Summer 2020

Synthesis of Alpha-Methylselenocysteine, Its Relevant Analogues, and an Unnatural Glutathione Disulfide Core

Robert J. Wehrle

SYNTHESIS OF ALPHA-METHYLSELENOCYSTEINE, ITS RELEVANT ANALOGUES, AND AN UNNATURAL GLUTATHIONE DISULFIDE CORE

by

Robert Joseph Wehrle

A Dissertation
Submitted to the Graduate School,
the College of Arts and Sciences
and the School of Mathematics and Natural Sciences
at The University of Southern Mississippi
in Partial Fulfillment of the Requirements
for the Degree of Doctor of Philosophy

Approved by:

Dr. Douglas Masterson, Committee Chair
Dr. Julie Pigza
Dr. Vijay Rangachari
Dr. Faqing Huang
Dr. Robert Hondal

August 2020

Published by the Graduate School

ABSTRACT

Selenoproteins, such as glutathione peroxidase, have gained interest for their ability to act as antioxidants, and their potential to act as anti-cancer agents. Synthesizing and studying selenoproteins can be problematic, however, due to their propensity to degrade from over-oxidation. The degradation from over-oxidation can be avoided by the incorporation of the unnatural amino acid, alpha-methylselenocysteine. A synthesis utilizing methyl malonic esters was used to synthesize protected (*R*)-alpha-methylselenocysteine efficiently (46% over four steps) and in high enantio-purity (88% enantiomeric excess). Using similar procedures, the (*S*)-enantiomer was also synthesized as well as a beta-analogue.

The use of enzymes in a chemical laboratory is beneficial as they provide an efficient enantioselective method to synthesize chiral materials. Unless known substrates are used, the stereochemistry of the product cannot be known with certainty. The Mosher method employs NMR to analyze an MTPA-derivatized version of a chiral compound, however, use on congested chiral centers is limited. While sitting in the MTPA-plane differently than the model predicts, the Mosher method can be used to determine unknown configurations in alpha-methyl amino acids. By synthesizing two MTPA-based diastereomers from enantio-enriched alpha-methylselenocysteine, the absolute configuration of the stereocenter at the alpha-carbon was determined to be an (*R*)-stereocenter.

Within the glutathione catalytic cycle, glutathione reduces the oxidized selenium of glutathione peroxidase to a selenol, allowing the enzyme to function again, however glutathione is oxidized to glutathione disulfide. Glutathione disulfide, while oxidized,

cannot operate normally and is needed to be reduced. The action of glutathione reductase reduces glutathione disulfide to two molar equivalents of glutathione. If both cysteines in glutathione disulfide are alpha-methyl amino acids, glutathione reductase is unable to perform the reduction. Work has been done to synthesize an asymmetric cystine and future work will be to elaborate to the asymmetric glutathione disulfide and study its inhibitory effects on glutathione reductase.

ACKNOWLEDGMENTS

I would first like to acknowledge the Chemistry and Biochemistry program at the University of Southern Mississippi for allowing me to pursue my Ph.D. I want to express my deepest gratitude for my advisor, Dr. Douglas Masterson, whose patience and guidance has allowed me to grow and develop as a graduate student. I would like to acknowledge my committee, who were always available to answer questions and to give feedback. I would like to thank Mrs. Tina Masterson, who helped me develop my teaching and presentation abilities. I would like to express my appreciation for the collaboration established with the Hondal research group, who performed all the biochemistry that lead to a shared publication. I would like to express thanks to Dr. Douglas Powell who performed the crystallography experiments, which were valued pieces of data for this dissertation. Finally, I would like to acknowledge past and present Masterson research group members who I have had the chance to interact and work with.

DEDICATION

I dedicate this manuscript to my late father, Bob Wehrle, who while alive, did everything in his power to help me succeed in life. He was lost suddenly during my tenure at USM, which was a difficult time. My wish is that he would be here to see me reach the monumental milestone, as it would have been one of the proudest moments in his life.

I would also like to dedication this manuscript to my wife, Jaclyn Wehrle, whose patience and determination was an inspiration and has allowed me to succeed in this program. Without her as my foundation, the difficult times would be much more so, and the good times much less.

TABLE OF CONTENTS

LIST OF TABLES

LIST OF ILLUSTRATIONS

LIST OF SCHEMES

LIST OF ABBREVIATIONS

α-MeAAs	α-methyl amino acids
α-MeSec	α-methylselenocysteine
α-MeSer	α-methylserine
α-MeTyr	α-methyltyrosine
1D	1-dimensional
Aib	α-methylalanine
Arg	Arginine
Asp	Aspartic Acid
ATP	Adenosine triphosphate
ATR	Attenuated total reflectance
Boc	*Tert*-butyloxycarbonyl
BtCl	1-chlorobenzotriazole
BtH	Benzotriazole
^{t}*Bu*	*Tert*-butyl
Cys	Cysteine
DCE	Dichloroethane
DCM	Dichloromethane
DMF	*N*,*N*-dimethylforamine
DMTST	Dimethyl(methylthio)sulfonium trifluoromethanesulfonate
DNA	Deoxyribonucleic acid
DPPA	Diphenylphosphoryl azide

ee	Enantiomeric excess
ESI	Electrospray ionization
Et	Ethyl
et al.	And others
Fmoc	Fluorenylmethyloxycarbonyl
FmocOH	9-fluorenylmethanol
FT-IR	Fourier transformed infrared spectroscopy
Gln	Glutamine
Gly	Glycine
GPx	Glutathione peroxidase
GPxOH	Oxidized glutathione peroxidase
GPxSG	Glutathione peroxidase-glutathione adduct
GSH	Glutathione
GSSG	Glutathione disulfide
GR	Glutathione reductase
HPLC	High pressure liquid chromatography
HRMS	High resolution mass spectrometry
in situ	In the reaction mixture
in vacuo	By vacuum
IR	Infrared spectroscopy
LRMS	Low resolution mass spectrometry
Me	Methyl
Mob	4-methoxybenzyl

MS	Mass spectrometry
Ms	Methylsulfonyl
MTPA	α-methoxy-α-trifluoromethylphenylacetate
NADPH	Nicotinamide adenine dinucleotide phosphate
NMR	Nuclear magnetic resonance
OAc	Acetate
PLE	Pig liver esterase
^{i}Pr	Isopropyl
Red-Al	Sodium bis(2-methoxyethoxy)aluminum hydride
R_f	Retention factor
ROS	Reactive oxygen species
R_t	Retention time
SBP-2	SECIS binding protein 2
Sec	Selenocysteine
SECIS	Selenocysteine insertion sequence
SeEF	Selenocysteine elongation factor
TEA	Triethylamine
tert	Tertiary
TFA	Trifluoroacetic acid
THF	Tetrahydrofuran
Thr	Threonine

TLC	Thin layer chromatography
tRNA	Transfer ribonucleic acid
Ts	4-tolylsulfonyl
Tyr	Tyrosine
UAAs	Unnatural amino acids
UV	Ultraviolet
Val	Valine

CHAPTER I – INTRODUCTION

1.1 Anti-oxidation in Biology

Respiration is an important biological process that allows for the conversion of small organic molecules to cellular energy in the form of ATP. During aerobic respiration oxygen is used in the electron transport chain to produce copious amounts of ATP, as well as water and carbon dioxide. During this process side reactions can occur, which can produce reactive oxygen species (ROS), such as superoxide radicals, hydrogen peroxide, and hydroxyl radicals. These ROS then proceed to cause oxidative damage to cellular machinery and DNA and if not suppressed can lead to chronic diseases, such as cancer, and even death.[1-4] To combat the propagation of the oxidative stress caused by ROS, organisms have developed a series of redox reactions utilizing antioxidant enzymes and substrates to reduce the level of ROS in the cell.[5] Many of the biomolecules are reversibly oxidized, converting the ROS to more benign materials, and are then subsequently reduced by a series of steps back to their original active form.

Many of these redox active biomolecules contain either sulfur or selenium in their active site, and it is these elements that directly interact with the ROS. Selenium is a trace metal in the Earth's crust and is an essential micronutrient for humans. With selenium labelled as a micronutrient, it unfortunately has a narrow range between deficiency and toxicity which can lead to several health issues, with deficiencies leading to diseases like Keshan disease[3, 6-7] and an excess leading to selenosis.[3, 8] It has been found in over 20 mammalian proteins mainly in the form of the amino acid selenocysteine (Sec).[9-12] All the proteins found containing Sec, such as glutathione peroxidase (GPx), have some

antioxidant function owing to selenium's low redox potential of -381 mV at pH 7.0[13] which are responsible for maintaining the homeostatic redox environment in cells.

Selenoenzymes work to reduce ROS and other forms of oxidative stress but have the potential to become overwhelmed. Much research has been undertaken to synthesize organoselenium compounds that have similar redox capabilities as GPx that are able to function more efficiently.[14-17] Synthesized in the 1920's, ebselen is an organoselenium compound that has been shown the exhibit GPx-like activities.[18-19] While used in clinical trials for to treat ischemia from cardiovascular occlusions as well as showing potential anti-cancer capabilities,[5, 20] it exhibits low solubility, as well as potential cytotoxicity.[21-22]

One class of selenium containing antioxidants that has not been studied extensively are synthetic peptide-based antioxidants which can exhibit water-solubility, as well as low cytotoxicity, but can be prone to degradation (See **Section 1.2**).[23]

GPx is a key selenoenzyme that reduces hydrogen peroxide. It acts in a catalytic redox cycle with glutathione (GSH) and glutathione reductase (GR). The catalytic cycle first starts with the selenium in GPx in the form of a selenol being oxidized by hydrogen peroxide to a selenenic acid (**Figure 1.1**).[24-25] The oxidized GPx (GPxOH) then oxidizes GSH to form a GPxSG complex, releasing water as a byproduct. The

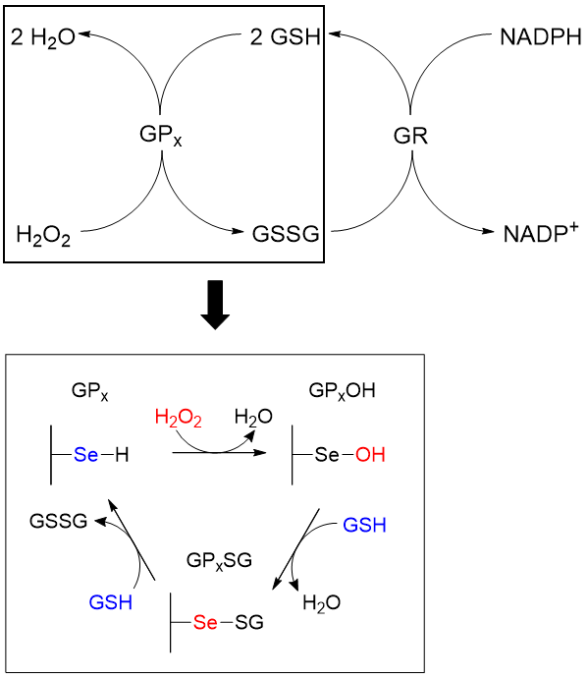

Figure 1.1 *Glutathione Peroxidase Enzyme Cycle*

selenium in the GPxSG complex is then reduced back to a selenol by an additional GSH producing glutathione disulfide (GSSG) and reforming the active GPx. The GSSG is then reduced by NADPH with GR acting as a catalyst, closing the catalytic cycle.

1.1.1 Sec and Selenium Incorporation into Proteins

Sec is considered by many to be the 21st natural amino acid. It shares many commonalities with the other 20 amino acids, such as having its own codon, tRNA, and is installed into peptides co-translationally verses a post-translational modification like many other unnatural amino acids.[12] The process in which it is added to a peptide, however, is not as trivial as the other 20 amino acids; since the codon for Sec is the stop codon UGA, it is needed to be retranslated for Sec insertion.[26-28]

This entire process, as explained by Turanov *et al*.,[29] and depicted in **Figure 1.2**, Sec is biosynthesized by its tRNA first being aminoacylated with serine,[30] followed by the hydroxyl on the serine moiety being phosphorylated. Selenophosphate then acts on this molecule yielding an active Sec tRNA producing diphosphate as a byproduct. This charged Sec-tRNA can then add Sec to a growing peptide chain.

Even though the biological pathway is known, there is still inherent difficulty incorporating Sec into proteins due to its codon being the stop codon sequence UGA. Without any modifications or secondary structure considerations to the RNA, peptide synthesis would cease at that point without adding in Sec or any additional amino acids that followed due to the UGA being treated as a stop codon. To overcome this, cells have installed a selenocysteine insertion sequence (SECIS) element directly downstream of a UGA sequence.

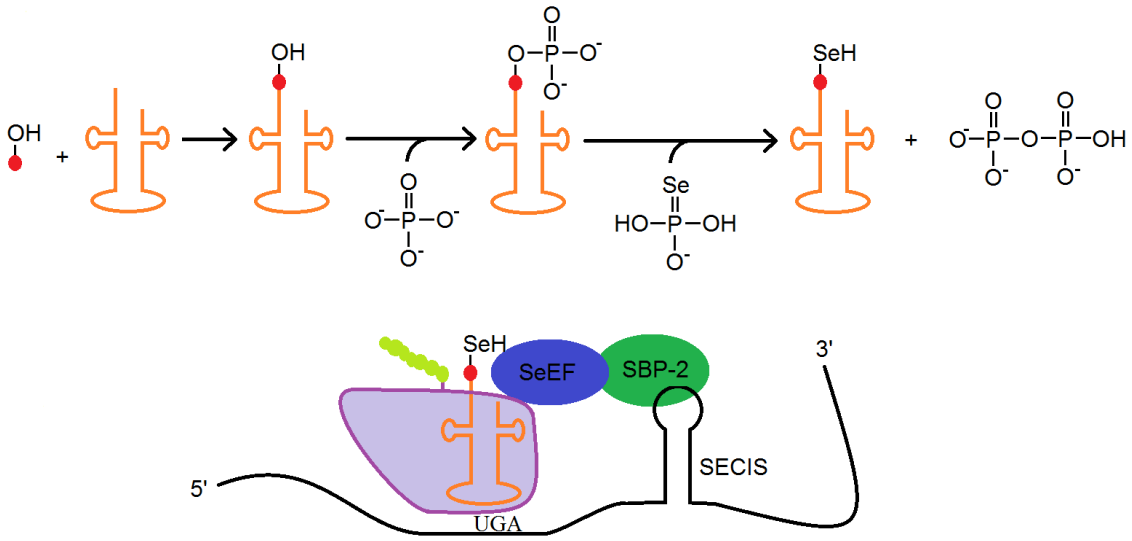

Figure 1.2 *Biosynthesis of a Sec Containing Peptide*

(Red) An amino acid with the R-group moiety shown. (Orange) Sec-tRNA. (Purple) Ribosome. (Yellow-green) Growing peptide chain

This SECIS, discovered by Berry et al.,[28] forms a stem loop structure at the 3' end in the RNA. With SECIS, coupled with SECIS binding protein 2 (SBP-2), selenocysteine elongation factor (SeEF), Sec-tRNA, and other cellular machinery, Sec is incorporated into the growing peptide chain as discussed by Krol in his review.[6] It is because of these extra processes needed for Sec incorporation that lower eukaryotes generally lack the ability to create selenoproteins.

1.1.2 Selenocysteine Versus Cysteine

Selenocysteine and cysteine (Cys) can perform biological redox processes in the biomolecules they are contained in. While both Sec and Cys have nearly identical redox chemistries, with a difference in their redox potential of 20-25 mV,[1] Sec is the preferred amino acid in some enzymes over Cys. Biologically, it seems counter-intuitive to have

this bias, specifically when specialized cellular machinery is required to add Sec into biomolecules, and Cys appearing to function identically to Sec. Both amino acids also have the same oxidation states and readily form dichalcogens when oxidized, which can then be easily reduced. Their differences become more obvious when the higher oxidation states are accessed. The work by Hondal *et al.*[31] demonstrated that at the 6^+ oxidation state of both sulfur and selenium are deactivated from further redox chemistries, however their ability to reach this oxidation state vary significantly (**Figure 1.3**). At the 4^+ oxidation state, the propensity of sulfur to be further oxidized to 6^+ is much higher than selenium. As shown by Hondal *et al.*, it only takes 2 equivalence of an oxidizer for sulfur to start converting to the 6^+ oxidation state, whereas selenium only starts converting to the 6^+ oxidation state after 3 equivalences.[31] Once oxidized, it is easier for selenium to be reduced and to proceed with additional redox reactions. This ability to readily cycle from higher oxidation states to lower and more active oxidation states may be why Sec is preferred over Cys in certain biological systems.

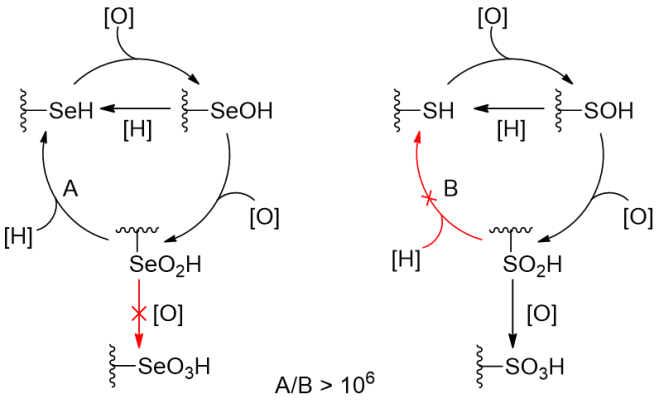

Figure 1.3 *Redox Cycles of Selenium and Sulfur*

Besides redox chemistry, there are other differences between Sec and Cys that biology can use to its advantage. The pK_a of the selenol in Sec is approximately 5.7,[32-33] which at physiological pH, the selenium is largely deprotonated. Conversely the pK_a of the thiol on Cys is 8.5 and at physiological pH the sulfur is only partially deprotonated.[34]

Since Sec is mostly deprotonated under these conditions the selenium would be more nucleophilic and be reactive towards the ROS than Cys. Many selenoproteins have known Cys homologues in biology, however they typically have several orders of magnitude lower activities when compared to the normal Sec containing protein.[35]

1.2 Sec Degradation

Under normal circumstances Sec, can easily reduce ROS to benign compounds, however there is a threshold at which it can become overwhelmed and become over-oxidized to form a seleninic acid. While selenium in this oxidation state can be easily reduced to lower oxidation states, the amino acid can degrade as this species. A typical reaction used in organoselenium chemistry is the β-elimination of a selenoxide to form an alkene.[36-38] The oxygen on the selenium can deprotonate the α-hydrogen of the amino acid which then eliminates selenium from the amino acid, forming dehydroalanine.[23, 39-40]

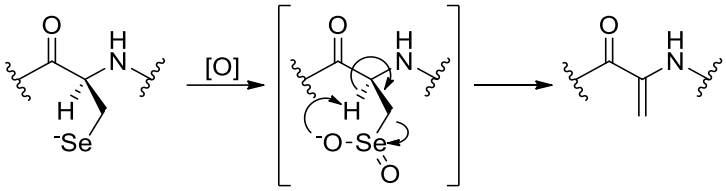

Scheme 1.1 *Selenocysteine Degradation*

Once dehydroalanine is formed, the biomolecule loses the ability to perform the redox chemistry that it could with Sec.[41] Without the α-hydrogen present, α-MeSec (α-methylselenocysteine) cannot degrade by this pathway. With this extra stability α-MeSec should have increased longevity, enabling it to cycle through more redox reactions, allowing the biomolecules to stay active longer.[42]

1.3 Unnatural Amino Acids

The normal 21 amino acids are readily used to make proteins, each amino acid with its difference in property, allowing for the many shapes and functions that proteins have. There, however, are many unnatural variations that the cell itself can create and utilize, typically formed from post-modifications to peptides.[43] These new amino acids offer new properties, and can possibly change protein folding.[44]

There are many unnatural amino acids (UAAs) that can be incorporated into a protein that are not biosynthesized, that scientists use, to purposely manipulate the protein in specific ways. These UAAs, just like their biosynthetic counterparts, can change the protein and give more desirable properties. One such class of UAAs is α-methyl amino acids (α-MeAAs), which replace the hydrogen on the α-carbon with a methyl group. This methyl group adds steric hindrance that the hydrogen atom would not, which results in added rigidity of the ψ and ϕ dihedral angles.[45] The values that ϕ and ψ for α-MeAAs take typically give helical structures or induce β-turns. Aib (α-methylalanine), the simplest α-MeAA, is a strong helix former, inducing either α- or 3_{10}-helical structures, as well as a β-turn promoter.

With the inclusion of α-MeAAs, the protein is typically more stable. All proteogenic amino acids, excluding glycine, are L-stereoisomers. Under basic enough conditions amino acids have the propensity to racemize at the α-carbon, which could cause the protein to misfold and degrade.[46-47] Within physiological pH, the rate of racemization is negligible, but racemization can be a problem when studying and

synthesizing peptides. Since there is no longer an acidic hydrogen on the α-carbon in α-MeAAs, racemization at this position is prevented, allowing for a more stable protein.

Besides racemization, α-MeAAs can also resist enzymatic cleavage. Khosla *et al.*[48] reported that when angiotensin II is modified to contain α-MeTyr (α-methyltyrosine) at the 4th position in the peptide, the molecule completely resists digestion by α-chymotrypsin, while the natural substrate degraded into two components from the scission of the N-terminal amide bond to the tyrosine. Based on their findings, the incorporation of α-MeTyr did very little to change the protein conformation and the protein retained almost all its biological function. Much of the enzymatic degradation resistance can be argued to be caused from the steric effects of the α-methyl group.

In biological systems, besides resisting enzymatic cleavage, α-MeAAs can inhibit enzymatic function. Inhibitors act by binding to the enzyme and preventing it from acting on its substrate.[49] Substrates with α-MeAAs may still have the ability to bind its enzyme, but the change in geometry afforded by the α-methyl groups may prevent enzymatic action. One example in literature is an unnatural form of glutathione disulfide which has α-methyl groups on both cysteines (G'SSG') as described by Kedrowski *et al.*[50] This molecule is able to enter the active site of GR, but because of the steric hinderance imposed by the α-methyl groups, G'SSG' is unable to be acted on. Another example reported by Nakazawa *et al.*[51] is the action of α-methylphenylalanine on aromatic L-amino acid decarboxylase. Without the addition of the cofactor pyridoxal phosphate, the enzymes function is inhibited.

1.4 Enzymes in Synthetic Chemistry

Many biological compounds that chemists synthesize contain at least one stereocenter, and careful consideration of reaction choice is needed to avoid the formation of epimers. To obtain a desired configuration from a reaction, chemists can employ several techniques: chiral catalysts, chromatographic resolutions, or enzymes. The benefit to chiral catalysts is that reactions do not need stoichiometric amounts of the catalyst, and many reactions can produce high enantioselectivity with very low loading amounts.[52] These catalysts, however, can be cost preventative to use as many of them use precious metals and expensive ligands to function.[53-54]

Another method that can be employed is utilizing chromatography for a chiral resolution of a racemic mixture. This method can allow for efficient separation of two racemates by using a chromatography column that has been functionalized with a chiral ligand. It is typically not known which enantiomer is which unless comparisons can be made with retention times of a known analyte. A benefit to this method, besides chiral resolution, is that enantiomeric excess (%ee) can be determined from the chromatographic trace on the HPLC system if an enantioselective reaction was used.

Enzymes are a ubiquitous resource to asymmetric synthetic chemistry. Many enzymes perform specific reactions have specific substrates that they act on,[55-56] however many enzymes are able to be used for more general reactions. Enzymes are useful because many of them are inexpensive, compared to chiral catalysts. Even though many are substrate dependent, enzymes typically offer high stereoselectivity, which can be altered depending on the specific enzyme and reaction conditions.[57-58] One common class of enzymes used are esterases which can selectively hydrolyze esters to carboxylic

acids.[59-61] A commonly used esterase is pig liver esterase (PLE) as it possesses a wide substrate scope. With PLE having a broad scope of substrates, its stereoselectivity has the potential to fluctuate depending on the substrate used. To aid in predicting which stereoisomer will be produced, Jones *et al*. created a model of the active site of PLE by computational methods from experimental data (**Figure 1.3**).[62] The Jones model, while adequate in initial predictions, cannot be used to accurately determine the stereochemistry of the hydrolysis product. Crude PLE was used to form the Jones model, however there are six isoenzymes within the crude enzyme. The isoenzymes can vary drastically from one another considering yield, enantioselectivity, and stereopreference.[57-58] To confirm absolute configuration and %ee of the enzymatic product, empirical methods, such as spectroscopy and polarimetry, must be used.

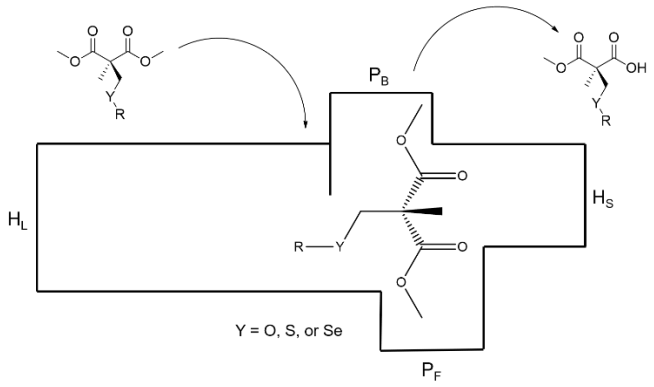

Figure 1.3 *Expected Orientation of α-MeSer, α-MeCys, and α-MeSec Malonic Esters in PLE Using the Jones Model*

1.5 Unnatural Amino Acids and Glutathione Reductase

The GSH catalytic cycle is a process that is critical for proper cellular function. Substituting α-MeAAs for key amino acids in peptides can allow for greater stability and prevent degradation associated with high levels of oxidative stress.[42] The incorporation of

α-MeAAs in this cycle can also change how enzymes interact with their substrates. When both cysteines are α-methylated in glutathione disulfide (G'SSG'), GR cannot reduce the disulfide bond present and G'SSG' acts as a competitive inhibitor.[50] With the activity of GR decreased from inhibition, the concentration of ROS will increase as the catalytic cycle becomes bottle-necked. It is unknown if the inhibition behavior will differ if an asymmetric glutathione disulfide is used instead, and future work will focus on its synthesis and function as a substrate for GR.

CHAPTER II – SYNTHESIS OF α-METHYLSELENOCYSTEINE AND ITS RELEVANT ANALOGUES

2.1 Introduction

Selenium is an essential trace nutrient needed for many higher organisms, which allows for the biosynthesis of selenocysteine (Sec) and selenoproteins. These selenoproteins typically have anti-oxidative properties which reduce oxidative stress within cells. The study and synthesis of selenoproteins is not a trivial endeavor, due to the potential degradation from β-elimination.[23] One of the first syntheses of Sec was performed by Fredga in 1936 by the action of potassium diselenide on 3-chloroalanine methyl ester.[63] Other routes have been used to synthesize Sec analogues, with a popular method being selenylating an activated serine with a nucleophilic selenium species,[33, 39, 64-65] which mirrors Fredga's method for selenylation. Another method first performed by Shirahama *et al*., and utilized by many chemists after, is the nucleophilic ring opening of a β-lactone by a selenylating agent.[66]

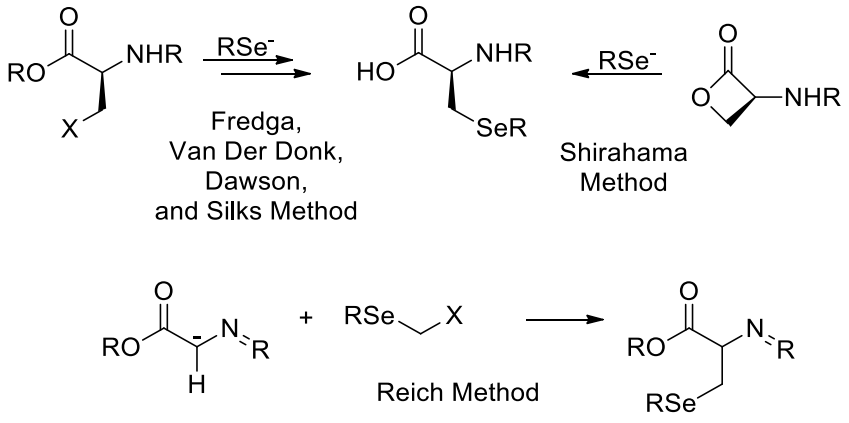

Scheme 2.1 *General Methods Previously Used to Synthesize Sec*

Both methods allow for high yielding reactions and enantiopure products if enantiopure materials are used. Finally, Reich *et al*. pioneered a synthesis from a glycine analogue forming a racemic Sec analogue from enolate chemistry,[67] using similar reagents to what the Masterson lab developed (**Scheme 2.2**).

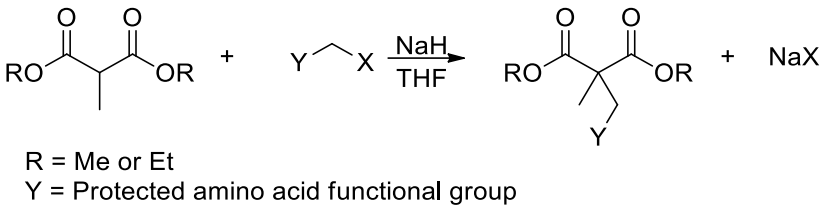

Scheme 2.2 *Masterson Lab Enolate Synthesis*

A few select α-MeSec analogues have been synthesized in the Masterson lab. All of them boast robust chemistries that can produce the target molecules in minimal steps, which will be discussed in this chapter: selenylation, desymmetrization, amine formation, and ester hydrolysis (**Scheme 2.3**).

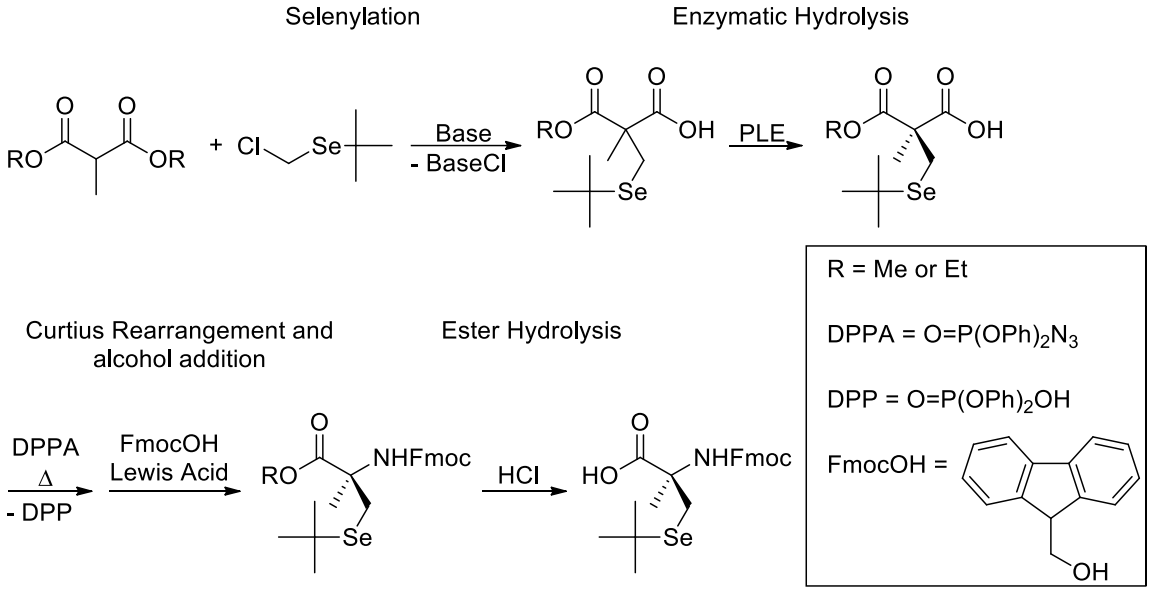

Scheme 2.3 *Synthetic Strategy to Synthesize α-MeSec Utilizing Enolate Chemistry*

2.2 Selenylation

2.2.1 Strategies in Literature

Chemists rely either on selenium's electrophilicity or nucleophilicity to selenylate molecules. Selenylation of an organic compound, depending on the necessary conditions and reagents used, can be a straightforward reaction, or quite complex. Once incorporated into the substrate, care is needed to avoid oxidation of the selenium, especially if there is a β-hydrogen to the selenium. With a β-hydrogen present, selenium can eliminate from the compound, leaving an alkene (see **Scheme 1.1** on page 6). Common oxidizers used for this process are peroxides, but other oxidants can be employed.[38]

Electrophilic selenylation occurs using a selenyl halide. The use of these types of species is in a selenoxide elimination reaction to from α,β-unsaturated ketones from enolates and proceeds through a *syn*-elimination process (**Scheme 2.4**).[68-69] Usually hydrogen peroxide is used as an oxidant in these reactions, however this leaves the ketone susceptible to a Baeyer-Villiger reaction, forming an unwanted ester. To avoid this problem, sodium periodate or ozone can be used.[38]

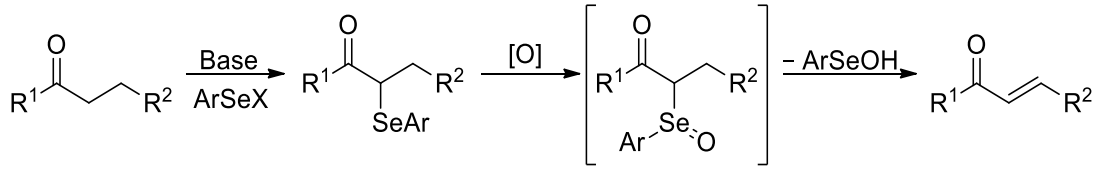

Scheme 2.4 *Selenoxide Elimination*

Another reaction that utilizes electrophilic selenium to selenylate a substrate is the oxidation of alkenes to form vinyl alcohols by utilizing selenium dioxide. Sharpless et al. explored this reaction mechanism (**Scheme 2.5**) and determined it to occur by the action

of the alkene attacking the selenium of selenous acid and the simultaneous deprotonation of the vinylogous proton by selenous acid, followed by a loss of water from the selenous acid moiety. Once at the seleninic acid intermediate, a [*2,3*]-sigmatropic rearrangement occurs, followed by solvolysis to produce the vinyl alcohol.[70-72]

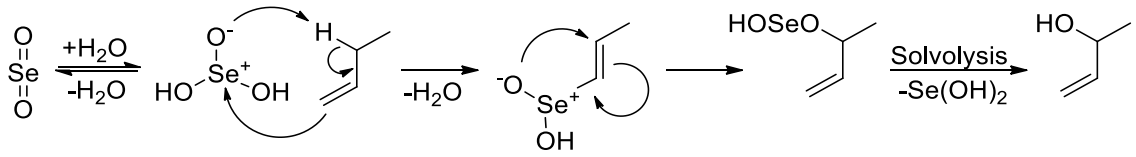

Scheme 2.5 *Selenium Dioxide Oxidation*

While electrophilic selenylation is an option to selenylate substrates, nucleophilic selenylation can also be used. Many of these reactions take advantage of selenium's high nucleophilicity, especially when in the selenolate form. Selenolates can attack electrophilic carbons, such as alkyl halides, to form a carbon selenium bond. Selenylation with these species acts through an S_N2 mechanism, and a sterically hindered carbon center will stifle the reaction.

Formation of nucleophilic selenium species has been previously done by the reduction of elemental selenium with alkali metals, such as sodium or potassium, creating a reactive metal selenide or diselenide depending on the stoichiometry used.[73] These reactive species can then be used to ultimately form selenides, diselenides, and polyselenides. Similar results can be achieved when using hydride sources, such as sodium borohydride, when forming a selenylating species from elemental selenium.[33, 74-76] Selenylating species can also be formed by reduction of diselenides using hydride sources, which will mostly result in selenide products being formed.[73]

More specialized reagents can also be used to selenylate substrates. One such compound is Woolins' reagent, which is the selenium equivalent to Lawesson's reagent.[77] This reagent exist as a dimer, but its active phenyldiselenophosphine intermediate can be readily created *in situ* by reflux (**Scheme 2.6**). The reactive intermediate of Woolins' reagent especially resembles selenophosphate, which is what the cells use to selenylate the phosphorylated serine (See **Figure 1.2** on page 4).

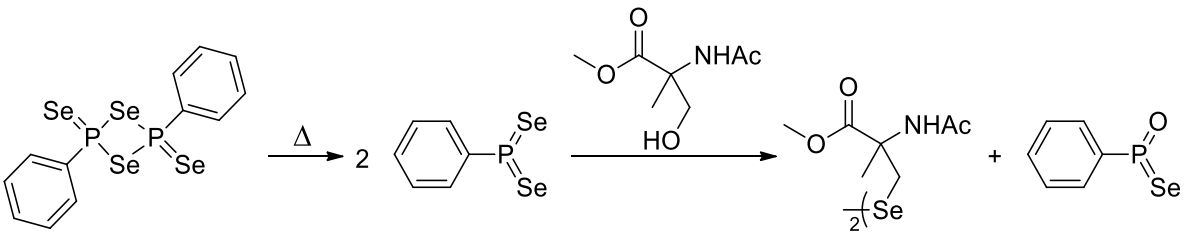

Woolins' Reagent

Scheme 2.6 *Woolins' Reagent and Its Action on α-MeSer*

Lawesson's and Woolins' reagents are routinely used to convert carbonyl containing functional groups to their higher chalcogen counterparts, however work has been done by Iwaoka *et al*.[78-79] that show that Lawesson's and Woolins' reagents can convert serine and α-methylserine (α-MeSer) to the Cys and Sec analogues, respectively (**Scheme 2.6**). There are problems with these conversions which include low to moderate yields as well as potential loss of optical purity.

2.2.2 α-Methylserine to α-Methylselenocysteine Hypothesis

It was hypothesized that synthesizing α-MeSec could be accomplished through a conversion from α-MeSer. Considering what substrates were on hand, it was decided to

explore the possibility to selenylate α-MeSer as a method of obtaining α-MeSec. It was hypothesized that because of selenium's superior nucleophilicity, selenylation should be possible on the hindered neopentyl-like methylene carbon, especially if the hydroxide group was activated by converting it to a sulfonic ester (**Scheme 2.7**).

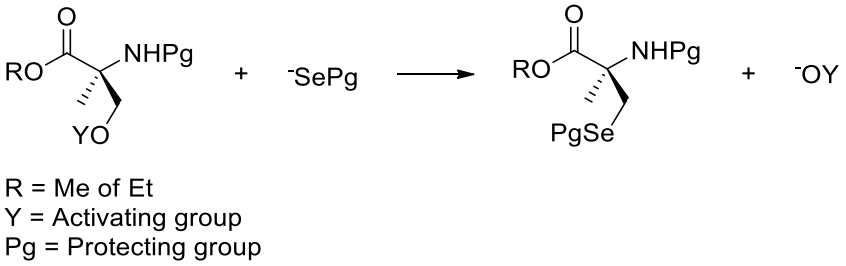

Scheme 2.7 *Selenylation Strategy of an Activated α-MeSer*

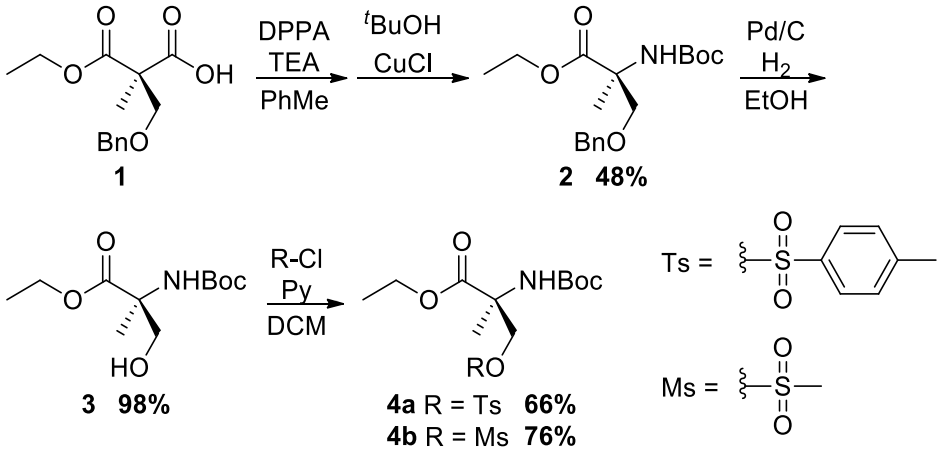

Scheme 2.8 *Synthesis of the Substrate to Selenylate*

The half-ester benzyl protected analogue **1** (70% ee) of α-MeSer was the starting material used in these attempts and needed to be converted to a substrate for selenylation (**Scheme 2.8**). The carboxylic acid of **1** was converted to a Boc protected amine **2** by using a Curtius rearrangement to form an isocyanate intermediate, which was then immediately

transformed to a carbamate by an alcohol addition with *tert*-butyl alcohol. The benzyl protected alcohol was then deprotected by hydrogenation with hydrogen gas and palladium in ethanol to afford **3** in high yields. The free alcohol was then converted to a sulfonic ester in the presence pyridine and the sulfonyl chloride to produce **4a** and **4b**.

With **4a** and **4b** in hand, different selenylating agents could then be used to attempt selenylation. The first one attempted, 4-methoxybenzyl diselenide **5**, was not commercially available and had to be synthesized. Elemental selenium was reduced with lithium triethylborohydride ($LiBEt_3H$) and then reacted with 4-methoxybenzyl chloride (MobCl) to produce **5** in low yields (**Scheme 2.9**).

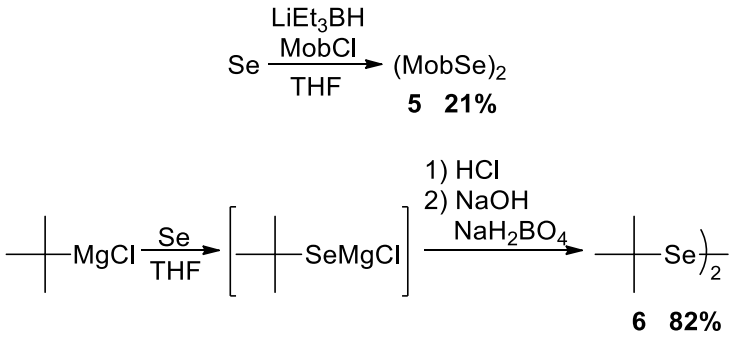

Scheme 2.9 *Synthesis of Non-commercial Selenylating Reagents*

A selenylation of **4a** was attempted using **5**, but **5** failed to reduce with sodium borohydride based on ^{77}Se NMR. Another selenylating agent was then tested, the selenide anion, Se^{2-}. The selenide anion was created *in situ* using $LiEt_3BH$, and then was used to selenylate **4** (**Scheme 2.10**), however only **4a** converted from starting material.

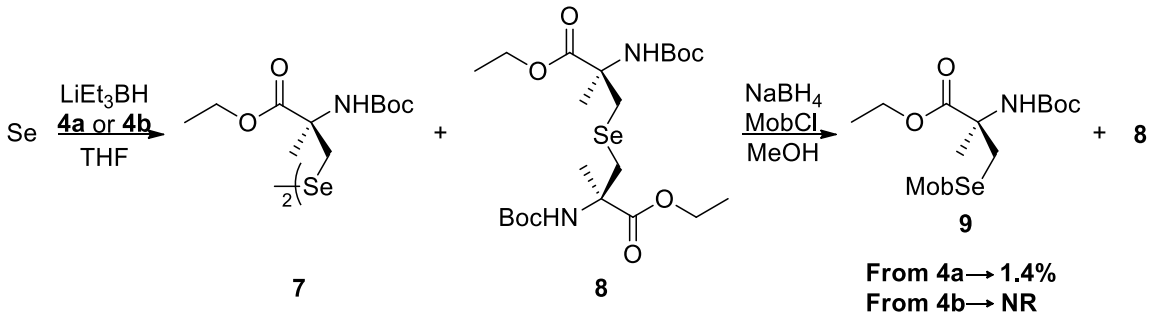

Scheme 2.10 *Initial Selenylation Attempt*

This, unfortunately, created a mixture of selenide **7** and diselenide **8**, which having very similar polarities, were unable to be separated by chromatography. Utilizing the chemical differences between a selenide and diselenide, it was possible to reduce **7**, and create an asymmetric selenide by trapping the formed selenolate with an alkyl halide. This was done by reducing **7** using $NaBH_4$ and then selenylating MobCl creating **9**. With a large difference in polarity, **9** was easily able to be isolated from **7**, but only a minute amount of **9** was able to be isolated.

With the poor yield from the previous selenylation attempts, other selenylating agents were considered, one being potassium selenocyanate (KSeCN). This was an attractive selenylating reagent because it should act as a non-bulky nucleophile and after the initial selenylation, the cyanate could be removed by hydrolysis, resulting in a diselenide.[73] While in principle the reaction should work, it failed to convert the substrate to a selenylated product.

A final selenating reagent considered was *tert*-butyl diselenide **6**. This reagent was chosen because of the previous experience using the sulfur variant used in the synthesis of α-MeCys. This was synthesized by first reacting *tert*-butyl magnesium

chloride with elemental selenium (**Scheme 2.9**). Selenium can insert itself between the carbon-magnesium bond, and with quenching, will form a selenol, which can then be easily oxidized to **6**. A selenylation was attempted with a reduced **6**, however the reaction failed to produce product.

With nucleophilic selenylation acting as a S_N2 mechanism there is a reasonable explanation as to why there was a low success rate with selenylation using **4** as a substrate; the selenylation site is on a neopentyl-like carbon. Normally, only the congestion of the electrophilic site is considered in the S_N2 mechanism, however, if the neighboring group is sterically hindered it can prevent the nucleophile from accessing the electrophilic center to the point which can be analogous to attempting a substitution on a tertiary carbon.[80-81]

2.2.3 Synthesis of α-MeSec Using Malonate Chemistry

With the low success of selenylation at the desired neopentyl-like carbon, another strategy the synthesis of α-MeSec is needed to be explored. In the Masterson group, several UAAs have been synthesized from a common starting material, methyl malonic esters. The functional groups of the UAAs can be added to the malonate backbone utilizing enolate chemistry. Further functionalization of the malonate allows for transformation to an amino acid which will be discussed in later sections. While this is a robust synthetic strategy, as proven with past syntheses, a stable selenium containing alkylating agent was needed to successfully alkylate the malonic ester using enolate chemistry (**Scheme 2.11**). The appropriate alkylating agent can be made from **6**, by

reduction and then chloroalkylation with DCM to incorporate the needed -CH_2X fragment.

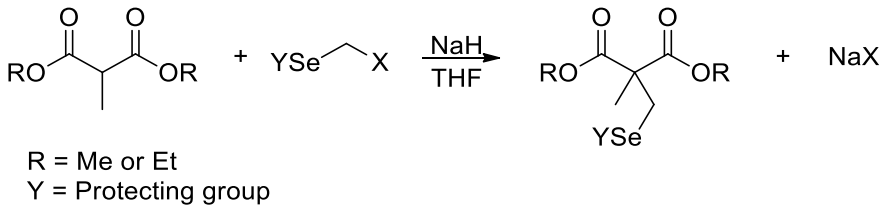

Scheme 2.11 *Seleno-Alkylation Utilizing the Enolate Strategy*

Before the alkylating agent could be made, an appropriate reducing agent needed to be found, due to the failure of the diselenide reductions in the earlier selenylation reactions. This was investigated utilizing ^{77}Se NMR before and after the addition of a reducing agent, which will show a large chemical shift for selenium if reduction took place. From these studies it was found that of the available reducing agents, $LiEt_3BH$ and sodium bis(2-methoxyethoxy)aluminum hydride (Red-Al) were the only reducing agent that were able to reduce **6** (**Table 2.1**). To confirm whether this selenylating reagent could overcome the steric effects of the neopentyl-like position, **4b** was added to the reduced form of **6**, unfortunately no selenylated product formed.

With a proper reducing agent discovered, the seleno-alkylating agent **10** could be made. This was done by reducing **6** in THF with $LiEt_3BH$, and then cannulating the formed selenolate to a round bottom containing DCM, which formed **10** (**Scheme 2.12**). Analysis by NMR revealed that **10** had a distinct shift difference from **6**, 488 ppm to 519 ppm, which was to be expected since selenium is quite sensitive to the electronic environment.[82] Upon sitting at room temperature for an extended length of time, **10** did seem to degrade to the dimer **11**, so creating it *in situ* was executed.

Table 2.1 *Reduction Studies of* ***6***[a]

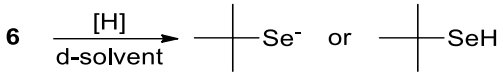

[H]	d-solvent	^{77}Se ppm	μmol **6**	μmol [H]	Notes
Blank	Ethanol-d6	486.5	198	0	
$NaBH_4$	Ethanol-d6	486.3		1450	White solid formed
Blank	THF-d8	487.6	121	0	
$LiEt_3BH$	THF-d8	164.5		200	Turned red
Blank	EtOH-(D_2O)[b]	486.1	247	0	
H_3PO_2	EtOH-(D_2O)[b]	484.5		1550	Without heating
H_3PO_2	EtOH-(D_2O)[b]	484.2			With heating, turned turbid
PPh_3	EtOH-(D_2O)[b]	484.3	394	1020	White solid formed
$LiEt_3BH$	THF-(D_2O)[b]	490.1[c]	228	500	**4b** was added after reduction
Red-Al[d]	THF-(D_2O)[b]	520.2[e]	313	900	Color changed from yellow to colorless

a) All reactions were performed in an NMR tube. b) D_2O was added as an external standard for non-deuterated solvents. c) ^{77}Se NMR data was obtained after workup d) Red-Al is sodium bis(2-methoxyethoxy)aluminum hydride e) DCM was used in the reaction to trap the selenolate through a chloroalkylation and the observed chemical shift is a result of that product

After the formation of **10**, the solvent was removed by vacuum and the resulting oil was then cannulated into a flask containing an enolate formed from the deprotonation of diethyl methylmalonate with sodium hydride. Based on NMR and mass spectrometry (MS), this method was successful in adding selenium to the desired substrate creating **12** with low yields (**Scheme 2.12**) which experienced a large chemical shift in ^{77}Se NMR. Besides creating **12**, a byproduct **11** was also formed, which seemed be an issue with the synthesis of **10** or a degradation product in the formation of **12**. With these low yields, the reactions can be later optimized.

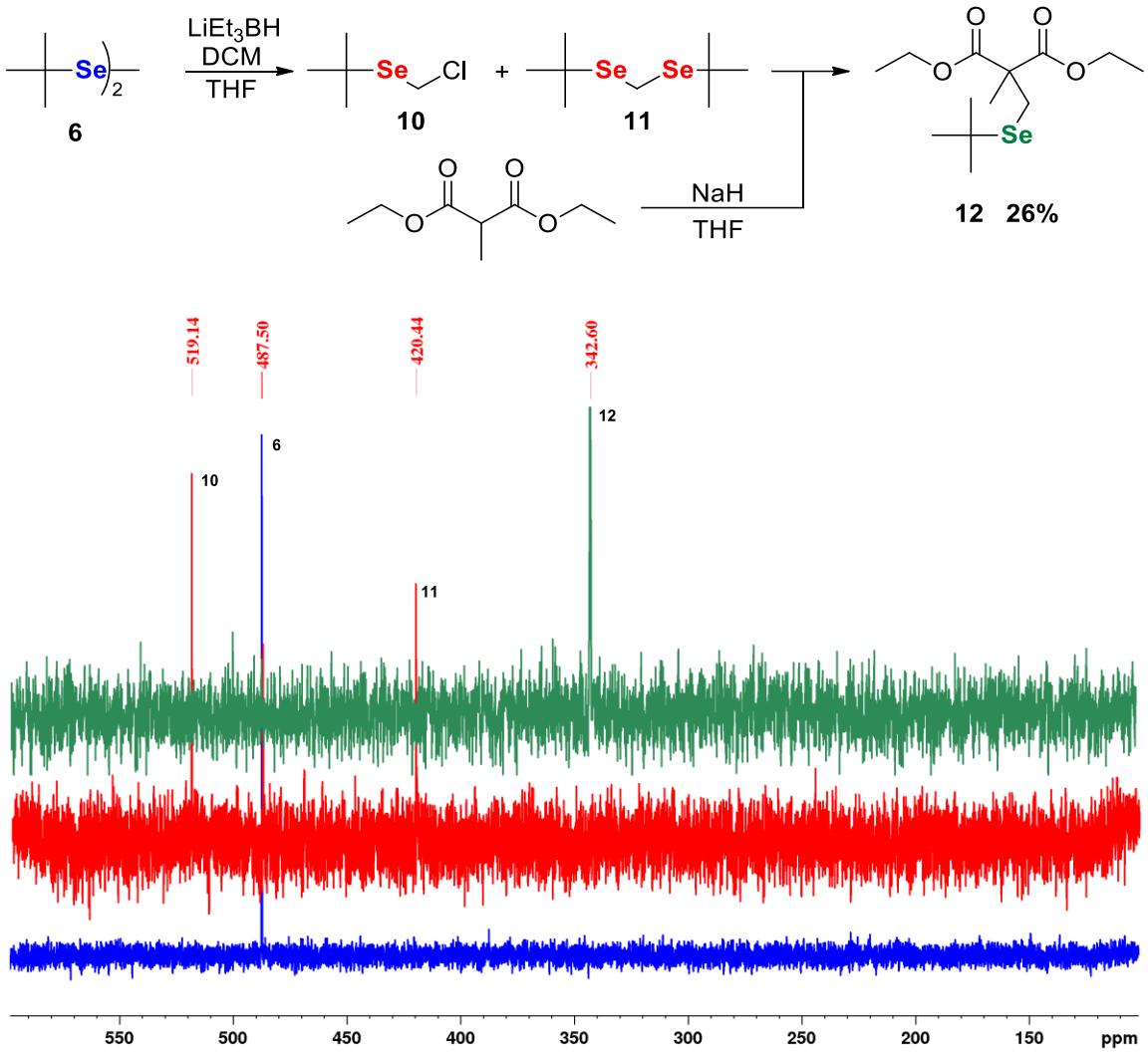

Scheme 2.12 *Synthesis of **11** and Its Use in Alkylating Diethyl Methylmalonate and ^{77}Se NMR of the Reactions*

^{77}Se NMRs of **6** and **12** were after purification.

2.2.3.2 Optimizations to Selenylation

With the successful, but low yields in the overall selenylation process, optimizations could be made. There were many places where optimizations could be made, from the synthesis of the diselenide, seleno-alkylating agent, as well as the alkylation itself. Synthesizing the diselenide was able to be accomplished with much

higher yields. Initially, once the selenium inserted into the carbon-magnesium bond, the reaction was quenched with ammonium chloride, however this sometimes caused the reaction to form a slurry, which was found to lower the yields.

Table 2.2 *Diselenide Synthesis*

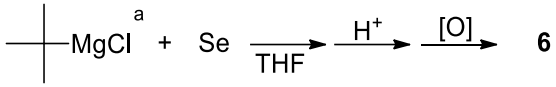

Trial	H^+	[O]	Yield of **6** (%)
1[b]	NH_4Cl	Air[c]	16
2[b]	NH_4Cl	Air[c]	12
3	NH_4Cl	Air	49
4	NH_4Cl	Air	18
5	NH_4Cl	Air	39
6	NH_4Cl	Air	13
7	NH_4Cl	Air	35
8	HCl	Air	57
9	HCl	Air	66
10	HCl	Air	62
11	HCl	Air	54
12	HCl	Air	53
13	HCl	Air[c]	21
14	HCl	O_2	27
15	HCl	Br_2	30
16	HCl	NaH_2BO_4[c,d]	82[e]

a) Grignard reagent was always in excess of selenium. b) Grignard was synthesized for the reaction instead of being purchased. c) Oxidation time was 3 hours or less. d) Oxidized from the selenolate instead of the selenol. e) Similar yields obtained by other lab members using this method.

It was later found that quenching with concentrated HCl was much more effective. Based on the work done by Mckillop *et al.*,[83] the rate of oxidation of the selenol is much slower than the rate of the selenolate. When previously oxidizing from the selenol, oxidation was found to be incomplete because some unoxidized selenol was removed by vacuum distillation lowering the yields of **6**. The highest yields (trial 16 **Table 2.2**) were obtained

by washing the selenol with base to deprotonate it to form a selenolate which partitioned to the aqueous phase. The oxidation was accomplished in a water/hexanes biphasic mixture, so once the selenolate was oxidized, it would partition from the aqueous phase to the organic phase, allowing for a much more facile isolation. As suggested by Mckillop *et al*., sodium perborate was used as the oxidizing agent instead of air since it was a reliable, consistent, and robust oxidant for selenium species. Using this method allowed for yields to improve to 82% after vacuum distillation.

Another potential for low yields within the alkylation process was the presence of boron compounds from the diselenide reduction interfering with the reaction. Using ^{11}B NMR, it was found that boron complexes existed in the reaction mixture from the synthesis of **10**, with these complexes persisting through different purification techniques (**Scheme 2.13**). Several alternative methods that avoided the use of boron-based reducing agents for the synthesis of **10** were attempted, but the best was the aluminum based reducing agent, Red-Al (**Scheme 2.14**).

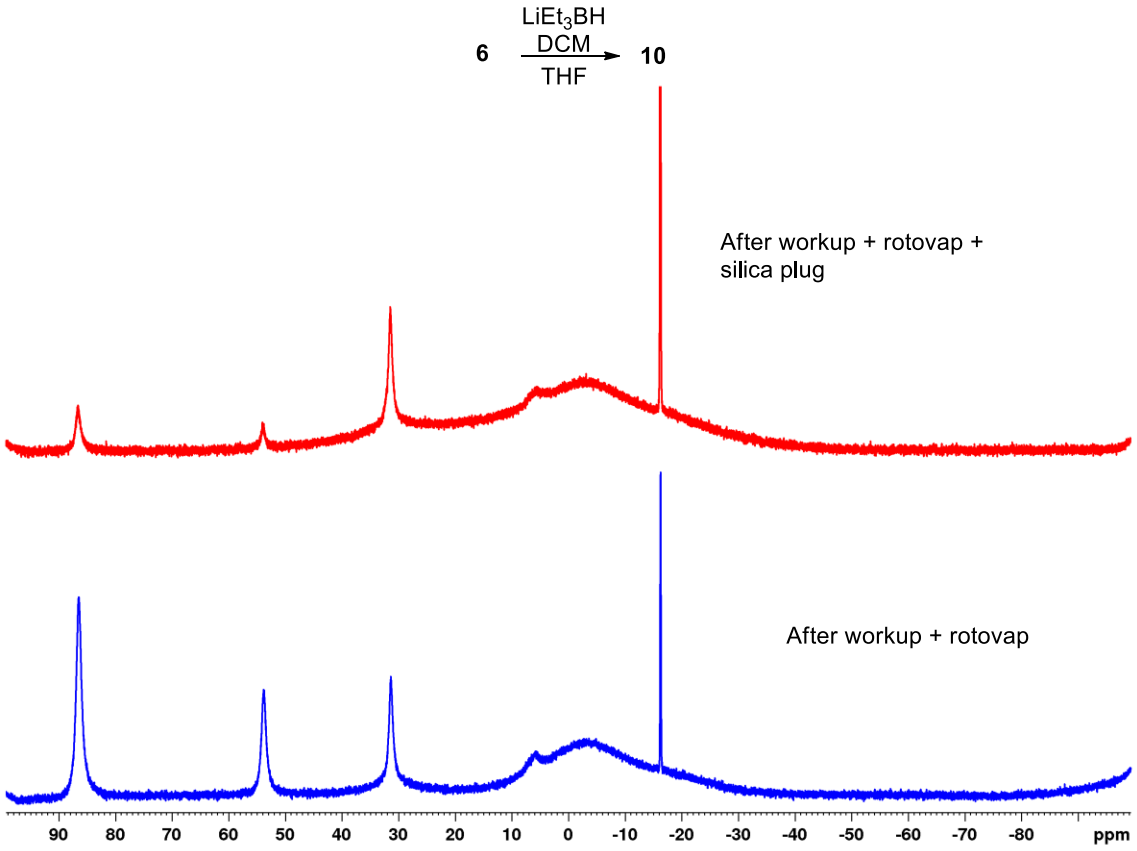

Scheme 2.13 *^{11}B NMR Analysis of **10** Attempting to Remove the Boron Species Through Different Workup Methods*

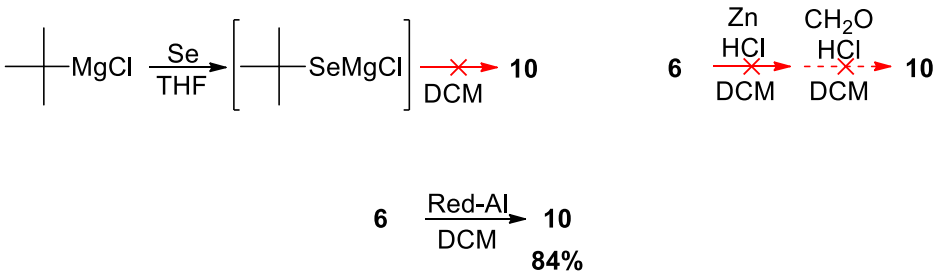

Scheme 2.14 *Attempts to Synthesize **10** Without a Boron Based Reducing Agent*

It was discovered that after the synthesis of **10**, with the aluminum byproducts were easily removed by a solution of sodium potassium tartrate. Previously the reduction was

performed in a separate flask and then the selenolate was cannulated into a flask containing DCM, but it was discovered that performing the reduction in DCM by adding Red-Al dropwise, was a very efficient process to cleanly produce **10**. This new reducing agent and method of synthesizing **10** directly increased the yield of the selenylation reaction from 26% to 80%.

2.3 Introduction of Chirality

With the successful synthesis of **12**, chirality needed to be introduced. Since **12** is a symmetrical molecule, a controlled desymmetrization is needed, specifically an enantioselective hydrolysis of one of the two esters. Enantioselective hydrolyses are carried out in the Masterson lab by employing enzymes, usually pig liver esterase (PLE). Previously it was discovered that PLE had great enantioselectivity with the α-MeCys malonic ester analogue, so it stood to reason that the α-MeSec variant should as well, since the only difference between the two is a single atom. Using phosphate buffer at pH 7.4, a biphasic mixture with **12** was made and PLE was added. The pH of this reaction was kept constant by the addition of NaOH and after the reaction the half-ester enzymatic hydrolysis product **13a** was isolated (**Scheme 2.15**). A racemic half-ester **13b** was also prepared by utilizing LiOH in a hydrolysis. With both compounds in hand, NMR samples were made that was spiked with an equimolar amount of (*S*)-α-methylbenzylamine to determine percent enantiomeric excess (%ee), however, neither the methylene protons or the ethyl ester protons were able to be resolved in the diastereomeric salts to give accurate results (**Scheme 2.16**).

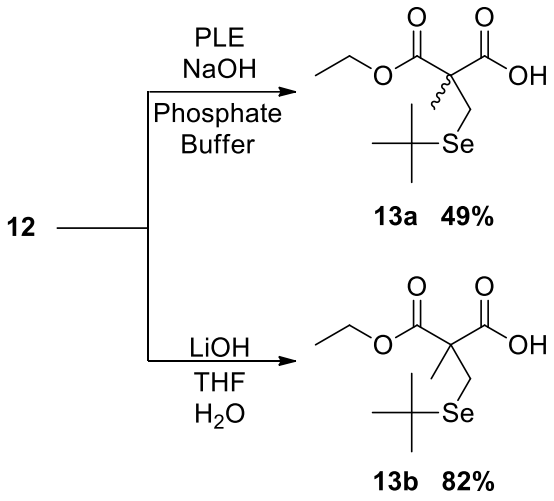

Scheme 2.15 *Enzymatic and Racemic Hydrolyses of Selenylated Malonate*

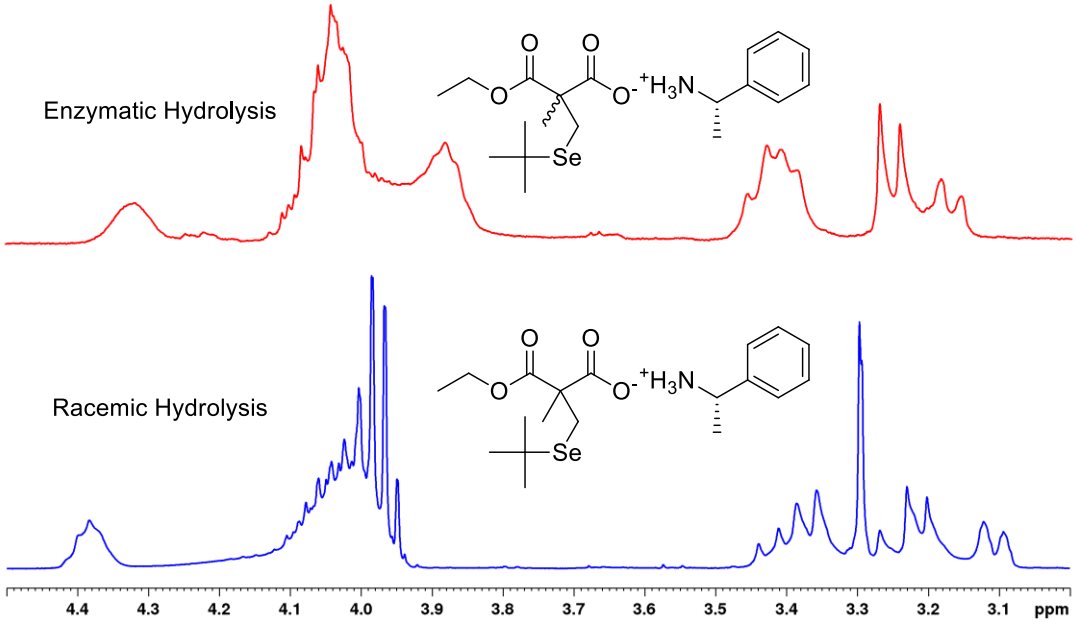

Scheme 2.16 *^{1}H NMR Spectra of the Downfield Aliphatic Signals to Determine %ee*

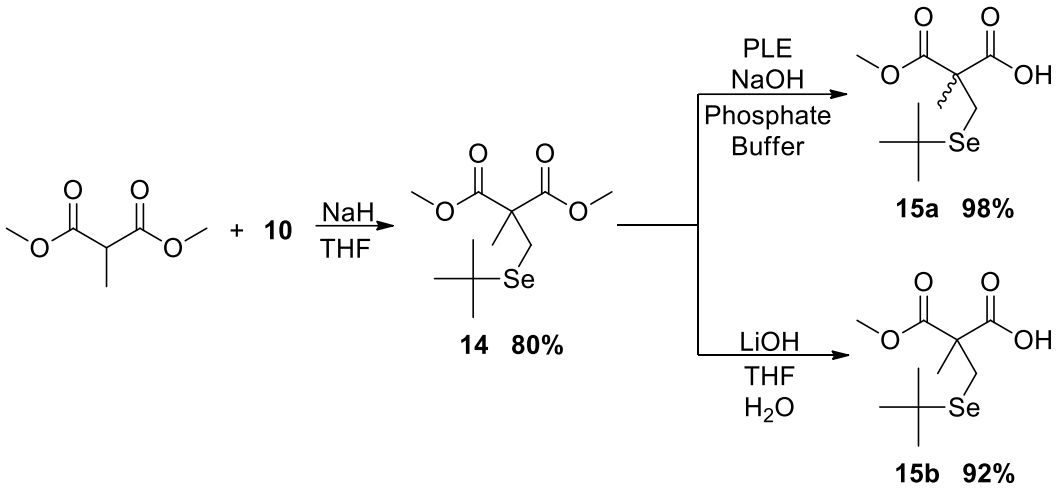

Scheme 2.17 *Synthesis of **15a** and **15b** from Dimethyl Methylmalonate*

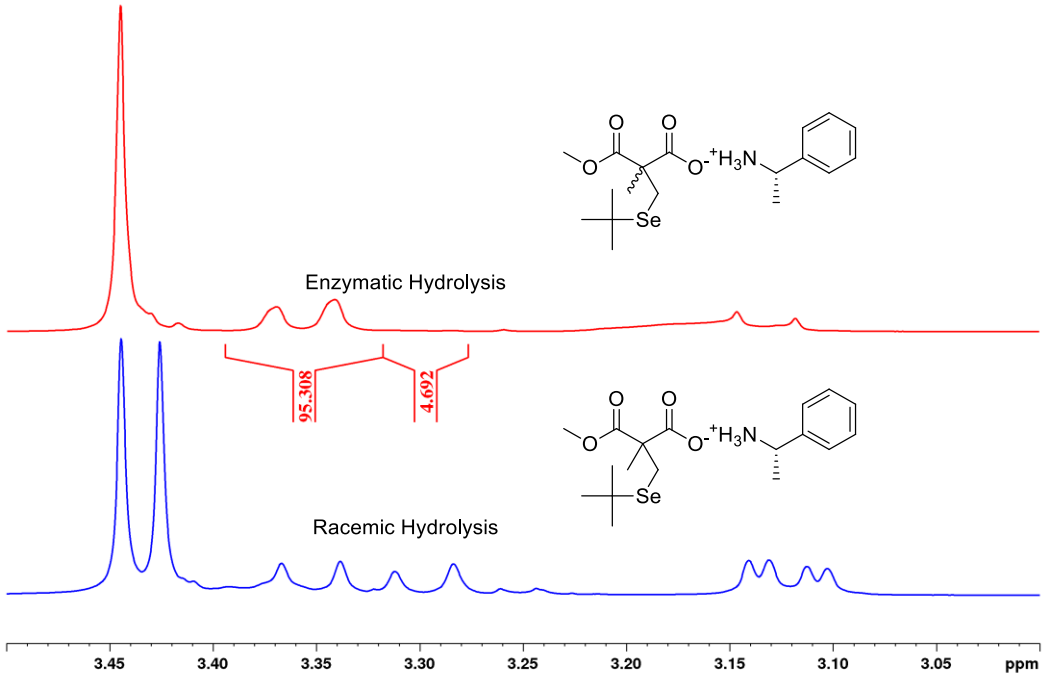

Scheme 2.18 *The Synthesis of **14** and **15** and the %EE Determination by ^{1}H NMR*

From these results, it was decided that performing the hydrolyses on the methyl diester could potentially allow for better resolution. A seleno-alkylation was implemented on dimethyl methylmalonate producing the selenylated diester **14**. Using identical procedures, enzymatic and racemic hydrolyses were carried out on **14** to produce the half-esters **15a** and **15b** (**Scheme 2.17**). Using (*S*)-α-methylbenzylamine in equimolar amounts to create the diastereomeric salts, NMR samples were made and analyzed by ^{1}H NMR. The peaks from the methyl ester proton signals were not resolved enough to use their integrations, but the methylene proton signals were, and it was determined that the PLE hydrolysis gave 88% ee (**Scheme 2.18**).

With the enantiomeric excess ascertained, the absolute configuration around the α-carbon was unknown. Based on comparisons to the ^{1}H NMR spectra of **15** (**Scheme 2.14)** with the spectra sulfur analogue of known configuration[84] the methoxy proton signals for both molecules share the same enantiomeric intensity patterns. The optical rotation of **15a** also shares the same direction of rotation with its sulfur analogue (-2.1° at c = 1.07 and -1.0° at c = 1.00 respectively), which suggests the absolute configuration of **15a** is (*R*) matching the sulfur analogue. This hypothesis was also supported by past literature which states that PLE does prefer to create the (*R*)-enantiomer from a diester.[60-62, 84] The determination of the absolute stereochemistry of the α-carbon will be discussed in Chapter III.

2.4 Curtius Rearrangement to Introduce Amine Functionality and Acid Hydrolysis of the Methyl Ester

Now that chirality has been introduced, amine functionality needs to be incorporated. With a carboxylic acid present, it can be easily converted to an acyl azide, and then, through a thermally induced Curtius Rearrangement an isocyanate can be formed. Once the isocyanate is formed, an alcohol can be added to create a carbamate. Depending on the alcohol added, the desired carbamate can be formed to allow for orthogonal deprotections; if *tert*-butyl alcohol is used, a Boc group is created, which is resistant to basic conditions, or if 9-fluorenylmethanol (FmocOH) is used, an Fmoc group is created, which is resistant to acidic conditions. To increase the reactivity of the alcohol towards the isocyanate, a Lewis acid is needed to facilitate the reaction, and titanium reagents normally are used, such as titanium isopropoxide ($Ti(O^iPr)_4$).

Creating the acyl azide and performing the Curtius Rearrangement efficiently converted to the isocyanate based on IR spectroscopy by monitoring the isocyanate stretch formation at 2252 cm^{-1}, however the alcohol addition was low yielding on the Fmoc product **16** (**Scheme 2.19**). Analysis with ^1H NMR revealed that the isopropoxide moiety from $Ti(O^iPr)_4$ was adding to the isocyanate instead of FmocOH, which created an isopropyl carbamate **17** instead of the desired Fmoc carbamate. To avoid this side reaction, hydrolyzing the isocyanate with sodium bicarbonate to an amine **18** was attempted, however based on MS, this led to multiple chain lengths of oligopeptides (**19**) to form. Another titanium-based Lewis acid was considered, titanium *tert*-butoxide ($Ti(O^tBu)_4$). Literature suggested that $Ti(O^tBu)_4$ is more resistant to hydrolysis than $Ti(O^iPr)_4$, and if hydrolysis does occur, *tert*-butoxide will be non-nucleophilic.[85]

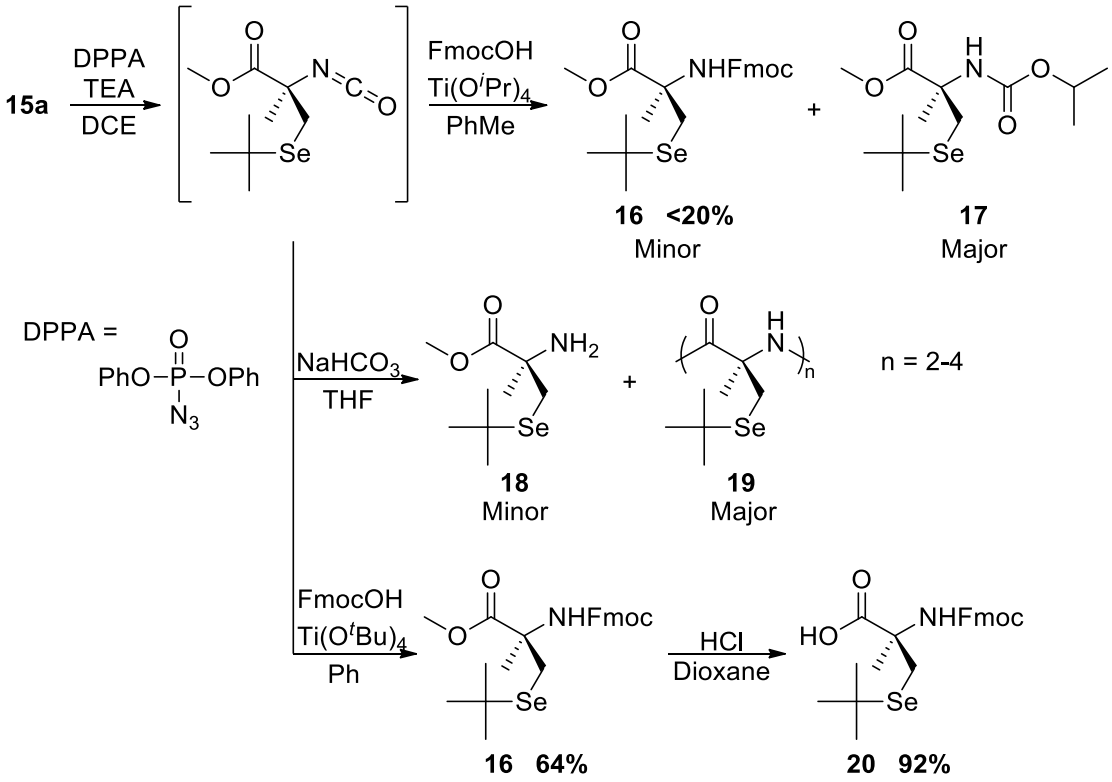

Scheme 2.19 *The Transformation of the Half-Ester **15a** to an Fmoc Protected Amine*

Yields of the unwanted products, **17** and **19**, were not calculated.

Another benefit to using Ti(O^{t}Bu)$_4$ is that it possesses dual Lewis acid – Lewis base character, which aids in the reaction. The titanium portion of the molecule would have acidic character, being attacked by the isocyanate oxygen, and in turn, activating the isocyanate carbon, and the *tert*-butoxide would have basic character deprotonating the oxonium cation from the alcohol addition. Using this new Lewis acid did allow for a cleaner reaction, which produced moderate yields of **16**.

With the successful Fmoc protection complete, the final step in the synthesis is to perform a hydrolysis on the methyl ester. The hydrolysis needs to be completed in acidic conditions due to Fmoc being base-labile. Using freshly made 5 M HCl in dioxane, the

methyl ester on **16** was successfully hydrolyzed forming a carboxylic acid **20** in high yields. The acid catalyzed ring opening of dioxane to form low molecular weight poly(ethylene glycol) was seen, but this byproduct was easily removed by aqueous washes.

2.5 Incorporation into Peptides

Once **20** was synthesized two peptides were synthesized in the Hondal lab with the sequence of H-XXX-Gly-Thr-Thr-Val-Arg-Asp-Tyr-Thr-Gln-OH. At the XXX position one peptide contained natural Sec, and the other contained α-MeSec created from **20**. This sequence was chosen because it corresponds to a sequence in the active site of GPx.[12] The anti-oxidative capabilities of these peptides were measured through a coupled glutathione reductase assay (**Scheme 2.20**) using the methods developed by Wilson *et al*.[15]

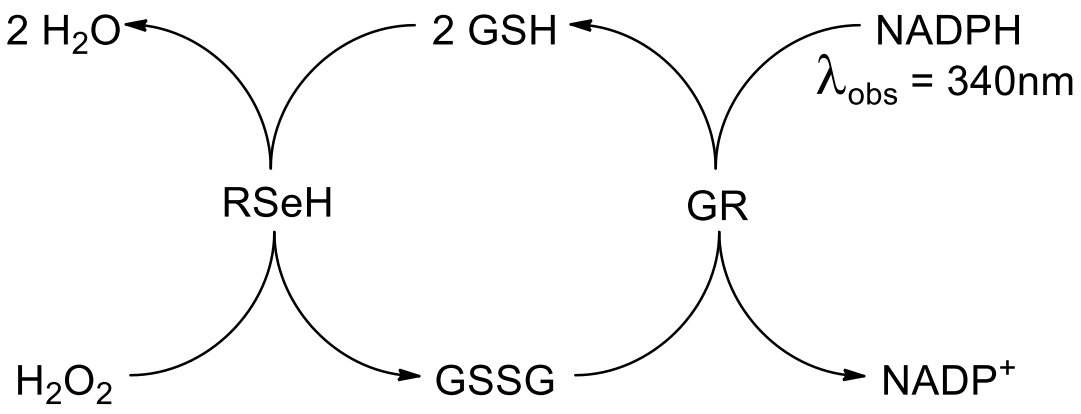

Scheme 2.20 *Coupled Glutathione Reductase Assay*

Without any hydrogen peroxide, both peptides had near zero activity, and once hydrogen peroxide was added the peptide containing α-MeSec did have a slight kinetic advantage

over the native peptide (**Figure 2.1**). The significant difference between the two peptides is seen in their stability. Their stability was tested by incubating each peptide in oxygenated buffer and measuring their normalized activity. It was discovered that after 96 hours, the peptide containing Sec lost 93% of its activity, while the peptide containing α-MeSec only lost 35% of its activity. Additionally, there was visible red precipitate in the sample of the Sec peptide from deselenylation of the over-oxidized peptide.

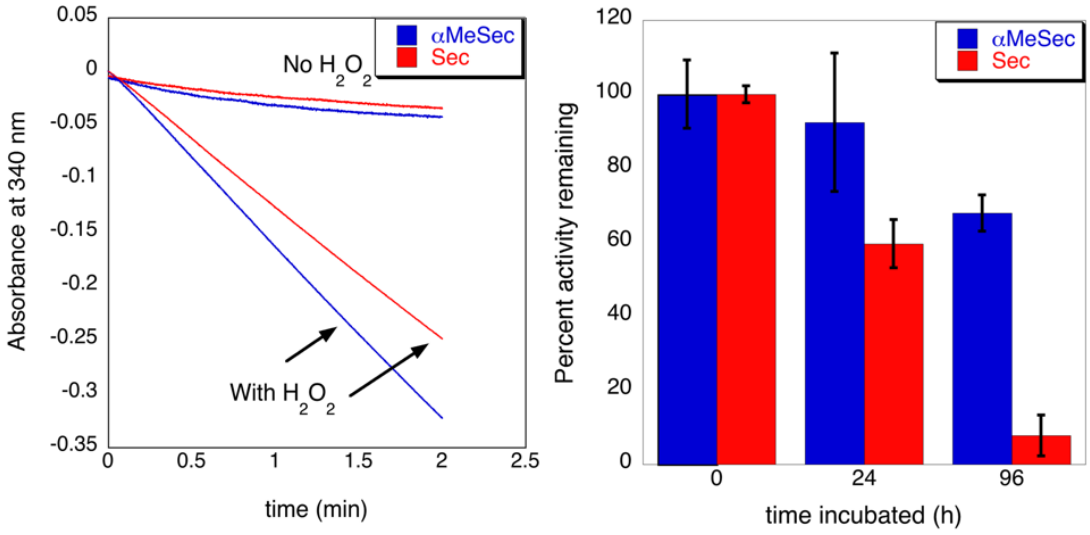

Figure 2.1 *Enzymatic Activity and Stability Assays of the Seleno-Peptides*

Obtained from Wehrle, R. J.; Ste Marie, E. J.; Hondal, R. J.; Masterson, D. S., Synthesis of alpha-methyl selenocysteine and its utilization as a glutathione peroxidase mimic. *J. Pept. Sci.* **2019**, e3173

2.6 Other α-MeSec Analogues Synthesized

With the synthesis of (*R*)-Fmoc-α-MeSec(^{t}Bu)-OH (**20**), syntheses of other analogues were attempted. One very important compound that was synthesized was the (*S*)-enantiomer of **20**. With both enantiomers of α-MeCys occurring naturally in several biomolecules,[84] studying how the opposite enantiomer of α-MeSec behaves in biological

systems is a topic of interest. The synthesis for this molecule essentially followed the same procedure, except of an extra esterification and a hydrolysis step after the enzymatic hydrolysis, as well as a variation of the acid hydrolysis at the end of the synthesis to afford the opposite enantiomer **24** (**Scheme 2.21**).

From a similar synthetic pathway to the α-methyl amino acids, a $\beta^{2,2}$-amino acid analogue was also able to be synthesized (**Scheme 2.22**). These molecules are important to synthesize because the quaternary α-carbon can cause problems with peptide coupling from steric hindrance. The methylene group adds distance from the steric congestion of the α-carbon which aids in peptide coupling. Starting from **15a**, an Arndt-Eistert Homologation, which contained a photolytic Wolff Rearrangement, was used to add a methylene group between the α-carbon and the carboxylic acid to form **26**.

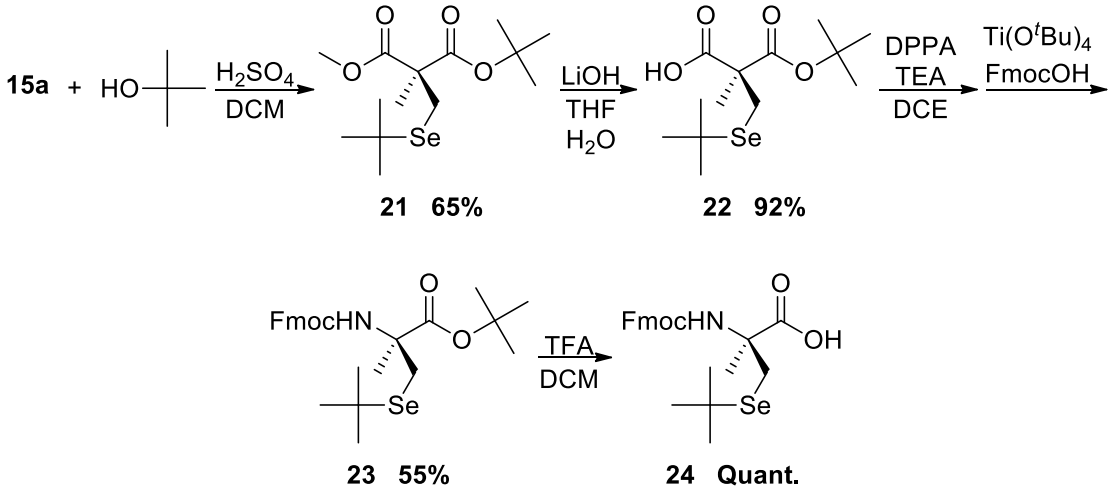

Scheme 2.21 *Synthesis of the (S)-Enantiomer from the PLE product*

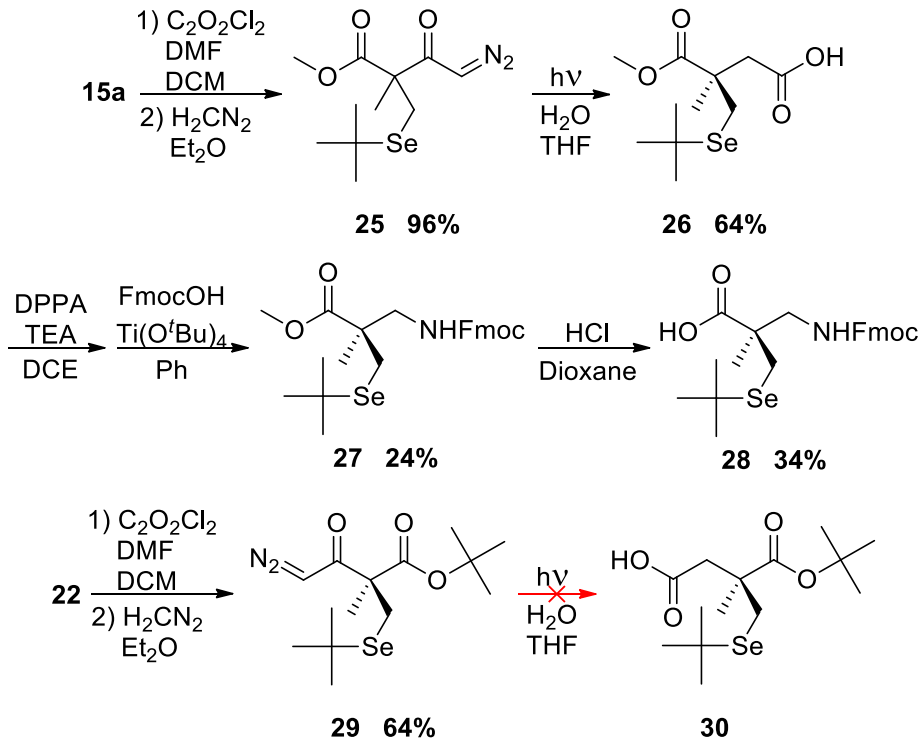

Scheme 2.22 *β[2,2]-Amino Acid Syntheses*

The acid-base workup of **26** produced a large amount of red precipitate, which suggests that elemental selenium is being liberated from the substrate from a degradation pathway as eliminated selenium does take on the appearance of a fine red precipitate. Allowing **26** sit for extended periods of time also formed red precipitate, which suggests that this degradation could be from oxidation and elimination of selenium. Recent literature[86] has found through calculations that malonic acid has the ability to self-catalyze tautomerization through dimerization. While **26** and **30** are not malonates, tautomerization is hypothetically possible forming a vinyl diol. If this vinyl diol can form, then a reaction akin to selenoxide elimination to form an α,β-unsaturated carbonyl can form, eliminating the selenium from the molecule, forming a fumaric acid-like

structure (**Scheme 2.23**). The eliminated organo-selenoxide can further degrade back to elemental selenium. This pathway could explain why **26** and **30** if left standing, does form a red precipitate.

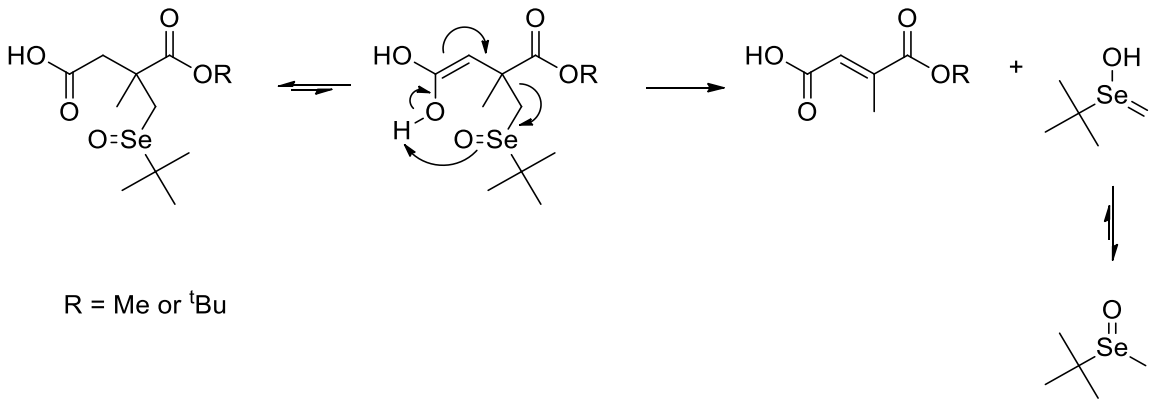

Scheme 2.23 *Hypothesized Degradation Pathway for β-Amino Acids*

From this point, the remaining **26** was converted to an acyl azide, and with a Curtius Rearrangement and an alcohol addition, an Fmoc protected amine **27** was synthesized in low yield. Once as the carbamate, the degradation seemed to not be as prevalent as the carboxylic acid once **27** was formed. The methyl ester was then hydrolyzed with 5M HCl in dioxane to form the carboxylic acid **28**.

Work towards the enantiomer of **28** was also done. Starting from **22**, the carboxylic acid was converted to a diazoketone, followed by a Wolff Rearrangement to form **30**, however upon sitting red precipitate formed just as what happened with **26**. From this degradation process, not enough material was able to be isolated.

An efficient route to synthesize an enantio-enriched sample of α-MeSec has been completed. This pathway has also been utilized to synthesis of the enantiomer of α-MeSec as well. The (*R*)-enantiomer was successfully integrated into a peptide and has

shown improved performance when compared to the native peptide. The (*S*)-$\beta^{2,2}$-amino acid was successfully synthesized but was found to have problems with degradation during key steps of the synthesis.

2.7 Experimental

2.7.1 Materials

Solvents for synthesis including *N*,*N*-dimethylformamide (DMF) and dichloromethane (DCM) were purchased from Fisher Scientific (Fair lawn, NJ) or Acros Organics (Morris Plains, New Jersey). Diphenylphosphoryl azide (DPPA) was purchased from TCI America (Portland, OR). 9-fluorenemethanol was purchased from Chempep Inc. (Miami, Fl). Titanium (IV) *tert*-butoxide was purchased from EMD Millipore. Silica gel (230-400 mesh) for purifications was purchased from Silicycle (Quebec City, QC, Canada). Deuterated solvents were purchased from Cambridge Isotope Laboratories (Andover, MA). All other chemicals were purchased from Sigma-Aldrich (Milwaukee, WI), Fisher Scientific (Waltham, MA), or ACROS Organics (Pittsburgh, PA). Hydrogenations were performed using a motorized Parr apparatus. High resolution mass spectral data on all synthesized compounds were obtained from positive electrospray ionization on a Bruker 12 Tesla APEX -Qe FTICR-MS with an Apollo II ion source (Old Dominion, Norfolk, VA) and were either analyzed as solutions in tetrahydrofuran (THF) or THF/Methanol. NMR spectra were acquired by a 400 MHz Bruker spectrometer. ^{1}H and ^{13}C chemical shifts (δ) were reported as downfield from tetramethylsilane. Both ^{13}C and ^{77}Se NMR spectra were ^{1}H decoupled. IR spectra were obtained from a Nicolet Nexus 470 FT-IR spectrometer with a Smart Orbit Thermo™ diamond plate ATR

attachment and samples were acquired as a solution from $CDCl_3$ or as neat samples. Optical rotation data were acquired by a Rudolph Research Analytical Autopol IV Automatic Polarimeter at 589 nm with a 100 mm quartz cell at ambient temperature.

2.7.2 Synthesis of (*S*)-N-Boc-α-MeSer(Bn)-OEt (2)

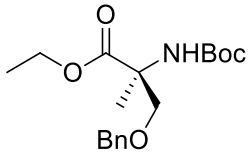

A 250 mL round bottom flask fitted with a reflux condenser was charged with a stir bar, **1** (4.19 g 15.7 mmol), toluene (50 mL), and triethylamine (TEA) (2.45 mL, 17.6 mmol). The reaction mixture was stirred for 5 minutes then diphenylphophoryl azide (DPPA) (3.60 mL, 16.7 mmol) was added and the solution was stirred at room temperature for 30 minutes and was then heated to reflux for 16 hours. The solution was then cooled to room temperature and *tert*-butanol (7.61 mL, 79.6 mmol) and copper (I) chloride (54.7 mg, 0.550 mmol) were added. The solvent was then heated to reflux for an additional 24 hours. After cooling to room temperature, the reaction was diluted with saturated $NaHCO_3$ (100 mL). The mixture was then extracted with diethyl ether (3 × 50 mL). The organic phases were pooled, dried over $MgSO_4$, filtered, and concentrated *in vacuo*. The crude oil was purified by gradient flash chromatography and eluted with hexanes/ethyl acetate (2:1 to 1:1). The product rich fractions (R_f = 0.60 1:1 hexanes/ethyl acetate) were pooled and concentrated *in vacuo* to afford 2.57 g (7.62 mmol, 48%) of a yellow oil. ^{1}H NMR (400 MHz, $CDCl_3$) δ 5.34 (br s, 1H), 4.56 (d, $^2J_{H\text{-}H}$ = 12.3 Hz, 1H), 4.50 (d, $^2J_{H\text{-}H}$ = 12.3 Hz, 1H), 4.20 (q, $^3J_{H\text{-}H}$ = 7.1 Hz, 2H), 3.76 (br d, $^2J_{H\text{-}H}$ = 9.0 Hz,

1H), 3.70 (br d, $^{2}J_{H\text{-}H}$ = 9.0 Hz, 1H), 1.52 (s, 3H), 1.44 (s, 9H), 1.25 (t, $^{3}J_{H\text{-}H}$ = 7.1 Hz, 3H).

2.7.3 Synthesis of (*S*)-N-Boc-α-MeSer-OEt (3)

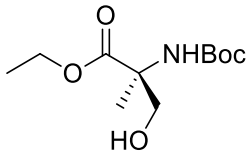

A 500 mL pressure tube was charged with **2** (2.06 g, 6.12 mmol), ethanol (50 mL) and 10% Pd/C (212 mg, 0.200 mmol) as a suspension in ethanol (20 mL). The atmosphere was exchanged for hydrogen and the reaction was agitated for 24 hours under 25 psi of H_2 at room temperature. The pressure was released, and the solution was filtered through Celite. The solvent was removed *in vacuo* affording 1.49 g (6.03 mmol, 98%) of a light-yellow oil. ^{1}H NMR (400 MHz, $CDCl_3$) δ 7.30 (m, 5H), 5.46 (br s, 1H), 4.22 (m, 2H), 3.99 (br d, $^{2}J_{H\text{-}H}$ = 11.0 Hz, 1H), 3.77 (br d, $^{2}J_{H\text{-}H}$ = 11.0 Hz, 1H), 1.47 (s, 3H), 1.44 (s, 9H), 1.29 (t, $^{3}J_{H\text{-}H}$ = 7.0 Hz, 3H).

2.7.4 Synthesis of (*S*)-N-Boc-α-MeSer(OTs)-OEt (4a)

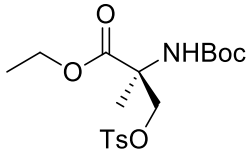

A 10 mL round bottom flask was charged with a stir bar, **3** (212 mg, 0.856 mmol), dichloromethane (DCM) (2 mL), and TEA (240 μL, 1.7 mmol). After cooling in an ice bath tosyl chloride (249 mg, 1.53 mmol) was added and the reaction was slowly warmed to room temperature. After stirring for 24 hours the solvent was removed *in vacuo* leaving a red oily solid. The crude solid was purified by gradient flash chromatography

and eluted with hexanes/ethyl acetate (4:1 to 1:1). The product rich fractions (R_f = 0.43 in 1:1 hexanes/ethyl acetate) were pooled and concentrated *in vacuo* to afford 226 mg (0.563 mmol, 66%) of a colorless solid. IR ($CDCl_3$, cm^{-1}) 3390, 2979, 2933, 1709, 1598; ^1H NMR (400 MHz, $CDCl_3$) δ 7.77 (d, $^3J_{H\text{-}H}$ = 8.0 Hz, 2H), 7.33 (d, $^3J_{H\text{-}H}$ = 8.0 Hz, 2H), 5.23 (br s, 1H), 4.42 (br d, $^2J_{H\text{-}H}$ = 9.3 Hz, 1H), 4.38 (d, $^2J_{H\text{-}H}$ = 9.5 Hz, 1H), 4.19 (m, 2H), 2.43 (s, 3H), 1.47 (s, 3H), 1.38 (s, 9H), 1.25 (t, $^3J_{H\text{-}H}$ = 7.4 Hz, 3H); ^{13}C NMR (100 MHz, $CDCl_3$) δ 171.4, 154.0, 144.9, 132.7, 129.9, 128.0, 80.2, 70.4, 62.1, 58.5, 28.2, 21.6, 20.6, 14.0; LRMS (ESI^+) Calcd for $C_{18}H_{27}NO_7S$ $[M + Na]^+$ 424.14 found 424.18.

2.7.5 Synthesis of (*S*)-N-Boc-α-MeSer(OMs)-OEt (4b)

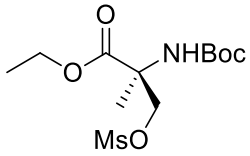

A 25 mL round bottom flask was charged with a stir bar, **3** (97 mg, 0.390 mmol), DCM (1.5 mL), and TEA (110 μL, 0.780 mmol). Once cooled in an ice bath, mesyl chloride (45 μL, 0.590 mmol) was added and the reaction was slowly warmed to room temperature. After stirring for 24 hours the solvent was removed *in vacuo* leaving a solid. The crude solid was dissolved in DCM (1 mL) and washed with water (1 mL), saturated $NaHCO_3$ (1 mL), and water (1 mL). The organic phase was filtered through a $MgSO_4$ plug and concentrated *in vacuo* to afford 89 mg (0.274 mmol, 70 %) of a colorless solid. IR ($CDCl_3$, cm^{-1}) 3378, 2974, 2939, 1704; ^1H NMR (400 MHz, $CDCl_3$) δ 5.37 (br s, 1H), 4.71 (br d, $^2J_{H\text{-}H}$ = 9.5 Hz, 1H), 4.59 (d, $^2J_{H\text{-}H}$ = 10.0 Hz, 1H), 4.26 (m, 2H), 3.01 (s, 3H), 1.53 (s, 3H), 1.44 (s, 9H), 1.30 (t, $^3J_{H\text{-}H}$ = 7.1 Hz, 3H); ^{13}C NMR (100 MHz, $CDCl_3$) δ

171.4, 154.2, 80.3, 70.3, 62.3, 58.6, 37.0, 28.2, 20.6, 14.0; LRMS (ESI^+) Calcd for $C_{12}H_{23}NO_7S$ $[M + Na]^+$ 348.11 found 348.19.

2.7.6 Synthesis of 4-Methoxybenzyl Diselenide (5)

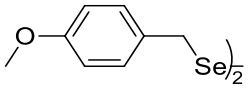

A 10 mL, dried round bottom flask fitted with a reflux condenser and a nitrogen atmosphere was charged with a stir bar, selenium (233 mg, 2.95 mmol) and tetrahydrofuran (THF) (1.5 mL). This suspension was stirred and $LiEt_3BH$ (3.0 mL, 3.0 mmol) was added and the solution was heated to solvent reflux for 1 hour. In another dry, 25 mL round bottom flask was added 4-methoxybenzyl chloride in THF (1.5 mL). Both flasks were cooled to -78 °C and the contents of the first flask were cannulated to the second flask. The reaction was slowly warmed to room temperature and stirred for 16 hours. The reaction was then filtered, and the filtrate was concentrated *in vacuo*. The crude oil was purified by recrystallization from ethanol to afford 247 mg (0.617 mmol, 21%) of a yellow solid. ^1H NMR (400 MHz, $CDCl_3$) δ 7.16 (d, $^3J_{H\text{-}H}$ = 8.6 Hz, 2H), 6.83 (d, $^3J_{H\text{-}H}$ = 8.7 Hz, 2H), 3.84 (s, 2H, Se satellites $^2J_{Se\text{-}H}$ = 7.2 Hz), 3.79 (s, 3H).

2.7.7 Synthesis of *tert*-butyl Diselenide (6)

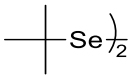

A flame dried 250 mL round bottom flask was charged with a stir bar, THF (100 mL), and *tert*-butylmagnesium chloride (48.0 mL, 96.0 mmol). The solution was chilled in an ice bath and to it was added selenium (5.77g, 73.1 mmol) in several small portions. The reaction mixture was stirred at room temperature for 30 minutes and was then quenched with concentrated HCl (8.0 mL, 97 mmol). The reaction mixture was diluted

with diethyl ether (100 mL) and washed with water (100 mL). The organic phase was extracted with 1M NaOH (3 × 100 mL). The aqueous phases were pooled and NaH_2BO_4 (9.0 g, 90 mmol) was added which slowly produced effervescence. To this solution was added hexanes (30 mL) and this mixture was stirred until effervescence ceased. The organic phase was decanted, and the aqueous phase was extracted with hexanes (3 × 30 mL). The resulting organic phases were pooled, dried over $MgSO_4$, filtered, and concentrated *in vacuo*. The crude product was distilled under reduced pressure collecting fractions that distilled above room temperature, yielding 8.13 g (29.9 mmol, 82%) of a yellow-orange liquid. ^{1}H NMR (400 MHz, $CDCl_3$) δ 1.47 (s, 18H, Se satellites $^3J_{Se\text{-}H}$ = 5.5 Hz); ^{77}Se NMR (76 MHz, $CDCl_3$) δ 487.8.

2.7.8 Synthesis of (*R*)-N-Boc-α-MeSec(Mob)-OEt (9)

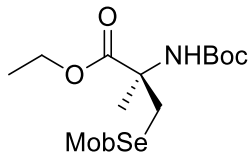

A flame dried, 25 mL round bottom flask fitted with a reflux condenser and a nitrogen atmosphere was charged with a stir bar, selenium (38 mg, 0.480 mmol), THF (2 mL), and $LiEt_3BH$ (500 μL, 0.500 mmol) which was heated to solvent reflux for 1 hour. The reaction was cooled to room temperature and **4a** (140 mg, 0.350 mmol) dissolved in THF (2 mL) was added. The reaction was heated to solvent reflux for an additional 15 hours after which the solution was filtered and concentrated *in vacuo*. The crude yellow oil (52 mg) was added to a 5 mL conical vial that was charged with a spin vane and methanol (2 mL). To this solution was added sodium borohydride (6 mg, 0.160 mmol) which caused effervescence and turned the solution from yellow to colorless. To this

solution was then added 4-methoxybenzyl chloride (23 μL, 0.170 mmol). The reaction mixture was stirred at 55 °C for 20 hours. The reaction was cooled to room temperature and diluted with diethyl ether (2 mL) and washed with water (3 × 2 mL). The aqueous phases were extracted with diethyl ether (2 × 1 mL). The organic phases were pooled, dried over $MgSO_4$, filtered, and concentrated *in vacuo*. The crude residue was dissolved in 10:1 hexanes/ethyl acetate and loaded onto the Chromatotron and eluted with hexanes/ethyl acetate (10:1 to 8:1). Product rich fractions (R_f = 0.06 in 10:1 hexanes/ethyl acetate) were pooled and concentrated *in vacuo* to afford 3.1 mg (.007 mmol, 1.4%). ^{1}H NMR (400 MHz, $CDCl_3$) δ 7.21 (d, $^3J_{H-H}$ = 8.6 Hz, 2H), 6.82 (d, $^3J_{H-H}$ = 8.7 Hz, 2H), 5.51 (br s, 1H), 4.20 (q, $^3J_{H-H}$ = 7.1 Hz, 2H), 3.79 (s, 3H), 3.77 (d, $^2J_{H-H}$ = 11.5 Hz, 1H), 3.74 (d, $^2J_{H-H}$ = 11.5 Hz, 1H), 3.35 (br d, $^2J_{H-H}$ = 11.5 Hz, 1H), 3.11 (d, $^2J_{H-H}$ = 13.1 Hz, 1H), 1.44 (s, 3H), 1.26 (t, $^3J_{H-H}$ = 7.2 Hz, 3H); LRMS (ESI^+) Calcd for $C_{19}H_{25}NO_5Se$ $[M + Na]^+$ 454.11 found 454.15.

2.7.9 Synthesis of *tert*-butyl Chloromethyl Selenide (10)

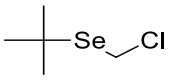

A flame dried, 250 mL, 3-necked round bottom flask with a nitrogen atmosphere was charged with a stir bar, **6** (7.52 g, 27.6 mmol), and dry DCM (75 mL 1.2 mol). The reaction mixture was cooled with an ice bath and Red-Al (18 mL, 55.4 mmol) was added dropwise until the solution turned colorless and turbid and effervescence ceased. The reaction mixture was stirred for an additional 30 minutes and the solution was diluted with diethyl ether (150 mL) and washed with a chilled 10% Rochelle salt solution (3 × 100 mL). The organic phase was dried over $MgSO_4$ and filtered, and the solvent was

removed *in vacuo* to afford 46.2 mmol (84%, determined by NMR) of a colorless oil, which was carried on directly to the following reaction. ^{1}H NMR (400 MHz, $CDCl_3$) δ 4.87 (s, 2H), 1.55 (s, 9H, Se satellites $^{3}J_{Se\text{-}H}$ = 5.6 Hz); ^{77}Se NMR (76 MHz, $CDCl_3$) δ 518.8.

2.7.10 Synthesis of Diethyl ((*tert*-butylselanyl)methyl)methylmalonate (12)

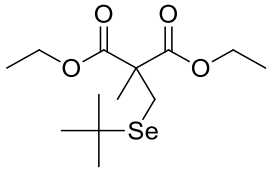

A flame dried, 250 mL, 3-necked round bottom flask with a nitrogen atmosphere was charged with a stir bar, sodium hydride (60% dispersion in mineral oil) (1.53 g, 38.3 mmol), and THF (25 mL). To this suspension was added diethyl methylmalonate (5.30 mL, 31.1 mmol) in THF (25 mL) producing effervescence and heat. This solution was stirred at room temperature for one hour. Another flame dried 100 mL round bottom flask with a nitrogen atmosphere was charged with a stir bar, **6** (4.37 g, 16.1 mmol) in THF (10 mL), and $LiEt_3BH$ (35 mL, 35 mmol). This solution was then cannulated to a flame dried, 100 mL round bottom flask containing a stir bar and DCM (10.0 mL, 156 mmol) and was left to react for 30 minutes at room temperature. The solvent was removed *in vacuo* and the residue was cannulated into the round bottom flask containing the enolate anion. A reflux condenser was fitted to the round bottom flask and the reaction mixture was brought to solvent reflux for 16.5 hours. The reaction mixture was cooled to room temperature and stirred for an additional 5 hours. The reaction mixture was diluted with diethyl ether (50 mL) and washed with water (4 × 50 mL). The aqueous phase was extracted with diethyl ether (2 × 20 mL). All organic phases were pooled, dried over

$MgSO_4$, filtered, and concentrated *in vacuo*. The crude liquid was purified by gradient flash chromatography and eluted with hexanes/ethyl acetate (12:1 to 10:1 to 6:1). The product rich fractions (R_f = 0.57 in 4:1 hexanes/ethyl acetate) were pooled and concentrated *in vacuo* to afford 2.65 g (8.20 mmol, 26%) of a colorless liquid. IR (Neat, cm^{-1}) 2978, 2939, 2893, 1729; ^{1}H NMR (400 MHz, $CDCl_3$) δ 4.19 (q, $^3J_{H\text{-}H}$ = 7.1 Hz, 4H), 3.05 (s, 2H), 1.49 (s, 3H), 1.43 (s, 9H, Se satellites $^3J_{Se\text{-}H}$ = 5.4 Hz), 1.26 (t, $^3J_{H\text{-}H}$ = 7.1 Hz, 6H); ^{13}C NMR (100 MHz, $CDCl_3$) δ 171.3, 61.5, 54.4 (Se satellites $^2J_{Se\text{-}C}$ = 4.6 Hz), 39.1 (Se satellites $^1J_{Se\text{-}C}$ = 29.8 Hz), 32.2 (Se satellites $^2J_{Se\text{-}C}$ = 6.6 Hz), 26.8 (Se satellites $^1J_{Se\text{-}C}$ = 36.9 Hz), 21.0, 14.0; ^{77}Se NMR (76 MHz, $CDCl_3$) δ 340.3; LRMS (ESI^+) Calcd for $C_{13}H_{24}O_4Se$ $[M + Na]^+$ 347.07 found 347.17.

2.7.11 Synthesis of 2-((*tert*-butylselanyl)methyl)-3-ethoxy-2-methyl-3-oxopropanoic acid (13)

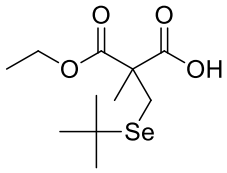

2.7.11.1 Enzymatic Hydrolysis (a)

A 50 mL beaker was charged with a stir bar, **12** (91 mg, 0.280 mmol), 7.6 pH phosphate buffer (20 mL), and crude porcine liver esterase (2 mg, 18 units/mg). The reaction was stirred vigorously with a constant pH = 7.4 by titrating 1M NaOH into the reaction. The reaction was complete after stirring for 17 hours. The solution pH was raised to 9 with the addition of 1M NaOH and was washed with DCM (20 mL). The aqueous phase was reacidified to pH = 3 with 1M HCl and extracted with diethyl ether

(20 mL). The organic phase was dried over $MgSO_4$, filtered, and concentrated *in vacuo* to afford 40 mg (0.135 mmol, 49%) of a slightly brown tinged oil. IR (Neat, cm^{-1}) 2972, 2957, 2938, 2892, 1709; ^{1}H NMR (400 MHz, $CDCl_3$) δ 6.80 (br s, 1H), 4.23 (q, $^3J_{H\text{-}H}$ = 7.1 Hz, 2H), 3.10 (d, $^2J_{H\text{-}H}$ = 11.6 Hz, 1H), 3.04 (d, $^2J_{H\text{-}H}$ = 11.6 Hz, 1H), 1.55 (s, 3H),1.44 (s, 9H, Se satellites $^3J_{Se\text{-}H}$ = 5.5 Hz), 1.30 (t, $^3J_{H\text{-}H}$ = 7.0, 3H); ^{13}C NMR (100 MHz, $CDCl_3$) δ 177.0, 171.2, 62.0, 54.5, 39.5, 32.2 (Se satellites $^2J_{Se\text{-}C}$ = 6.6 Hz), 26.6, 21.1, 14.0; ^{77}Se NMR (76 MHz, CDCl3) δ 343.9; LRMS (ESI^+) Calcd for $C_{11}H_{20}O_4Se$ $[M - {}^tBu]^+$ 238.98 found 238.92; $[\alpha]_D^{23} = -0.8°$ (c = 4.4, $CHCl_3$).

2.7.11.2 Racemic Hydrolysis (b)

A 50 mL round bottom flask was charged with a stir bar, **12** (514 mg, 1.59 mmol), THF (10 mL), lithium hydroxide (44 mg, 1.9 mmol), and water (10 mL). The reaction mixture was stirred at room temperature for 19 hours and 1M HCl was added to lower the pH to 3. The solution was diluted with diethyl ether (10 mL) and washed with 0.1M HCl (3 × 10 mL). The aqueous phases were extracted with diethyl ether (10 mL). The organic phases were pooled, dried over $MgSO_4$, filtered, and concentrated *in vacuo* to afford 385 mg (1.30 mmol, 82%) of a colorless liquid. ^{1}H NMR (400 MHz, $CDCl_3$) δ 9.98 (br s, 1H), 4.23 (q, $^3J_{H\text{-}H}$ = 7.1 Hz, 2H), 3.10 (d, $^2J_{H\text{-}H}$ = 11.6 Hz, 1H), 3.04 (d, $^2J_{H\text{-}H}$ = 11.6 Hz, 1H), 1.55 (s, 3H),1.44 (s, 9H, Se satellites $^3J_{Se\text{-}H}$ = 5.5 Hz), 1.30 (t, $^3J_{H\text{-}H}$ = 7.0, 3H); ^{77}Se NMR (76 MHz, CDCl3) δ 342.9

2.7.12 Synthesis of Dimethyl ((*tert*-butylselanyl)methyl)methylmalonate (14)

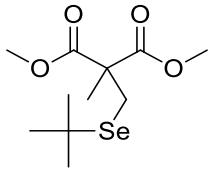

A flame dried, 250 mL, 3-necked round bottom flask with a nitrogen atmosphere was charged with a stir bar and sodium hydride (60% dispersion in mineral oil) (1.61 g, 40.3 mmol). The sodium hydride was washed with two portions of pentane. A suspension was created with the addition of THF (60 mL). The suspension was cooled with an ice bath and dimethyl methylmalonate (4.84 g, 33.1 mmol) was added dropwise, which produced effervescence. The reaction mixture was stirred at room temperature for 90 minutes and **10** (46.1 mmol) was added. The reaction mixture was stirring at room temperature for 2 hours and then heated to solvent reflux for 60 hours. The reaction mixture was cooled to room temperature, filtered through a bed of Celite, and concentrated *in vacuo*. The residue was reconstituted with diethyl ether (100 mL) and washed with water (5 × 100 mL). The organic phase was dried over $MgSO_4$, filtered, and concentrated *in vacuo*. The crude oil was purified by gradient flash chromatography and eluted with hexanes/ethyl acetate (8:1 to 4:1). The product rich fractions (R_f = 0.50 in 4:1 hexanes/ethyl acetate) were pooled and concentrated *in vacuo* to afford 7.81 g (26.5 mmol, 80%) of a colorless oil. IR ($CDCl_3$, cm^{-1}) 2953, 2891, 2861, 1731; ^1H NMR (400 MHz, $CDCl_3$) δ 3.74 (s, 6H), 3.05 (s, 2H), 1.51 (s, 3H), 1.43 (s, 9H, Se satellites $^3J_{Se-H}$ = 5.5 Hz); ^{13}C NMR (100 MHz, $CDCl_3$) δ 171.7, 54.5 (Se satellites $^2J_{Se-C}$ = 4.8 Hz), 52.7, 39.3 (Se satellites $^1J_{Se-C}$ = 29.0 Hz), 32.2 (Se satellites $^2J_{Se-C}$ = 6.6 Hz), 26.8 (Se satellites $^1J_{Se-C}$ = 37.0 Hz), 21.0; ^{77}Se NMR (76 MHz, $CDCl_3$) δ 342.6; HRMS (ESI^+) Calcd for $C_{11}H_{20}O_4Se$ $[M + Na]^+$ 319.0419 found 319.0420.

2.7.13 Synthesis of 2-((*tert*-butylselanyl)methyl)-3-methoxy-2-methyl-3-oxopropanoic acid (15)

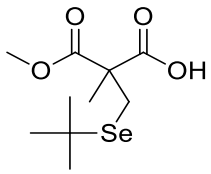

2.7.13.1 Enzymatic Hydrolysis (a)

A 100 mL beaker was charged with a stir bar, **14** (3.24 g, 11.0 mmol), 7.6 pH phosphate buffer (40 mL), and crude porcine liver esterase (52 mg, 18 units/mg). The reaction was stirred vigorously with a constant pH = 7.4 by titrating 1M NaOH into the reaction. The reaction was complete after stirring for 4 hours. The solution pH was raised to 9 with the addition of 1M NaOH and was washed with diethyl ether (60 mL). The aqueous phase was reacidified to pH = 3 with 4M HCl and extracted with DCM (3 × 60 mL). The organic phase was filtered through a bed of Celite, dried over $MgSO_4$, and concentrated *in vacuo* to afford 3.03 g (10.8 mmol, 98%, ee = 88%) of a slightly brown tinged oil. IR ($CDCl_3$, cm^{-1}) 2955, 2889, 1709, 1636; ^1H NMR (400 MHz, $CDCl_3$) δ 9.26 (br s, 1H), 3.77 (s, 3H), 3.09 (d, $^2J_{H\text{-}H}$ = 11.6 Hz, 1H), 3.04 (d, $^2J_{H\text{-}H}$ = 11.6 Hz, 1H), 1.54 (s, 3H),1.43 (s, 9H, Se satellites $^3J_{Se\text{-}H}$ = 5.5 Hz); ^{13}C NMR (100 MHz, $CDCl_3$) δ 177.2, 171.5, 54.5 (Se satellites $^2J_{Se\text{-}C}$ = 5.1 Hz), 52.9, 39.6 (Se satellites $^1J_{Se\text{-}C}$ = 29.3 Hz), 32.2 (Se satellites $^2J_{Se\text{-}C}$ = 6.6 Hz), 26.5 (Se satellites $^1J_{Se\text{-}C}$ = 37.8 Hz), 21.1; ^{77}Se NMR (76 MHz, $CDCl_3$) δ 344.5; HRMS (ESI^+) Calcd for $C_{10}H_{18}O_4Se$ $[M + Na]^+$ 305.0263 found 305.0267; $[\alpha]_D^{23} = -2.1°$ (c = 1.07, $CHCl_3$).

2.7.13.2 Racemic Hydrolysis (b)

A 25 mL round bottom flask was charged with a stir bar, **14** (514 mg, 1.74 mmol), THF (5 mL), lithium hydroxide (47 mg, 1.9 mmol), and water (5 mL). The reaction mixture was stirred at room temperature for 30 hours, and 1M NaOH was added to raise

the pH to 9. The solution was diluted with water (6 mL) and washed with DCM (2 × 6 mL). The aqueous phase was reacidified with 1M HCl to pH = 3 and then extracted with diethyl ether (9 mL). The organic phase was dried over $MgSO_4$, filtered, and concentrated *in vacuo* to afford 450 mg (1.60 mmol, 92%) of a colorless liquid. ^{1}H NMR (400 MHz, $CDCl_3$) δ 5.99 (br s, 1H), 3.76 (s, 3H), 3.09 (d, $^2J_{H\text{-}H}$ = 11.6 Hz, 1H), 3.04 (d, $^2J_{H\text{-}H}$ = 11.6 Hz, 1H), 1.53 (s, 3H),1.43 (s, 9H, Se satellites $^3J_{Se\text{-}H}$ = 5.5 Hz).

2.7.14 Synthesis of (*R*)-N-Fmoc-α-MeSec(*t*Bu)-OMe (16)

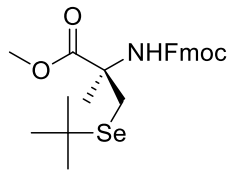

A 25 mL round bottom flask with a nitrogen atmosphere was charged with a stir bar, **15** (578 mg, 2.06 mmol), dichloroethane (DCE) (5 mL), and TEA (0.35 mL, 2.5 mmol). The reaction mixture was stirred for 5 minutes and DPPA (0.50 mL, 2.3 mmol) was added. A reflux condenser was fitted to the round bottom flask and the reaction mixture was stirred for 5 hours at room temperature and heated to solvent reflux for 19 hours. The reaction mixture was cooled to room temperature, diluted with DCE (10 mL), washed with chilled saturated NH_4Cl (15 mL), dried over $MgSO_4$, filtered, and concentrated *in vacuo* to afford a yellow tinged turbid oil. The oil was reconstituted in benzene (5 mL) and added to a 25 mL round bottom flask with a stir bar. To the solution was added 9-fluorenemethanol (416 mg, 2.12 mmol) and titanium (IV) *tert*-butoxide (0.10 mL, 0.260 mmol). The reaction mixture was stirred at room temperature for 29 hours and then diluted with diethyl ether (15 mL). This solution was washed with saturated NH_4Cl (4 × 15 mL). The aqueous phases were extracted with DCM (25 mL).

All organic phases were pooled, dried over $MgSO_4$, filtered, and concentrated in vacuo to afford a crude yellow oil. The crude product was purified by flash chromatography and eluted with 2:3 diethyl ether/hexanes. The product rich fractions (R_f = 0.36 in 2:3 diethyl ether/hexanes) were pooled and concentrated *in vacuo* to afford 626 mg (1.32 mmol, 64%) of a colorless oil. IR ($CDCl_3$, cm^{-1}) 3415, 3349, 2952, 2890, 1721, 1500, 1478, 1449; ^1H NMR (400 MHz, $CDCl_3$) δ 7.75 (d, *J* = 7.5 Hz, 2H), 7.61 (d, *J* = 7.5 Hz, 2H), 7.39 (t, *J* = 7.4 Hz, 2H), 7.31 (td, *J* = 7.4, 1.1 Hz, 2H), 5.85 (br s, 1H), 4.29 (m, 3H), 3.78 (s, 3H), 3.48 (br d, $^2J_{H\text{-}H}$ = 11.2 Hz, 1H), 3.09 (br d, $^2J_{H\text{-}H}$ = 11.1 Hz, 1H), 1.69 (s, 3H), 1.41 (s, 9H); ^{13}C NMR (100 MHz, $CDCl_3$) δ 173.6, 154.6, 143.9, 141.3, 127.7, 127.1, 125.2, 120.0, 66.8, 60.1, 53.0, 47.2, 39.4, 32.3 (Se satellites $^2J_{Se\text{-}C}$ = 6.6 Hz), 28.7, 24.1; ^{77}Se NMR (76 MHz, $CDCl_3$) δ 334.9; HRMS (ESI^+) Calcd for $C_{24}H_{29}NO_4Se$ $[M + Na]^+$ 498.1154 found 498.1161; $[\alpha]_D^{23}$ = +8.9° (c = 1.01, $CHCl_3$).

2.7.15 Synthesis of (*R*)-N-Fmoc-α-MeSec(^{t}Bu)-OH (20)

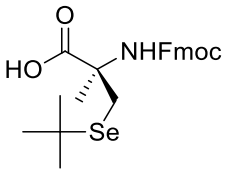

A 50 mL round bottom flask fitted with a reflux condenser was charged with a stir bar, **16** (1.29 g, 2.73 mmol), 1,4-dioxane (10 mL), and 5M HCl (10 mL). The reaction mixture was heated to solvent reflux for 50 hours. The reaction mixture was cooled to room temperature and extracted with DCM (3 × 10 mL). The organic phases were concentrated *in vacuo*, and the resulting viscous yellow residue was reconstituted with diethyl ether (30 mL). The solution was washed with 0.1M HCl (5 × 20 mL). The organic phase was dried over $MgSO_4$, filtered, and concentrated *in vacuo*. Residual solvent was

removed by azeotropic drying with pentane to afford 1.15 g (2.50 mmol, 92%) of a yellow tinged viscous oil. IR ($CDCl_3$, cm^{-1}) 3404, 2955, 1707, 1502, 1450; ^1H NMR (400 MHz, $CDCl_3$) δ 7.75 (d, *J* = 7.8 Hz, 2H), 7.60 (d, *J* = 7.4 Hz, 2H), 7.39 (t, *J* = 7.4 Hz, 2H), 7.31 (td, *J* = 7.4, 0.8 Hz, 2H), 5.77 (br s, 1H), 4.28 (m, 3H), 3.39 (d, *J* = 11.1 Hz, 1H), 3.18 (d, *J* = 10.9 Hz, 1H), 1.71 (s, 3H), 1.41 (s, 9H); ^{13}C NMR (100 MHz, $CDCl_3$) δ 177.7, 154.9, 143.8, 141.3, 127.7, 127.1, 125.2, 120.0, 67.0, 59.7, 47.1, 39.6, 32.3 (Se satellites $^2J_{Se\text{-}C}$ = 6.6 Hz), 28.7, 24.1; ^{77}Se NMR (76 MHz, $CDCl_3$) δ 331.0; HRMS (ESI^+) Calcd for $C_{23}H_{27}NO_4Se$ $[M + Na]^+$ 484.0998 found 484.1001; $[\alpha]_D^{23}$ = +2.6° (c = 1.01, $CHCl_3$).

2.7.16 Synthesis of (*S*)-1-*tert*-butyl 3-methyl 2-((*tert*-butylselanyl)methyl)-2-methylmalonate (21)

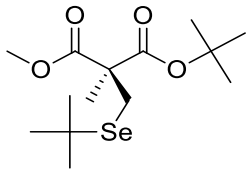

A 50 mL round bottom flask was charged with a stir bar, DCM (13 mL), $MgSO_4$ (1.77 g, 14.8 mmol), and concentrated sulfuric acid (0.20 mL, 3.7 mmol). Clumped $MgSO_4$ was broken up by vigorously stirring. To this suspension was added a solution of **15a** (1.03 g, 3.67 mmol) in DCM (7 mL). *Tert*-butanol (1.75 mL, 18.3 mmol) was added dropwise, and the flask was tightly sealed and stirred for 47 hours. The reaction mixture was filtered washed with saturated $NaHCO_3$ (20 mL) and brine (20 mL). The organic phase was dried over $MgSO_4$, filtered, and concentrated *in vacuo* to afford 807 mg (2.39 mmol, 65%) of an amber-tinged liquid. IR ($CDCl_3$, cm^{-1}) 2975, 2952, 1728; ^1H NMR (400 MHz, $CDCl_3$) δ 3.73 (s, 3H), 3.03 (d, $^2J_{H\text{-}H}$ = 11.4 Hz, 1H), 3.00 (d, $^2J_{H\text{-}H}$ = 11.4 Hz,

1H), 1.46 (s, 3H), 1.45 (s, 9H), 1.43 (s, 9H, Se satellites $^{3}J_{Se\text{-}H}$ 5.3 Hz); ^{13}C NMR (100 MHz, $CDCl_3$) δ 172.2, 170.3, 82.0, 55.0 (Se satellites $^{2}J_{Se\text{-}C}$ = 4.8 Hz), 52.4, 39.0 (Se satellites $^{1}J_{Se\text{-}C}$ = 29.3 Hz), 32.2 (Se satellites $^{2}J_{Se\text{-}C}$ = 6.6 Hz), 27.8, 26.8 (Se satellites $^{1}J_{Se\text{-}C}$ = 37.0 Hz), 20.8; ^{77}Se NMR (76 MHz, $CDCl_3$) δ 339.3; HRMS (ESI^+) Calcd for $C_{14}H_{26}O_4Se$ $[M + Na]^+$ 361.0889 found 361.0893; $[\alpha]_D^{23}$ = −9.6° (c = 1.00, $CHCl_3$).

2.7.17 Synthesis of (*S*)-3-(*tert*-butoxy)-2-((*tert*-butylselanyl)methyl)-2-methyl-3-oxopropanoic acid (22)

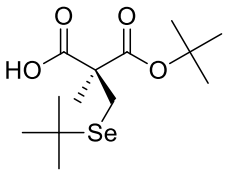

A 25 mL round bottom flask was charged with a stir bar, **21** (498 mg, 1.48 mmol), THF (6.0 mL), lithium hydroxide (117 mg, 4.9 mmol), and water (6.0 mL). The reaction mixture was stirring at room temperature for 16 hours. The pH was reduced to 3 using 4M HCl, diluted with diethyl ether (15 mL), and washed with saturated NH_4Cl (3 × 15 mL). The organic phase was then dried over $MgSO_4$, filtered, and concentrated *in vacuo* to afford 437 mg (1.35 mmol, 92%) of a yellow tinged oil. IR ($CDCl_3$, cm^{-1}) 2977, 1707; ^{1}H NMR (400 MHz, $CDCl_3$) δ 10.69 (br s, 1H), 3.06 (d, $^{2}J_{H\text{-}H}$ = 11.4 Hz, 1H), 3.00 (d, $^{2}J_{H\text{-}H}$ = 11.4 Hz, 1H), 1.50 (s, 3H), 1.47 (s, 9H), 1.44 (s, 9H, Se satellites $^{3}J_{Se\text{-}H}$ 5.6 Hz); ^{13}C NMR (100 MHz, $CDCl_3$) δ 177.3, 170.4, 82.7, 54.9 (Se satellites $^{2}J_{Se\text{-}C}$ = 4.8 Hz), 39.2 (Se satellites $^{1}J_{Se\text{-}C}$ = 29.0 Hz), 32.2 (Se satellites $^{2}J_{Se\text{-}C}$ = 6.6 Hz), 27.8, 26.7 (Se satellites $^{1}J_{Se\text{-}C}$ = 37.0 Hz), 21.1; ^{77}Se NMR (76 MHz, $CDCl_3$) δ 342.3; HRMS (ESI^+) Calcd for $C_{13}H_{24}O_4Se$ $[M + Na]^+$ 347.0732 found 347.0734; $[\alpha]_D^{23}$ = −2.4° (c = 1.00, $CHCl_3$).

2.7.18 Synthesis of (*S*)-N-Fmoc-α-MeSec(^{t}Bu)-O^{t}Bu (23)

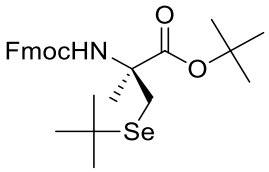

A 25 mL round bottom flask with a nitrogen atmosphere was charged with a stir bar, **22** (888 mg, 2.75 mmol), DCE (10 mL), and TEA (0.50 mL, 3.6 mmol). The reaction mixture was stirring for 5 minutes and DPPA (650 μL, 3.0 mmol) was added. The round bottom flask was fitted with a reflux condenser and the reaction mixture was stirred for an additional hour and then heated to solvent reflux for 17 hours. The reaction mixture was cooled to room temperature, diluted with DCE (10 mL), and washed with chilled saturated NH_4Cl (20 mL). The organic phase was dried over $MgSO_4$, filtered, and concentrated *in vacuo* to afford a turbid oil. The oil was reconstituted in a 25 mL round bottom flask using benzene (10 mL). This flask was charged with a stir bar, 9-fluorenemethanol (545 mg, 2.78 mmol), and titanium (IV) *tert*-butoxide (0.10 mL, 0.260 mmol). The reaction mixture was stirred at room temperature for 47 hours. Saturated NH_4Cl (10 mL) was added, and the reaction mixture was stirred for 3.5 hours. The reaction mixture was diluted with diethyl ether (20 mL), washed with saturated NH_4Cl (2 × 20 mL), and water (20 mL). The emulsion was extracted with diethyl ether (20 mL). The organic phases were pooled, dried over $MgSO_4$, filtered, and concentrated in vacuo to afford a crude oil. This oil was purified by gradient flash chromatography and eluted with hexanes/diethyl ether (8:1 to 4:1). The product rich fractions (R_f = 0.57 in 2:3 diethyl ether/hexanes) were pooled and concentrated *in vacuo* to afford 786 mg (1.52 mmol, 55%) of a colorless, gummy solid. IR ($CDCl_3$,cm^{-1}) 3413, 2973, 1715; ^{1}H NMR

(400 MHz, $CDCl_3$) δ 7.76 (d, *J* = 8.0 Hz, 2H), 7.62 (dd, *J* = 7.4, 2.9 Hz, 2H), 7.39 (t, *J* = 7.4 Hz, 2H), 7.31 (td, *J* = 7.4, 1.1 Hz, 2H), 5.96 (s, 1H), 4.28 (m, 3H), 3.51 (d, ^2J = 11.2 Hz, 1H), 3.05 (d, ^2J = 11.2 Hz, 1H), 1.69 (s, 3H), 1.50 (s, 9H), 1.41 (s, 9H); ^{13}C NMR (100 MHz, $CDCl_3$) δ 172.2, 154.5, 144.1, 143.9, 141.3, 127.6, 127.0, 125.3, 119.9, 82.7, 66.7, 60.2 (Se satellites $^2J_{Se\text{-}C}$ = 4.0 Hz), 47.2, 39.0, 32.4 (Se satellites $^2J_{Se\text{-}C}$ = 6.6 Hz), 28.4, 27.9, 24.2; ^{77}Se NMR (76 MHz, $CDCl_3$) δ 336.8; HRMS (ESI^+) Calcd for$C_{27}H_{35}NO_4Se$ $[M + Na]^+$ 540.1624 found 540.1626; $[\alpha]_D^{23}$ = +7.7° (c = 1.00, $CHCl_3$).

2.7.19 Synthesis of (*S*)-N-Fmoc-α-MeSec(*t*Bu)-OH (24)

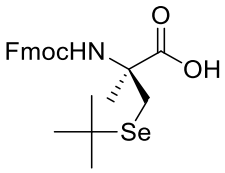

A 25 mL round bottom flask was charged with a stir bar, **23** (546 mg, 1.06 mmol), DCM (10 mL), and trifluoroacetic acid (10.0 mL, 14.9 mmol). The reaction mixture was stirred for 2 hours at room temperature and the solvent was removed *in vacuo*. The residue was reconstituted in diethyl ether (10 mL) and washed with saturated NH_4Cl (3 × 10 mL). The organic phase was dried over $MgSO_4$, filtered, and concentrated *in vacuo*. Residual solvent was removed by azeotropic drying with pentane to afford 487 mg (1.06 mmol, quantitative) of a gummy, foamy solid. IR ($CDCl_3$,cm^{-1}) 3400, 3065, 2955, 1707, 1503, 1450; ^{1}H NMR (400 MHz, $CDCl_3$) δ 8.99 (br s, 1H), 7.76 (d, *J* = 7.5 Hz, 2H), 7.60 (d, *J* = 7.4 Hz, 2H), 7.39 (d, *J* = 7.4 Hz, 2H), 7.31 (td, *J* = 7.4, 0.8 Hz, 2H), 5.77 (br s, 1H), 4.29 (m, 3H), 3.36 (d, *J* = 10.5 Hz, 1H), 3.18 (d, *J* = 10.6 Hz, 1H), 1.70 (s, 3H), 1.41 (s, 9H); ^{13}C NMR (100 MHz, $CDCl_3$) δ 178.0, 155.1, 143.7, 141.3, 127.7, 127.1, 125.1, 120.0, 67.2, 59.7, 39.8, 32.3 (Se satellites $^2J_{Se\text{-}C}$ = 6.2 Hz), 28.6, 24.0; ^{77}Se NMR (76

MHz, $CDCl_3$) δ 330.2; HRMS (ESI^+) Calcd for $C_{23}H_{27}NO_4Se$ $[M + Na]^+$ 484.0998 found 484.1000; $[\alpha]_D^{23} = -2.7°$ (c = 1.07, $CHCl_3$).

2.7.20 Synthesis of (*R*)-methyl 2-((*tert*-butylselanyl)methyl)-4-diazo-2-methyl-3-oxobutanoate (25)

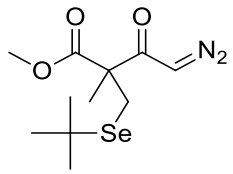

A flame dried, 50 mL round bottom flask was charged with a stir bar, **15a** (506 mg, 1.80 mmol), DCM (10 mL), and oxalyl chloride (500 μL, 5.83 mmol). To this solution was then added DMF (1 drop) causing effervescence. The reaction mixture was stirred for 14 hours at room temperature and the volatiles were removed *in vacuo*. The residue was reconstituted in diethyl ether (10 mL) and cooled to -10 °C. To this solution was added 0.1715 M ethereal solution of diazomethane (52 mL, 8.9 mmol) was added. The reaction mixture placed in a freezer set at -10 °C for 15 hours. The reaction mixture was warmed to room temperature and bubbled with N_2. The solvent was removed *in vacuo* to afford 529 mg (1.73 mmol, 96%) of a yellow oil. IR ($CDCl_3$,cm^{-1}) 3099, 2953, 2107, 1732, 1633; ^1H NMR (400 MHz, $CDCl_3$) δ 5.49 (s, 1H), 3.74 (s, 3H), 3.08 (d, $^2J_{H-H}$ = 11.4 Hz, 1H, Se satellites $^2J_{Se-H}$ 3.1 Hz), 2.98 (d, $^2J_{H-H}$ = 11.5 Hz, 1H, Se satellites $^2J_{Se-H}$ 3.0 Hz), 1.48 (s, 3H), 1.43 (s, 9H, Se satellites $^3J_{Se-H}$ 5.5 Hz); ^{13}C NMR (100 MHz, $CDCl_3$) δ 191.8, 172.4, 58.3 (Se satellites $^2J_{Se-C}$ = 4.4 Hz), 54.0, 52.8, 39.5 (Se satellites $^1J_{Se-C}$ = 29.0 Hz), 32.2 (Se satellites $^2J_{Se-C}$ = 6.6 Hz), 27.0 (Se satellites $^1J_{Se-C}$ = 37.0 Hz), 20.8; ^{77}Se NMR (76 MHz, $CDCl_3$) δ 343.5; HRMS (ESI^+) Calcd for $C_{11}H_{18}N_2O_3Se$ $[M + Na]^+$ 329.0375 found 329.0378.

2.7.21 Synthesis of (*R*)-3-((*tert*-butylselanyl)methyl)-4-methoxy-3-methyl-4-oxobutanoic acid (26)

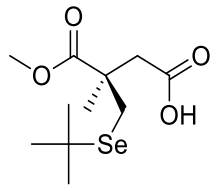

A 50 mL round bottom flask was charged with a stir bar, **25** (1.07 g, 3.50 mmol), THF (14 mL), and water (6 mL). The reaction mixture was sparged with N_2 for 15 minutes. The reaction mixture was placed 11.5 cm away from a UV lamp and exposed to UV radiation for 42 hours at room temperature with positive N_2 pressure. The volatiles were removed *in vacuo* and the residues pH was brought to 9 with 1M NaOH. The solution was washed with diethyl ether (20 mL). The aqueous phase was acidified with 4M HCl to pH = 3 which caused red precipitate to form. The solution was extracted with diethyl ether (40 mL). The organic phase was dried over $MgSO_4$, filtered, and concentrated *in vacuo* to afford 662 mg (2.24 mmol, 64%) of a yellow liquid. IR ($CDCl_3$,cm^{-1}) 2953, 2891, 1729, 1708; ^{1}H NMR (400 MHz, $CDCl_3$) δ 10.12 (br s, 1H), 3.71 (s, 3H), 2.94 (d, $^2J_{H\text{-}H}$ = 11.5 Hz, 1H), 2.92 (d, $^2J_{H\text{-}H}$ = 16.8 Hz, 1H), 2.91 (d, $^2J_{H\text{-}H}$ = 11.5 Hz, 1H), 2.69 (d, J = 16.7 Hz, 1H), 1.42 (s, 9H, Se satellites $^3J_{Se\text{-}H}$ = 5.0 Hz), 1.36 (s, 3H); ^{13}C NMR (100 MHz, $CDCl_3$) δ 177.1, 175.5, 52.3, 44.5 (Se satellites $^2J_{Se\text{-}C}$ = 4.0 Hz), 41.8, 39.3 (Se satellites $^1J_{Se\text{-}C}$ = 29.0 Hz), 32.3 (Se satellites $^2J_{Se\text{-}C}$ = 6.2 Hz), 30.1 (Se satellites $^1J_{Se\text{-}C}$ = 37.4 Hz), 23.3; ^{77}Se NMR (76 MHz, $CDCl_3$) δ 328.6; HRMS (ESI^+) Calcd for $C_{11}H_{20}O_4Se$ $[M + Na]^+$ 319.0419 found 319.0424; $[\alpha]_D^{25}$ = 4.1° (c = 1.01, $CHCl_3$).

2.7.22 Synthesis of (*R*)-methyl 3-((((9*H*-fluoren-9-yl)methoxy)carbonyl)amino)-2-((*tert*-butylselanyl)methyl)-2-methylpropanoate (27)

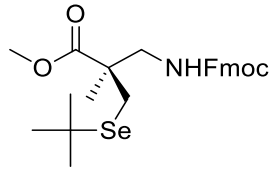

A 25 mL round bottom flask was charged with a stir bar, **26** (359 mg, 1.21 mmol), DCE (5 mL), and TEA (210 μL, 1.51 mmol). The reaction mixture was stirring for 5 minutes and DPPA (290 μL, 1.35 mmol) was added. The round bottom flask was fitted with a reflux condenser and the reaction mixture was stirred for an additional 1.5 hours and then heated to solvent reflux for 28 hours. The reaction mixture was cooled to room temperature, diluted with DCE (10 mL), and washed with chilled saturated NH_4Cl (15 mL). The organic phase was dried over $MgSO_4$, filtered, and concentrated *in vacuo* to afford a turbid oil. The oil was reconstituted in a 50 mL round bottom flask using benzene (10 mL). This flask was charged with a stir bar, 9-fluorenemethanol (246 mg, 1.25 mmol), and titanium (IV) *tert*-butoxide (50 μL, 0.129 mmol). The reaction mixture was stirred at room temperature for 4 days. Saturated NH_4Cl (10 mL) was added, and the reaction mixture was stirred for 30 minutes. The reaction mixture was diluted with diethyl ether (20 mL), washed with saturated NH_4Cl (3 × 20 mL). The organic phase was pooled, dried over $MgSO_4$, filtered, and concentrated in vacuo to afford a crude oil. This oil was purified by gradient flash chromatography and eluted with 2:3 diethyl ether/hexanes. The product rich fractions (R_f = 0.27 in 2:3 diethyl ether/hexanes) were pooled and concentrated *in vacuo* to afford 142 mg (0.291 mmol, 24%) of a colorless, gummy solid. IR (Et_2O,cm^{-1}) 3363, 3064, 2971, 2950, 2889, 1716, 1611, 1600; ^1H NMR

(400 MHz, $CDCl_3$) δ 7.75 (d, J_{H-H} = 7.0 Hz, 2H), 7.59 (d, J_{H-H} = 7.4 Hz, 2H), 7.38 (t, J_{H-H} = 7.4 Hz, 2H), 7.30 (t, J_{H-H} = 7.4 Hz, 2H), 5.30 (br t, J_{H-H} = 6.3 Hz, 1H), 4.30 (m, 3H), 3.71 (s, 3H), 3.47 (dd, J_{H-H} = 14.0, 6.1 Hz, 1H) 3.41 (dd, J_{H-H} = 13.9, 7.3 Hz, 1H), 2.79 (s, 2H), 1.41 (s, 9H, Se satellites $^3J_{Se-H}$ = 5.4 Hz), 1.29 (s, 3H); ^{13}C NMR (100 MHz, $CDCl_3$) δ 175.7, 156.7, 144.0, 141.3, 127.7, 127.1, 125.1, 120.0, 66.9, 52.2, 47.9, 47.7, 47.3, 39.2 (Se satellites $^1J_{Se-C}$ = 29.0 Hz), 32.2 (Se satellites $^2J_{Se-C}$ = 6.6 Hz), 28.2 (Se satellites $^1J_{Se-C}$ = 37.4 Hz), 21.7; ^{77}Se NMR (76 MHz, $CDCl_3$) δ 336.4; HRMS (ESI^+) Calcd for $C_{25}H_{31}NO_4Se$ $[M + Na]^+$ 512.1311 found 512.1305; $[\alpha]_D^{24}$ = 3.4° (c = 0.88, $CHCl_3$).

2.7.23 Synthesis of (*R*)-3-((((9*H*-fluoren-9-yl)methoxy)carbonyl)amino)-2-((*tert*-butylselanyl)methyl)-2-methylpropanoic acid (28)

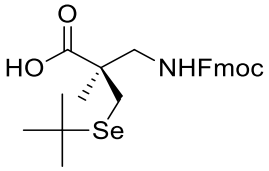

A 10 mL round bottom flask fitted with a reflux condenser was charged with a stir bar, **27** (90 g, 0.180 mmol), 1,4-dioxane (3 mL), and 5M HCl (3 mL). The reaction mixture was heated to solvent reflux for 48 hours. The reaction mixture was cooled to room temperature and extracted with diethyl ether (20 mL) and washed with 0.1M HCl (5 × 20 mL). The organic phase was dried over $MgSO_4$, filtered, and concentrated *in vacuo*. Residual solvent was removed by azeotropic drying with pentane to afford 29 mg (0.062 mmol, 34%) of a yellow tinged viscous oil. IR ($CDCl_3$, cm^{-1}) ; ^{1}H NMR (400 MHz, $CDCl_3$) δ 9.81 (br s), 7.74 (d, *J* = 7.0 Hz, 2H), 7.58 (d, *J* = 7.3 Hz, 2H), 7.37 (t, *J* = 7.1 Hz, 2H), 7.29 (t, *J* = 7.2 Hz, 2H), 5.38 (br t, J_{H-H} = 5.9 Hz, 1H), 4.34 (m, 3H), 3.34 (m,

2H), 2.81 (s, 2H), 1.41 (s, 9H), 1.32 (s, 3H); ^{77}Se NMR (76 MHz, $CDCl_3$) δ 334.2; HRMS (ESI^+) Calcd for $C_{24}H_{29}NO_4Se$ $[M + Na]^+$ 498.1154 found 498.1149.

2.7.24 Synthesis of (*S*)-*tert*-butyl 2-((*tert*-butylselanyl)methyl)-4-diazo-2-methyl-3-oxobutanoate (29)

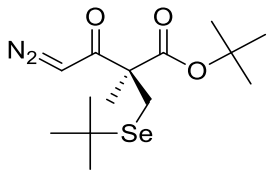

A flame dried, 50 mL round bottom flask was charged with a stir bar, **22** (430 mg, 1.24 mmol), DCM (10 mL), and oxalyl chloride (500 μL, 5.83 mmol). To this solution was then added DMF (1 drop) which caused effervescence. The reaction mixture was stirred for 16 hours at room temperature and the volatiles were removed *in vacuo*. The residue was reconstituted in diethyl ether (10 mL) and cooled to -10 °C. To this solution was added 0.2206 M ethereal solution of diazomethane (51 mL, 11 mmol) was added. The reaction mixture placed in a freezer set at -10 °C for 16 hours. The reaction mixture was warmed to room temperature and bubbled with N_2. The solvent was removed *in vacuo* to afford 276 mg (0.794 mmol, 64%) of a yellow oil. IR ($CDCl_3$,cm^{-1}) 2977, 2937, 2893, 2112, 1722, 1635; ^{1}H NMR (400 MHz, $CDCl_3$) δ 5.46 (s, 1H), 3.08 (d, $^2J_{H\text{-}H}$ = 11.2 Hz, 1H), 2.90 (d, $^2J_{H\text{-}H}$ = 11.4 Hz, 1H), 1.47 (s, 9H), 1.43 (s, 12H); ^{13}C NMR (100 MHz, $CDCl_3$) δ 192.5, 170.8, 82.3, 58.7, 53.5, 39.0, 32.2, 27.7, 27.0, 20.7; ^{77}Se NMR (76 MHz, $CDCl_3$) δ 340.5.

CHAPTER III – DIRECT DETERMINATION OF ABSOLUTE STEREOCHEMISTRY OF α-METHYLSELENOCYSTEINE USING THE MOSHER METHOD

3.1 Background

Enzymatic hydrolysis utilizing pig liver esterase (PLE) can be a reliable method to form chiral carboxylic acids. Based on literature precedence, PLE prefers to create the (*R*)-enantiomer, however there are substrates known to cause PLE to produce the (*S*)-enantiomer.[60-62, 84] Because there is uncertainty with the configuration of the resulting stereocenter with untested substrates, empirical methods are needed to ascertain the absolute configuration of the newly generated stereocenter.

One method for determining absolute configuration is polarimetry. Polarimetry is a nondestructive method that passes plane polarized monochromatic light through a solution containing a chiral compound. As the plane polarized light passes through the sample, the plane is rotated the from the normal, with enantiomers rotating the plane in directions opposed to each other. One drawback to this method is to determine absolute stereochemistry, specific rotations need to be compared to appropriate analogues with known configurations because direction of rotation does not establish (*R*)- or (*S*)-stereochemistry. While having the same designation, (*R*)-serine and (*R*)-cysteine rotate plane polarized light in opposite directions. This method, while excellent at determining optical purity, lacks a means to independently and unambiguously determine absolute configuration.

Another method to determine absolute configuration is x-ray crystallography. X-ray crystallography functions by hitting a high purity crystal with a beam of x-rays and

measuring the diffraction pattern produced. From this diffraction pattern and computational analysis, a very accurate 3-dimensional molecular structure can be determined. One of the problems that prevents this method from being utilized routinely is the process of creating a single crystal large and pure enough for analysis. Many organic materials are liquids under standard conditions, and some materials, if able to become solid under standard conditions, only form as amorphous solids and are unable to be analyzed by this technique. While this method can produce a precise 3-dimensional representation of a molecule, its utility is limited to crystalline solids. Crystalline materials can also be problematic, as twinning or cracking can form in the crystal preventing easy structure elucidation with the crystallography technique.

Another method of determining the absolute configuration of a stereocenter is through synthetic means, such as kinetic resolutions. Enantiomers will react at different rates, producing enantio-enriched products, if chiral catalysts or chiral reagents are used.[87-89] Modelling the intermediate complex in models such as the Zimmerman-Traxler model, one enantiomer will form a more stabilized intermediate from spatial and electrostatic interactions, which can be used to explain the difference in reaction kinetics between the enantiomers.[90] The differences in kinetic rates, combined with the modelling the intermediate complex, can be used to determine the stereochemistry of the starting material. While kinetic resolution is a powerful tool to determine absolute configuration, the substrate may be incompatible with the asymmetric reactions needed for the process; the functional group needed in the reaction may be absent in the substrate, or other functional groups present could be sensitive to the required reaction conditions, affecting the reaction kinetics in unpredictably.

The Mosher method is another method to determine absolute configuration and has seen numerous uses as a reliable method to analyze stereocenters and chirality of organic molecules by utilizing NMR spectroscopy,[91-93] which is especially useful when X-ray crystallography cannot be used. It can not only establish %ee, but also the absolute stereochemistry of an ambiguous stereocenter when applied correctly. This method relies on the principle of magnetic anisotropy, or a nonuniform magnetic environment.[94] This magnetic inequivalence is caused by local magnetic fields created by the valence and bonding electrons that resist the external magnetic field produced by the spectrometer, which has the effect of shielding the nucleus giving it a slightly different frequency. This effect is felt by nuclei by through-bond interactions and can be influenced by induction effects caused by dipoles, or electron delocalization from bond resonance. Magnetic anisotropy can also occur from through-space interactions which occurs through electrons in π-systems. The movement of these π-electrons creates large, conical shaped, shielding environments, with the ability to shield any NMR active nuclei that sit spatially inside of them (**Figure 3.1**).

Magnetic anisotropy from spatial interactions was recognized very early on in the development of practical NMR in the mid 1960's with the differences in diastereomers and enantiomers in chiral solvents well established,[95] but it wasn't until Mosher's article in 1973, where his method was initially developed, that the physics of the spatial interactions of these systems directly correlated absolute stereochemistry to chemical shifts.[91] Before that time, anisotropic effects were used by many, as it is still used today, to determine optical purity.[96-99]

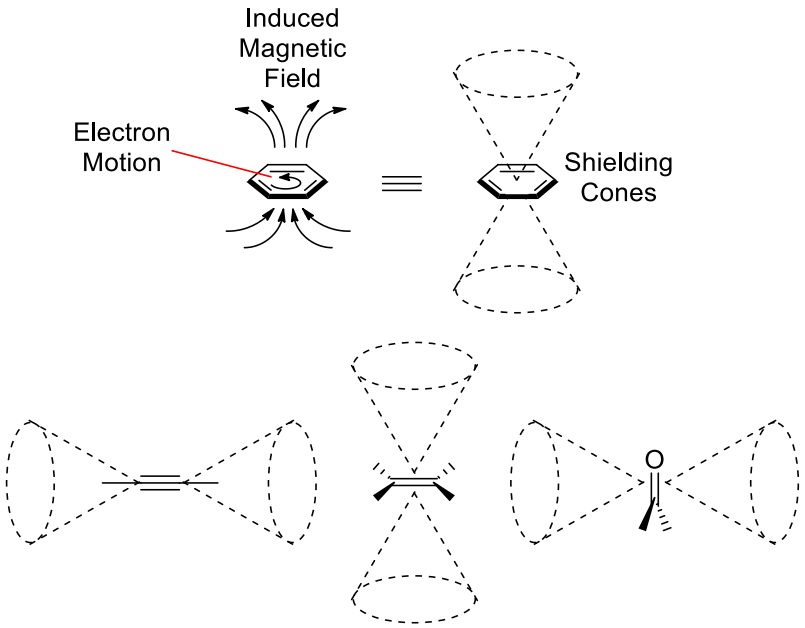

Figure 3.1 *Magnetic Anisotropy in π-Systems and Shielding Effects from These Systems*

Mosher synthesized esters (or amides) using enantiopure carboxylic acids or acyl chlorides of known configurations at the α-carbon, containing an aromatic group, which were coupled with secondary alcohols (amines). When modeling these esters (amides) with a specific conformation, he found an upfield shift from groups that were on the same side of the MTPA-plane as, or ipsilateral to, the MTPA-phenyl group (**Figure 3.2**). While it may not be the lowest energy conformer, this conformation is thought be significant on the NMR timescale.[93, 100] Early in this work, three aromatic containing carboxylic acids were used, mandelic acid, *O*-methylmandelic acid, and α-methoxy-α-trifluoromethylphenylacetic acid (MTPA), however Mosher found that MTPA gave more straightforward and consistent results than the other two molecules since mandelates and *O*-methylmandelates have the potential to epimerize.[96-97]

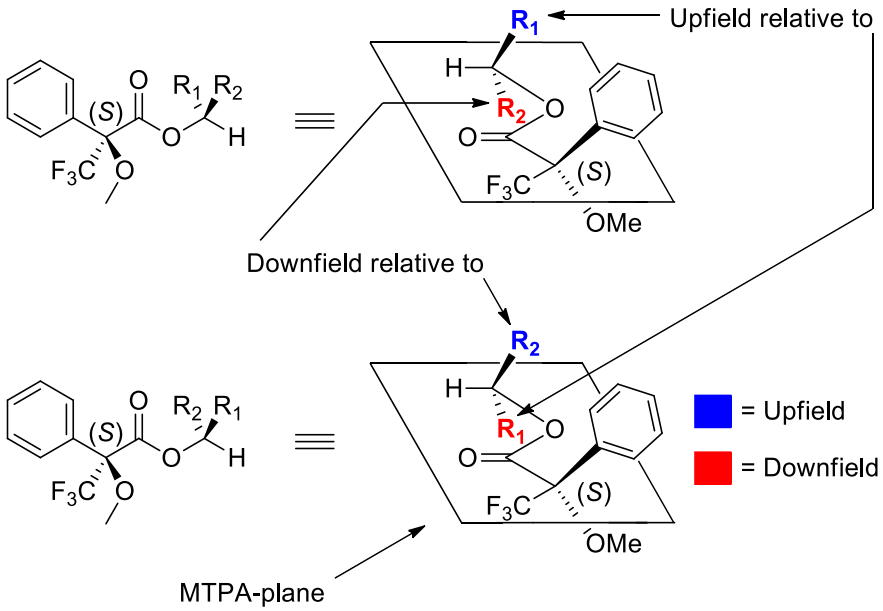

Figure 3.2 *Anisotropic Trends Seen with MTPA with Required Conformation*

MTPA also allows for the option to use ^{19}F NMR to be used for analysis as well which allows for additional confirmation of optical purity determination or stereocenter assignment, however for stereocenter assignment it may be difficult to utilize.[101-102]

For the Mosher method to produce predictable results, an alcohol or amine is needed to be on a chiral, secondary carbon. If this carbon is tertiary, the formed ester or amide will not sit in the MTPA-plane as proposed by Mosher due to the steric congestion around this carbon, and will instead have a different conformation than what is expected for accurate assignment; instead without a hydrogen present on the carbinyl carbon (carbon attached to the heteroatom) to sit in the MTPA-plane, the molecule would be expected to adopt one of the available staggered conformations (**Figure 3.3**). When the carbon is tertiary, many opt to use the Mosher method to determine enantio-purity and use other empirical methods instead to determine absolute stereochemistry. To date, there

is only one source that has utilized the Mosher method to determine the configuration of a tertiary carbon, but the authors used computational analysis to approximate what to expect for the non-ideal conformation to aid in the interpretation of the spectra to identify the stereochemistry.[103]

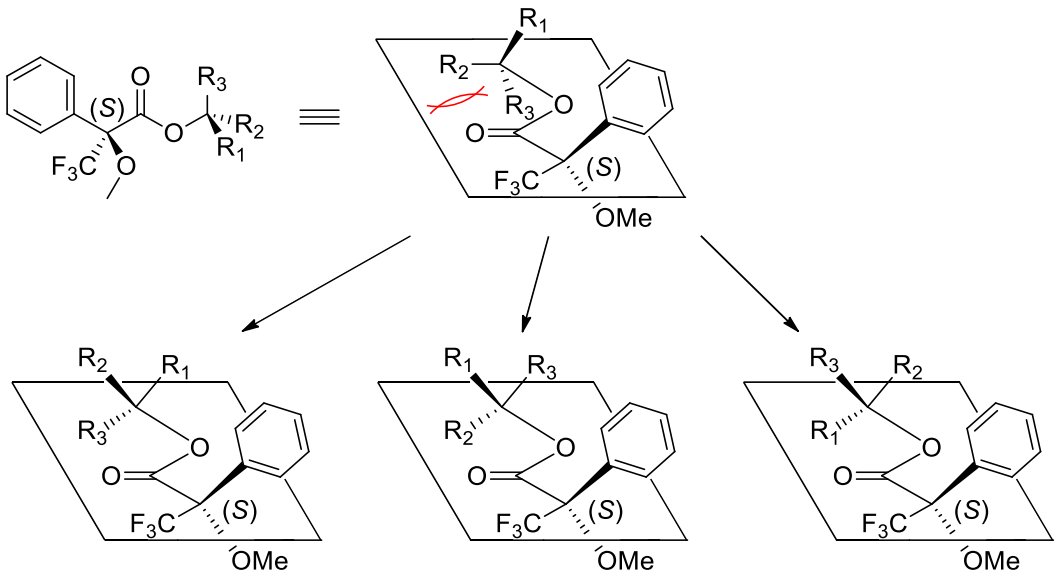

Figure 3.3 *Steric Interactions from a Tertiary Carbinyl Carbon*

Currently, there seems to be a gap in knowledge using the Mosher method to analyze amides with a tertiary carbinyl carbon. With the correct substrates, amides should accurately predict unknown configurations over their ester counterparts, especially if a group around the carbinyl carbon has the capability to hydrogen bond with the amide hydrogen atom (**Figure 3.4**). Mosher found that when either mandelic or atrolactic acids were used to make the diastereomeric esters and amides, the $\Delta\delta$ were greater than that of the MTPA analogues.[91, 97]

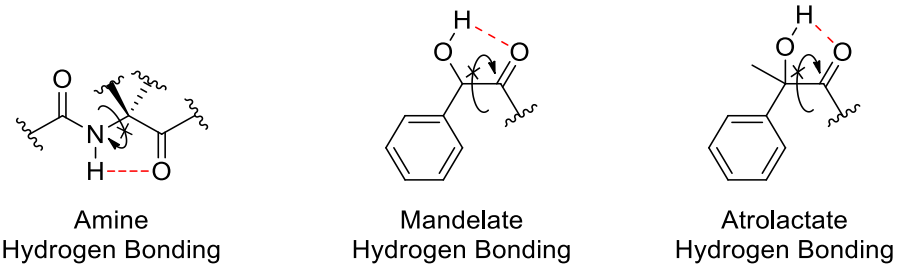

Figure 3.4 *Rigidity of Conformers Caused by Hydrogen Bonding*

He postulated that large Δδ was caused by the mandelates having the ability to hydrogen bond to the carbonyl allowing for more rigidity of the acid moiety of the ester.[91] With the substrate having the ability to hydrogen bond with the amide hydrogen, it should be possible to accurately assign the absolute configuration of the α-carbon of an α-MeAA with the Mosher method.

3.2 Synthesis and Analysis of the Mosher Amides

With the potential for hydrogen bonding between the amide hydrogen and the ester carbonyl, it is hypothesized that the conformation of the parent amino ester will sit in a predictable orientation that will allow for the determination of its unknown stereocenter (**Figure 3.5**).

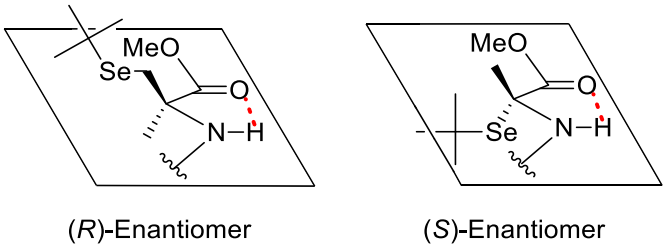

Figure 3.5 *Hypothesized Amino Ester Conformations in the MPTA-Plane*

The Mosher method was used to accurately assign the configuration of the α-MeSec analogue that was previously synthesized **20**, which was hypothesized to be of (*R*)-configuration based on comparisons to the optical rotation of its α-MeCys counterpart[104] of known stereochemistry. Amino ester **31** was converted to two diastereomeric MTPA amides, (*X*,*R*)-**32** and (*X*,*S*)-**32**, where X is the unassigned stereocenter on the carbinyl carbon, through a series of reactions with known retention of stereochemistry (**Scheme 3.1**). Several spectra were obtained for each diastereomer and were compared to observe any magnetic anisotropy present.

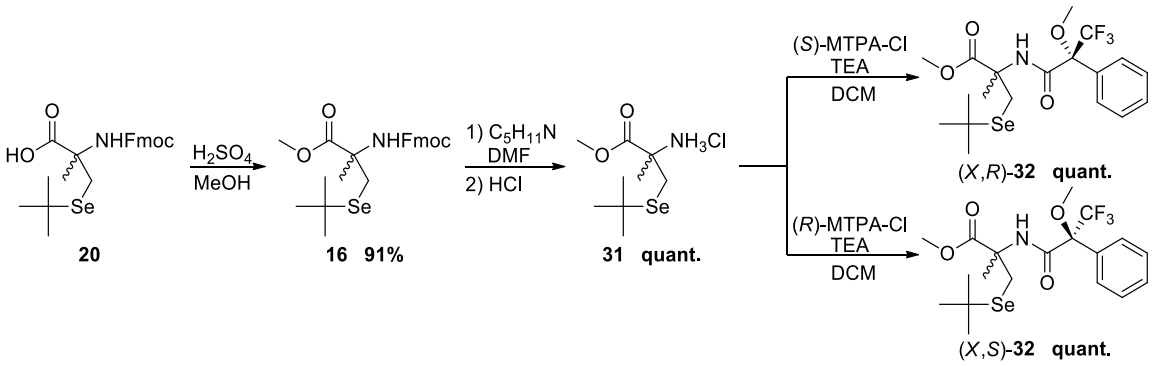

Scheme 3.1 *Synthesis of the MTPA-Amides*

In the ^{1}H spectra, the α-methyl hydrogen atoms show strong shielding effects from the MTPA-phenyl group (+13.4 Hz using the δ(*X*,*S*) - δ(*X*,*R*) convention) which correlates to the α-methyl group of the carbinyl carbon being ipsilateral to the MTPA-phenyl group in (*X*,*R*)-**32** and not in (*X*,*S*)-**32** (**Figure 3.6**). Due to the diastereotopic nature of the methylene protons adjacent to the selenium (Δδ +1.7 and Δδ +11.6 Hz), these protons did not shift as expected. The unexpected shift could be caused by other effects, such as the electronic environment imposed by the selenium atom, interfering

with the anisotropy caused by the MTPA-phenyl.[91] The *tert*-butyl group protons (Δδ -6.2 Hz), experienced a small anisotropic effect believed to be caused by the large distance from the MTPA-phenyl group. With the data presented in the ^{1}H spectra, the side groups take the configurations that presented in **Figure 3.6** for each diastereomer.

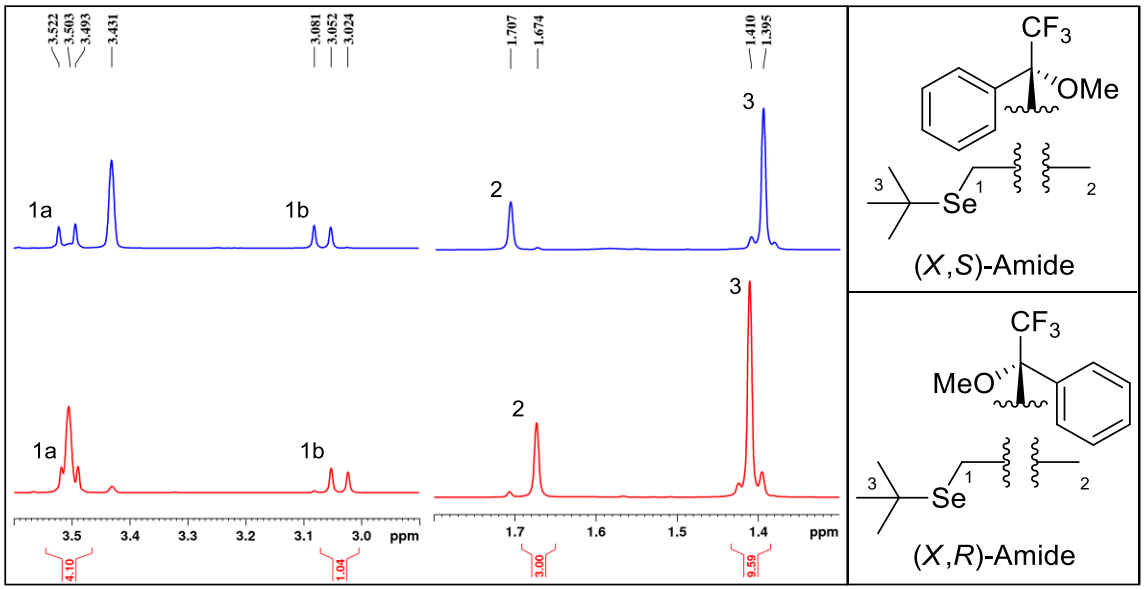

Figure 3.6 *^{1}H NMR Spectra of the sp^{3} regions of (X,S)-**32** and (X,R)-**32***

More agreeable evidence for stereocenter assignment is gained from ^{13}C NMR, especially from the carbons adjacent to the carbinyl carbon. In agreement with ^{1}H spectra, the α-methyl carbon (Δδ +28.6 Hz) experienced a large anisotropic shift, with the α-methyl carbon ipsilateral to the MTPA-phenyl group in (*X*,*R*)-**32** (**Figure 3.7**). The methylene carbon (Δδ -43.5 Hz) also experienced a large anisotropic effect that corroborates the previous configurational assignment (**Figure 3.6**). The quaternary *tert*-butyl carbon (Δδ -14.8 Hz) also experienced a shift in the same direction of the

methylene carbon, but much more diminished, due to an increased distance from the MTPA-phenyl group.

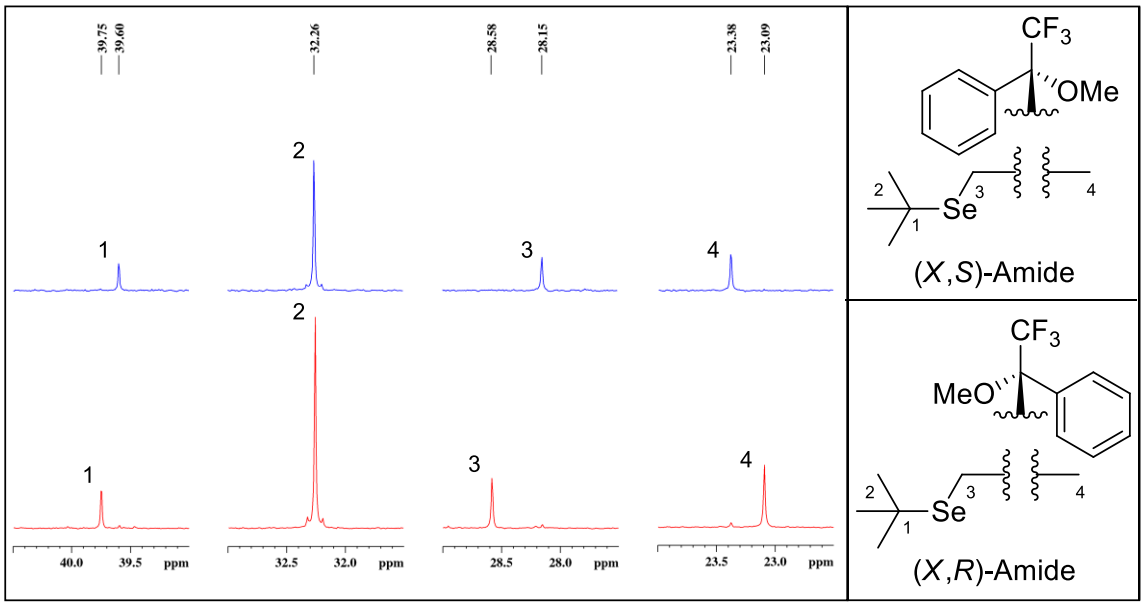

Figure 3.7 *^{13}C NMR Spectra of the sp^3 regions of (X,S)-**32** and (X,R)-**32***

The methyl carbons of the *tert*-butyl group did not experience any measurable shift difference, which is caused by the increased distance from the MTPA-phenyl group tapering the effect of the anisotropy that the phenyl group confers. With all the ^{13}C resonances analyzed, the configuration of the side groups can be more confidently assigned (**Figure 3.7**), which agrees with the assignment proposed from the ^{1}H spectra.

Useful configurational information can be gained from the ^{19}F NMR spectra as well. The signals from the trifluoromethyl groups of the MTPA are magnetically inequivalent (**Figure 3.8**) with (*X*,*S*)-**32** experiencing an upfield anisotropic shift when compared to (*X*,*R*)-**32**. Based on past literature precedence,[91, 100-102] this can be caused by steric interactions between a bulky side group and the MTPA-phenyl group causing a destabilization of the preferred conformation, forcing trifluoromethyl group to sit outside

the preferred deshielding cone of the MTPA-carbonyl longer than average. This destabilization results in fluorine atoms ultimately showing an upfield shift in the spectrum.

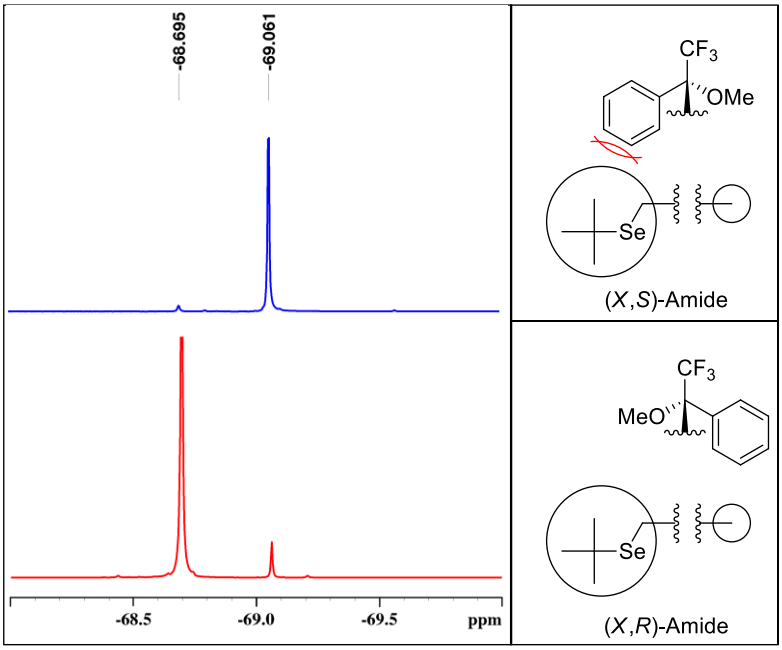

Figure 3.8 *[19]F NMR Spectra of the Trifluoromethyl Groups Showing Steric Interactions*

Bearing in mind the size of the side groups, there is a direct relationship with whether the phenyl group and the *tert*-butyl selenide group share the same side of the MTPA-plane and the chemical shift of the trifluoromethyl group (**Figure 3.8**).

Since selenium has a wide chemical shift range for the selenide functionality, and high sensitivity to the electronic environment,[7, 82, 105] it was hypothesized that ^{77}Se NMR could give large anisotropic shifts assignment of the configuration of the unknown stereocenter. The selenium shifts observed (**Figure 3.9**) opposed the configuration that the ^{1}H, ^{13}C, and ^{19}F spectra predicted. An effect that could have influenced the anisotropic shift the selenium experiences is the large electron cloud around selenium.

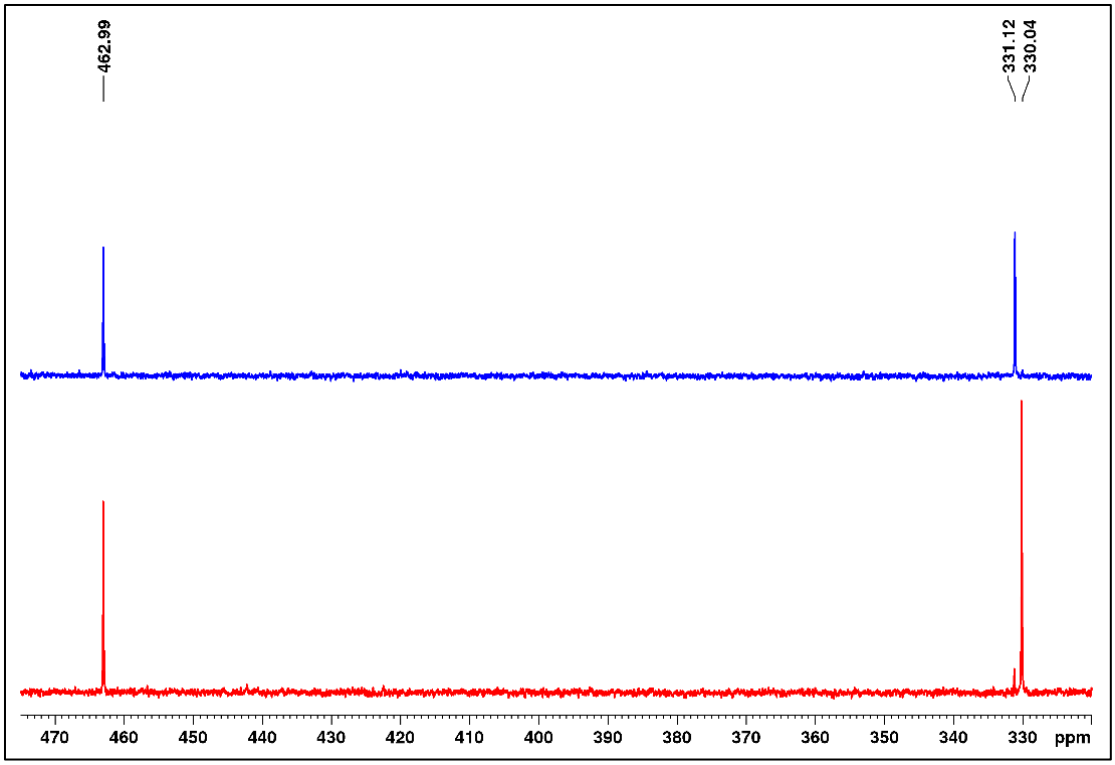

Figure 3.9 *^{77}Se Spectra of (X,S)-**32** and (X,R)-**32** Spiked with Diphenyl Diselenide*

This large electron cloud shields the nucleus from the magnetic field and prevents the expected anisotropic effects from the MTPA-phenyl group.[82]

Based on all the spectra collected, there is strong supporting evidence that the side groups sit in the positions proposed in **Figures 3.6-3.8** leaving the ester to sit in the MTPA-plane. With the ester carbonyl sitting anti to the amide hydrogen, there will be repulsive electrostatic forces exerted between the ester and amide carbonyls (**Figure 3.10a**). The inverse is true if the ester carbonyl sits syn to the amide hydrogen, since a stabilization occurs from the amide hydrogen atom hydrogen bonding to ester carbonyl (**Figure 3.10b**). This would be very similar to what Mosher *et al*. observed when working with mandelates.[91] With the ester in the expected *syn*-orientation, the absolute

configuration of the α-carbon of **20** is (*R*). This assignment confirms the expected configuration when comparing the optical rotation of **20** ($[\alpha]_D^{23}$ = 2.6° (c = 1.01, $CHCl_3$)) to its α-MeCys analogue ($[\alpha]_D^{24}$ = 2.0° (c = 1.0 CH_2Cl_2)).[104]

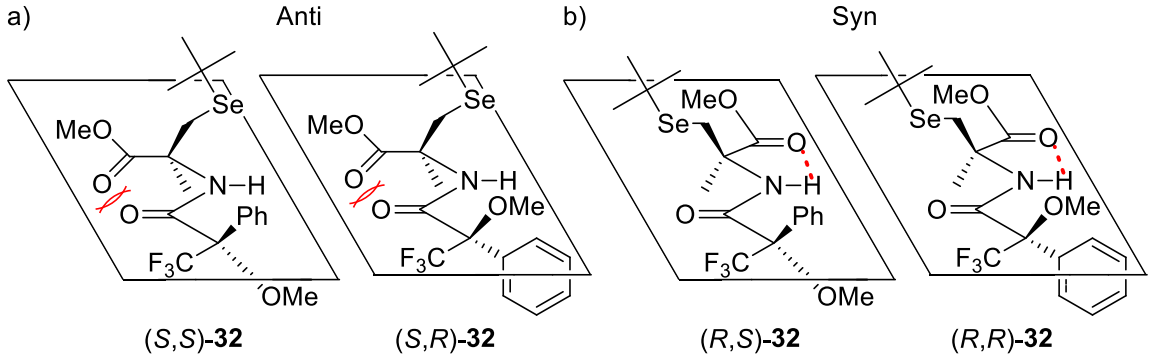

Figure 3.10 *The Anti and Syn Arrangements of the Ester of Each Amide*

After the Mosher analysis was complete, it was discovered that x-ray quality crystals were able to be grown from the enzymatic hydrolysis product **15a**. While **15a** was not used directly in the Mosher study, it was used in the synthesis of **20** using reactions that retain stereochemistry. The crystal was formed by dissolving **15a** in a minimal amount of n-octane and allowing for slow evaporation of the solvent. Single crystal x-ray diffraction was performed by Dr. Douglas Powell at the University of Oklahoma. The data confirmed an (*R*)-stereochemistry of the α-carbon, validating the results of the independent Mosher analysis (**Figure 3.11**). The crystallography was completed with ellipsoid displacement probability of 50%.

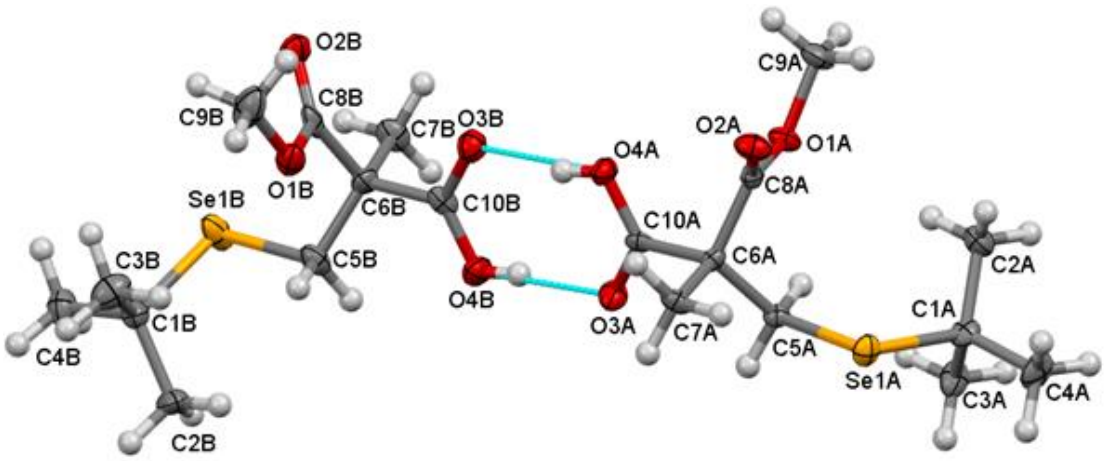

Figure 3.11 *X-Ray Crystal Structure of* ***15a***

Based on these results, the Mosher method can be used to determine the absolute configuration of a quaternary α-carbon of an enantiopure α-MeAA. To confirm the conclusions from the NMR spectral analysis, X-ray crystallography was performed on a synthetically related structure which validated the procedure. Even with the parent molecule sitting in an unconventional orientation in the MTPA-plane for the Mosher method, the magnetic anisotropy is still able to be used to correctly interpret the unknown stereochemistry by analyzing standard NMR nuclei. While only implemented on α-MeSec, the Mosher method could be extended to other α-MeAA's to determine ambiguous stereocenter configurations especially if crystallography is unable to be performed.

3.3 Experimental

3.3.1 General Procedures

All NMR spectra were obtained using a Bruker 400 MHz spectrometer in $CDCl_3$ or CD_3CN. Chemical shifts for ^1H and ^{13}C spectra are referenced from TMS (δ 0.00 ppm) with TMS as an internal standard. Chemical shifts for ^{77}Se spectra are referenced with diphenyl diselenide (δ 463 ppm) as an internal standard. All heteronuclear NMR experiments were ^1H decoupled. IR spectra were obtained from a Nicolet Nexus 470 FT-IR spectrometer with a Smart Orbit Thermo™ diamond plate ATR attachment as a solution in $CDCl_3$. Reverse phase HPLC was performed using a C18 (250 x 10 mm) Vydac column eluting with MeCN:H_2O (0-100% over 20 min.).

X-ray data was collected by Dr. Powell and obtained from a colorless, needle-shaped crystal of dimensions 0.018 x 0.018 x 0.204 mm. Intensity data for this compound were collected using a D8 Quest κ-geometry diffractometer with a Bruker Photon II CMOS area detector and an Incoatec Iμs microfocus Mo Kα source (λ = 0.71073 Å). The sample was cooled to 100 K. Cell parameters were determined from a least-squares fit of 4170 peaks in the range $2.41 < \theta < 23.51°$. A total of 33580 data were measured in the range $2.406 < \theta < 26.388°$ using ϕ and ω oscillation frames. The data were corrected for absorption by the empirical method[106] giving minimum and maximum transmission factors of 0.6704 and 0.7454. The data were merged to form a set of 5315 independent data with R(int) = 0.1288 and a coverage of 99.9 %.

The orthorhombic space group $P2_12_12_1$ was determined by systematic absences and statistical tests and verified by subsequent refinement. The structure was solved by direct methods and refined by full-matrix least-squares methods on F^2.[107-108] The

positions of hydrogens bonded to carbons were initially determined by geometry and were refined using a riding model. Hydrogens bonded to oxygens were located on a difference map, and their positions were refined independently with a restraint on the O-H distance. Non-hydrogen atoms were refined with anisotropic displacement parameters. Hydrogen atom displacement parameters were set to 1.2 (1.5 for methyl) times the isotropic equivalent displacement parameters of the bonded atoms. A total of 277 parameters were refined against 1 restraint and 5315 data to give $wR(F^2) = 0.1110$ and S = 1.008 for weights of $w = 1/[\sigma^2 (F^2) + (0.0460 P)^2]$, where $P = [F_o^2 + 2F_c^2] / 3$. The final R(*F*) was 0.0521 for the 3830 observed, [$F > 4\sigma(F)$], data. The largest shift/s.u. was 0.001 in the final refinement cycle. The final difference map had maxima and minima of 0.468 and -0.619 e/Å^3, respectively. The absolute structure was determined by refinement of the Flack parameter.[109]

3.3.2 Synthesis of (*R*)-N-Fmoc-α-MeSec(ᵗBu)-OMe (16)

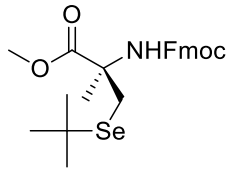

A 25 mL round bottom flask fitted with a reflux condenser was charged with a stir bar, **20** (295.0 mg, 0.640 mmol), methanol (10 mL), and concentrated sulfuric acid (20.0 µL, 0.360 mmol). The reaction mixture was heated to solvent reflux for 43 hours and the volatiles were removed *in vacuo*. The residue was reconstituted in diethyl ether (5 mL) and washed with water (3 x 3 mL). The organic phase was dried over magnesium sulfate, filtered, and concentrated *in vacuo* to afford 276.6 mg (0.582 mmol, 91%) of **16** as a

colorless oil. Spectra were identical to what was previously synthesized (See pages 50-51).

3.3.3 Synthesis of (*R*)-α-MeSec(^{t}Bu)-OMe HCl (31)

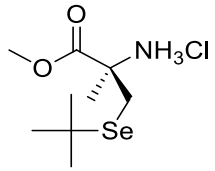

A 25 mL round bottom flask containing was charged with a stir bar, **16** (314.2 mg, 0.662 mmol), and a 20% piperidine in DMF solution (10 mL). After stirring for 30 min. at room temperature the reaction was diluted with diethyl ether (20 mL) and extracted with 0.25 M HCl (3 x 20 mL). The aqueous phase was filtered and concentrated *in vacuo* to afford 191.1 mg (0.662 mmol, quant.) of **31** as a white solid. ^{1}H NMR (400 MHz, $CDCl_3$) δ 3.83 (s, 3H), 3.19 (d, $^2J_{H\text{-}H}$ = 12.8 Hz, 1H,), 3.09 (d, $^2J_{H\text{-}H}$ = 12.8 Hz, 1H), 1.74 (s, 3H), 1.45 (s, 9H, Se satellites $^3J_{Se\text{-}H}$ 5.9 Hz); ^{13}C NMR (100 MHz, CD_3CN) δ 171.0, 61.0, 53.8, 41.6, 31.9, 27.8, 22.6; ^{77}Se NMR (76 MHz, CD_3CN) δ 327.1; HRMS (ESI^+) Calcd for $C_9H_{20}NO_2Se^+$ 254.0654 found 254.0652.

3.3.4 Synthesis of the Mosher acid chloride

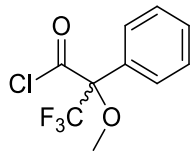

The synthesis was carried out on a 100-150 mg scale with the appropriate MTPA enantiomer based on previously reported literature procedures.[110] The reactions afforded a yellow oil (74-79%) that were pure enough to carry forward without distillation based on literature spectra.

3.3.5 General synthetic procedure N-MTPA-α-MeSec(^{t}Bu)-OMe ((*X*,*R*)-32 and (*X*,*S*)-32)

A 25 mL round bottom flask was charged with a stir bar, the appropriate Mosher acid chloride (75-150 mg), **25** (1.1-1.2 molar equivalence), DCM (3 mL), and TEA (2 molar equivalence). After stirring for 23 hrs. at room temperature the reaction was diluted with diethyl ether (5 mL) and filtered. The filtrate was concentrated *in vacuo* to afford a crude yellow-orange solid. The solid was dissolved in acetonitrile (5 mL) and purified by reverse phase HPLC (R_t = 17.1 min.) resulting in pure **26** (quantitative) as a colorless oil.

3.3.5.1 (*X*,*S*)-32

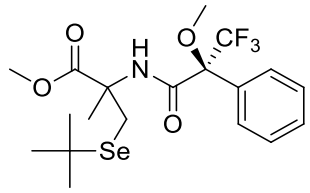

IR ($CDCl_3$, cm^{-1}) 3383, 2954, 1740, 1698, 1505, 1449; ^{1}H NMR (400 MHz, $CDCl_3$) δ 7.72 (br s, 1H), 7.60 (m, 2H), 7.40 (m, 3H), 3.78 (s, 3H), 3.50 (d, $^2J_{H\text{-}H}$ = 11.5 Hz, 1H), 3.43 (s, 3H), 3.07 (d, $^2J_{H\text{-}H}$ = 11.5 Hz, 1H), 1.71 (s, 3H), 1.40 (s, 9H, Se satellites $^3J_{Se\text{-}H}$ 5.4 Hz); ^{13}C NMR (100 MHz, $CDCl_3$) δ 173.1, 165.6, 132.2, 129.4, 128.4 128.2, 127.7, 123.8 (q, $^1J_{C\text{-}F}$ = 290.0 Hz), 84.1 (q, $^2J_{C\text{-}F}$ = 26.2 Hz), 60.2, 55.1, 53.0, 39.6, 32.3 (Se satellites $^2J_{Se\text{-}C}$ = 6.6 Hz), 28.1, 23.4; ^{19}F NMR (376 MHz, $CDCl_3$) δ -69.1; ^{77}Se NMR (76 MHz, $CDCl_3$) δ 331.1; HRMS (ESI^+) Calcd for $C_{19}H_{26}F_3NO_4Se$ $[M + H]^+$ 470.1052 found 470.1055.

3.3.5.2 (*X*,*R*)-32

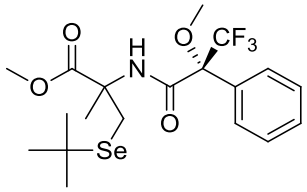

IR ($CDCl_3$, cm^{-1}) 3383, 2954, 1740, 1698, 1505, 1448; ^1H NMR (400 MHz, $CDCl_3$) δ 7.61 (br s, 1H), 7.58 (m, 2H), 7.39 (m, 3H), 3.75 (s, 3H), 3.51 (s, 3H), 3.50 (d, $^2J_{H\text{-}H}$ = 11.5 Hz, 1H), 3.04 (d, $^2J_{H\text{-}H}$ = 11.6 Hz, 1H), 1.67 (s, 3H), 1.41 (s, 9H, Se satellites $^2J_{Se\text{-}H}$ 5.5 Hz); ^{13}C NMR (100 MHz, $CDCl_3$) δ 173.0, 165.6, 132.7, 129.4, 128.4, 128.2, 127.7, 123.7 (q, $^1J_{C\text{-}F}$ = 290.0 Hz), 83.9 (q, $^2J_{C\text{-}F}$ = 26.2 Hz), 60.0 (Se satellites $^2J_{Se\text{-}C}$ = 4.0 Hz), 55.3, 52.9, 39.7 (Se satellites $^1J_{Se\text{-}C}$ = 28.6 Hz), 32.3 (Se satellites $^2J_{Se\text{-}C}$ = 6.6 Hz), 28.6 (Se satellites $^1J_{Se\text{-}C}$ = 37.4 Hz), 23.1; ^{19}F NMR (376 MHz, $CDCl_3$) δ -68.7; ^{77}Se NMR (76 MHz, $CDCl_3$) δ 330.1; HRMS (ESI^+) Calcd for $C_{19}H_{26}F_3NO_4Se$ $[M + Na]^+$ 492.0864 found 492.0871.

3.3.6 Crystal Data

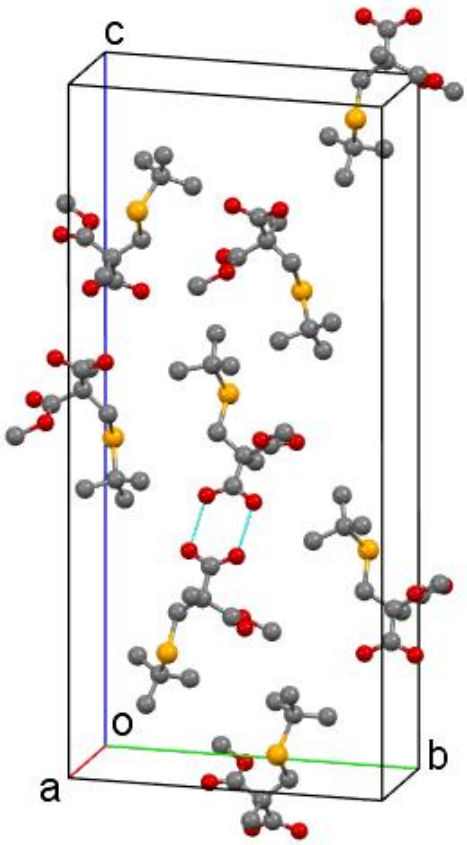

Figure 3.12 *Unit cell of* ***15a***

Table 3.1 *Crystal Data and Structure Refinement for* ***15a***

Empirical formula	$C_{10}H_{18}O_4Se$	
Formula weight	281.20	
Crystal system	orthorhombic	
Space group	$P2_12_12_1$	
Unit cell dimensions	a = 5.7779(3) Å	α= 90°
	b = 14.2158(9) Å	β= 90°
	c = 31.605(3) Å	γ= 90°
Volume	2596.0(3) $Å^3$	
Z, Z'	8, 2	
Density (calculated)	1.439 g/mL	
Wavelength	0.71073 Å	
Temperature	100(2) K	
F(000)	1152	
Absorption coefficient	2.886 mm^{-1}	
Absorption correction	Semi-empirical from equivalents	
Max. and min. transmission	0.7454 and 0.6704	
Theta range for data collection	2.406 to 26.388°	
Reflections collected	33580	
Independent reflections	5315 [R(int) = 0.1288]	
Data / restraints / parameters	5315 / 1 / 277	
wR(F2 all data)	wR2 = 0.1110	
R(F obsd data)	R1 = 0.0521	
Goodness-of-fit on F^2	1.008	
Observed data [I > 2σ(I)]	3830	
Absolute structure parameter	0.003(10)	
Largest and mean shift / s.u.	0.001 and 0.000	
Largest diff. peak and hole	0.468 and -0.619 e/$Å^3$	

Table 3.2 *Atomic coordinates and equivalent isotropic displacement parameters for* ***15a****.*

U(eq) is defined as one third of the trace of the orthogonalized Uij tensor.

	x	y	z	U(eq)
Se(1A)	0.09631(14)	0.40465(6)	0.52499(3)	0.0226(2)
O(1A)	0.5841(9)	0.5642(3)	0.48619(16)	0.0210(13)
O(2A)	0.2526(9)	0.6393(4)	0.4703(2)	0.0263(14)
O(3A)	0.5068(10)	0.3822(4)	0.39683(18)	0.0257(14)
O(4A)	0.5460(9)	0.5374(4)	0.39408(18)	0.0227(15)
C(1A)	0.2904(14)	0.3749(5)	0.5751(3)	0.0212(19)
C(2A)	0.4615(14)	0.4529(6)	0.5836(3)	0.029(2)
C(3A)	0.4168(16)	0.2817(5)	0.5690(3)	0.029(2)
C(4A)	0.1139(16)	0.3667(6)	0.6113(3)	0.033(2)
C(5A)	0.3274(11)	0.3949(5)	0.4798(2)	0.0158(17)
C(6A)	0.3054(12)	0.4778(5)	0.4483(3)	0.0166(18)
C(7A)	0.0627(12)	0.4851(5)	0.4291(3)	0.0207(19)
C(8A)	0.3726(13)	0.5706(5)	0.4694(2)	0.0189(17)
C(9A)	0.6735(13)	0.6506(6)	0.5040(3)	0.029(2)
C(10A)	0.4668(12)	0.4625(5)	0.4111(3)	0.0164(18)
Se(1B)	1.10849(16)	0.32673(7)	0.19572(3)	0.0342(3)
O(1B)	0.7181(9)	0.5208(4)	0.23474(18)	0.0280(15)
O(2B)	1.0845(10)	0.5721(4)	0.23841(17)	0.0288(14)
O(3B)	0.7974(9)	0.5120(4)	0.32698(19)	0.0270(14)
O(4B)	0.7559(11)	0.3555(4)	0.3279(2)	0.0307(16)
C(1B)	0.8856(16)	0.2771(5)	0.1532(2)	0.0234(18)
C(2B)	0.7610(16)	0.1911(6)	0.1710(3)	0.035(2)
C(3B)	0.7106(15)	0.3528(6)	0.1415(3)	0.037(2)
C(4B)	1.0382(14)	0.2509(6)	0.1160(3)	0.031(2)
C(5B)	0.9098(14)	0.3370(6)	0.2456(2)	0.0255(19)
C(6B)	0.9781(13)	0.4232(6)	0.2718(3)	0.023(2)
C(7B)	1.2309(12)	0.4184(6)	0.2867(3)	0.027(2)
C(8B)	0.9430(13)	0.5135(6)	0.2464(3)	0.024(2)
C(9B)	0.6548(15)	0.6076(7)	0.2147(3)	0.041(3)
C(10B)	0.8292(12)	0.4318(6)	0.3114(3)	0.0193(19)

Table 3.3 *Bond Lengths [Å]* ***15a***

Bond	Length	Bond	Length
Se(1A)-C(5A)	1.960(7)	Se(1B)-C(5B)	1.956(8)
Se(1A)-C(1A)	1.985(8)	Se(1B)-C(1B)	1.991(8)
O(1A)-C(8A)	1.335(9)	O(1B)-C(8B)	1.355(9)
O(1A)-C(9A)	1.447(9)	O(1B)-C(9B)	1.434(10)
O(2A)-C(8A)	1.198(8)	O(2B)-C(8B)	1.195(9)
O(3A)-C(10A)	1.250(9)	O(3B)-C(10B)	1.256(9)
O(4A)-C(10A)	1.278(9)	O(4B)-C(10B)	1.275(10)
O(4A)-H(4A)	0.75(6)	O(4B)-H(4B)	0.75(6)
C(1A)-C(2A)	1.511(11)	C(1B)-C(4B)	1.515(11)
C(1A)-C(3A)	1.524(10)	C(1B)-C(3B)	1.522(11)
C(1A)-C(4A)	1.538(11)	C(1B)-C(2B)	1.526(11)
C(2A)-H(2A1)	0.98	C(2B)-H(2B1)	0.98
C(2A)-H(2A2)	0.98	C(2B)-H(2B2)	0.98
C(2A)-H(2A3)	0.98	C(2B)-H(2B3)	0.98
C(3A)-H(3A1)	0.98	C(3B)-H(3B1)	0.98
C(3A)-H(3A2)	0.98	C(3B)-H(3B2)	0.98
C(3A)-H(3A3)	0.98	C(3B)-H(3B3)	0.98
C(4A)-H(4A1)	0.98	C(4B)-H(4B1)	0.98
C(4A)-H(4A2)	0.98	C(4B)-H(4B2)	0.98
C(4A)-H(4A3)	0.98	C(4B)-H(4B3)	0.98
C(5A)-C(6A)	1.547(10)	C(5B)-C(6B)	1.531(11)
C(5A)-H(5A1)	0.99	C(5B)-H(5B1)	0.99
C(5A)-H(5A2)	0.99	C(5B)-H(5B2)	0.99
C(6A)-C(10A)	1.515(10)	C(6B)-C(10B)	1.524(11)
C(6A)-C(8A)	1.528(10)	C(6B)-C(8B)	1.529(12)
C(6A)-C(7A)	1.531(10)	C(6B)-C(7B)	1.536(10)
C(7A)-H(7A1)	0.98	C(7B)-H(7B1)	0.98
C(7A)-H(7A2)	0.98	C(7B)-H(7B2)	0.98
C(7A)-H(7A3)	0.98	C(7B)-H(7B3)	0.98
C(9A)-H(9A1)	0.98	C(9B)-H(9B1)	0.98
C(9A)-H(9A2)	0.98	C(9B)-H(9B2)	0.98
C(9A)-H(9A3)	0.98	C(9B)-H(9B3)	0.98

Table 3.4 *Bond Angles [°] for* ***15a***

Bonds	Angle	Bonds	Angle
C(5A)-Se(1A)-C(1A)	100.5(3)	C(5B)-Se(1B)-C(1B)	101.0(3)
C(8A)-O(1A)-C(9A)	115.1(6)	C(8B)-O(1B)-C(9B)	115.5(7)
C(10A)-O(4A)-H(4A)	110(7)	C(10B)-O(4B)-H(4B)	111(8)
C(2A)-C(1A)-C(3A)	110.3(7)	C(4B)-C(1B)-C(3B)	111.8(7)
C(2A)-C(1A)-C(4A)	110.9(7)	C(4B)-C(1B)-C(2B)	111.3(7)
C(3A)-C(1A)-C(4A)	110.2(7)	C(3B)-C(1B)-C(2B)	110.0(7)
C(2A)-C(1A)-Se(1A)	110.8(6)	C(4B)-C(1B)-Se(1B)	103.5(6)
C(3A)-C(1A)-Se(1A)	110.9(6)	C(3B)-C(1B)-Se(1B)	110.1(6)
C(4A)-C(1A)-Se(1A)	103.6(5)	C(2B)-C(1B)-Se(1B)	109.9(6)
C(1A)-C(2A)-H(2A1)	109.5	C(1B)-C(2B)-H(2B1)	109.5
C(1A)-C(2A)-H(2A2)	109.5	C(1B)-C(2B)-H(2B2)	109.5
H(2A1)-C(2A)-H(2A2)	109.5	H(2B1)-C(2B)-H(2B2)	109.5
C(1A)-C(2A)-H(2A3)	109.5	C(1B)-C(2B)-H(2B3)	109.5
H(2A1)-C(2A)-H(2A3)	109.5	H(2B1)-C(2B)-H(2B3)	109.5
H(2A2)-C(2A)-H(2A3)	109.5	H(2B2)-C(2B)-H(2B3)	109.5
C(1A)-C(3A)-H(3A1)	109.5	C(1B)-C(3B)-H(3B1)	109.5
C(1A)-C(3A)-H(3A2)	109.5	C(1B)-C(3B)-H(3B2)	109.5
H(3A1)-C(3A)-H(3A2)	109.5	H(3B1)-C(3B)-H(3B2)	109.5
C(1A)-C(3A)-H(3A3)	109.5	C(1B)-C(3B)-H(3B3)	109.5
H(3A1)-C(3A)-H(3A3)	109.5	H(3B1)-C(3B)-H(3B3)	109.5
H(3A2)-C(3A)-H(3A3)	109.5	H(3B2)-C(3B)-H(3B3)	109.5
C(1A)-C(4A)-H(4A1)	109.5	C(1B)-C(4B)-H(4B1)	109.5
C(1A)-C(4A)-H(4A2)	109.5	C(1B)-C(4B)-H(4B2)	109.5
H(4A1)-C(4A)-H(4A2)	109.5	H(4B1)-C(4B)-H(4B2)	109.5
C(1A)-C(4A)-H(4A3)	109.5	C(1B)-C(4B)-H(4B3)	109.5
H(4A1)-C(4A)-H(4A3)	109.5	H(4B1)-C(4B)-H(4B3)	109.5
H(4A2)-C(4A)-H(4A3)	109.5	H(4B2)-C(4B)-H(4B3)	109.5
C(6A)-C(5A)-Se(1A)	111.1(5)	C(6B)-C(5B)-Se(1B)	110.2(5)
C(6A)-C(5A)-H(5A1)	109.4	C(6B)-C(5B)-H(5B1)	109.6
Se(1A)-C(5A)-H(5A1)	109.4	Se(1B)-C(5B)-H(5B1)	109.6
C(6A)-C(5A)-H(5A2)	109.4	C(6B)-C(5B)-H(5B2)	109.6
Se(1A)-C(5A)-H(5A2)	109.4	Se(1B)-C(5B)-H(5B2)	109.6
H(5A1)-C(5A)-H(5A2)	108	H(5B1)-C(5B)-H(5B2)	108.1
C(10A)-C(6A)-C(8A)	107.8(6)	C(10B)-C(6B)-C(8B)	106.9(7)
C(10A)-C(6A)-C(7A)	105.5(6)	C(10B)-C(6B)-C(5B)	111.3(6)
C(8A)-C(6A)-C(7A)	110.3(6)	C(8B)-C(6B)-C(5B)	110.7(7)

Table 3.4 *(continued)*

Bonds	Angle	Bonds	Angle
C(10A)-C(6A)-C(5A)	109.8(6)	C(10B)-C(6B)-C(7B)	106.8(7)
C(8A)-C(6A)-C(5A)	110.8(6)	C(8B)-C(6B)-C(7B)	108.9(7)
C(7A)-C(6A)-C(5A)	112.4(6)	C(5B)-C(6B)-C(7B)	112.1(7)
C(6A)-C(7A)-H(7A1)	109.5	C(6B)-C(7B)-H(7B1)	109.5
C(6A)-C(7A)-H(7A2)	109.5	C(6B)-C(7B)-H(7B2)	109.5
H(7A1)-C(7A)-H(7A2)	109.5	H(7B1)-C(7B)-H(7B2)	109.5
C(6A)-C(7A)-H(7A3)	109.5	C(6B)-C(7B)-H(7B3)	109.5
H(7A1)-C(7A)-H(7A3)	109.5	H(7B1)-C(7B)-H(7B3)	109.5
H(7A2)-C(7A)-H(7A3)	109.5	H(7B2)-C(7B)-H(7B3)	109.5
O(2A)-C(8A)-O(1A)	125.1(7)	O(2B)-C(8B)-O(1B)	123.1(8)
O(2A)-C(8A)-C(6A)	124.6(7)	O(2B)-C(8B)-C(6B)	127.3(7)
O(1A)-C(8A)-C(6A)	110.3(6)	O(1B)-C(8B)-C(6B)	109.6(7)
O(1A)-C(9A)-H(9A1)	109.5	O(1B)-C(9B)-H(9B1)	109.5
O(1A)-C(9A)-H(9A2)	109.5	O(1B)-C(9B)-H(9B2)	109.5
H(9A1)-C(9A)-H(9A2)	109.5	H(9B1)-C(9B)-H(9B2)	109.5
O(1A)-C(9A)-H(9A3)	109.5	O(1B)-C(9B)-H(9B3)	109.5
H(9A1)-C(9A)-H(9A3)	109.5	H(9B1)-C(9B)-H(9B3)	109.5
H(9A2)-C(9A)-H(9A3)	109.5	H(9B2)-C(9B)-H(9B3)	109.5
O(3A)-C(10A)-O(4A)	122.9(7)	O(3B)-C(10B)-O(4B)	124.4(8)
O(3A)-C(10A)-C(6A)	121.7(7)	O(3B)-C(10B)-C(6B)	118.5(8)
O(4A)-C(10A)-C(6A)	115.3(7)	O(4B)-C(10B)-C(6B)	117.0(7)

Table 3.5 *Anisotropic displacement parameters ($Å^2 x\ 10^3$) for* ***15a***.

The anisotropic displacement factor exponent takes the form: $-2\ \pi^2[\ h^2\ a^{*2}\ U_{11} + ... + 2\ h\ k\ a^*\ b^*\ U_{12}]$

	U_{11}	U_{22}	U_{33}	U_{23}	U_{13}	U_{12}
Se(1A)	16(1)	31(1)	21(1)	1(1)	3(1)	1(1)
O(1A)	16(3)	19(3)	29(3)	-5(2)	-2(3)	-1(3)
O(2A)	22(3)	20(3)	38(4)	-5(3)	-2(3)	1(3)
O(3A)	37(3)	17(3)	23(3)	-1(3)	6(3)	5(2)
O(4A)	28(4)	21(3)	20(3)	-1(3)	8(3)	-2(3)
C(1A)	24(4)	14(4)	26(5)	3(4)	3(4)	5(4)
C(2A)	33(5)	28(5)	25(5)	-6(4)	-2(4)	-4(4)
C(3A)	35(5)	27(5)	24(5)	2(4)	7(5)	11(5)
C(4A)	30(5)	38(5)	30(5)	2(4)	18(5)	0(5)
C(5A)	15(3)	14(4)	19(4)	0(4)	0(3)	1(3)
C(6A)	15(4)	17(4)	17(5)	3(4)	3(3)	0(3)
C(7A)	15(4)	21(4)	26(5)	-5(4)	-5(4)	-1(3)
C(8A)	23(4)	18(4)	15(4)	-1(3)	5(4)	-1(4)
C(9A)	28(5)	26(5)	32(6)	-12(4)	-1(4)	-7(4)
C(10A)	12(4)	16(4)	22(5)	-1(4)	-3(3)	-3(3)
Se(1B)	22(1)	52(1)	28(1)	-18(1)	7(1)	-9(1)
O(1B)	21(3)	40(4)	24(4)	4(3)	-2(3)	-5(3)
O(2B)	23(3)	38(4)	26(3)	3(3)	2(3)	-4(3)
O(3B)	30(3)	27(4)	24(4)	-1(3)	4(3)	2(3)
O(4B)	36(4)	31(4)	26(4)	-3(3)	12(3)	-11(3)
C(1B)	28(4)	23(4)	20(5)	-1(4)	1(4)	-3(4)
C(2B)	48(6)	28(5)	29(6)	7(5)	-3(5)	-19(5)
C(3B)	31(5)	33(6)	46(7)	7(5)	9(5)	4(4)
C(4B)	36(5)	32(5)	24(5)	-1(4)	2(4)	5(4)
C(5B)	19(4)	31(5)	27(5)	-8(4)	-3(4)	-2(4)
C(6B)	21(4)	27(5)	21(5)	-1(4)	5(4)	-7(4)
C(7B)	15(4)	36(6)	30(5)	-7(4)	0(4)	1(4)
C(8B)	18(5)	39(5)	14(5)	-11(4)	3(4)	-2(4)
C(9B)	32(6)	60(7)	32(6)	16(5)	-5(4)	-3(5)
C(10B)	11(4)	23(5)	24(5)	-7(4)	-2(3)	4(3)

Table 3.6 *Hydrogen coordinates and isotropic displacement parameters for* ***15a***

	x	y	z	U(eq)
H(4A)	0.600(15)	0.526(6)	0.373(2)	0.03
H(2A1)	0.38	0.51	0.59	0.04
H(2A2)	0.55	0.44	0.61	0.04
H(2A3)	0.57	0.46	0.56	0.04
H(3A1)	0.3	0.23	0.56	0.04
H(3A2)	0.52	0.29	0.54	0.04
H(3A3)	0.5	0.27	0.59	0.04
H(4A1)	0	0.32	0.61	0.05
H(4A2)	0.2	0.35	0.64	0.05
H(4A3)	0.03	0.43	0.61	0.05
H(5A1)	0.48	0.39	0.49	0.02
H(5A2)	0.31	0.33	0.46	0.02
H(7A1)	-0.05	0.5	0.45	0.03
H(7A2)	0.06	0.54	0.41	0.03
H(7A3)	0.03	0.43	0.41	0.03
H(9A1)	0.83	0.64	0.52	0.04
H(9A2)	0.68	0.7	0.48	0.04
H(9A3)	0.57	0.67	0.53	0.04
H(4B)	0.698(15)	0.365(7)	0.349(2)	0.04
H(2B1)	0.66	0.21	0.19	0.05
H(2B2)	0.66	0.16	0.15	0.05
H(2B3)	0.88	0.14	0.18	0.05
H(3B1)	0.62	0.37	0.17	0.06
H(3B2)	0.79	0.41	0.13	0.06
H(3B3)	0.61	0.33	0.12	0.06
H(4B1)	1.15	0.2	0.12	0.05
H(4B2)	0.94	0.23	0.09	0.05
H(4B3)	1.12	0.31	0.11	0.05
H(5B1)	0.75	0.34	0.24	0.03
H(5B2)	0.93	0.28	0.26	0.03
H(7B1)	1.33	0.41	0.26	0.04
H(7B2)	1.27	0.48	0.3	0.04
H(7B3)	1.25	0.36	0.31	0.04
H(9B1)	0.49	0.61	0.21	0.06
H(9B2)	0.68	0.66	0.23	0.06
H(9B3)	0.75	0.62	0.19	0.06

Table 3.7 *Torsion angles [°] for* ***15a***

Bonds	Angle
Se(1A)-C(5A)-C(6A)-C(10A)	-173.5(5)
Se(1A)-C(5A)-C(6A)-C(8A)	67.5(7)
Se(1A)-C(5A)-C(6A)-C(7A)	-56.5(8)
C(9A)-O(1A)-C(8A)-O(2A)	-4.2(11)
C(9A)-O(1A)-C(8A)-C(6A)	175.2(6)
C(10A)-C(6A)-C(8A)-O(2A)	113.9(8)
C(7A)-C(6A)-C(8A)-O(2A)	-0.7(11)
C(5A)-C(6A)-C(8A)-O(2A)	-125.9(8)
C(10A)-C(6A)-C(8A)-O(1A)	-65.4(8)
C(7A)-C(6A)-C(8A)-O(1A)	179.9(6)
C(5A)-C(6A)-C(8A)-O(1A)	54.7(8)
C(8A)-C(6A)-C(10A)-O(3A)	155.8(7)
C(7A)-C(6A)-C(10A)-O(3A)	-86.3(9)
C(5A)-C(6A)-C(10A)-O(3A)	35.0(10)
C(8A)-C(6A)-C(10A)-O(4A)	-28.5(9)
C(7A)-C(6A)-C(10A)-O(4A)	89.4(8)
C(5A)-C(6A)-C(10A)-O(4A)	-149.3(7)
Se(1B)-C(5B)-C(6B)-C(10B)	-178.8(5)
Se(1B)-C(5B)-C(6B)-C(8B)	62.5(7)
Se(1B)-C(5B)-C(6B)-C(7B)	-59.3(8)
C(9B)-O(1B)-C(8B)-O(2B)	-4.6(11)
C(9B)-O(1B)-C(8B)-C(6B)	173.2(7)
C(10B)-C(6B)-C(8B)-O(2B)	115.5(9)
C(5B)-C(6B)-C(8B)-O(2B)	-123.1(9)
C(7B)-C(6B)-C(8B)-O(2B)	0.5(12)
C(10B)-C(6B)-C(8B)-O(1B)	-62.1(8)
C(5B)-C(6B)-C(8B)-O(1B)	59.2(8)
C(7B)-C(6B)-C(8B)-O(1B)	-177.1(7)
C(8B)-C(6B)-C(10B)-O(3B)	-31.8(9)
C(5B)-C(6B)-C(10B)-O(3B)	-152.7(7)
C(7B)-C(6B)-C(10B)-O(3B)	84.7(9)
C(8B)-C(6B)-C(10B)-O(4B)	152.0(7)
C(5B)-C(6B)-C(10B)-O(4B)	31.1(10)
C(7B)-C(6B)-C(10B)-O(4B)	-91.6(9)

Table 3.8 *Hydrogen bonds for **15a** [Å and °]*

D-H...A	d(D-H)	d(H...A)	d(D...A)	<(DHA)
O(4A)-H(4A)...O(3B)	0.75(6)	1.87(6)	2.596(8)	166(10)
O(4B)-H(4B)...O(3A)	0.75(6)	1.90(6)	2.640(8)	171(10)
C(2B)-H(2B2)...O(4A)#1	0.98	2.55	3.485(11)	159
C(4B)-H(4B2)...O(2A)#1	0.98	2.61	3.576(11)	169
C(9B)-H(9B1)...O(2B)#2	0.98	2.58	3.416(10)	143

CHAPTER IV – SYNTHESIS TOWARDS AN ASYMMETRIC GLUTATHIONE DISULFIDE

4.1 Background

Glutathione peroxidase (GPx) is a selenoprotein that can reduce hydrogen peroxide, radical species, and other reactive oxidative species to benign and unreactive compounds. During the catalytic cycle, the selenium of GPx is oxidized to a selenenic acid[24, 111] and needs to be reduced to become reactivated. The reduction is completed in two steps using two molar equivalence of the tripeptide glutathione (GSH), with GSH leaving as the oxidized disulfide, glutathione disulfide (GSSG). As GSSG, it is unable to perform any other reductions and needs to be reduced to a thiol. The enzyme glutathione reductase (GR) is responsible for the reduction of GSSG back to GSH.

Glutathione reductase was first discovered in pea cells in 1951,[112] was later discovered in animal tissues in 1952,[113] and was isolated from yeast in 1955.[114] It has a very limited substrate scope only known to catalyze the reduction of GSSG; not even cystine or homocystine can be reduced. These results suggest that the amino acids adjacent to Cys in GSSG are important in substrate reactivity. Past research has incorporated α-MeCys within GSSG to form an unnatural glutathione disulfide (G'SSG'), this however acted as a competitive inhibitor of GR.[50] Acting as a competitive inhibitor, G'SSG' is able to fit in the active site, however the enzyme is unable to act upon it. Based on computational analysis, this is caused by a deviation in the dihedral angle, χ_3, from the normal range of approximately 90° while in the active site. The steric effects of the α-methyl groups present in G'SSG' causes the dihedral angle to constrict to

62°, which prevents GR from acting on G'SSG' (**Figure 4.1**). To enable normal or partially inhibited enzymatic function, a χ_3 dihedral angle closer to the normal value will be required. It is hypothesized that normal or partial inhibition of GR can be achieved through the asymmetric glutathione disulfide G'SSG. The reduced steric bulk should allow for increased mobility around the disulfide bond in G'SSG, allowing for χ_3 to approach closer to normal angles in the active site of GR.

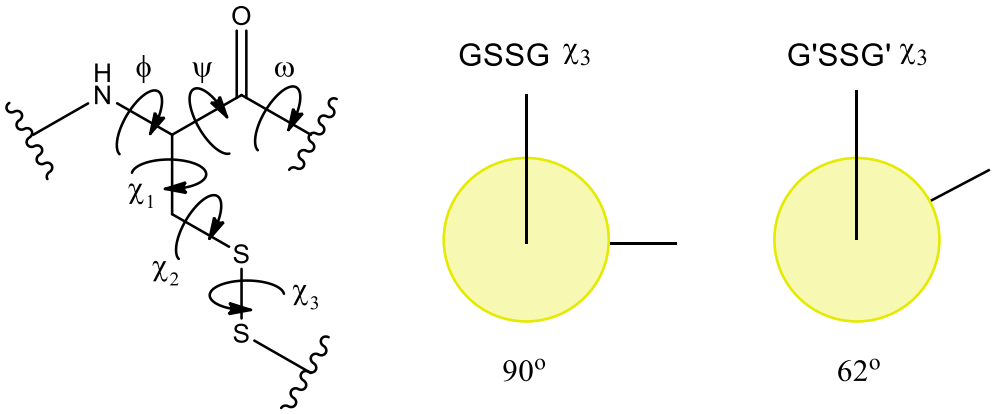

Figure 4.1 *The χ_3 Dihedral Angles of GSSG and G'SSG' as Modelled in GR*

Biologically, GSSG is created by the oxidation of two molar equivalences of GSH to form a symmetric disulfide. Using hydrogen peroxide as the oxidant, GSSG can be synthesized in an identical manner in a laboratory setting. Previously, G'SH was synthesized in the Masterson lab utilizing solution phase peptide synthesis, and then oxidized to G'SSG' with oxygen.[115] This method cannot be used to efficiently create an asymmetric disulfide, such as G'SSG, otherwise a mixture of products will form, GSSG, G'SSG, and G'SSG'.

Different synthetic methods are used to create asymmetric disulfides with peptides and other biomacromolecular structures. Taking advantage of sulfur's

nucleophilicity, the thiolate can attack a disulfide bond, substituting one thiolate for another creating a new disulfide linkage.[116] In past literature, the kinetics of the thiol-disulfide exchange have been examined, and it was discovered that without catalytic base the exchange is extremely slow since the thiol is much less nucleophilic than the thiolate.[117] The thiol exchange happens as an S_N2 mechanism forming a three membered intermediate between the sulfurs with the negative charge delocalized between the exterior sulfurs (**Figure 4.2**).[118]

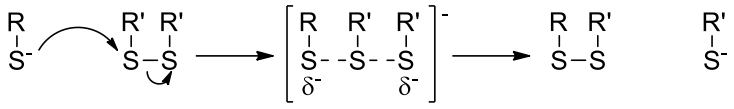

Figure 4.2 *General Mechanism for Thiol-Disulfide Exchange*

While this method is straightforward, there are issues that can arise when attempting this chemistry with small molecules. Many of the exchanges are reversible which can cause a mixture of products. Another problem with the thiol-disulfide exchange method is that any trace amounts of thiol present with the desired mixed disulfide can cause an exchange, even at a lower pH since the ionization of a thiol is in equilibrium.[118]

To overcome the problem of byproducts, many chemists choose to activate one of the thiols, by either creating a sulfenyl halide,[119-120] Bunte salts,[121-122] sulfonium salts,[123-124] or many other electrophilic sulfur species.[125-127] Many of these methods, however, rely on employing harsh reagents, or involve multiple steps with purifications. After the first thiol is activated and purified, the second thiol is added creating the asymmetric disulfide (**Scheme 4.1**).

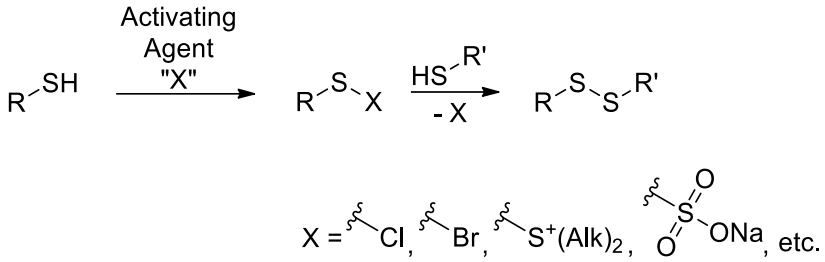

Scheme 4.1 *Asymmetric Disulfide Synthesis*

Hunter *et al*. developed a method using 1-chlorobenzotriazole (BtCl) in tandem with benzotriazole (BtH) to activate a thiol, which can then be reacted with the second thiol in one pot to produce an asymmetric disulfide (**Scheme 4.2**).[128] This method allows for the direct synthesis of the asymmetric disulfide without intermediary purification steps using mild reagents.

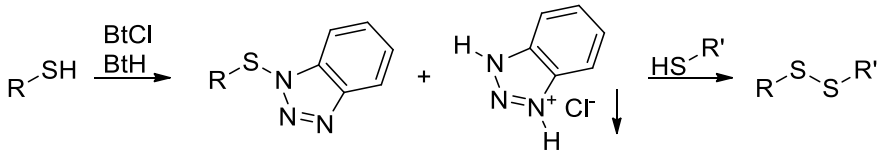

Scheme 4.2 *Hunter's Approach to Asymmetric Disulfides*

4.2 Asymmetric Glutathione Core Synthesis

With the synthesis of *N*-Boc-α-MeCys-OMe, it is hypothesized that using the strategy established by Hunter *et* al.[128] an asymmetric cystine core can be created and then elaborated to form G'SSG.

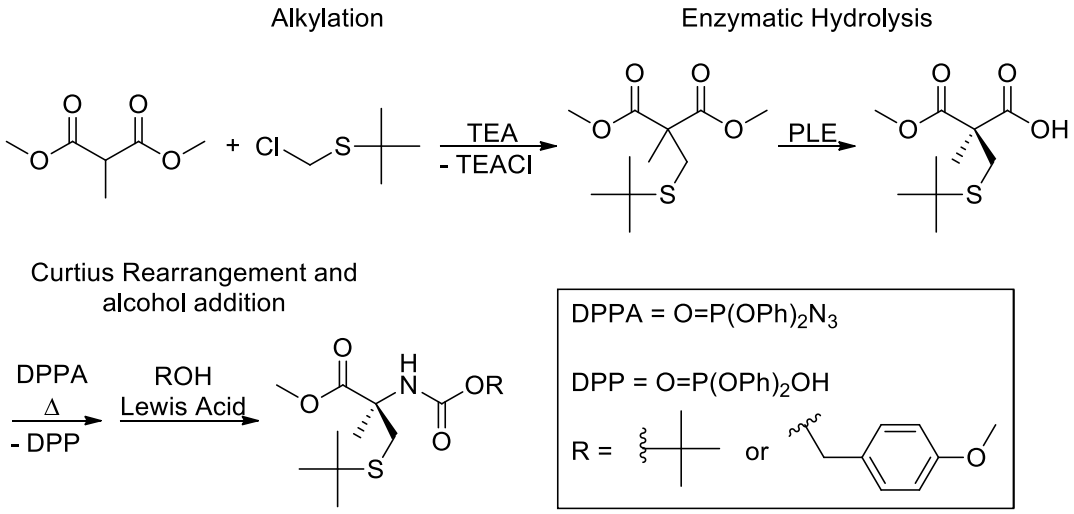

Scheme 4.3 *Route to Synthesize the Protected Cysteine Amino Ester*

The first step in forming the glutathione core was to first synthesize an appropriate α-MeCys analogue. In most steps the chemistry is analogous to the synthesis of α-MeSec, including an initial alkylation, enzymatic hydrolysis, Curtius rearrangement, and an alcohol addition (**Scheme 4.3**).

Synthesis of the thio-alkylated malonate **34** was straightforward and did not suffer from the synthetic problems that the selenium analogue possessed (**Scheme 4.4**). The alkylating agent **33** was directly synthesized from the commercially available *tert*-butylthiol, with no need for reducing agents that could interfere with later reactions. The synthesis of **33** was very high yielding and did not require purification.

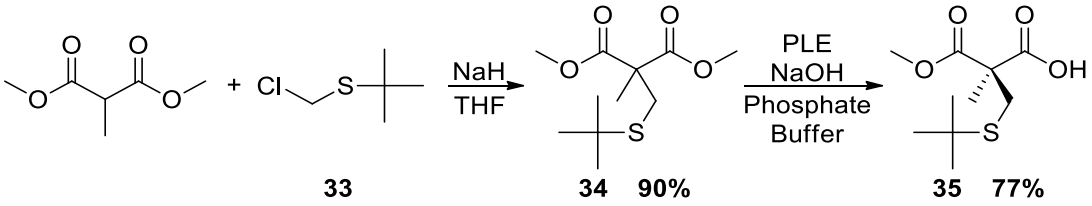

Scheme 4.4 *Synthesis the Half-Ester **35***

The enzymatic hydrolysis of **34** to produce the half-ester **35** was an efficient reaction obtaining yields comparable to what is in the literature.[115]

Once **35** was synthesized, a Curtius rearrangement was used to create an isocyanate intermediate (**Scheme 4.5**). Following what has been done in the literature, 4-methoxybenzyl alcohol was used in the alcohol addition to the isocyanate, producing the Moz-protected amine **36** in reasonable yields. In addition, *tert*-butyl alcohol was used forming the Boc-protected amine **37**. The benefit to synthesizing **37** is that purification is simplified by passing the crude material through silica, eluting with 8:1 hexanes/ethyl acetate, and collecting eluant until colorless, while the purification of **36** involves traditional column chromatography, monitoring each fraction for product. The disadvantage to synthesizing **37** is that a Lewis acid is needed to overcome the steric effects imposed by *tert*-butyl alcohol.

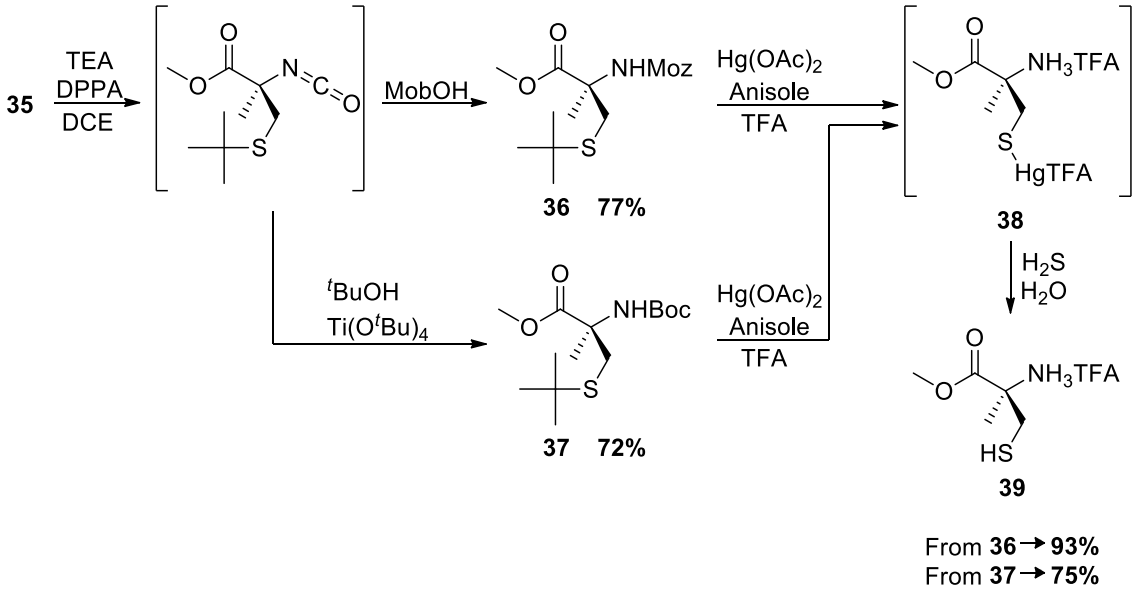

Scheme 4.5 *Transformation of Half-Ester **35** to Thiol **39***

Both **36** and **37** can be used to in the thiol deprotection step to produce **39**, however better yields are obtained when proceeding from **36**. This deprotection is accomplished with mercury acetate in TFA, creating the mercury adduct **38**.[129] The adduct is converted into the desired thiol **39** by bubbling hydrogen sulfide through an aqueous suspension.

Once **39** was synthesized, the amine needed to be reprotected for the asymmetric disulfide step. Attempting an *N*-Boc protection with di-*tert*-butyl dicarbonate (Boc_2O) resulted in low yields of the desired *N*-Boc protected amine **40** (**Scheme 4.6**). From NMR analysis a major unwanted product from this reaction is the *S*-Boc protected compound **41** (**Figure 4.3**). From literature precedence, it was possible to selectively deprotect the sulfur of **41** with sodium hydroxide,[130] however this method was only successful in hydrolyzing the methyl ester.

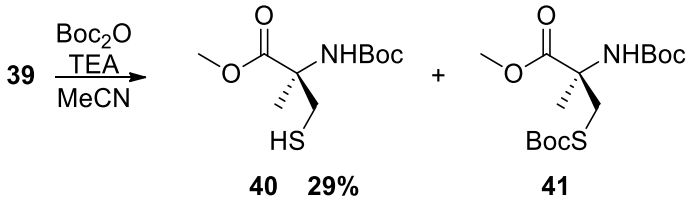

40 **29%** **41**

Scheme 4.6 *N-Boc Protection of the Free Amine*

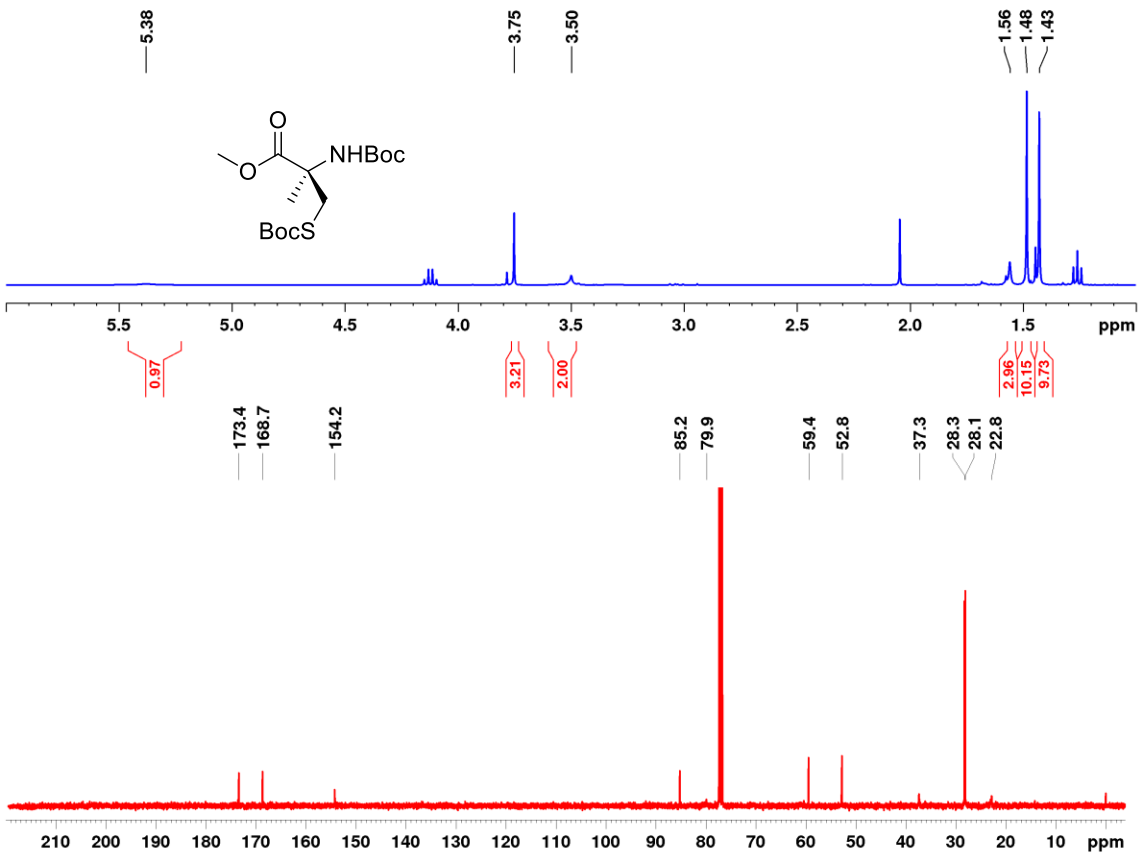

Figure 4.3 *The ^{1}H and ^{13}C NMR Spectra of the Byproduct* ***41***

In attempts to find an efficient route to **40**, alternative deprotection methods were explored. One method explored was utilizing dimethyl(methylthio)sulfonium triflate (DMTST). Under these conditions, **37** should be converted into a mixed disulfide, which could then be reduced to form **40** without affecting the *N*-Boc (**Scheme 4.7**),[131] however this reaction failed to produce the intermediate mixed disulfide. Another strategy attempted was Boc protecting the ammonium salt of **38** before the mercury was removed, but this method was unsuccessful.

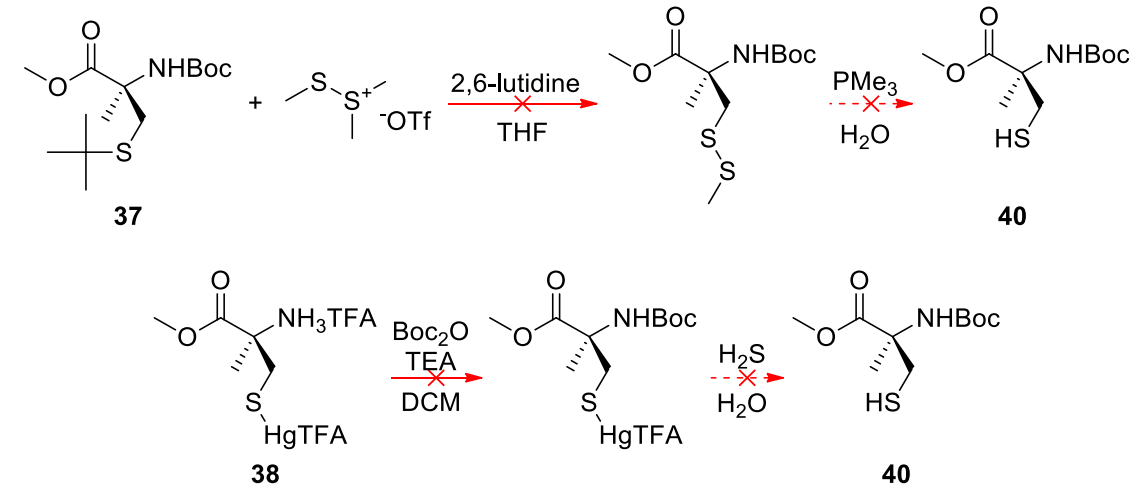

Scheme 4.7 *Failed Alternative Routes to* ***40***

With the isolation of **40**, the asymmetric G'SSG core could be synthesized applying the method proposed by Hunter *et al.*[128] Using the method as proposed, **42** was produced in low yield, with thiourea adducts and cystine contributing to the loss of yield (**Scheme 4.8**) which was verified by MS (**Figure 4.4**).

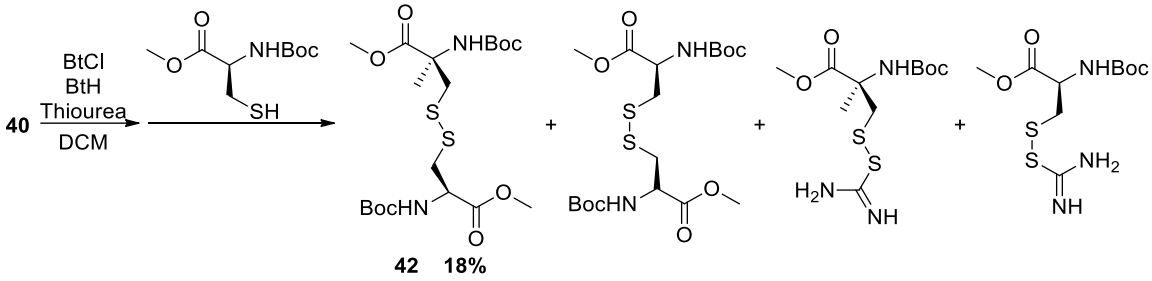

Scheme 4.8 *Formation of the Asymmetric G'SSG core*

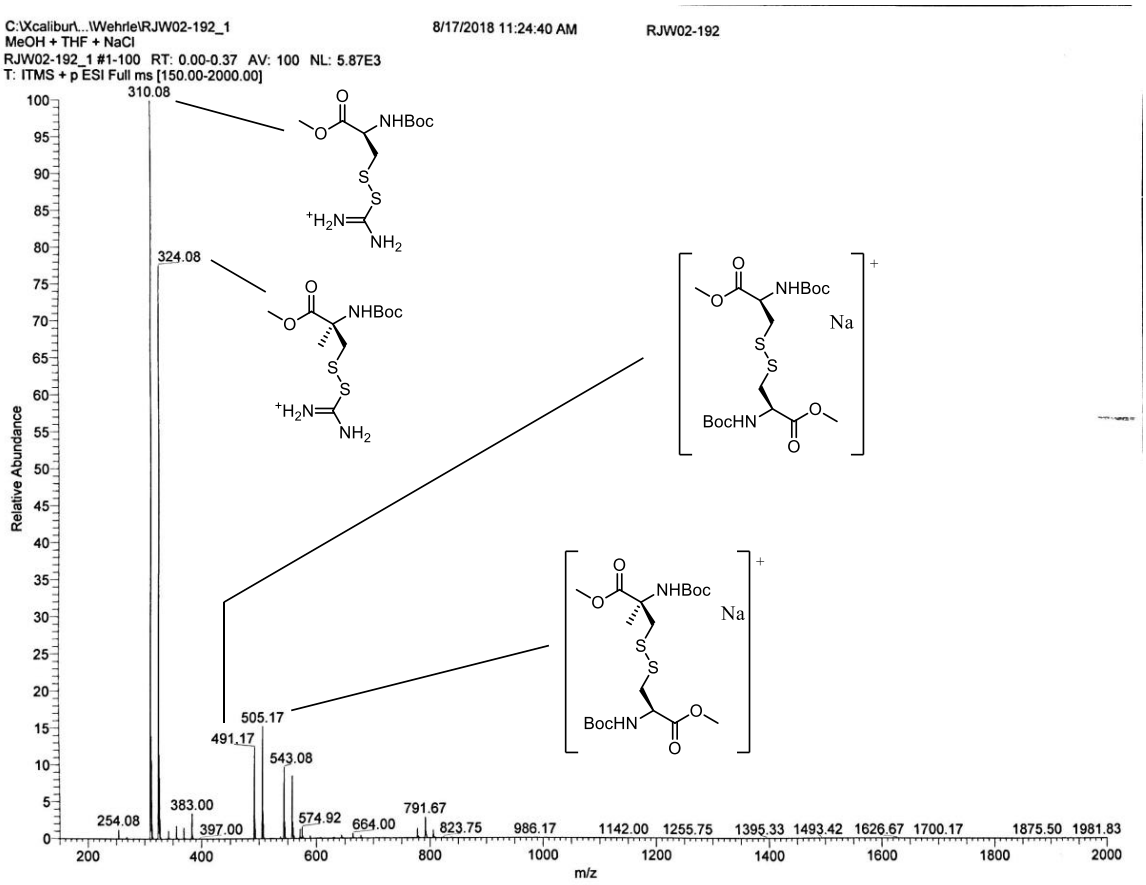

Figure 4.4 *Mass Spectrograph of the Crude Product from the Asymmetric Disulfide Synthesis*

Based on the literature, the yield was expected to be higher, however based on the byproducts formed, the stoichiometry recommended seems incorrect. To ensure complete conversion to the activated thiol as seen in **Scheme 4.2**, excess BtCl is used. To quench the excess BtCl, thiourea is employed, however the paper uses a large excess which is the probable cause of most of the byproducts.

4.3 Future Work

With the synthesis of the G'SSG core **42** synthesized, elaboration to form G'SSG is needed. Using solution phase peptide synthesis, the asymmetric cystine core can be elaborated to synthesize G'SSG. The first main step in the synthesis would be the hydrolysis of the methyl ester to allow for the coupling of a glycine analogue (**Scheme 4.9**). An acid catalyzed ester hydrolysis can potentially cause a Boc deprotection of the amine, which would ruin the following coupling step, and a base catalyzed ester hydrolysis could induce disulfide shuffling, causing a mixture of disulfides to form. The best course of action would be an enzymatic hydrolysis to form **43**, which prevents the potential for side reactions. A glycine alkyl ester can be coupled to the carboxylic acid of **43** to produce the tetrapeptide **44**, which the nitrogen can be then be deprotected with TFA to yield the free amine **45**.

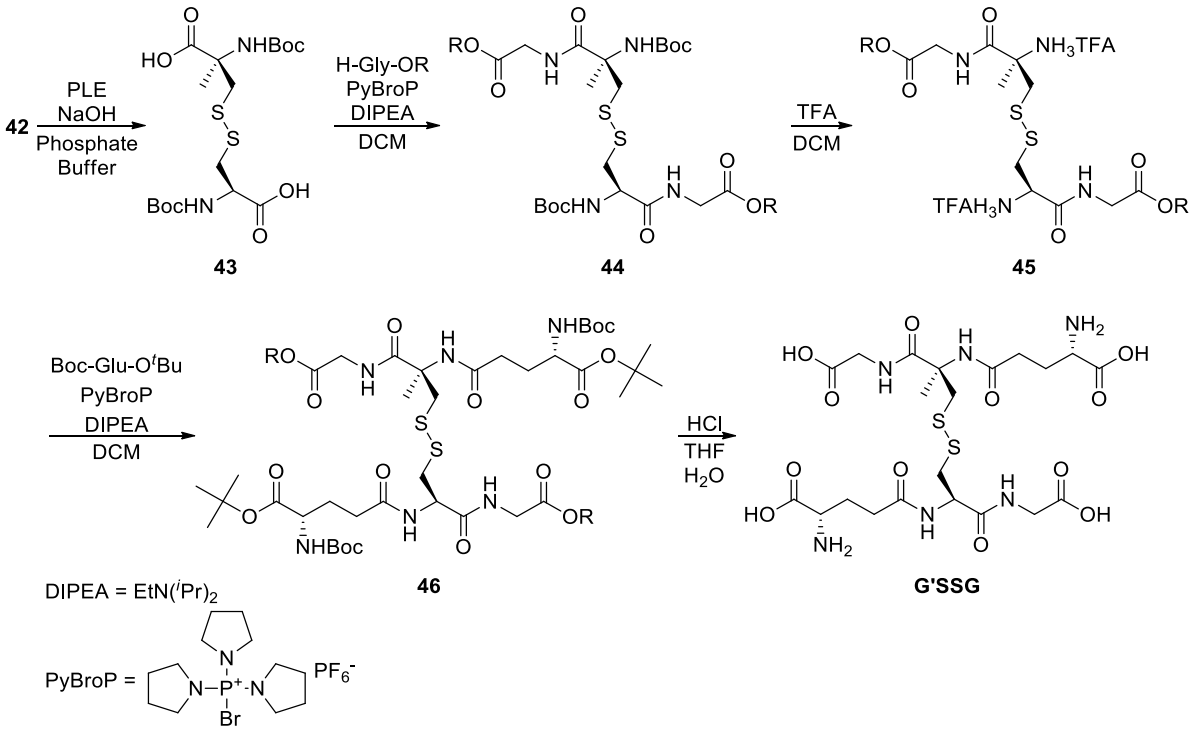

Scheme 4.9 *The Core-Out Synthesis of G'SSG*

To **45**, a backbone protected glutamic acid can be coupled to the free amine to yield **46**. After **46** is formed, a standard acidic hydrolysis can be done to liberate the carboxylic acid and amines of their protecting groups forming G'SSG. With G'SSG synthesized, enzymatic testing with GR can be performed to analyze the activity of G'SSG towards GR.

4.4 Experimental

4.4.1 Materials

Solvents for synthesis from Fisher Scientific (Fair lawn, NJ) or Acros Organics (Morris Plains, New Jersey). Diphenylphosphoryl azide (DPPA) was purchased from TCI America (Portland, OR). Titanium (IV) *tert*-butoxide was purchased from EMD Millipore. Silica gel (230-400 mesh) for purifications was purchased from Silicycle (Quebec City, QC, Canada). Deuterated solvents were purchased from Cambridge Isotope Laboratories (Andover, MA). All other chemicals were purchased from Sigma-Aldrich (Milwaukee, WI), Fisher Scientific (Waltham, MA), or ACROS Organics (Pittsburgh, PA). NMR spectra were obtained from a 400 MHz Bruker spectrometer. ^{1}H and ^{13}C chemical shifts (δ) were reported as downfield from tetramethylsilane and ^{13}C experiments were ^{1}H decoupled. IR spectra were obtained from a Nicolet Nexus 470 FT-IR spectrometer with a Smart Orbit Thermo™ diamond plate ATR attachment and samples were acquired as neat samples.

4.4.2 Synthesis of *tert*-butyl(chloromethyl)sulfane (33)

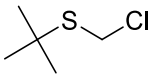

Compound **33** was prepared according to the reported procedures.[84, 115] A 3-necked, 500 mL round bottom flask was charged with a stir bar, DCM (175 mL), paraformaldehyde (6.65 g, 222 mmol), and *tert*-butylthiol (20.0 mL, 177 mmol). The reaction mixture was cooled in an ice bath, and with stirring hydrogen chloride was bubbled through the reaction mixture for 15 minutes. Nitrogen was bubbled through the reaction mixture for 2 hours to purge excess hydrogen chloride from the system. The aqueous phase was removed, and the organic phase was dried with $MgSO_4$, filtered, and concentrated *in vacuo* to afford 167 mmol (94%) of a yellow tinged liquid. ^{1}H NMR (400 MHz, $CDCl_3$) δ 4.85 (s, 2H), 1.42 (s, 9H).

4.4.3 Synthesis of dimethyl 2-((*tert*-butylthio)methyl)-2-methylmalonate (34)

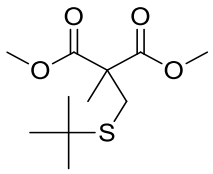

Compound **34** was prepared according to the reported procedures.[115, 132] A flame dried, 500 mL, 3-necked round bottom flask with a nitrogen atmosphere was charged with a stir bar and sodium hydride (60% dispersion in mineral oil) (6.30 g, 40.3 mmol). The sodium hydride was washed with two portions of pentane. A suspension was created with the addition of THF (200 mL). The suspension was cooled with an ice bath and dimethyl methylmalonate (19.07 g, 130.5 mmol) was added dropwise, which produced effervescence. The reaction mixture was stirred at room temperature for 2 hours and **33** (157 mmol) was added. The reaction mixture was stirring at room temperature for 1 hour and then heated to solvent reflux for 17.5 hours. The reaction mixture was cooled to room temperature, filtered through a bed of Celite, diluted with diethyl ether (150 mL), and

washed with water (7 × 100 mL). The organic phase was dried over $MgSO_4$, filtered, and concentrated *in vacuo* to afford 29.23 g (117.7 mmol, 90%) of a colorless oil. ^{1}H NMR (400 MHz, $CDCl_3$) δ 3.74 (s, 6H), 3.03 (s, 2H), 1.50 (s, 3H), 1.31 (s, 9H).

4.4.4 Synthesis of (*R*)-2-((*tert*-butylthio)methyl)-3-methoxy-2-methyl-3-oxopropanoic acid (35)

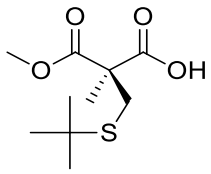

Compound **35** was prepared according to the reported procedures.[115, 132] A 400 mL beaker was charged with a stir bar, **34** (29.30 g, 118.0 mmol), 7.4 pH phosphate buffer (250 mL), and crude porcine liver esterase (497 mg, 18 units/mg). The reaction was stirred vigorously with a constant pH = 7.4 by titrating 1M NaOH into the reaction. The reaction was complete after stirring for 30 hours. The solution pH was raised to 9 with the addition of 1M NaOH and was washed with diethyl ether (300 mL). The aqueous phase was reacidified to pH = 3 with 4M HCl and extracted with $CHCl_3$ (3 × 400 mL). The organic phase was filtered through a bed of Celite, dried over $MgSO_4$, and concentrated *in vacuo* to afford 21.41 g (91.37 mmol, 77%) of a yellow liquid. ^{1}H NMR (400 MHz, $CDCl_3$) δ 10.05 (br s, 1H), 3.77 (s, 3H), 3.07 (d, $^2J_{H\text{-}H}$ = 12.0 Hz, 1H), 3.02 (d, $^2J_{H\text{-}H}$ = 12.3 Hz, 1H), 1.53 (s, 3H), 1.31 (s, 9H).

4.4.5 Synthesis of (*R*)-*N*-Moz-α-MeCys(^{t}Bu)-OMe (36)

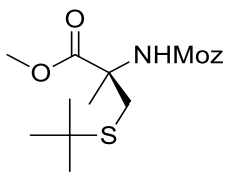

Compound **36** was prepared according to the reported procedures.[115, 132] A 250 mL round bottom flask with a nitrogen atmosphere was charged with a stir bar, **35** (5.01 g, 21.4 mmol), dichloroethane (DCE) (75 mL), and TEA (3.60 mL, 25.8 mmol). The reaction mixture was stirred for 5 minutes and DPPA (5.10 mL, 23.7 mmol) was added. A reflux condenser was fitted to the round bottom flask and the reaction mixture was stirred for 1 hour at room temperature and heated to solvent reflux for 16.5 hours. The reaction mixture was cooled to room temperature, and to the mixture was added 4-methoxybenzyl alcohol (14.86 g, 107.3 mmol). The reaction mixture was heated to solvent reflux for 24 hours and the solvent was removed *in vacuo*. The residue was reconstituted in diethyl ether (100 mL) and was washed with water (5 × 100 mL). The organic phase was dried over $MgSO_4$, filtered, and concentrated in vacuo to afford a crude orange oil. The crude product was purified by flash chromatography and eluted with 2:1 hexanes/ethyl acetate (R_f = 0.61 in 1:1 hexanes/ethyl acetate spiked with 2% TEA). The product rich fractions were pooled and concentrated *in vacuo* to afford 6.13 g (16.6 mmol, 78%) of a yellow liquid. ^{1}H NMR (400 MHz, $CDCl_3$) δ 7.29 (d, $J_{H\text{-}H}$ = 8.9 Hz, 2H), 6.88 (d, $J_{H\text{-}H}$ = 8.7 Hz, 2H), 5.72 (br s, 1H), 5.01 (s, 2H), 3.80 (s, 3H), 3.76 (br s, 3H), 3.30 (br d, $^2J_{H\text{-}H}$ = 11.9 Hz, 1H), 3.01 (d, $^2J_{H\text{-}H}$ = 12.2 Hz, 1H), 1.63 (br s, 3H), 1.27 (s, 9H).

4.4.6 Synthesis of (*R*)-*N*-Boc-α-MeCys(^{t}Bu)-OMe (37)

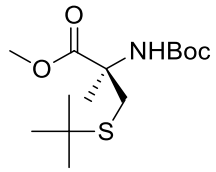

A 500 mL round bottom flask with a nitrogen atmosphere was charged with a stir bar, **35** (18.47 g, 78.83 mmol), DCE (150 mL), and TEA (13.2 mL, 94.7 mmol). The

reaction mixture was stirred for 5 minutes and DPPA (18.0 mL, 83.5 mmol) was added. A reflux condenser was fitted to the round bottom flask and the reaction mixture was stirred for 1.5 hours at room temperature and heated to solvent reflux for 20.5 hours. The reaction mixture was cooled to room temperature, and to the mixture was added *tert*-butanol (23.5 mg, 247 mmol) and titanium (IV) *tert*-butoxide (3.00 mL, 7.77 mmol). The reaction mixture was heated to solvent reflux for 2.5 days and was washed with saturated NH_4Cl (3 × 150 mL). The organic phase was pooled, dried over $MgSO_4$, filtered, and concentrated in vacuo to afford a crude brown oil. The crude product was filtered through silica gel with 8:1 hexanes/ethyl acetate until the eluate became colorless. The eluate was concentrated *in vacuo* to afford 17.37 g (56.87 mmol, 72%) of a yellow liquid. IR ($CDCl_3$, cm^{-1}) 3431, 3370, 2964, 2902, 2866, 1740, 1714; ^1H NMR (400 MHz, $CDCl_3$) δ 5.43 (br s, 1H), 3.76 (s, 3H), 3.24 (br d, $^2J_{H\text{-}H}$ = 11.4 Hz, 1H), 3.05 (d, $^2J_{H\text{-}H}$ = 12.2 Hz, 1H), 1.58 (s, 3H), 1.43 (s, 9H), 1.30 (s, 9H); ^{13}C NMR (100 MHz, $CDCl_3$) δ 173.8, 154.2, 79.6, 59.2, 52.6, 42.2, 34.9, 30.8, 28.3, 23.5.

4.4.7 Synthesis of (*R*)-H-α-MeCys-OMe TFA (39)

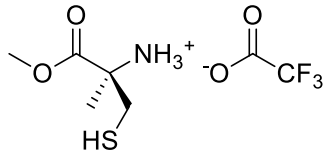

A 250 mL round bottom flask in an ice bath was charged with a stir bar, TFA (100 mL), anisole (4.0 mL, 37 mmol), and **36** (6.68 g, 18.1 mmol). To the reaction mixture was added mercury acetate (5.78 g, 18.2 mmol). After stirring for 30 minutes at 0 °C the volatiles were removed *in vacuo*. The residue was washed with diethyl ether several times until a fine grey powder remained. Water (100 mL) was used to create

suspension a from this powder. A separate 100 mL round bottom flask was charged with sodium sulfide nonahydrate (19.11 g, 79.57 mmol) and sulfuric acid (4.5 mL, 83 mmol) which generated hydrogen sulfide. The generated hydrogen sulfide was bubbled through the suspension creating a black precipitate which was removed by gravity filtration. The volatiles were removed *in vacuo* yielding 4.44 g (16.8 mmol, 93%) of a yellow tinged oil. ^{1}H NMR (400 MHz, $CDCl_3$) δ 8.62 (br s, 3H), 3.86 (s, 3H), 3.15 (br d, $^{2}J_{H\text{-}H}$ = 14.3 Hz, 1H), 3.04 (br d, $^{2}J_{H\text{-}H}$ = 14.9 Hz, 1H), 1.83 (br s, 1H), 1.70 (s, 3H).

4.4.8 Synthesis of (*R*)-*N*-Boc-α-MeCys-OMe (40)

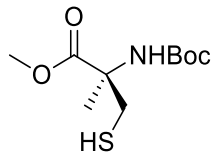

A 50 mL round bottom flask was charged with a stir bar, **39** (846 mg, 3.21 mmol), acetonitrile (20 mL), and Boc_2O (800 μL, 3.48 mmol). To this suspension was added TEA (450 μL, 3.23 mmol). After stirring for 22 hours at room temperature the reaction mixture was diluted with diethyl ether (40 mL) and washed with water (3 × 40 mL), dried over $MgSO_4$, filtered, and concentrated *in vacuo*. The remaining impurities were removed by distillation under reduced pressure, until no further distillate formed. The pot fraction yielded 235 mg (0.943 mmol, 29%) of a cream colored solid. ^{1}H NMR (400 MHz, $CDCl_3$) δ 5.86 (br s, 1H), 3.78 (s, 3H), 3.66 (br d, $^{2}J_{H\text{-}H}$ = 15.1 Hz, 1H), 3.50 (d, $^{2}J_{H\text{-}H}$ = 14.2 Hz, 1H), 1.60 (s, 3H), 1.53 (s, 1H), 1.46 (s, 9H).

4.4.9 Synthesis of (*R*)-methyl 2-((*tert*-butoxycarbonyl)amino)-3-(((*R*)-2-((*tert*-butoxycarbonyl)amino)-3-methoxy-3-oxopropyl)disulfanyl)-2-methylpropanoate (42)

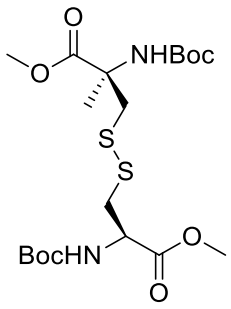

Compound **42** was prepared according to the reported procedure.[128] A 25 mL round bottom flask was charged with a stir bar, BtCl (215 mg, 1.40 mmol), BtH (85 mg, 0.71 mmol), and DCM (5 mL). The solution was cooled to -63 °C by a liquid nitrogen/chloroform slurry and a solution of **40** (174 mg, 0.697 mmol) in DCM (1 mL) was added dropwise. After stirring for 20 minutes at -63 °C, TLC confirmed the absence of **40** (R_f = 0.61 in 1:1 hexanes/ethyl acetate) and to the reaction mixture was added a solution of thiourea (152 mg, 2.00 mmol) in THF (2 mL). After stirring for an additional 10 minutes a solution of *N*-Boc-Cys-OMe (220 μL, 1.07 mmol) in DCM (1 mL) was added dropwise. Slowly warming to room temperature and stirring for 18 hours the reaction mixture was filtered. The filtrate was concentrated *in vacuo* and purified by gradient flash chromatography and eluted with hexanes/ethyl acetate (4:1 to 1:1). The product rich fractions (R_f = 0.58 in 1:1 hexanes/ethyl acetate) were pooled and concentrated *in vacuo* to afford 61 mg (0.126 mmol, 18%) of a colorless gummy solid. ^{1}H NMR (400 MHz, $CDCl_3$) δ 5.52 (br s, 1H), 5.41 (br d, *J* = 7.6 Hz, 1H), 4.61 (m, 1H), 3.77 (s, 3H), 3.76 (s, 3H), 3.56 (br d, *J* = 13.4 Hz, 1H), 3.36 (d, *J* = 14.1 Hz, 1H), 3.13 (d,

J = 5.4 Hz, 2H), 1.57 (s, 3H), 1.45 (s, 9H), 1.44 (s, 9H); ^{13}C NMR (100 MHz, $CDCl_3$) δ 173.5, 171.3, 155.1, 154.1, 80.2, 79.8, 59.9, 52.8, 52.6, 45.0, 41.4, 28.3, 28.3, 23.5; LRMS (ESI^+) Calcd for $C_{19}H_{34}N_2O_8S_2$ $[M + Na]^+$ 505.17 found 505.17.

APPENDIX A – CHARACTERIZATION DATA FROM SYNTHESES

A.1 Chapter 2 Spectra

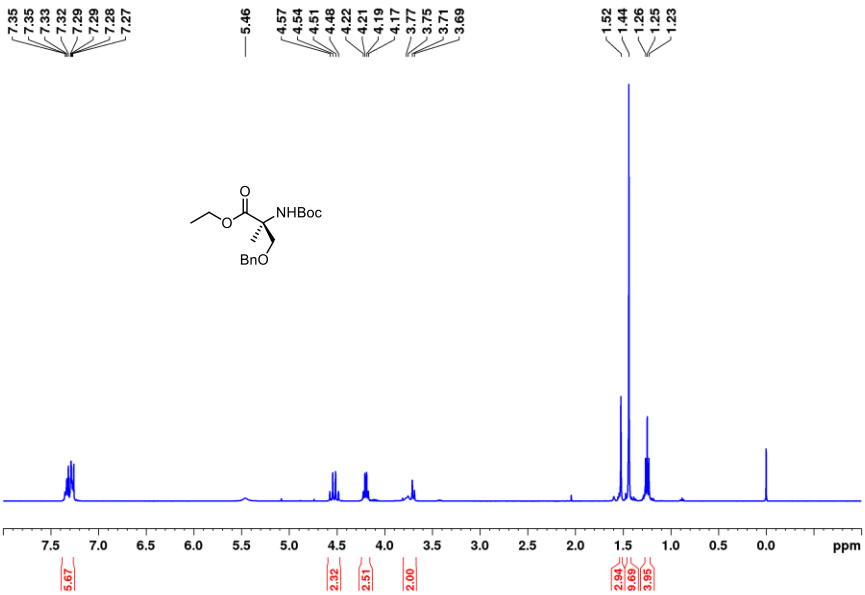

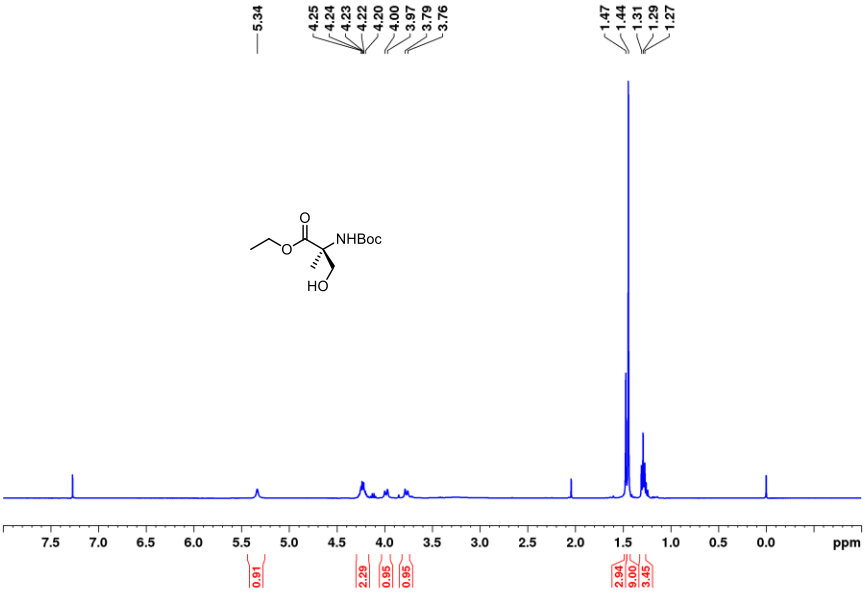

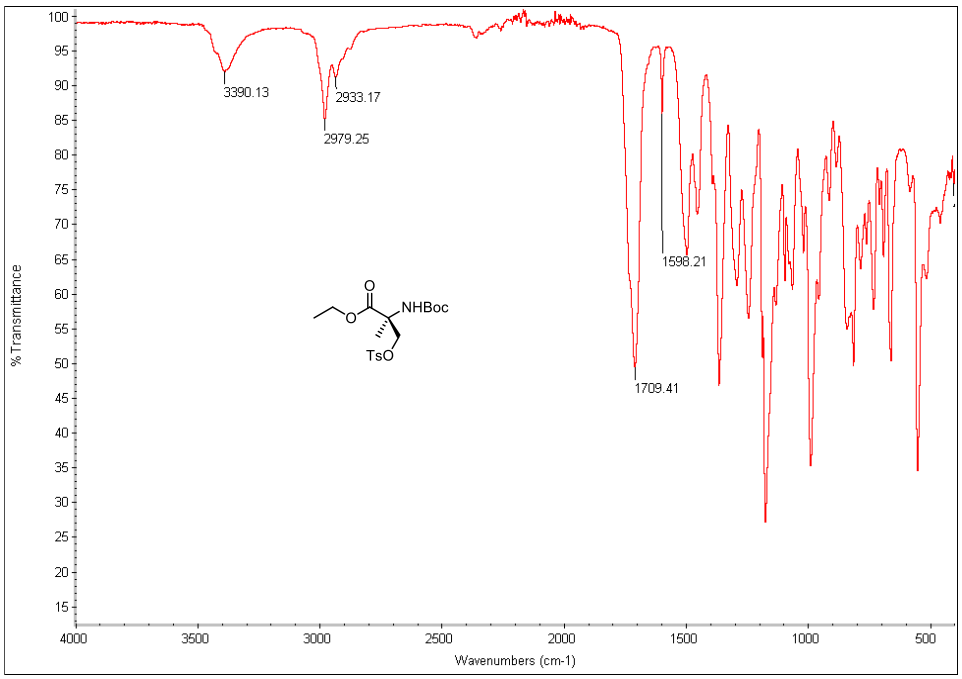
% Transmittance
Wavenumbers (cm-1)
3390.13
2933.17
2979.25
1598.21
1709.41
NHBoc
TsO

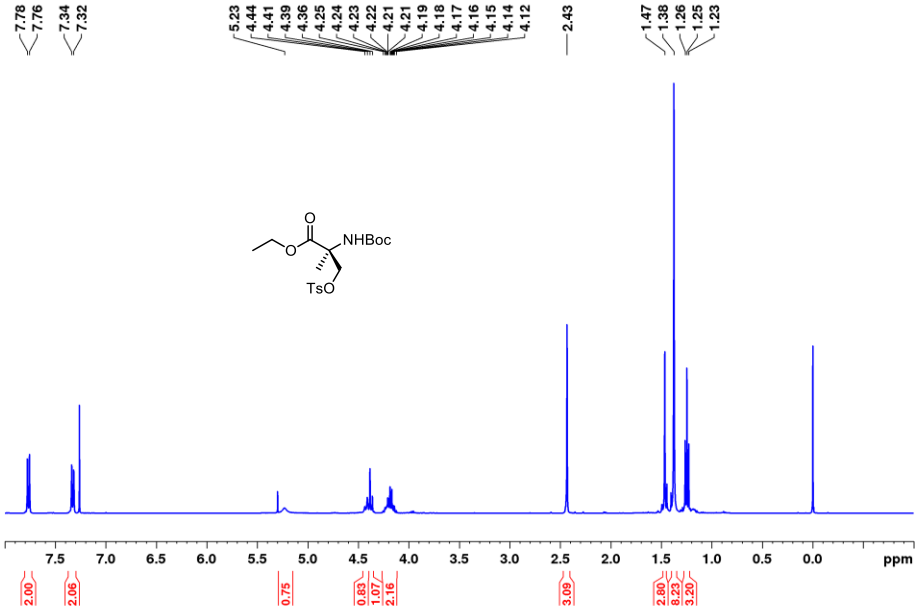
7.78
7.76
7.34
7.32
5.23
4.44
4.41
4.39
4.36
4.25
4.24
4.23
4.22
4.21
4.21
4.19
4.18
4.17
4.16
4.15
4.14
4.12
2.43
1.47
1.38
1.26
1.25
1.23
NHBoc
TsO
ppm
2.00
2.06
0.75
0.83
1.07
2.16
3.09
2.80
8.23
3.20

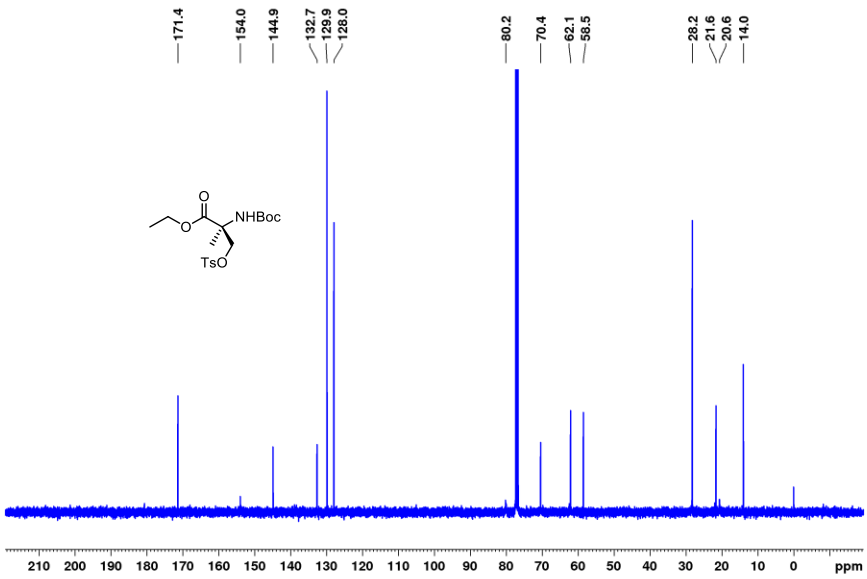
171.4
154.0
144.9
132.7
129.9
128.0
80.2
70.4
62.1
58.5
28.2
21.6
20.6
14.0
NHBoc
TsO
210 200 190 180 170 160 150 140 130 120 110 100 90 80 70 60 50 40 30 20 10 0 ppm

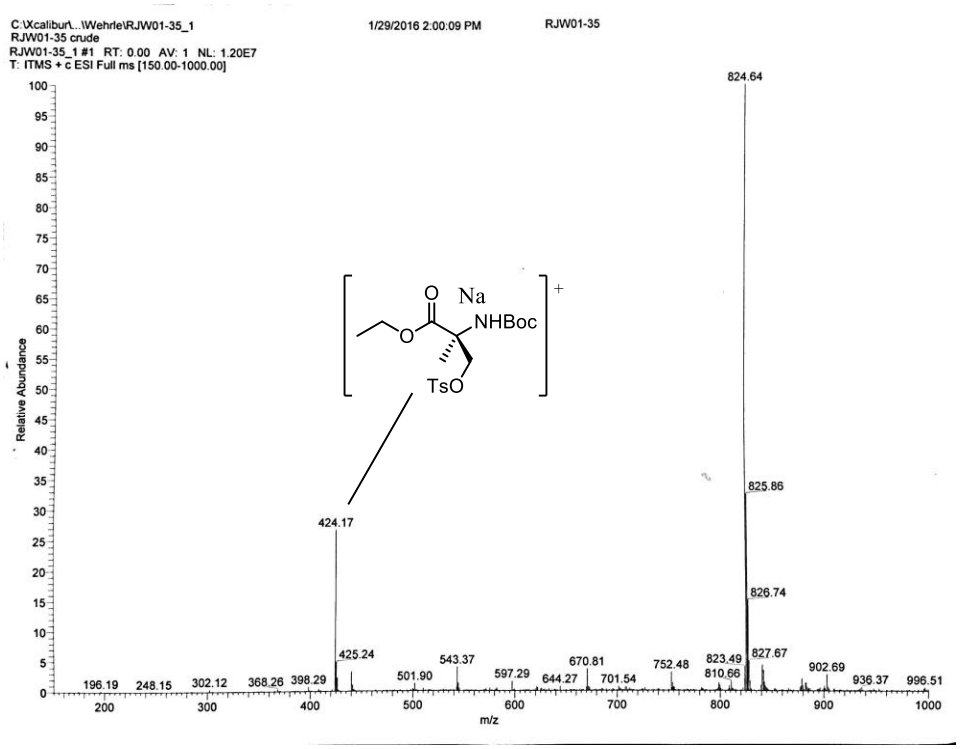
C:\Xcalibur\...\Wehrle\RJW01-35_1
RJW01-35 crude
RJW01-35_1 #1 RT: 0.00 AV: 1 NL: 1.20E7
T: ITMS + c ESI Full ms [150.00-1000.00]
1/29/2016 2:00:09 PM
RJW01-35
Relative Abundance
m/z
824.64
825.86
826.74
827.67
424.17
425.24
Na
NHBoc
TsO

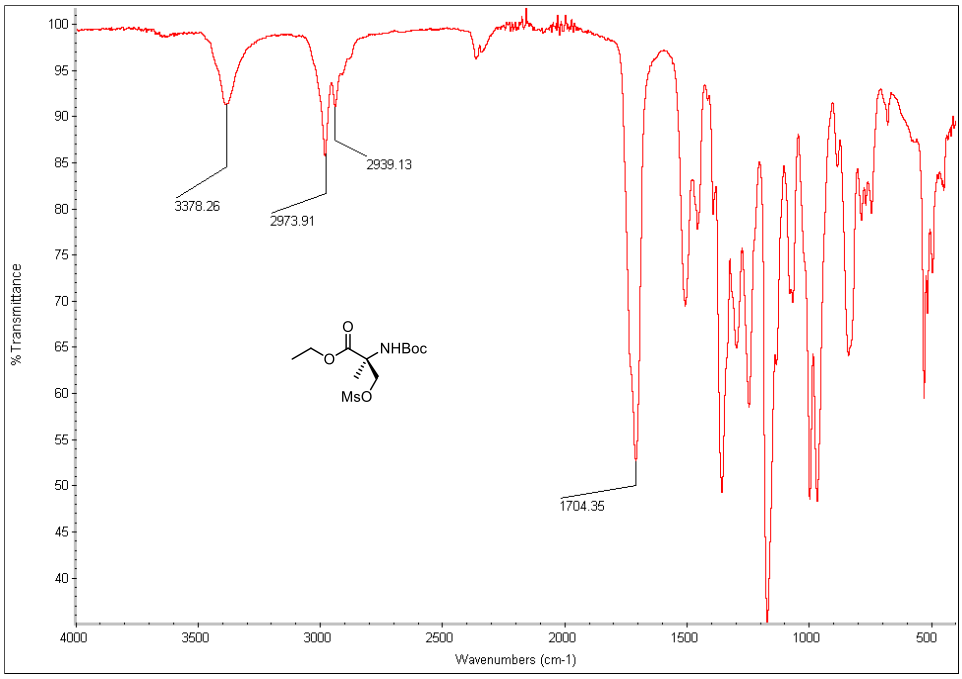
% Transmittance
Wavenumbers (cm-1)
3378.26
2973.91
2939.13
1704.35
NHBoc
MsO

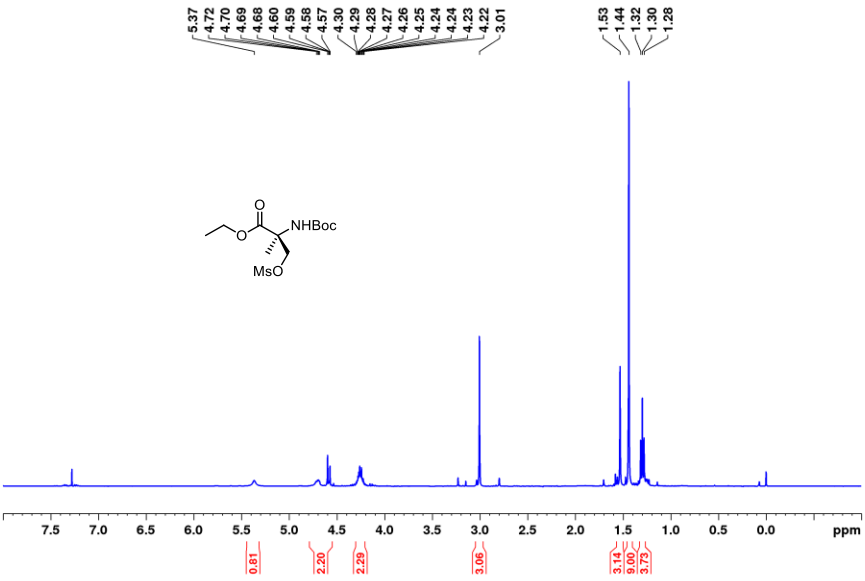
5.37
4.72
4.70
4.69
4.68
4.60
4.59
4.58
4.57
4.30
4.29
4.28
4.27
4.26
4.25
4.24
4.24
4.23
4.22
3.01
1.53
1.44
1.32
1.30
1.28
NHBoc
MsO
ppm
0.61
2.20
2.29
3.06
3.14
9.00
3.73

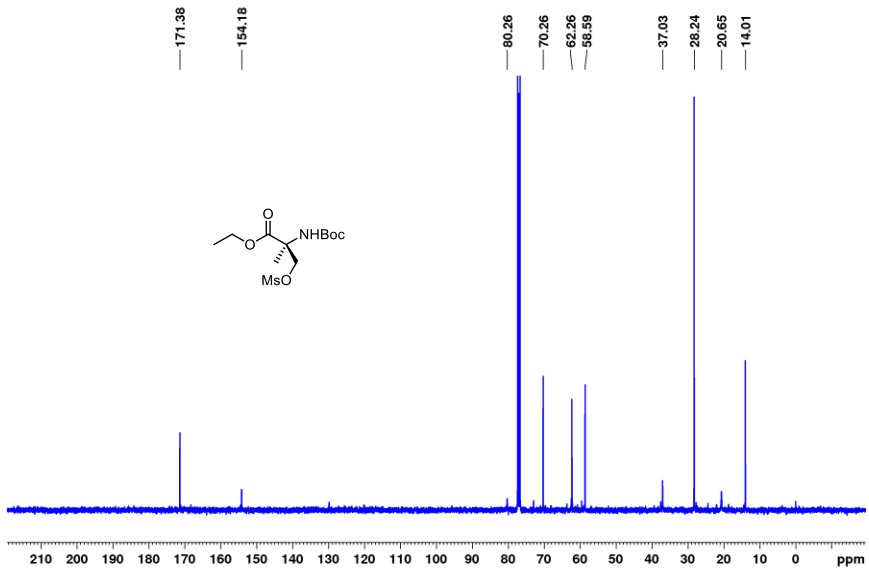
171.38
154.18
80.26
70.26
62.26
58.59
37.03
28.24
20.65
14.01
O
NHBoc
O
MsO
210 200 190 180 170 160 150 140 130 120 110 100 90 80 70 60 50 40 30 20 10 0 ppm

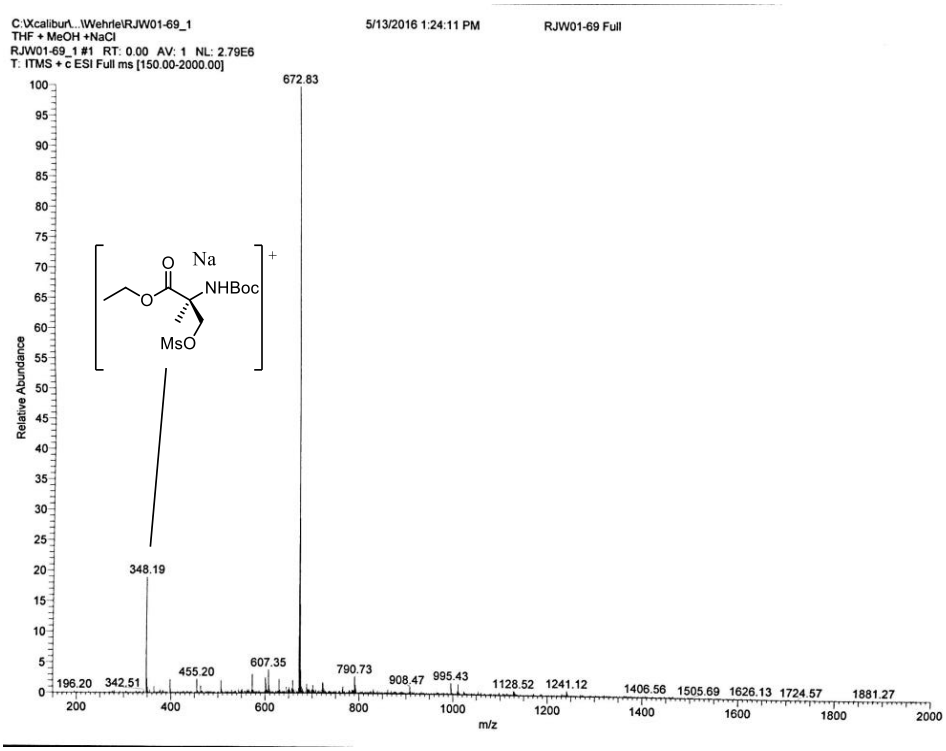
C:\Xcalibur\...\Wehrle\RJW01-69_1
THF + MeOH +NaCl
RJW01-69_1 #1 RT: 0.00 AV: 1 NL: 2.79E6
T: ITMS + c ESI Full ms [150.00-2000.00]
5/13/2016 1:24:11 PM
RJW01-69 Full
672.83
Na
O
NHBoc
O
MsO
+
348.19
Relative Abundance
196.20
342.51
455.20
607.35
790.73
908.47
995.43
1128.52
1241.12
1406.56
1505.69
1626.13
1724.57
1881.27
m/z

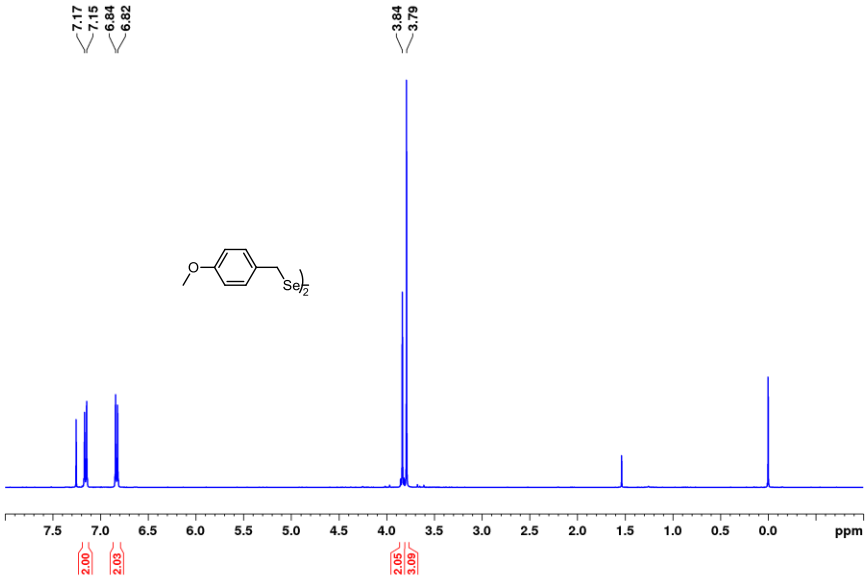
7.17
7.15
6.84
6.82
3.84
3.79
O
Se
2
7.5
7.0
6.5
6.0
5.5
5.0
4.5
4.0
3.5
3.0
2.5
2.0
1.5
1.0
0.5
0.0
ppm
2.00
2.03
2.05
3.09

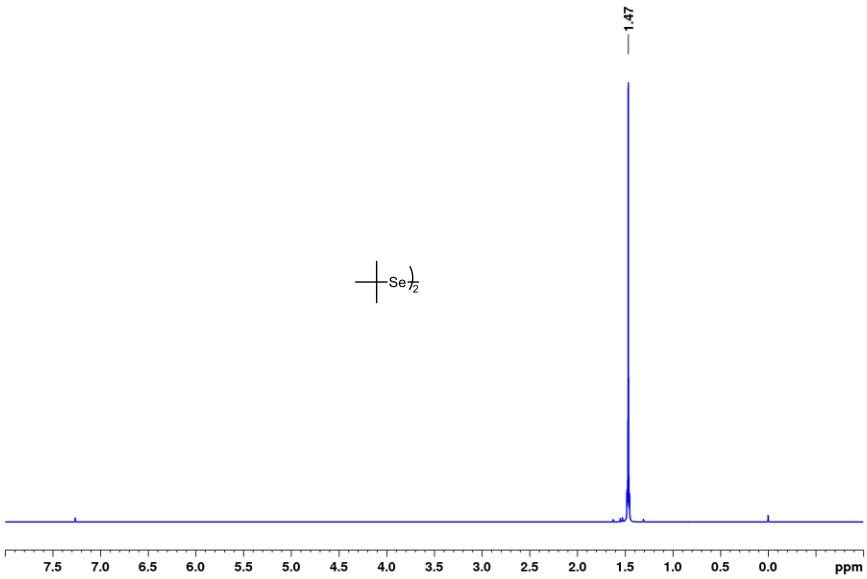
1.47
Se
2
7.5
7.0
6.5
6.0
5.5
5.0
4.5
4.0
3.5
3.0
2.5
2.0
1.5
1.0
0.5
0.0
ppm

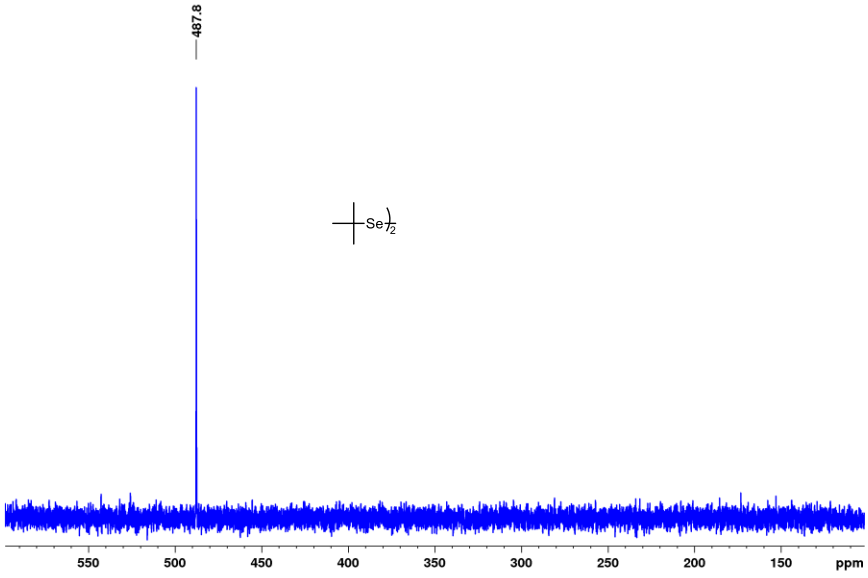
487.8
Se
2
550
500
450
400
350
300
250
200
150
ppm

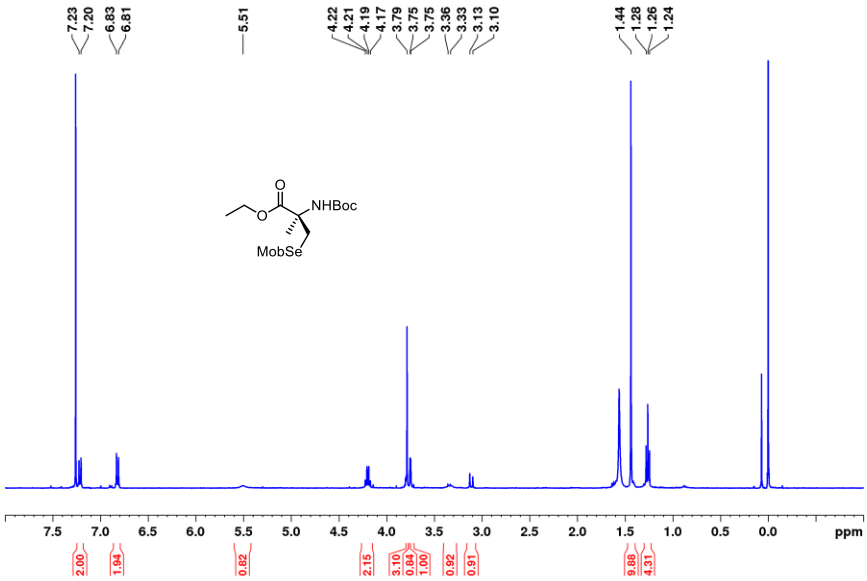
7.23
7.20
6.83
6.81
5.51
4.22
4.21
4.19
4.17
3.79
3.75
3.75
3.36
3.33
3.13
3.10
1.44
1.28
1.26
1.24
O
O
NHBoc
MobSe
7.5
7.0
6.5
6.0
5.5
5.0
4.5
4.0
3.5
3.0
2.5
2.0
1.5
1.0
0.5
0.0
ppm
2.00
1.94
0.82
2.15
3.10
0.84
1.00
0.92
0.91
9.68
4.31

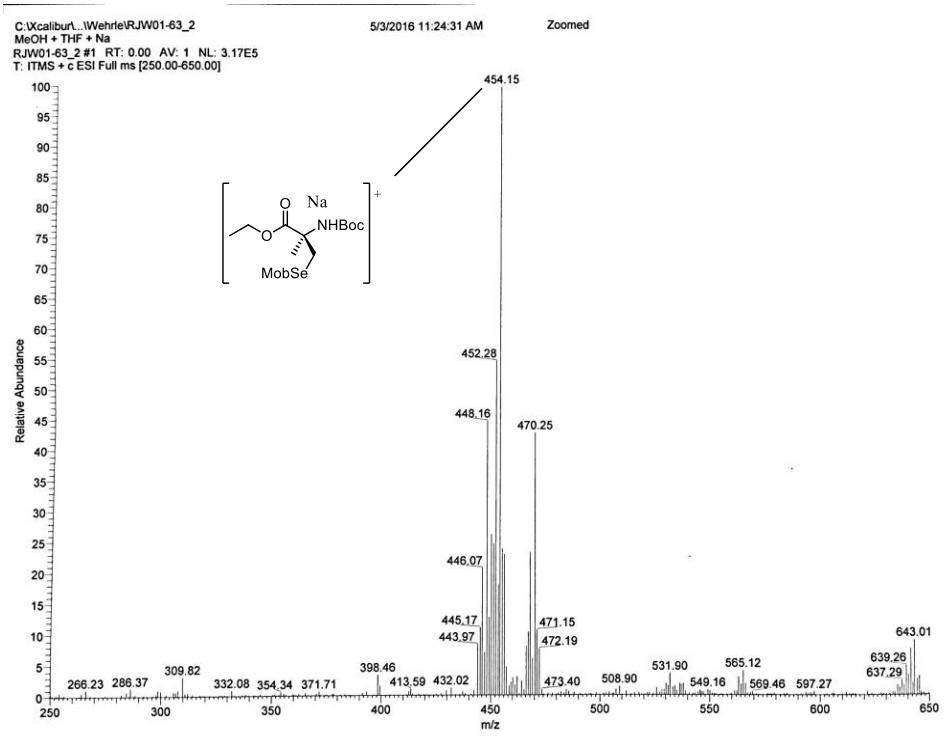
C:\Xcalibur\...\Wehrle\RJW01-63_2
MeOH + THF + Na
RJW01-63_2 #1 RT: 0.00 AV: 1 NL: 3.17E5
T: ITMS + c ESI Full ms [250.00-650.00]
5/3/2016 11:24:31 AM
Zoomed
Relative Abundance
m/z
454.15
452.28
448.16
470.25
446.07
445.17
443.97
471.15
472.19
643.01
639.26
637.29
565.12
531.90
549.16
569.46
597.27
508.90
473.40
398.46
413.59
432.02
309.82
266.23
286.37
332.08
354.34
371.71
Na
NHBoc
MobSe
O

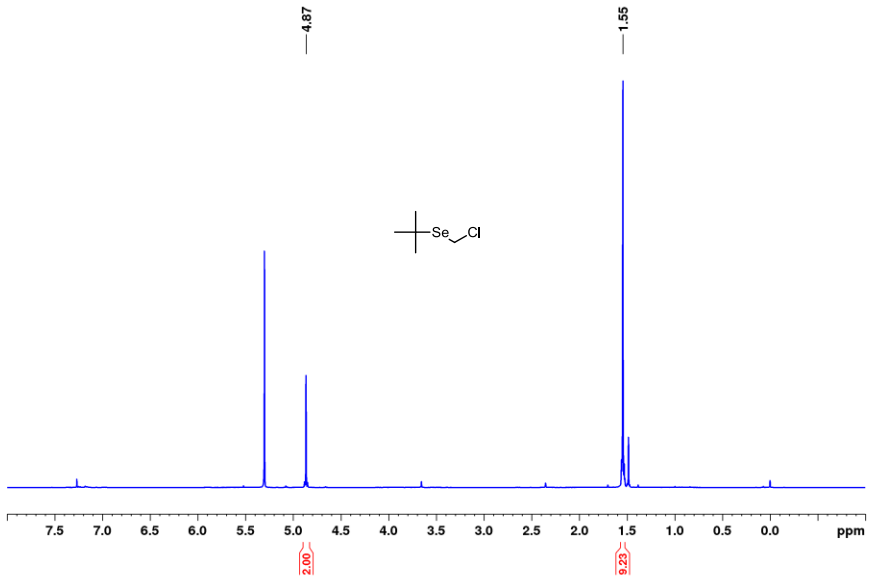
4.87
1.55
Se
Cl
ppm
2.00
9.23

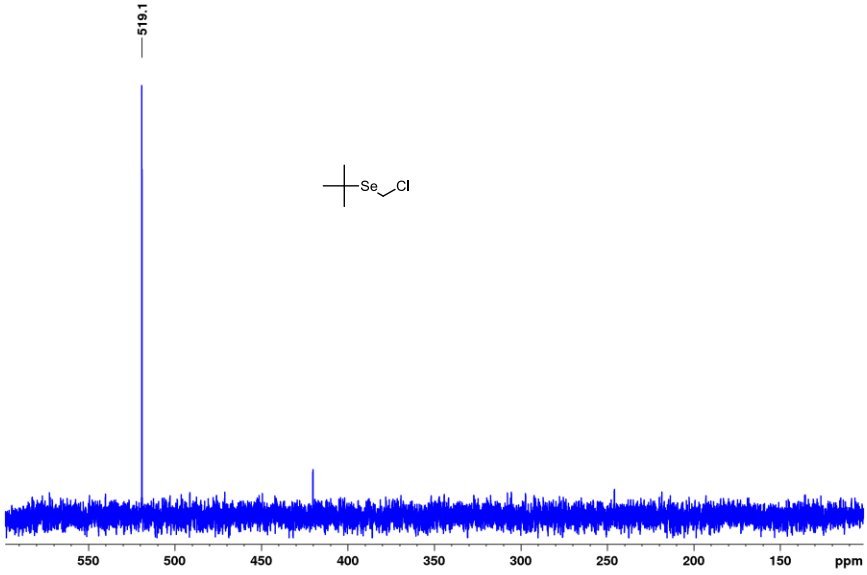
519.1
Se
Cl
550
500
450
400
350
300
250
200
150
ppm

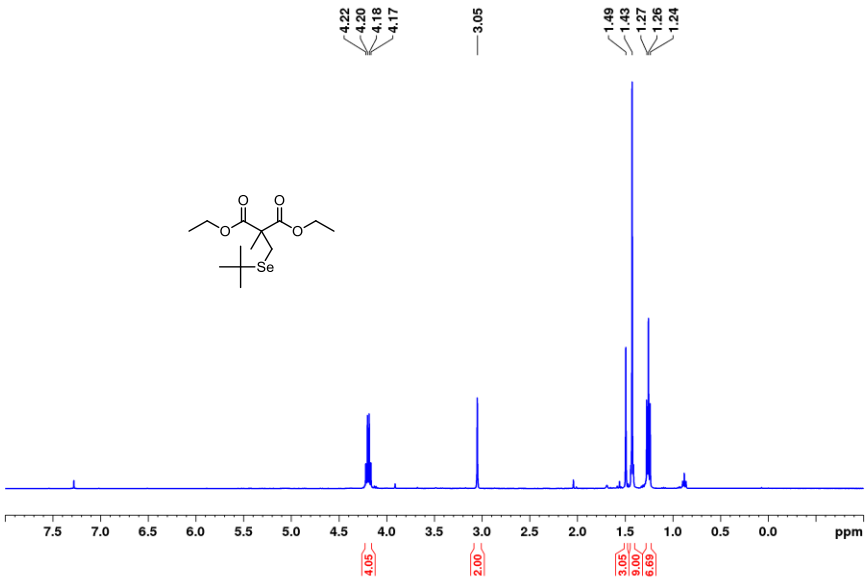
4.22
4.20
4.18
4.17
3.05
1.49
1.43
1.27
1.26
1.24
O
O
O
O
Se
7.5
7.0
6.5
6.0
5.5
5.0
4.5
4.0
3.5
3.0
2.5
2.0
1.5
1.0
0.5
0.0
ppm
4.05
2.00
3.05
9.00
6.69

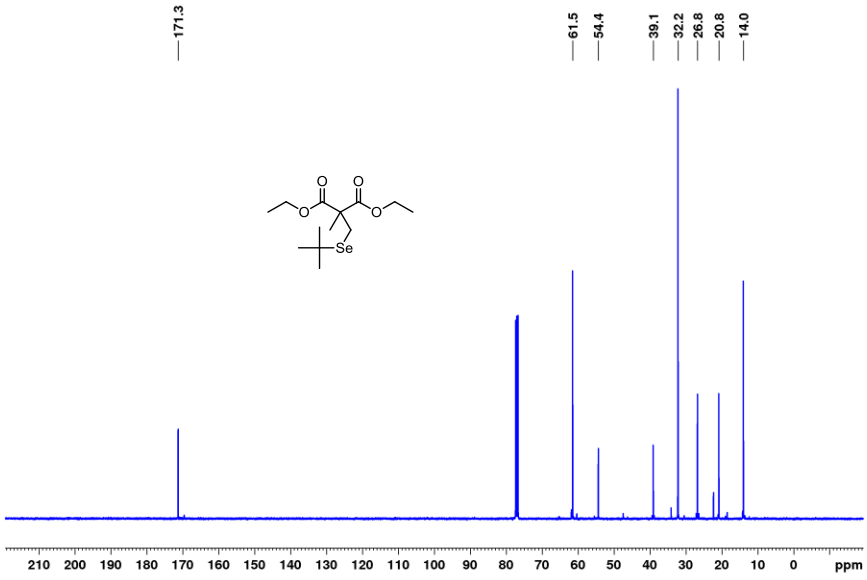
171.3
61.5
54.4
39.1
32.2
26.8
20.8
14.0
O
O
O
O
Se
210 200 190 180 170 160 150 140 130 120 110 100 90 80 70 60 50 40 30 20 10 0 ppm

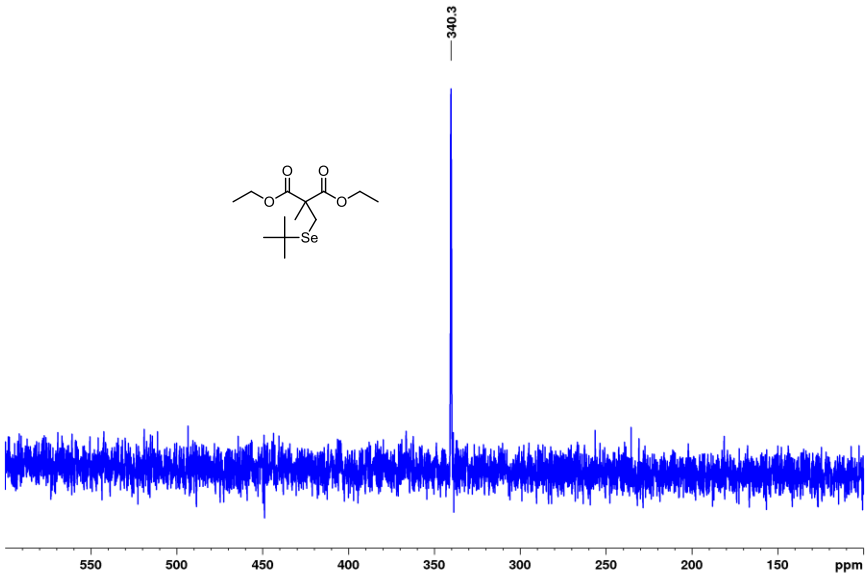
340.3
O
O
O
O
Se
550 500 450 400 350 300 250 200 150 ppm

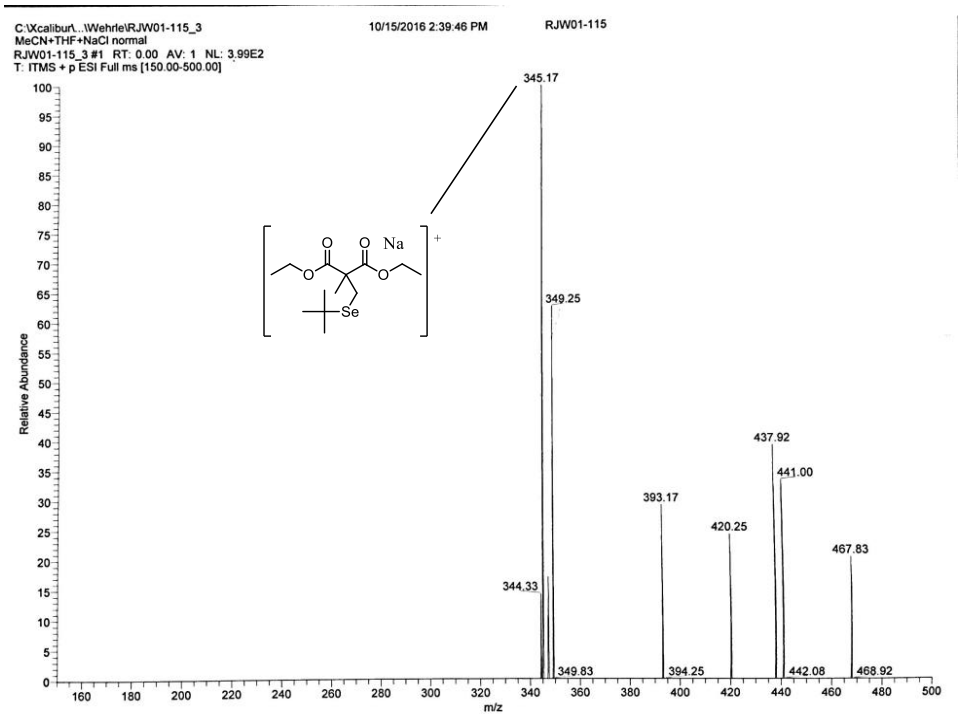
C:\Xcalibur\...\Wehrle\RJW01-115_3
MeCN+THF+NaCl normal
RJW01-115_3 #1 RT: 0.00 AV: 1 NL: 3.99E2
T: ITMS + p ESI Full ms [150.00-500.00]
10/15/2016 2:39:46 PM
RJW01-115
345.17
349.25
437.92
441.00
393.17
420.25
467.83
344.33
349.83
394.25
442.08
468.92
Relative Abundance
m/z
Na
Se

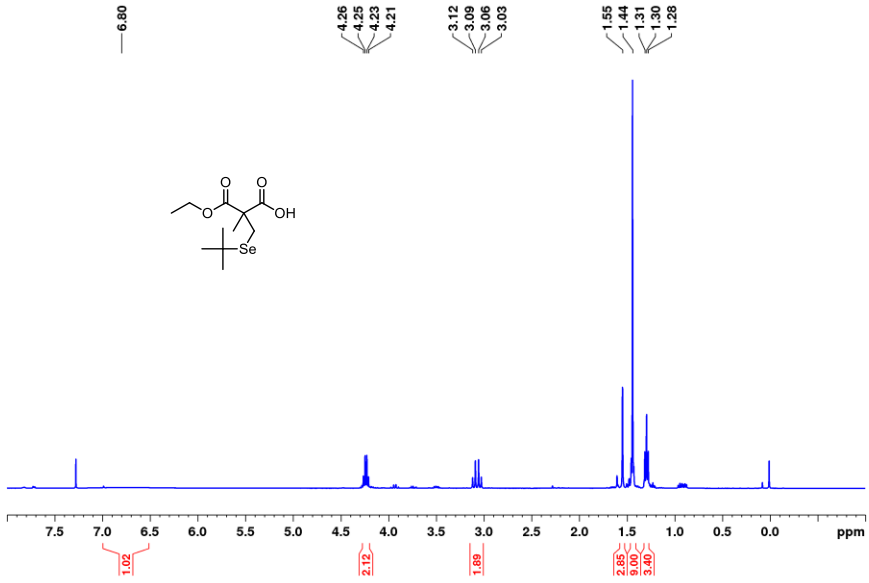
6.80
4.26
4.25
4.23
4.21
3.12
3.09
3.06
3.03
1.55
1.44
1.31
1.30
1.28
OH
Se
ppm
1.02
2.12
1.89
2.85
9.00
3.40

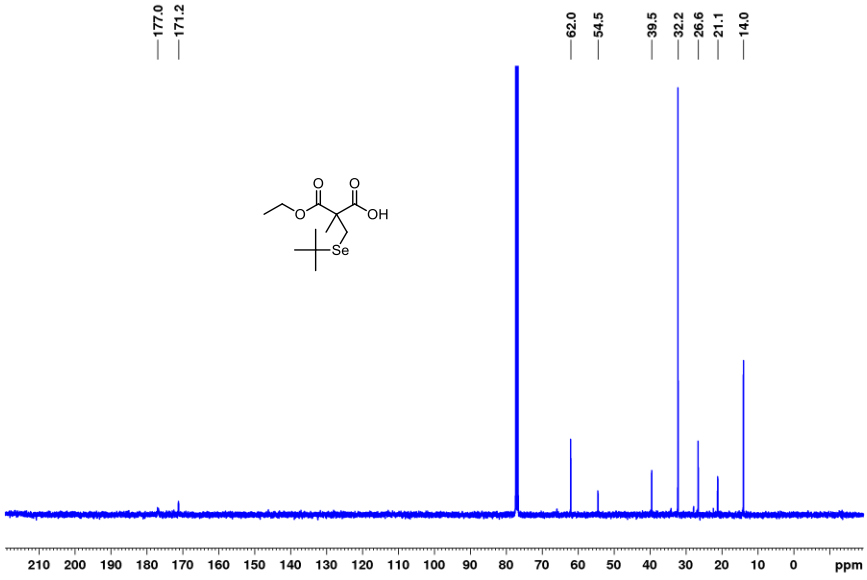
177.0
171.2
62.0
54.5
39.5
32.2
26.6
21.1
14.0
O
O
O
OH
Se
210 200 190 180 170 160 150 140 130 120 110 100 90 80 70 60 50 40 30 20 10 0 ppm

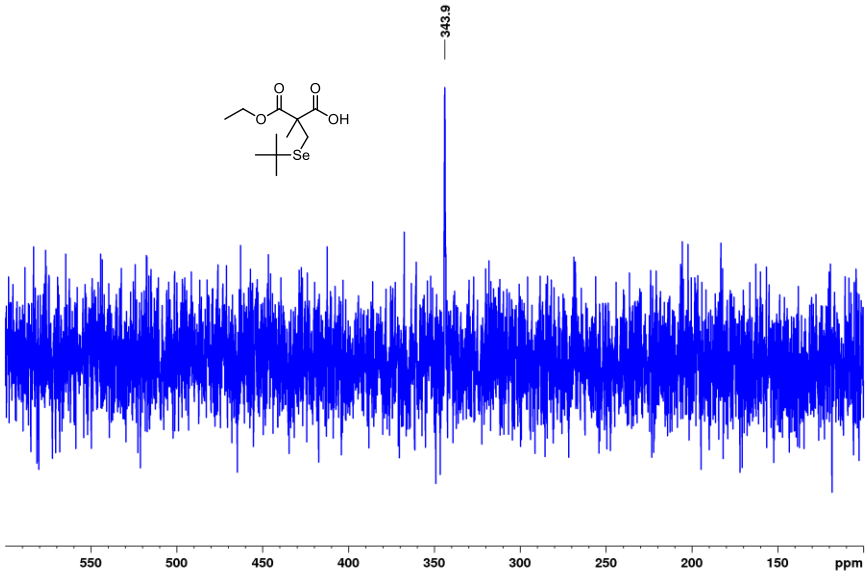
343.9
O
O
O
OH
Se
550 500 450 400 350 300 250 200 150 ppm

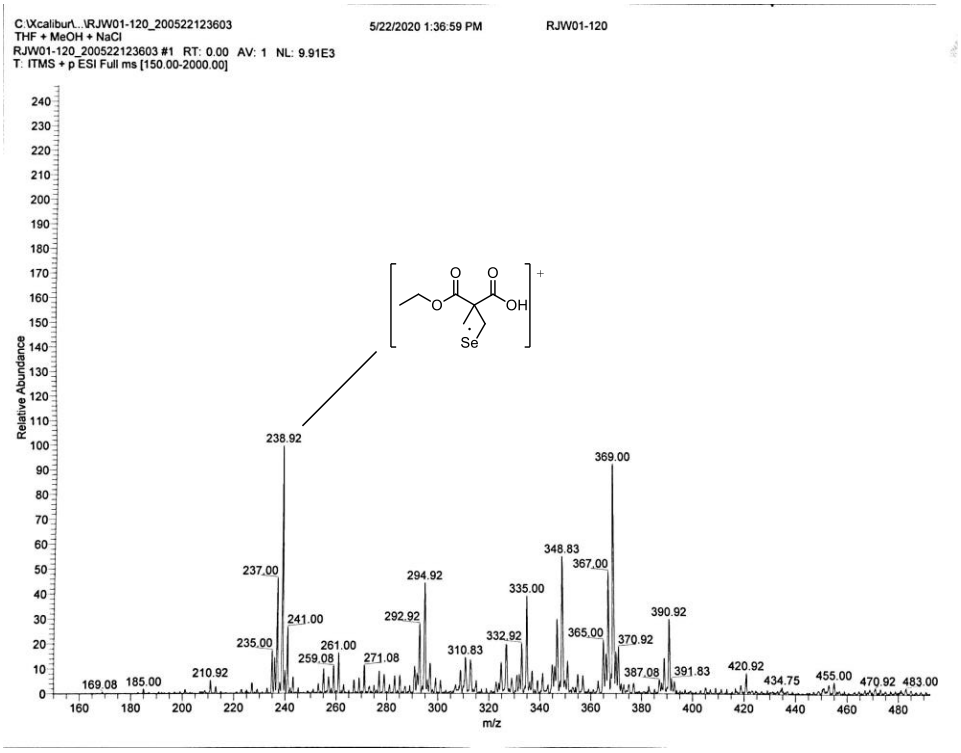
C:\Xcalibur\...\RJW01-120_200522123603
THF + MeOH + NaCl
RJW01-120_200522123603 #1 RT: 0.00 AV: 1 NL: 9.91E3
T: ITMS + p ESI Full ms [150.00-2000.00]
5/22/2020 1:36:59 PM
RJW01-120
Relative Abundance
m/z
238.92
369.00
348.83
367.00
237.00
294.92
335.00
241.00
292.92
390.92
235.00
261.00
332.92
365.00
370.92
259.08
271.08
310.83
387.08
391.83
420.92
169.08
185.00
210.92
434.75
455.00
470.92
483.00
OH
Se

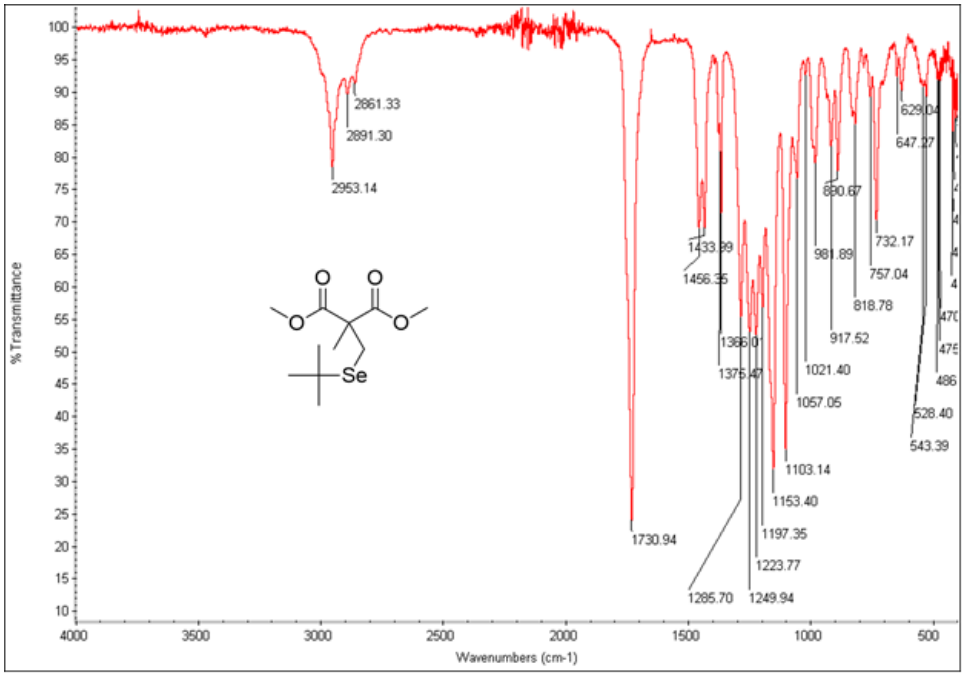
% Transmittance
Wavenumbers (cm-1)
2861.33
2891.30
2953.14
1730.94
1433.99
1456.35
1366.01
1375.47
1285.70
1249.94
1223.77
1197.35
1153.40
1103.14
1057.05
1021.40
981.89
917.52
880.67
818.78
757.04
732.17
647.27
629.04
543.39
528.40
Se

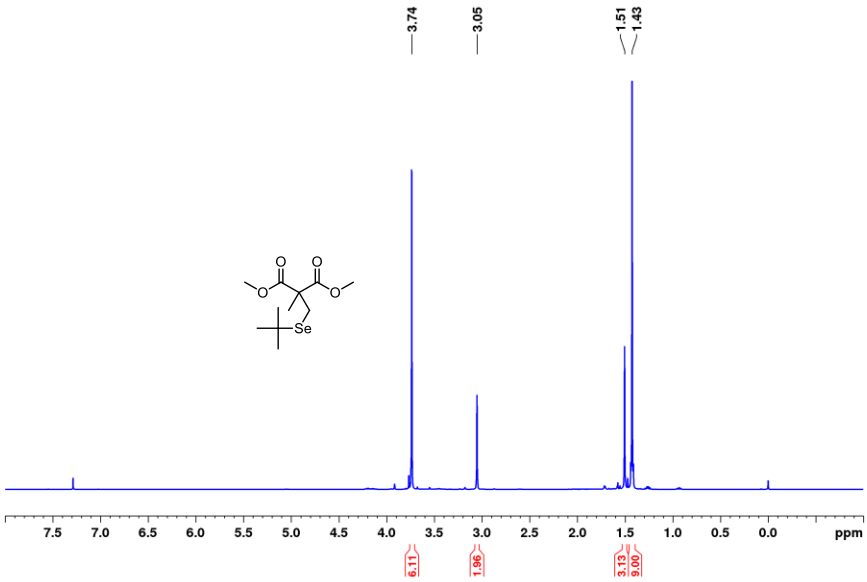
3.74
3.05
1.51
1.43
O
O
O
O
Se
7.5 7.0 6.5 6.0 5.5 5.0 4.5 4.0 3.5 3.0 2.5 2.0 1.5 1.0 0.5 0.0 ppm
6.11
1.96
3.13
9.00

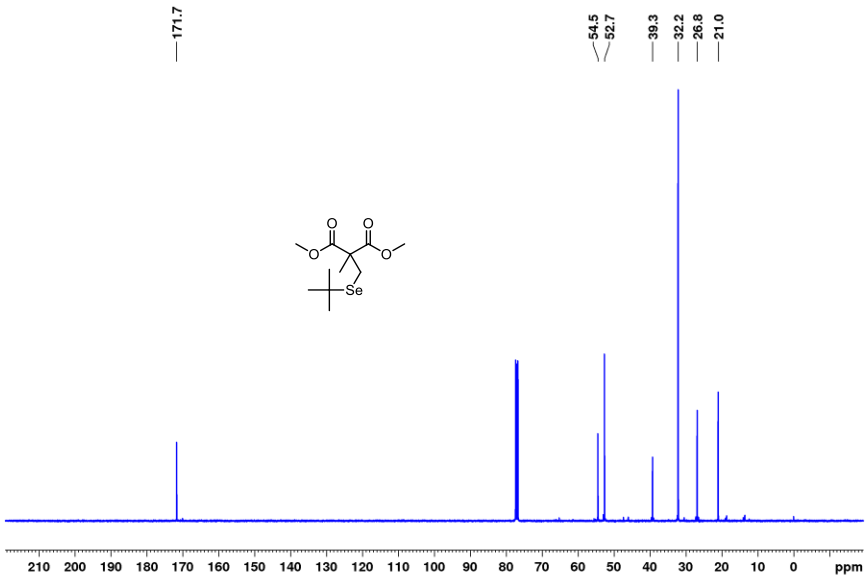
171.7
54.5
52.7
39.3
32.2
26.8
21.0
O
O
O
O
Se
210 200 190 180 170 160 150 140 130 120 110 100 90 80 70 60 50 40 30 20 10 0 ppm

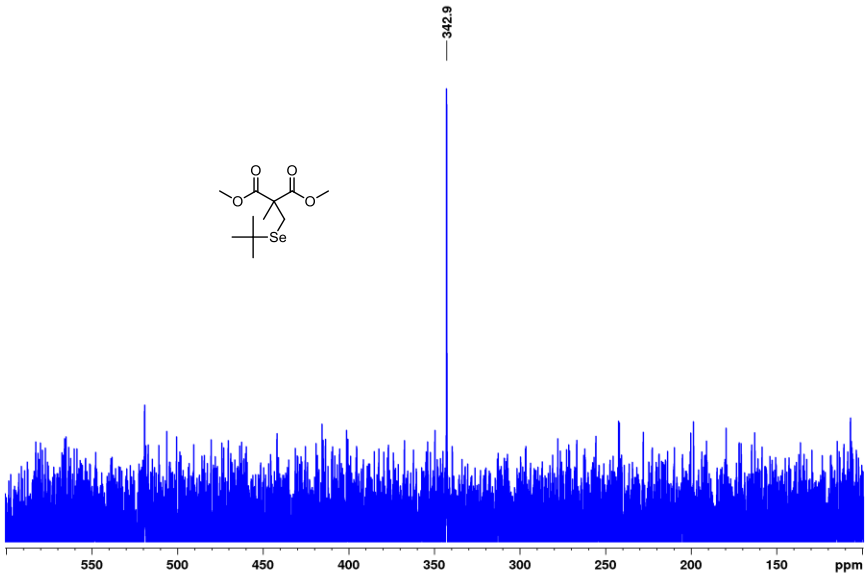
342.9
O
O
O
O
Se
550
500
450
400
350
300
250
200
150
ppm

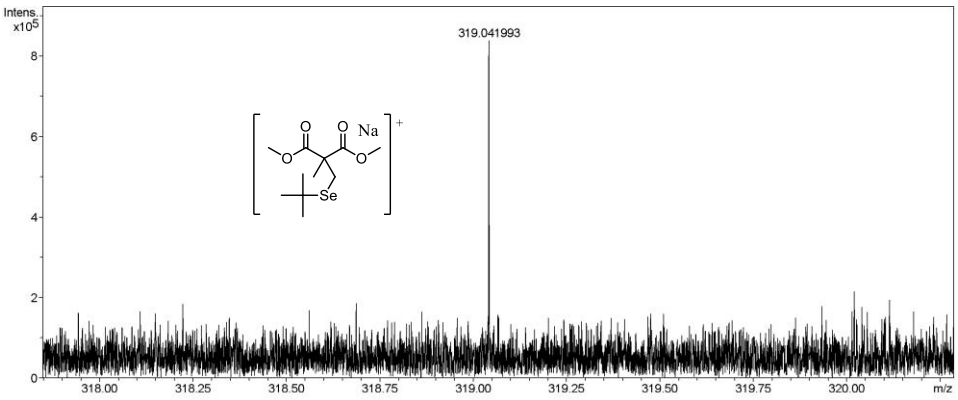
Intens.
x10^5
8
6
4
2
0
319.041993
O
O
O
O
Na
+
Se
318.00
318.25
318.50
318.75
319.00
319.25
319.50
319.75
320.00
m/z

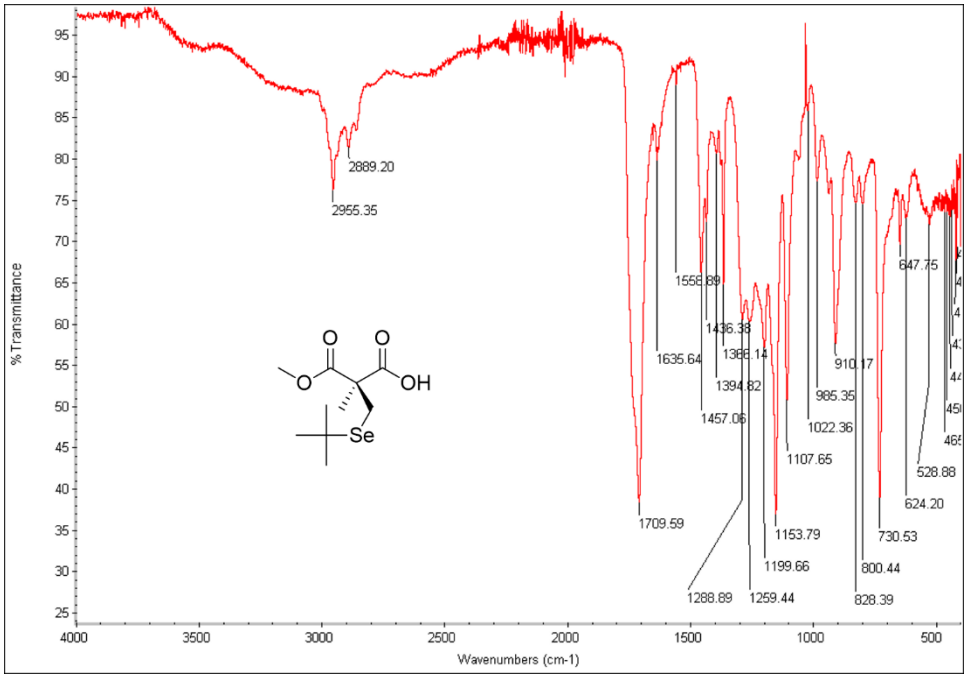
% Transmittance
Wavenumbers (cm-1)
2955.35
2889.20
1709.59
1635.64
1558.89
1457.06
1436.38
1394.82
1366.14
1288.89
1259.44
1199.66
1153.79
1107.65
1022.36
985.35
910.17
828.39
800.44
730.53
647.75
624.20
528.88
O
O
O
OH
Se

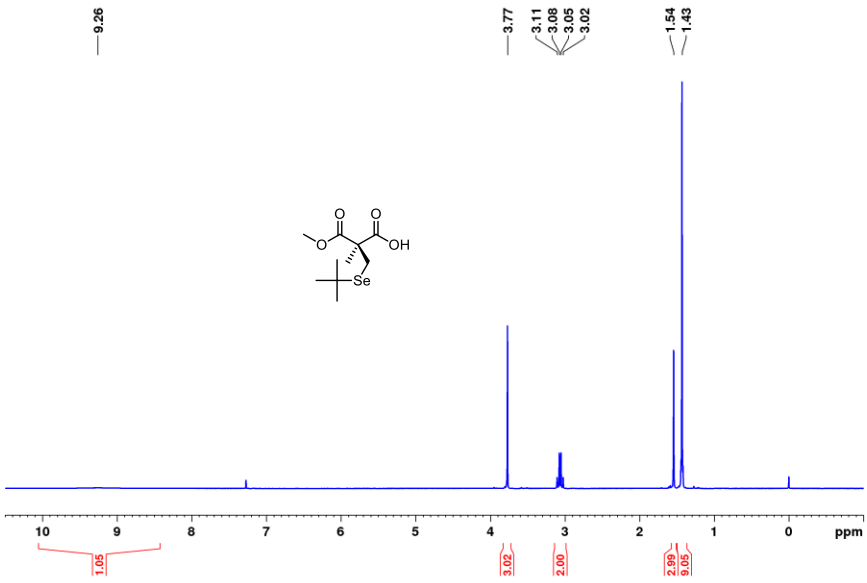
9.26
3.77
3.11
3.08
3.05
3.02
1.54
1.43
ppm
1.05
3.02
2.00
2.99
9.05
O
O
O
OH
Se

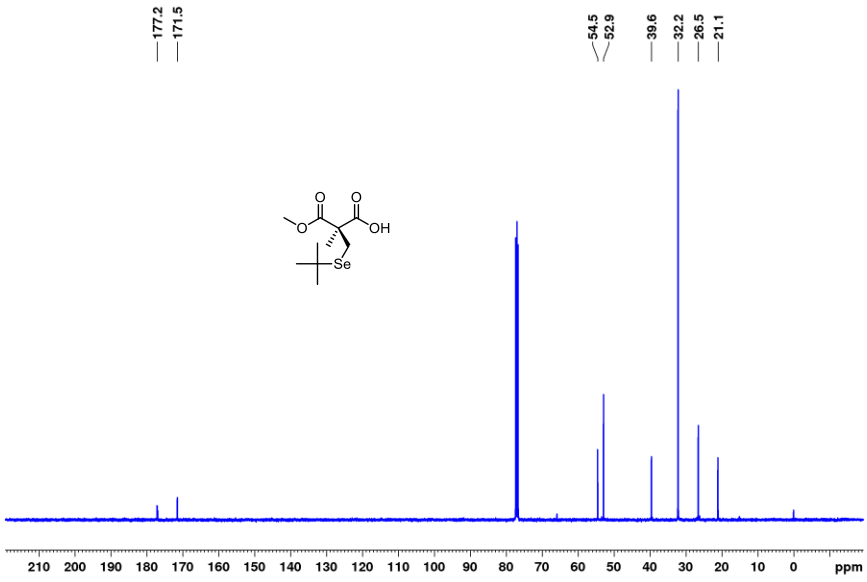
177.2
171.5
54.5
52.9
39.6
32.2
26.5
21.1
O
O
O
OH
Se
210 200 190 180 170 160 150 140 130 120 110 100 90 80 70 60 50 40 30 20 10 0 ppm

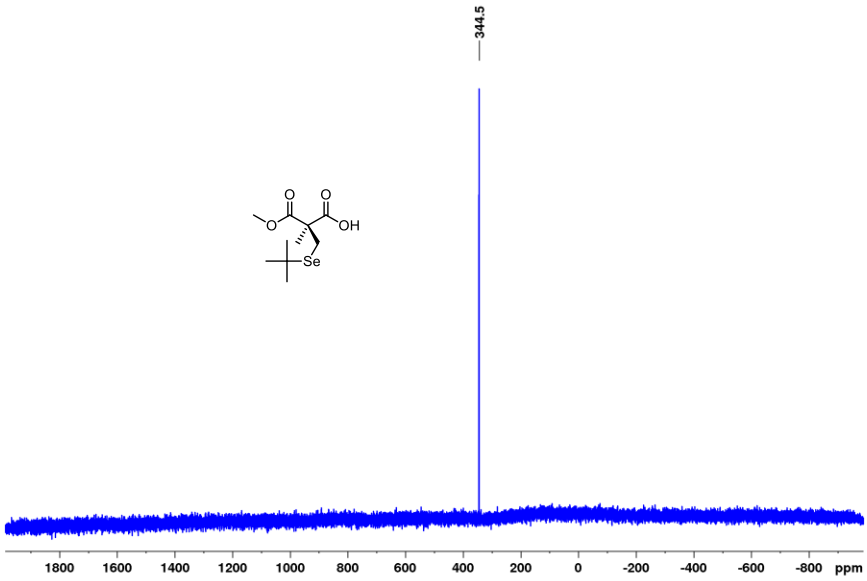
344.5
O
O
O
OH
Se
1800 1600 1400 1200 1000 800 600 400 200 0 -200 -400 -600 -800 ppm

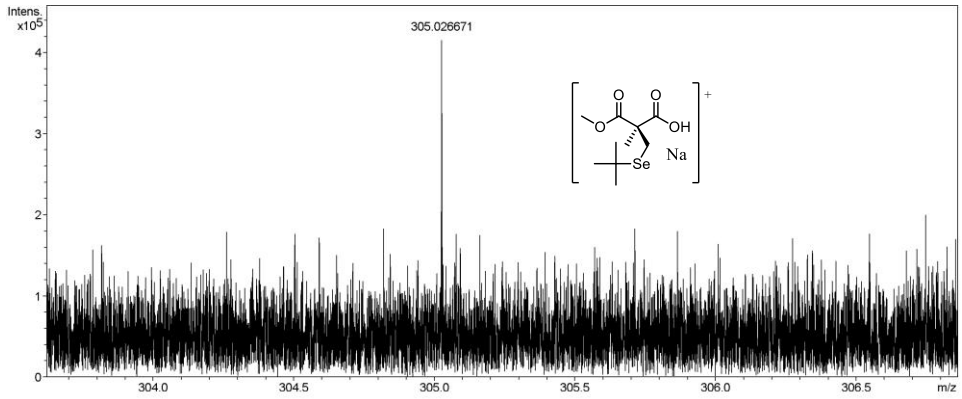
Intens.
x10^5
305.026671
Na
304.0
304.5
305.0
305.5
306.0
306.5
m/z

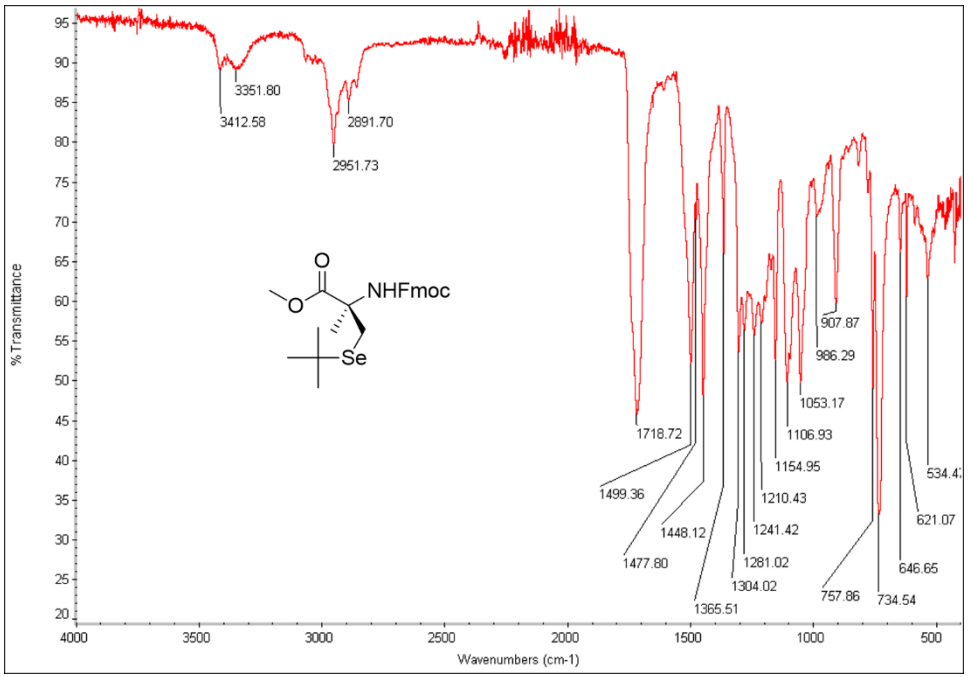
% Transmittance
3412.58
3351.80
2891.70
2951.73
NHFmoc
1718.72
1499.36
1448.12
1477.80
1365.51
1281.02
1304.02
1241.42
1210.43
1154.95
1106.93
1053.17
986.29
907.87
757.86
734.54
646.65
621.07
534.4
Wavenumbers (cm-1)

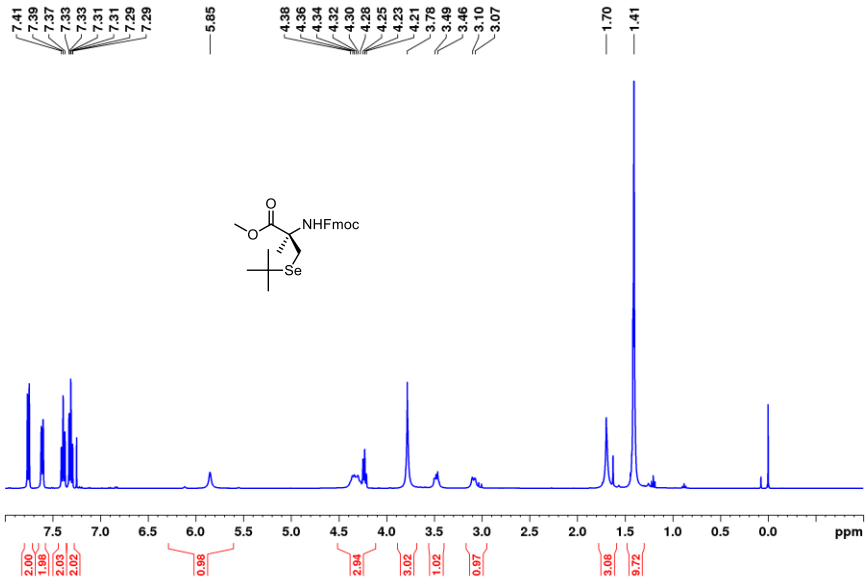
7.41
7.39
7.37
7.33
7.33
7.31
7.31
7.29
7.29
5.85
4.38
4.36
4.34
4.32
4.30
4.28
4.25
4.23
4.21
3.78
3.49
3.46
3.10
3.07
1.70
1.41
NHFmoc
Se
7.5
7.0
6.5
6.0
5.5
5.0
4.5
4.0
3.5
3.0
2.5
2.0
1.5
1.0
0.5
0.0
ppm
2.00
1.98
2.03
2.02
0.96
2.94
3.02
1.02
0.97
3.06
9.72

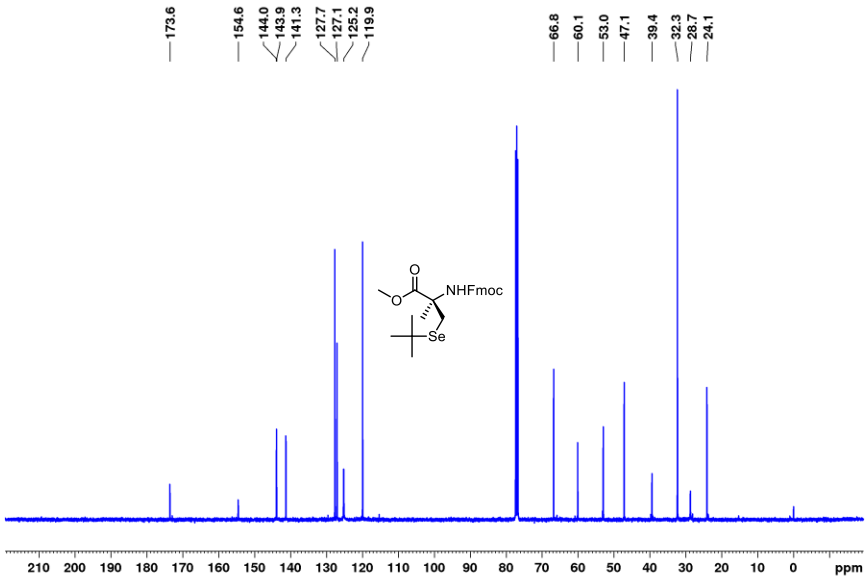
173.6
154.6
144.0
143.9
141.3
127.7
127.1
125.2
119.9
66.8
60.1
53.0
47.1
39.4
32.3
28.7
24.1
NHFmoc
Se
210
200
190
180
170
160
150
140
130
120
110
100
90
80
70
60
50
40
30
20
10
0
ppm

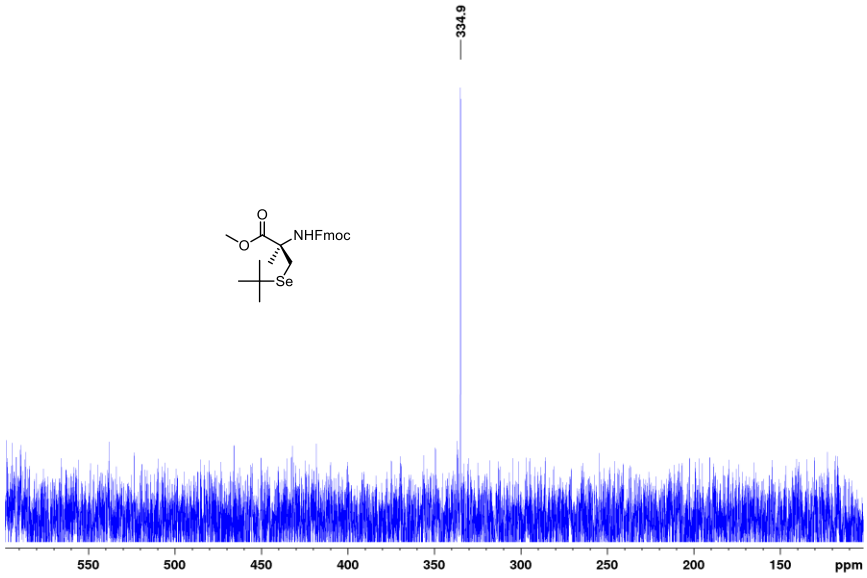
334.9
O
O
NHFmoc
Se
550
500
450
400
350
300
250
200
150
ppm

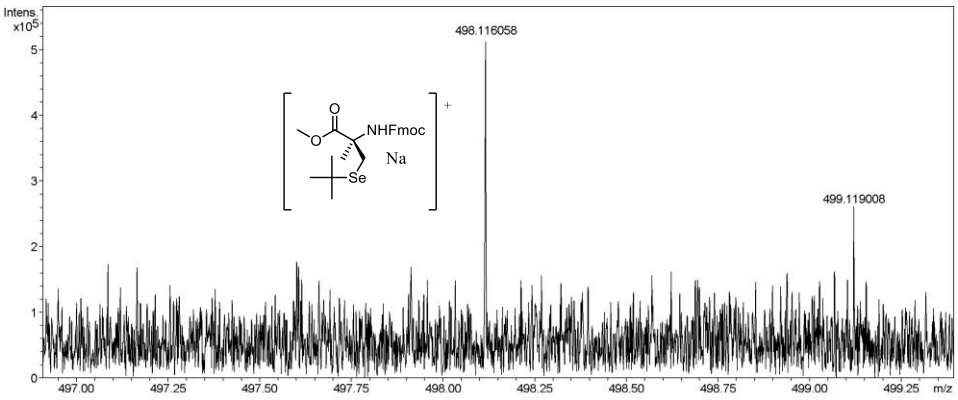
Intens.
x10^5
5
4
3
2
1
0
498.116058
499.119008
O
O
NHFmoc
Na
Se
+
497.00
497.25
497.50
497.75
498.00
498.25
498.50
498.75
499.00
499.25
m/z

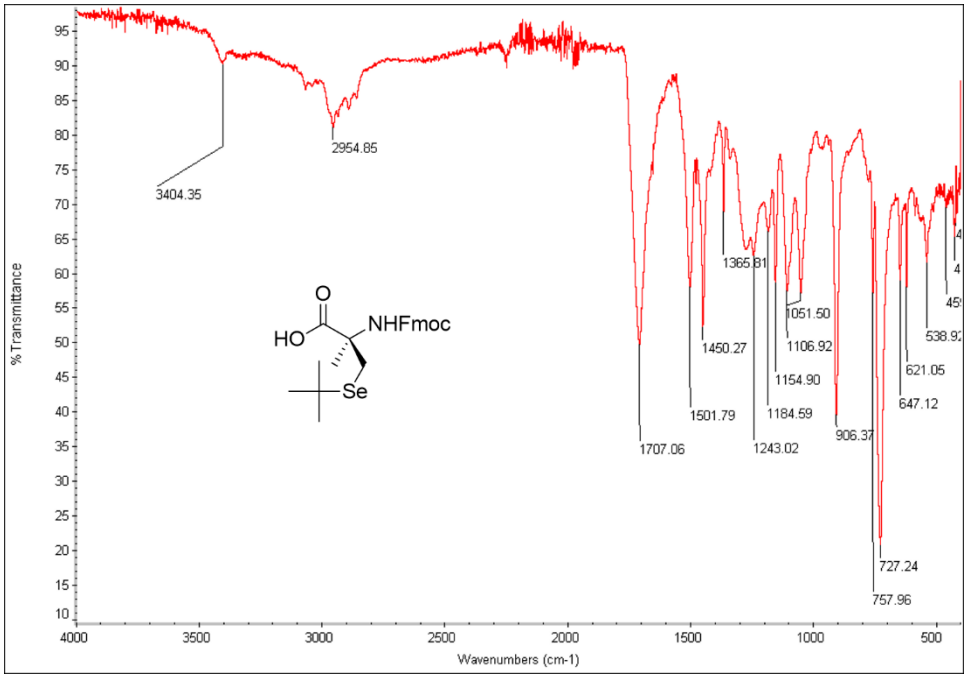
% Transmittance
Wavenumbers (cm-1)
3404.35
2954.85
1707.06
1501.79
1450.27
1365.81
1243.02
1184.59
1154.90
1106.92
1051.50
906.37
757.96
727.24
647.12
621.05
538.92
HO
O
NHFmoc
Se

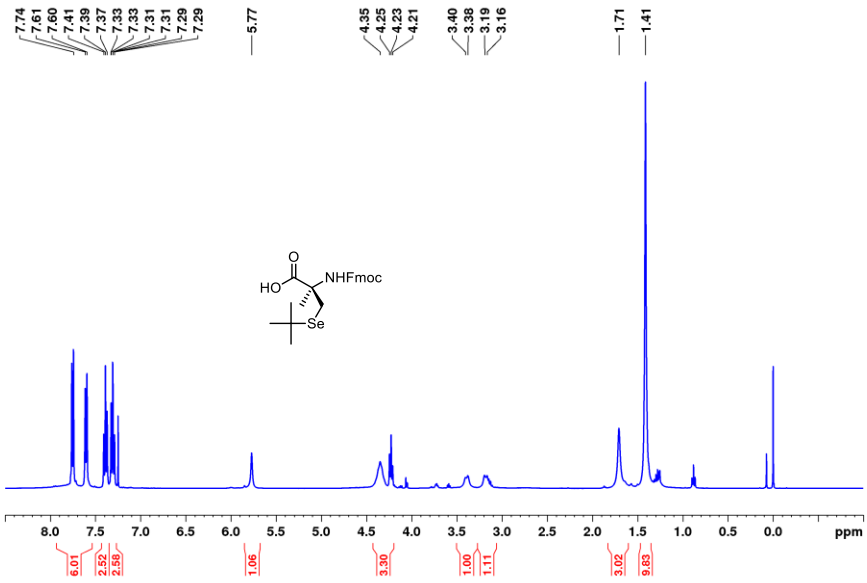
7.74
7.61
7.60
7.41
7.39
7.37
7.33
7.33
7.31
7.31
7.29
7.29
5.77
4.35
4.25
4.23
4.21
3.40
3.38
3.19
3.16
1.71
1.41
HO
O
NHFmoc
Se
ppm
6.01
2.52
2.58
1.06
3.30
1.00
1.11
3.02
9.83

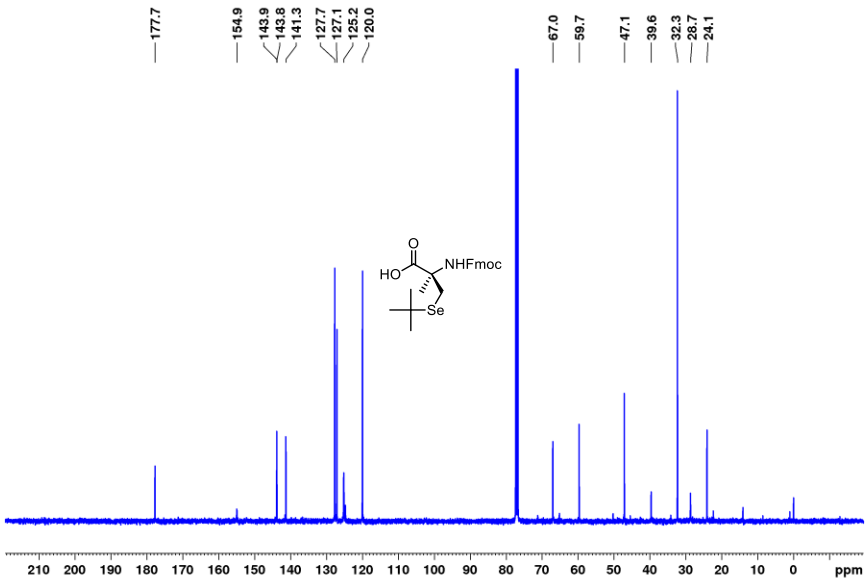
177.7
154.9
143.9
143.8
141.3
127.7
127.1
125.2
120.0
67.0
59.7
47.1
39.6
32.3
28.7
24.1
O
HO
NHFmoc
Se
210 200 190 180 170 160 150 140 130 120 110 100 90 80 70 60 50 40 30 20 10 0 ppm

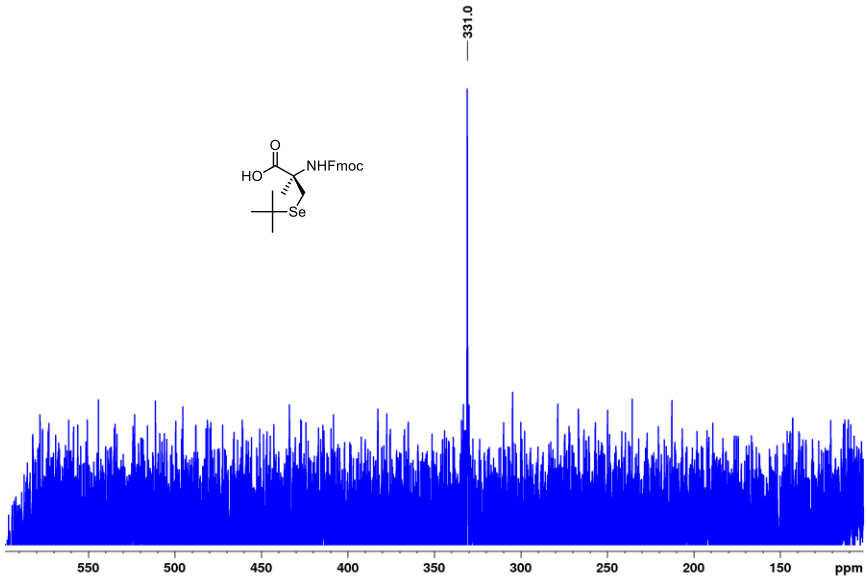
331.0
O
HO
NHFmoc
Se
550 500 450 400 350 300 250 200 150 ppm

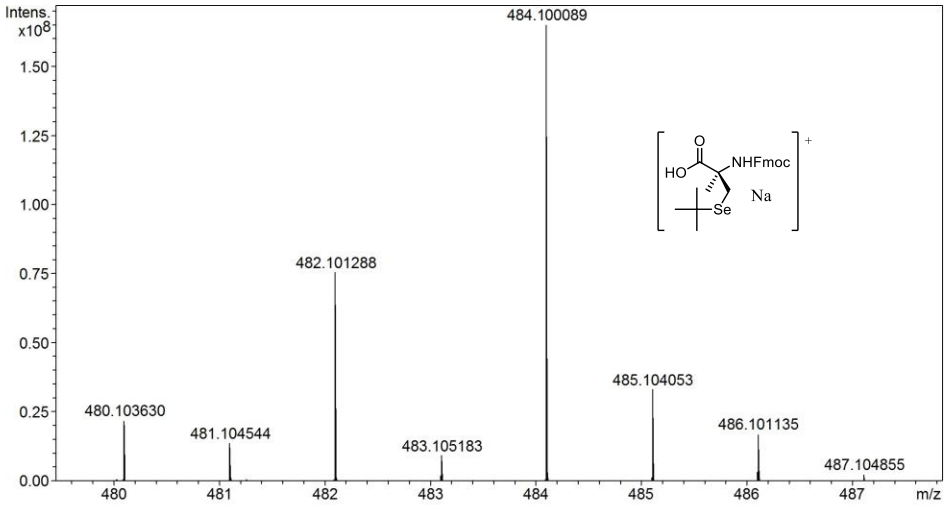
Intens.
x10^8
1.50
1.25
1.00
0.75
0.50
0.25
0.00
484.100089
482.101288
485.104053
480.103630
481.104544
483.105183
486.101135
487.104855
480
481
482
483
484
485
486
487
m/z
HO
O
NHFmoc
Na
Se

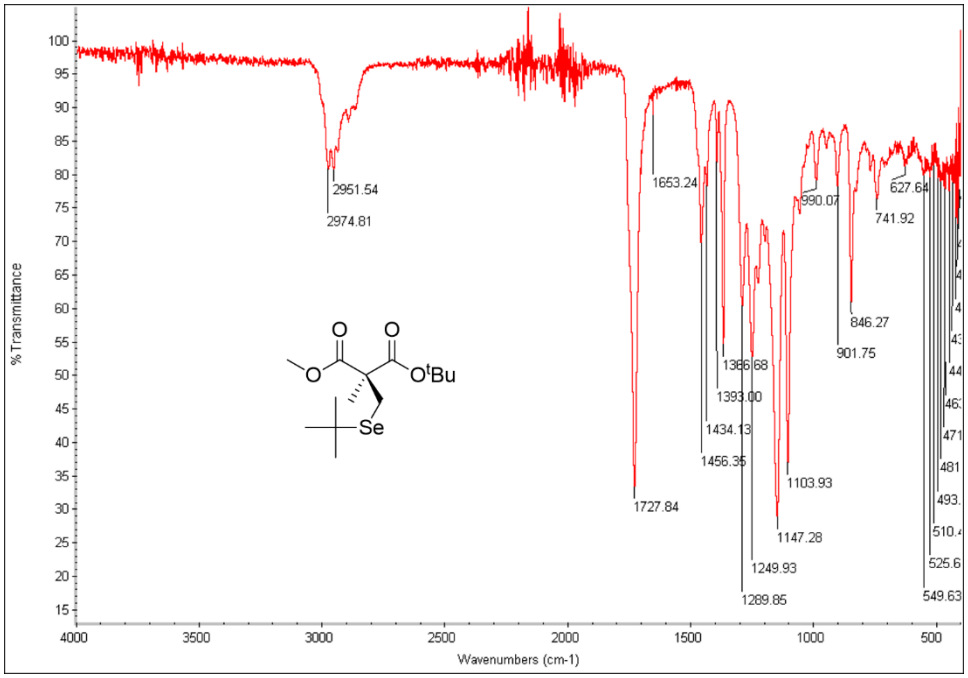
% Transmittance
100
95
90
85
80
75
70
65
60
55
50
45
40
35
30
25
20
15
2951.54
2974.81
1653.24
990.07
627.64
741.92
846.27
901.75
1386.68
1393.00
1434.13
1456.35
1103.93
1727.84
1147.28
1249.93
1289.85
549.63
525.6
510.
493.
481
471
4000
3500
3000
2500
2000
1500
1000
500
Wavenumbers (cm-1)
O
O
O
O^tBu
Se

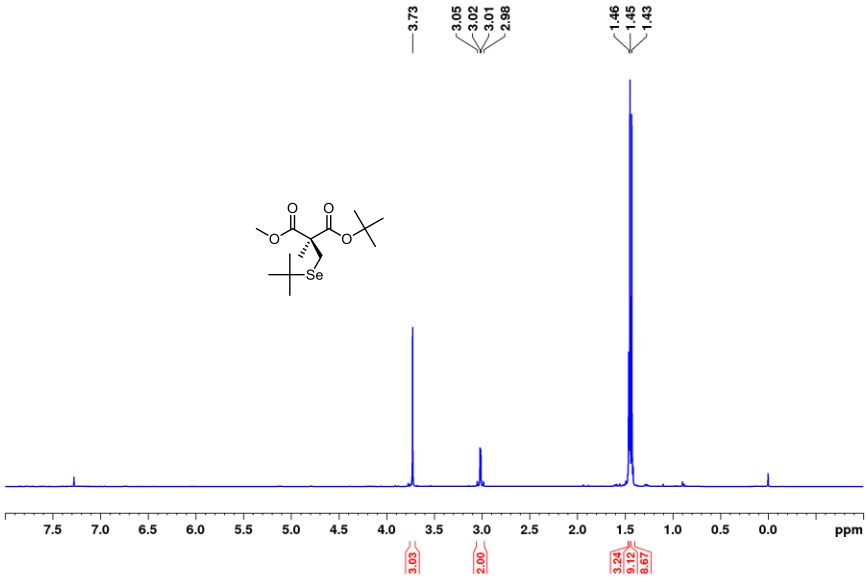
3.73
3.05
3.02
3.01
2.98
1.46
1.45
1.43
Se
7.5 7.0 6.5 6.0 5.5 5.0 4.5 4.0 3.5 3.0 2.5 2.0 1.5 1.0 0.5 0.0 ppm
3.03
2.00
3.24
9.12
8.67

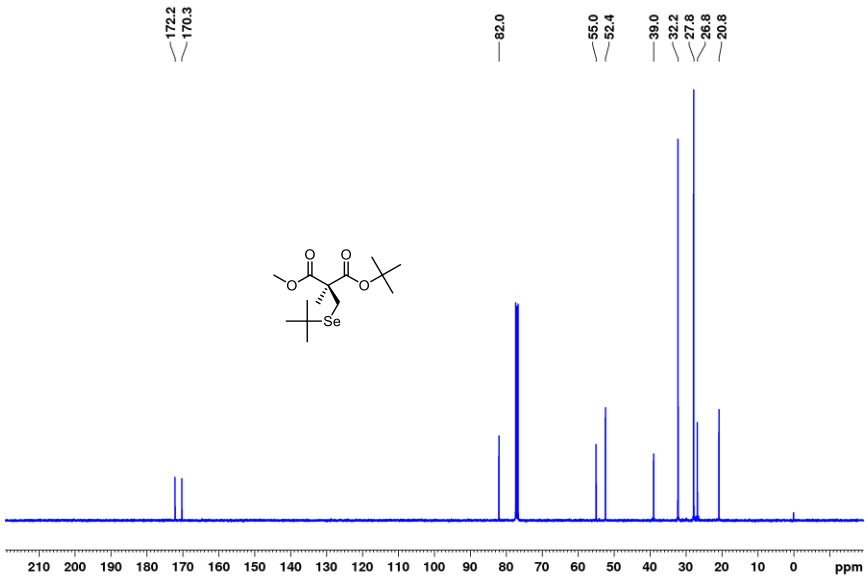
172.2
170.3
82.0
55.0
52.4
39.0
32.2
27.8
26.8
20.8
Se
210 200 190 180 170 160 150 140 130 120 110 100 90 80 70 60 50 40 30 20 10 0 ppm

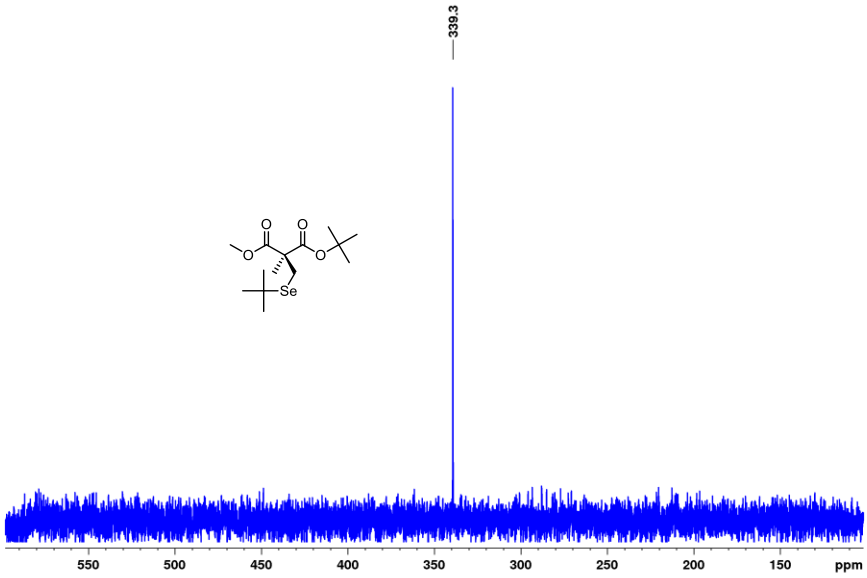
339.3
Se
550
500
450
400
350
300
250
200
150
ppm

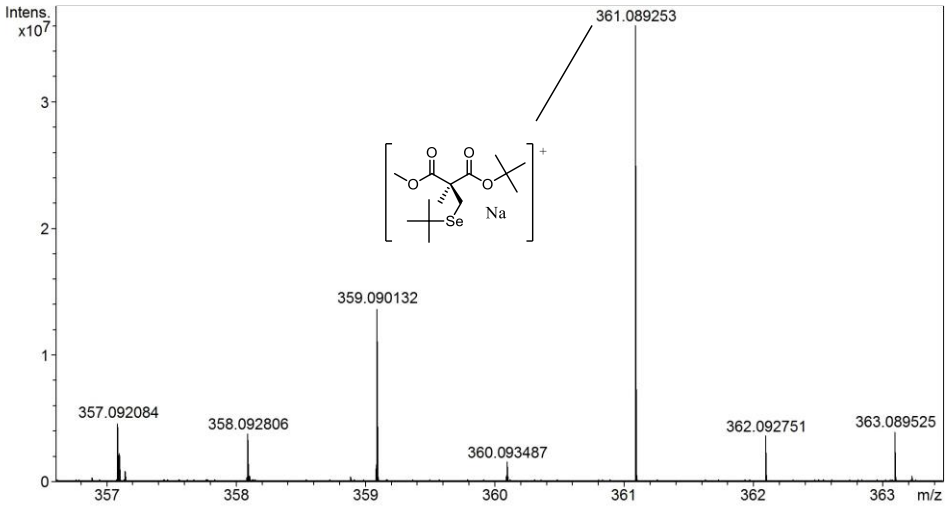
Intens.
x10^7
3
2
1
0
361.089253
359.090132
357.092084
358.092806
360.093487
362.092751
363.089525
Na
Se
357
358
359
360
361
362
363
m/z

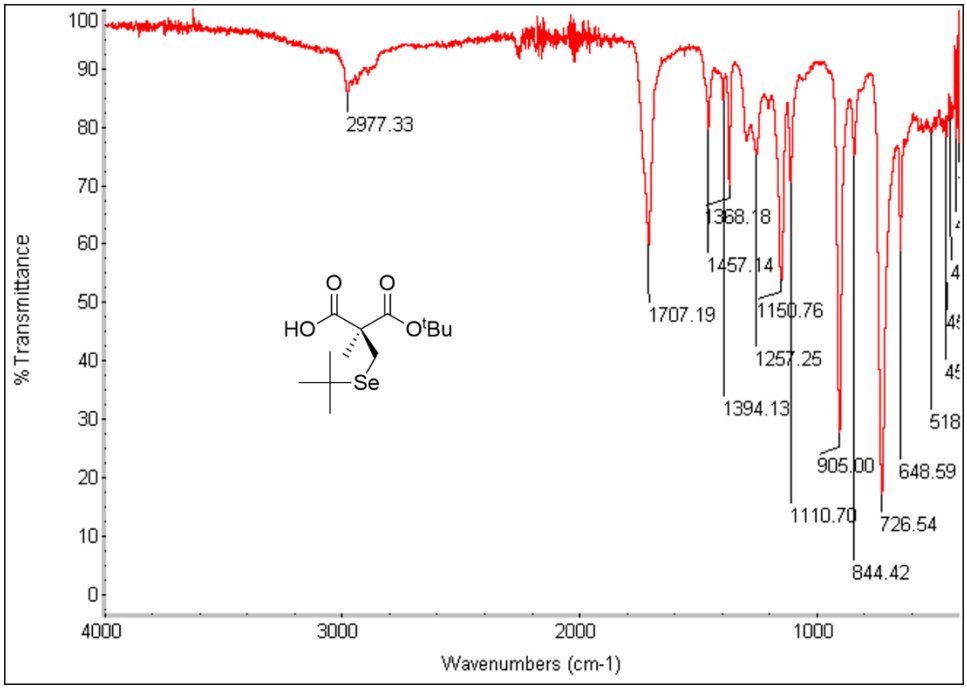
% Transmittance
Wavenumbers (cm-1)
2977.33
1707.19
1457.14
1368.18
1394.13
1257.25
1150.76
1110.70
905.00
844.42
726.54
648.59
HO
O
O
OtBu
Se

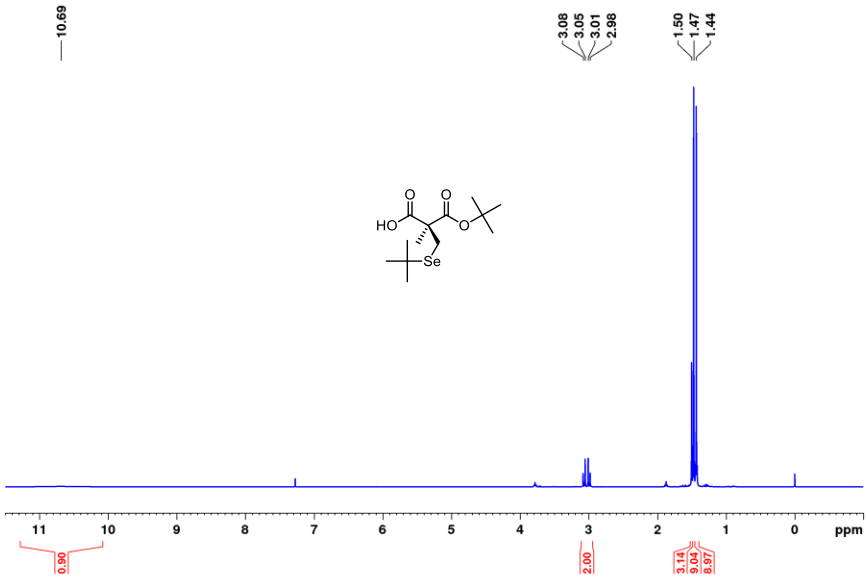
10.69
3.08
3.05
3.01
2.98
1.50
1.47
1.44
HO
O
O
Se
ppm

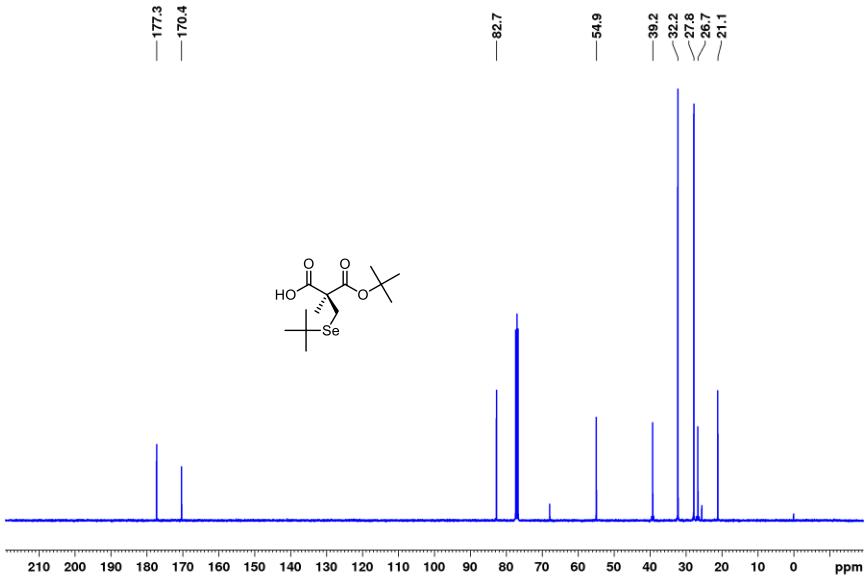
177.3
170.4
82.7
54.9
39.2
32.2
27.8
26.7
21.1
HO
O
O
O
Se
210 200 190 180 170 160 150 140 130 120 110 100 90 80 70 60 50 40 30 20 10 0 ppm

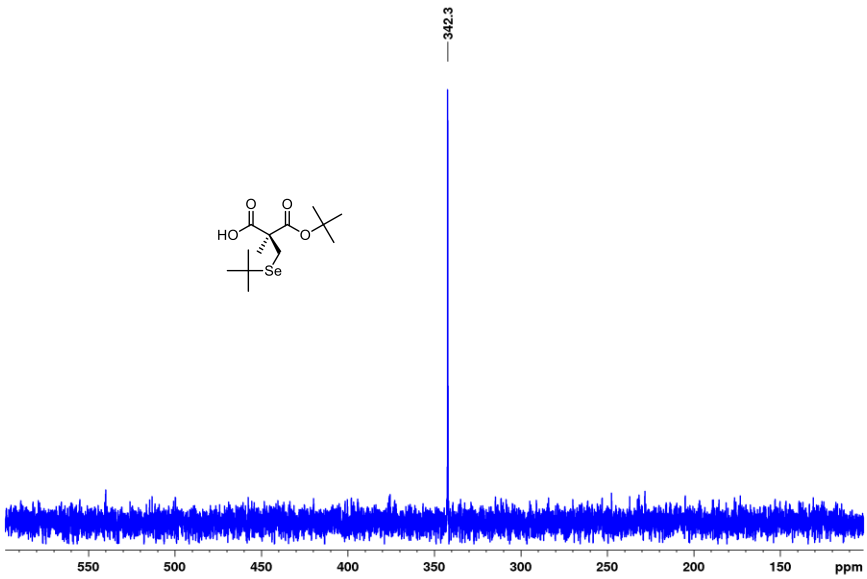
342.3
HO
O
O
O
Se
550 500 450 400 350 300 250 200 150 ppm

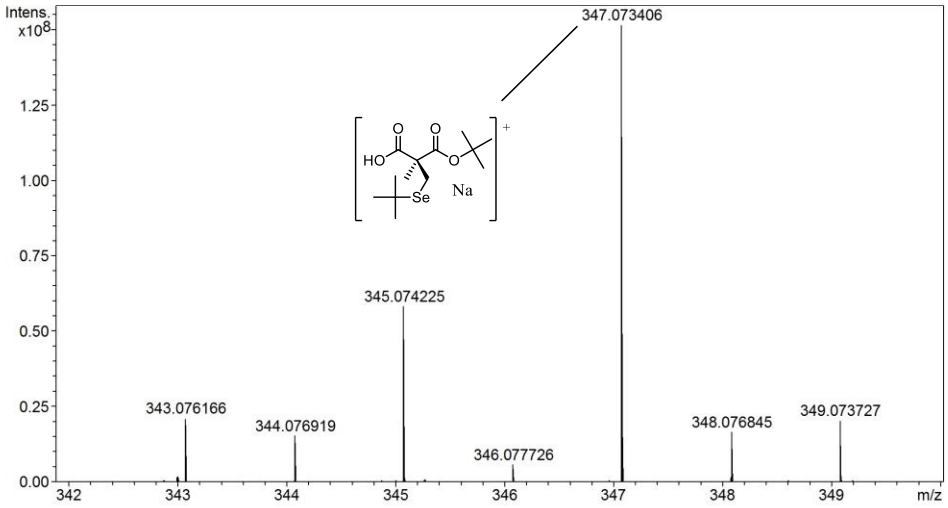
Intens.
x10^8
1.25
1.00
0.75
0.50
0.25
0.00
347.073406
345.074225
343.076166
344.076919
346.077726
348.076845
349.073727
342
343
344
345
346
347
348
349
m/z
HO
O
O
O
Se
Na
+

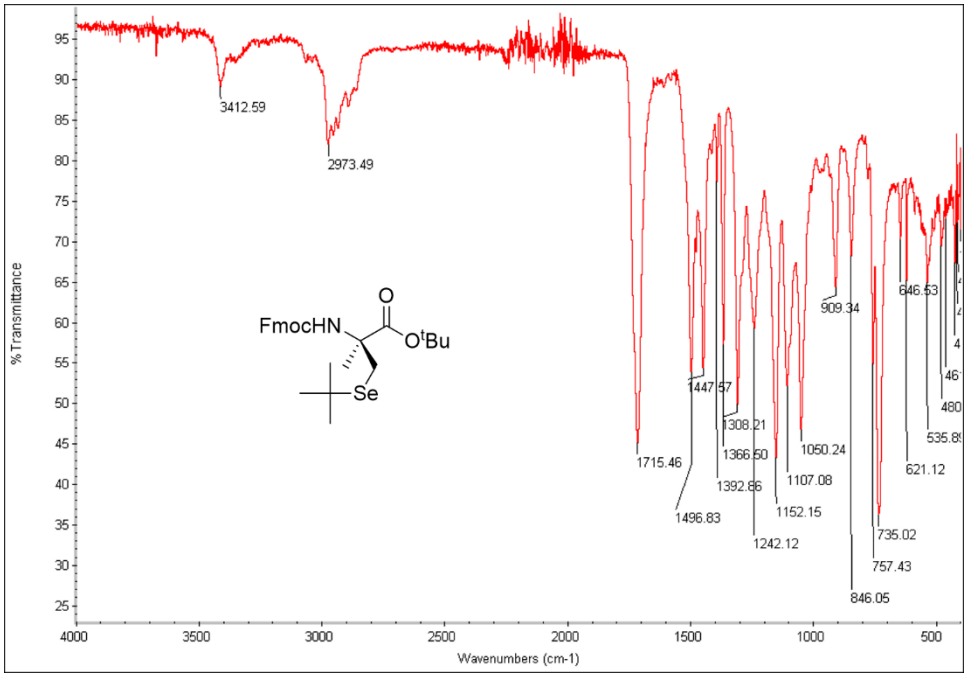
% Transmittance
95
90
85
80
75
70
65
60
55
50
45
40
35
30
25
3412.59
2973.49
1715.46
1496.83
1447.57
1392.86
1366.60
1308.21
1242.12
1152.15
1107.08
1050.24
909.34
846.05
757.43
735.02
646.53
621.12
FmocHN
O
O^tBu
Se
4000
3500
3000
2500
2000
1500
1000
500
Wavenumbers (cm-1)

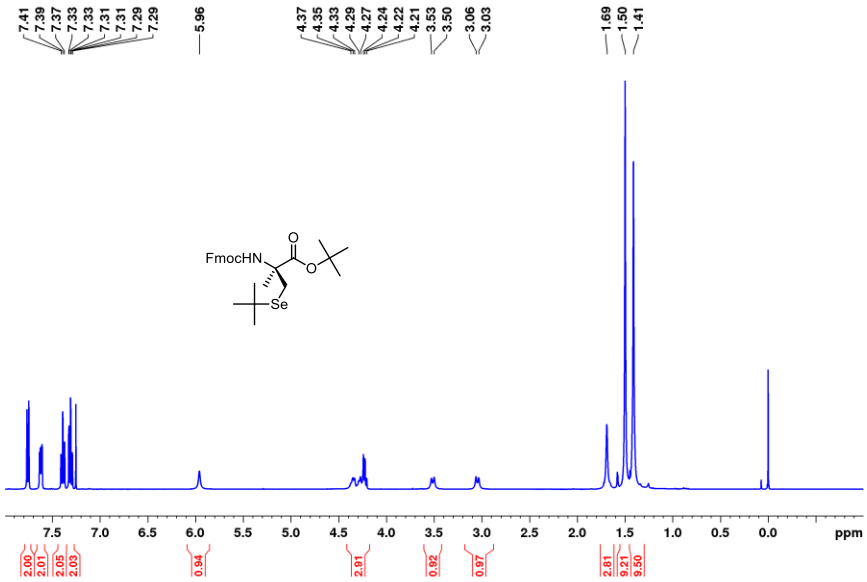
7.41
7.39
7.37
7.33
7.33
7.31
7.31
7.29
7.29
5.96
4.37
4.35
4.33
4.29
4.27
4.24
4.22
4.21
3.53
3.50
3.06
3.03
1.69
1.50
1.41
FmocHN
O
O
Se
7.5
7.0
6.5
6.0
5.5
5.0
4.5
4.0
3.5
3.0
2.5
2.0
1.5
1.0
0.5
0.0
ppm
2.00
2.01
2.05
2.03
0.94
2.91
0.92
0.97
2.81
9.21
9.50

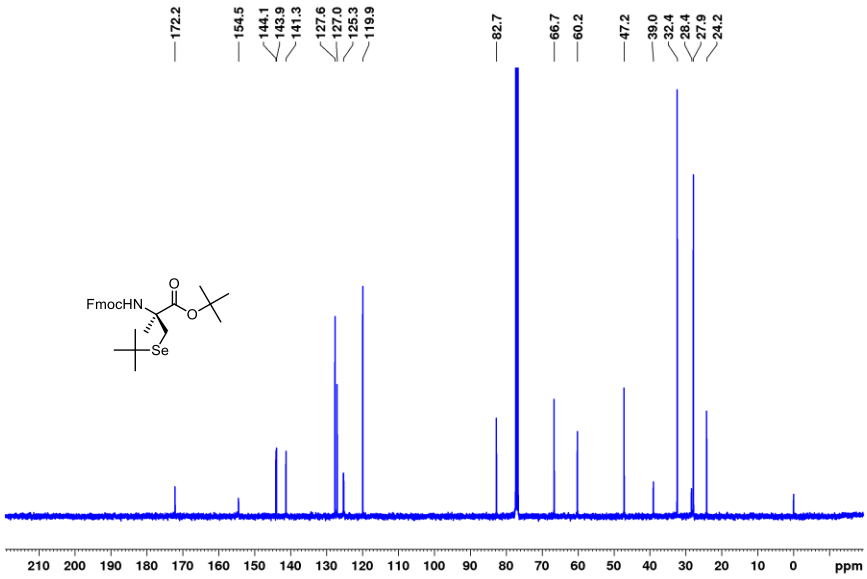
172.2
154.5
144.1
143.9
141.3
127.6
127.0
125.3
119.9
82.7
66.7
60.2
47.2
39.0
32.4
28.4
27.9
24.2
FmocHN
O
O
Se
210
200
190
180
170
160
150
140
130
120
110
100
90
80
70
60
50
40
30
20
10
0
ppm

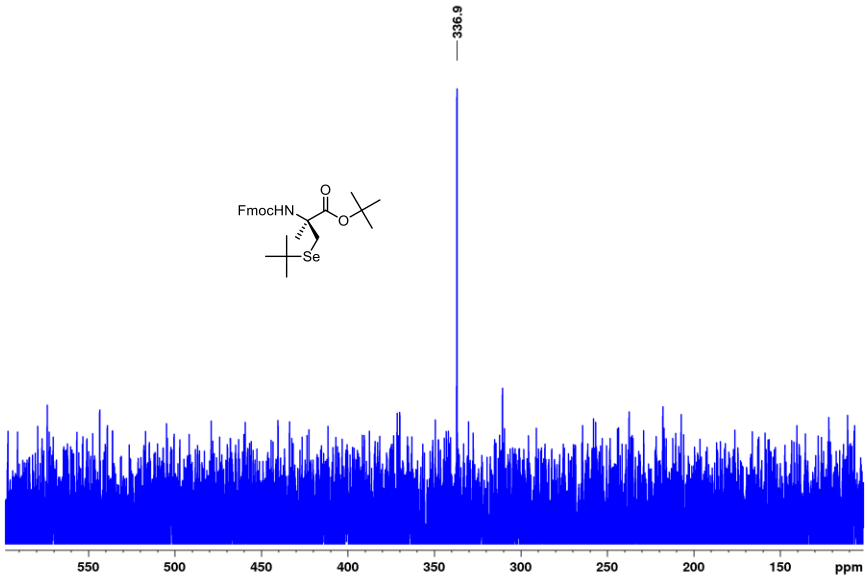
336.9
FmocHN
O
O
Se
550
500
450
400
350
300
250
200
150
ppm

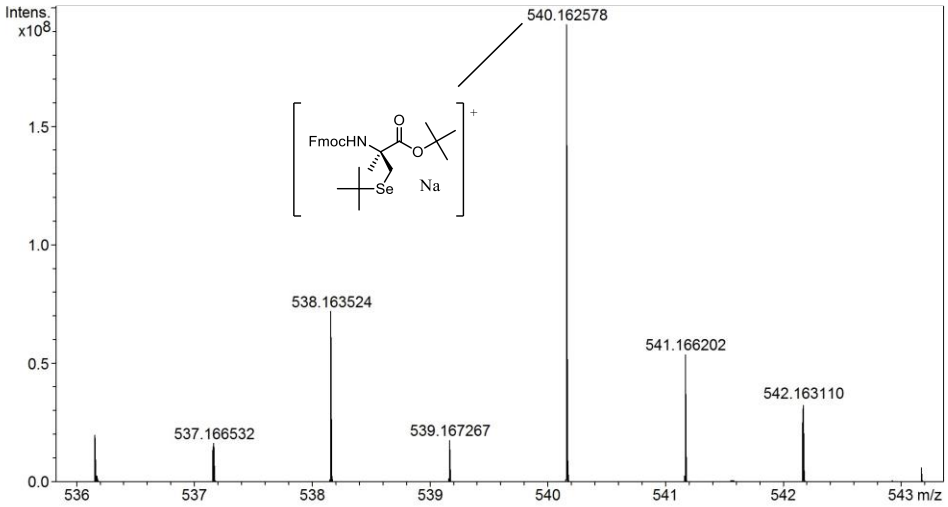
Intens.
x10^8
1.5
1.0
0.5
0.0
540.162578
538.163524
541.166202
542.163110
537.166532
539.167267
FmocHN
Se
Na
+
536
537
538
539
540
541
542
543 m/z

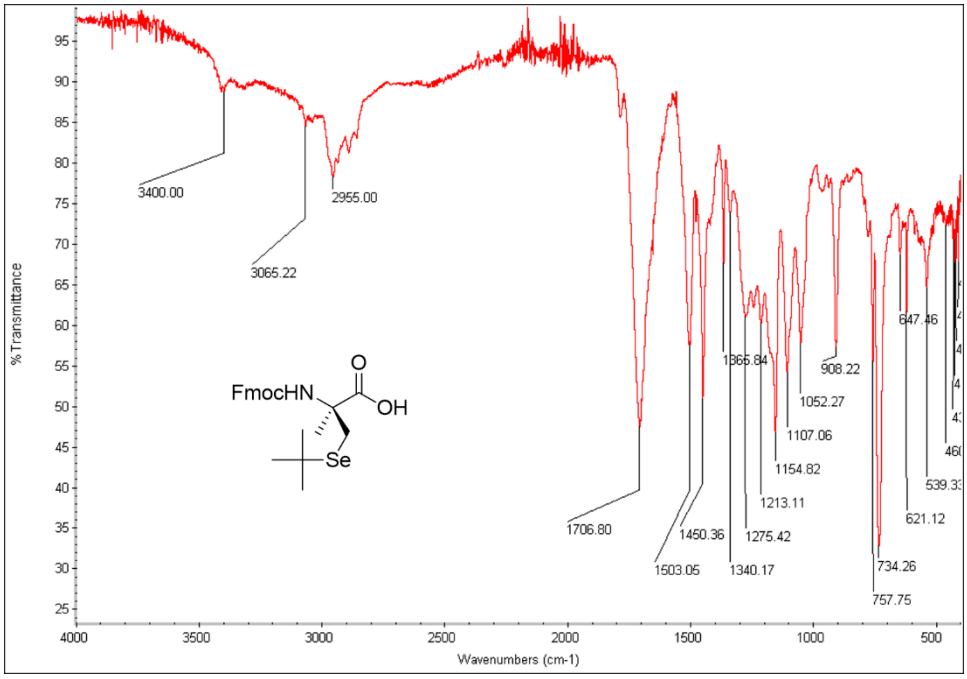
% Transmittance
Wavenumbers (cm-1)
3400.00
3065.22
2955.00
1706.80
1503.05
1450.36
1340.17
1275.42
1213.11
1154.82
1107.06
1052.27
908.22
757.75
734.26
621.12
539.33
647.46
FmocHN
OH
O
Se

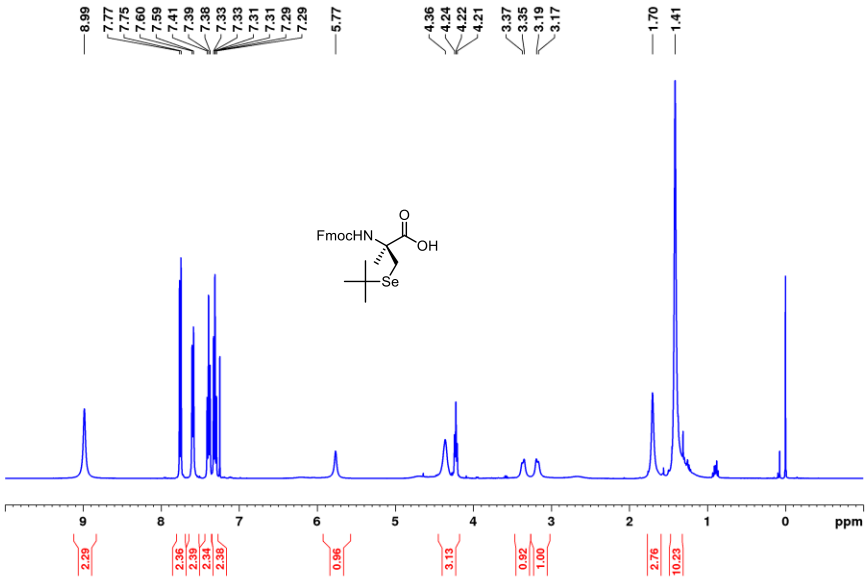
8.99
7.77
7.75
7.60
7.59
7.41
7.39
7.38
7.33
7.33
7.31
7.31
7.29
7.29
5.77
4.36
4.24
4.22
4.21
3.37
3.35
3.19
3.17
1.70
1.41
FmocHN
OH
O
Se
ppm
2.29
2.36
2.39
2.34
2.38
0.96
3.13
0.92
1.00
2.76
10.23

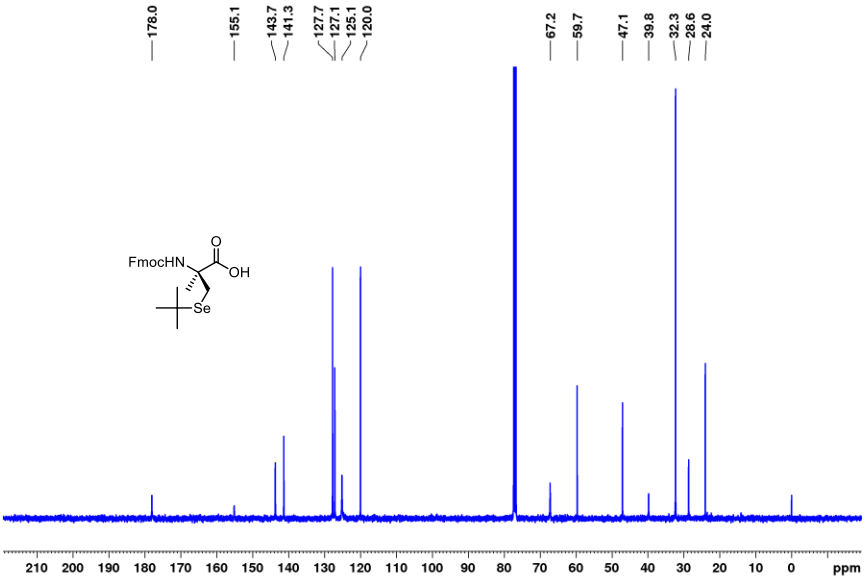
178.0
155.1
143.7
141.3
127.7
127.1
125.1
120.0
67.2
59.7
47.1
39.8
32.3
28.6
24.0
FmocHN
O
OH
Se
210 200 190 180 170 160 150 140 130 120 110 100 90 80 70 60 50 40 30 20 10 0 ppm

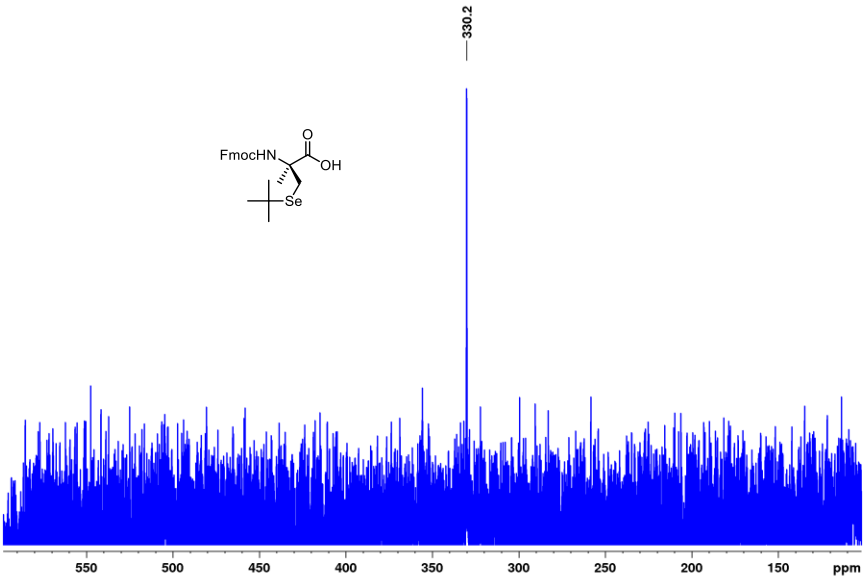
330.2
FmocHN
O
OH
Se
550 500 450 400 350 300 250 200 150 ppm

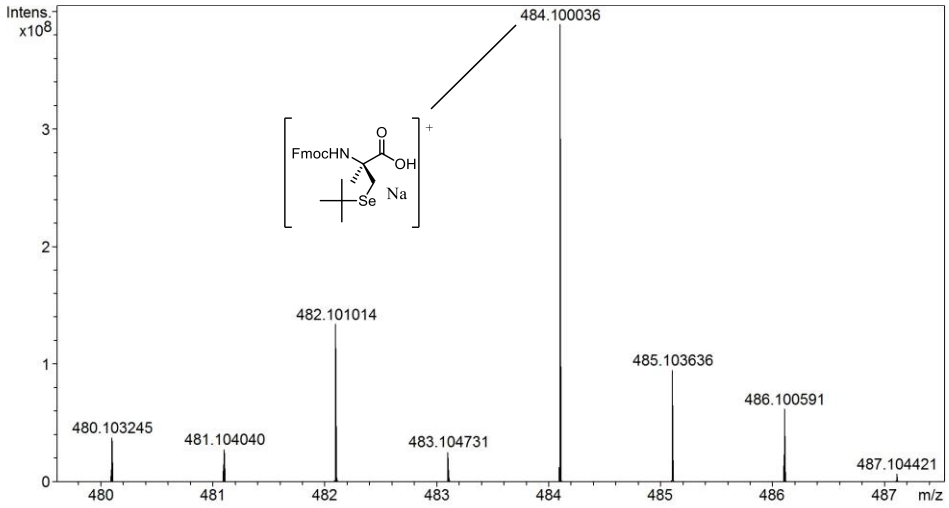
Intens.
x10^8
484.100036
482.101014
485.103636
486.100591
480.103245
481.104040
483.104731
487.104421
m/z
FmocHN
OH
Se
Na

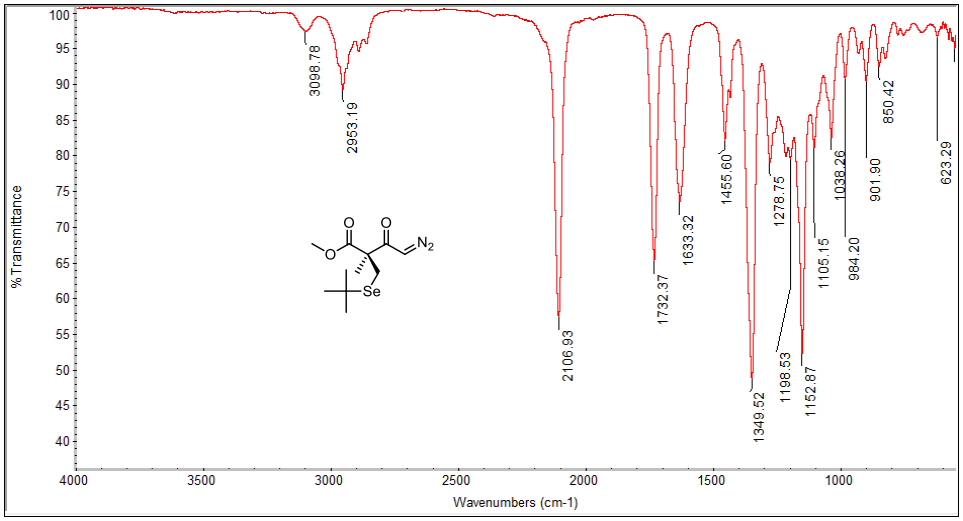
%Transmittance
Wavenumbers (cm-1)
3098.78
2953.19
2106.93
1732.37
1633.32
1455.60
1349.52
1278.75
1198.53
1152.87
1105.15
1038.26
984.20
901.90
850.42
623.29
N2
Se

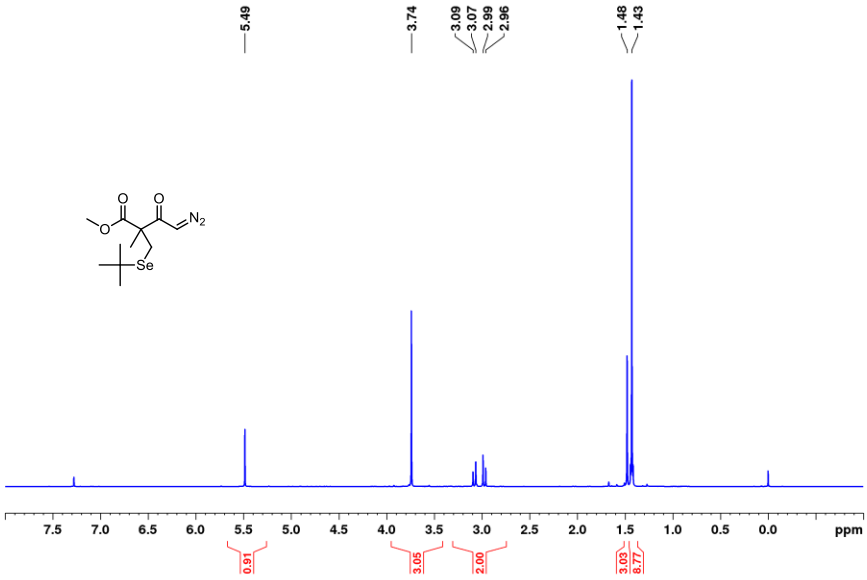
5.49
3.74
3.09
3.07
2.99
2.96
1.46
1.43
O
O
O
N2
Se
7.5 7.0 6.5 6.0 5.5 5.0 4.5 4.0 3.5 3.0 2.5 2.0 1.5 1.0 0.5 0.0 ppm
0.91
3.05
2.00
3.03
9.77

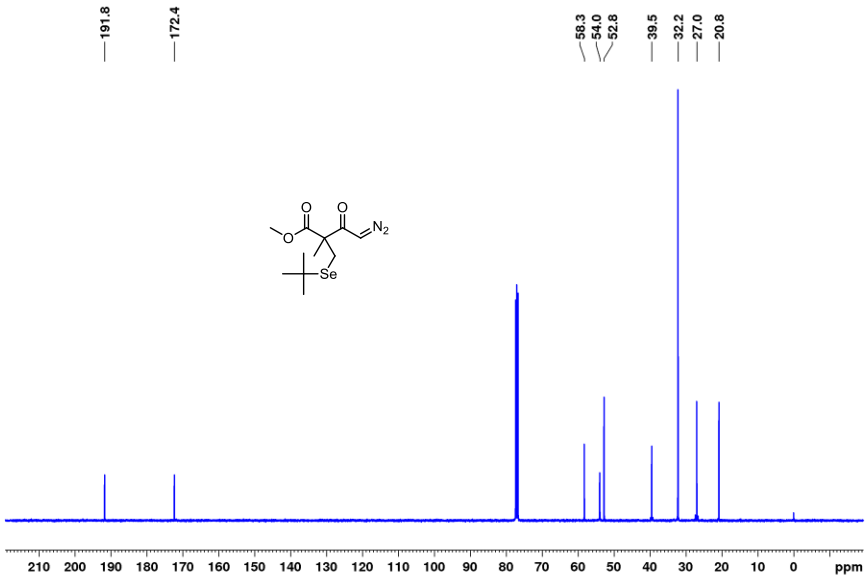
191.8
172.4
58.3
54.0
52.8
39.5
32.2
27.0
20.8
O
O
O
N2
Se
210 200 190 180 170 160 150 140 130 120 110 100 90 80 70 60 50 40 30 20 10 0 ppm

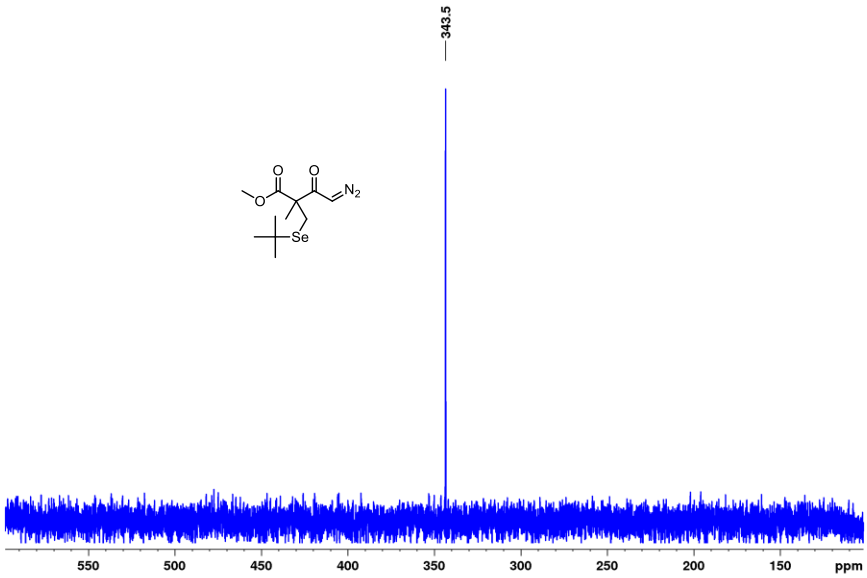
343.5
550
500
450
400
350
300
250
200
150
ppm

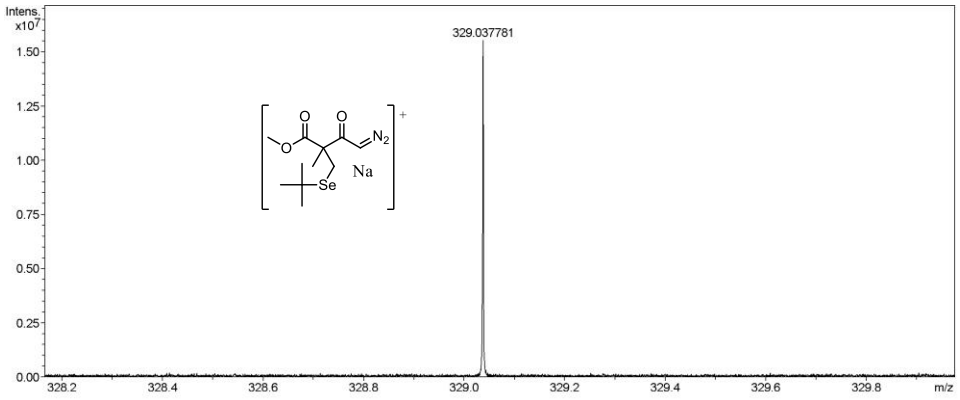
Intens.
x10^7
1.50
1.25
1.00
0.75
0.50
0.25
0.00
329.037781
328.2
328.4
328.6
328.8
329.0
329.2
329.4
329.6
329.8
m/z
Na

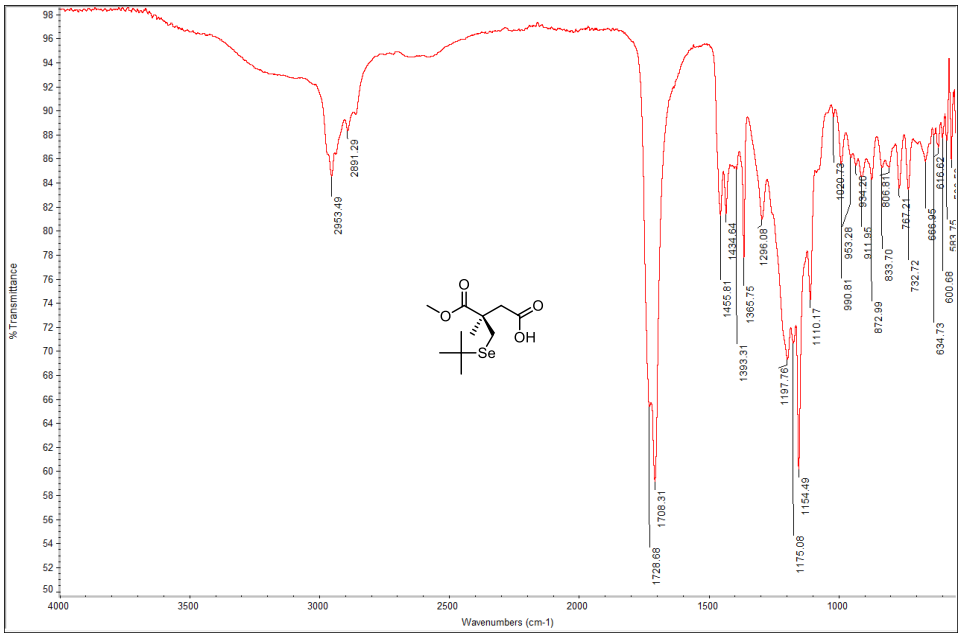
% Transmittance
Wavenumbers (cm-1)
2953.49
2891.29
1728.68
1708.31
1455.81
1434.64
1393.31
1365.75
1296.08
1197.76
1175.08
1154.49
1110.17
1020.73
990.81
953.28
934.26
911.95
872.99
833.70
806.81
767.21
732.72
666.96
634.73
616.62
600.68
OH
Se

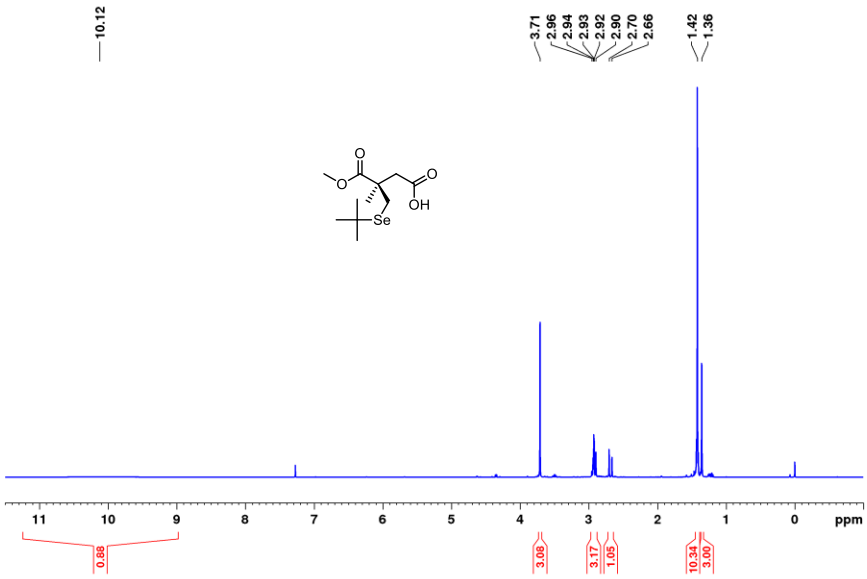
10.12
3.71
2.96
2.94
2.93
2.92
2.90
2.70
2.66
1.42
1.36
ppm
0.88
3.08
3.17
1.05
10.34
3.00
OH
Se

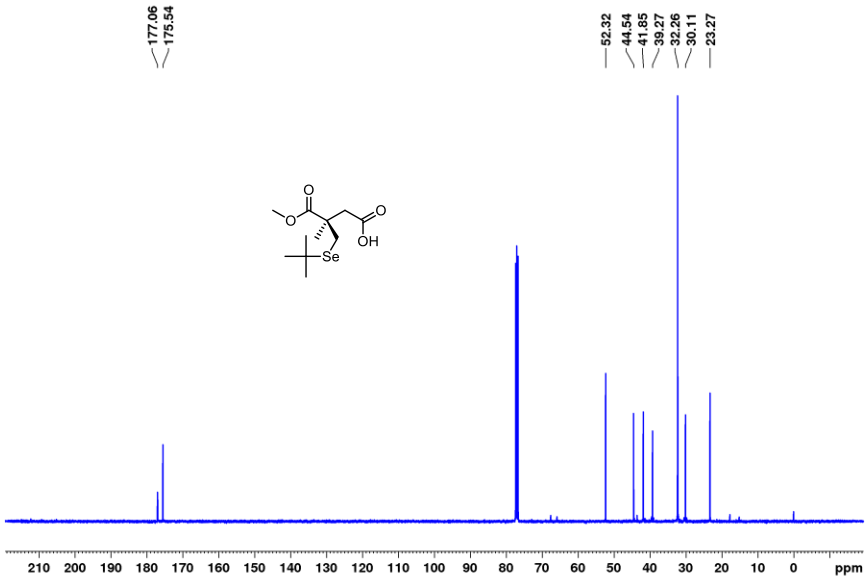
177.06
175.54
52.32
44.54
41.85
39.27
32.26
30.11
23.27
O
O
O
OH
Se
210 200 190 180 170 160 150 140 130 120 110 100 90 80 70 60 50 40 30 20 10 0 ppm

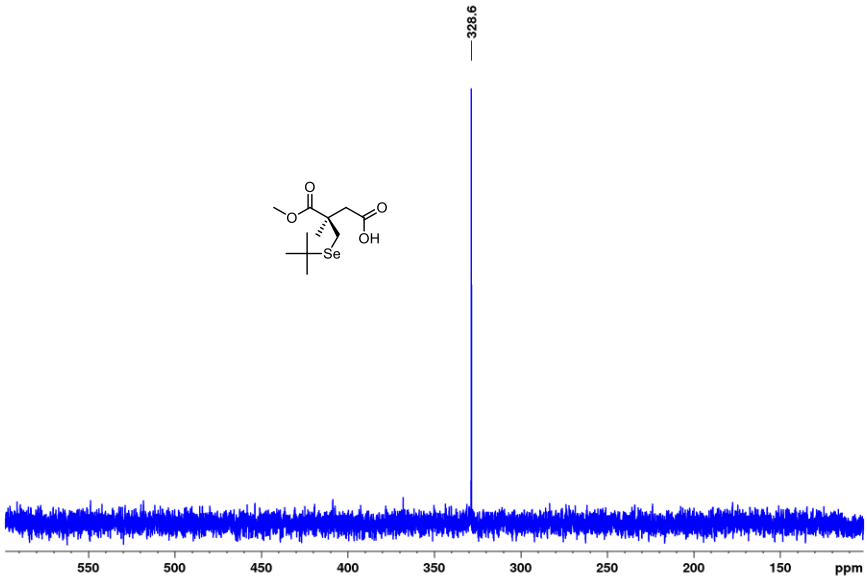
328.6
O
O
O
OH
Se
550 500 450 400 350 300 250 200 150 ppm

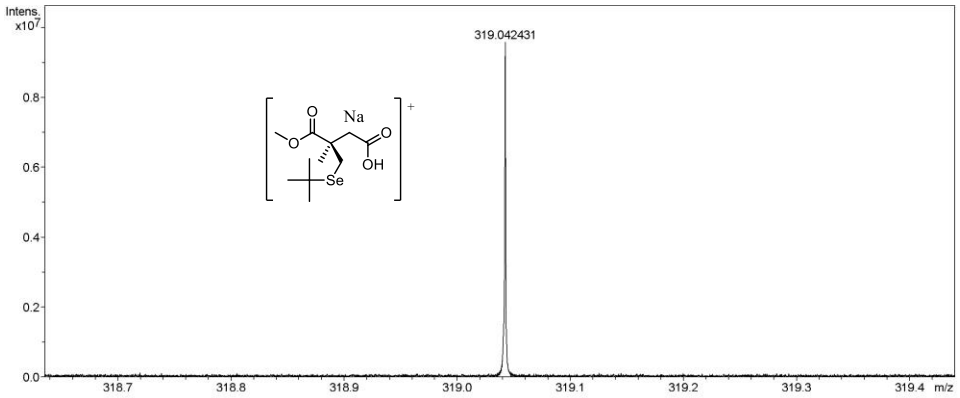
Intens.
x10^7
0.8
0.6
0.4
0.2
0.0
319.042431
318.7
318.8
318.9
319.0
319.1
319.2
319.3
319.4
m/z
Na
O
O
OH
Se

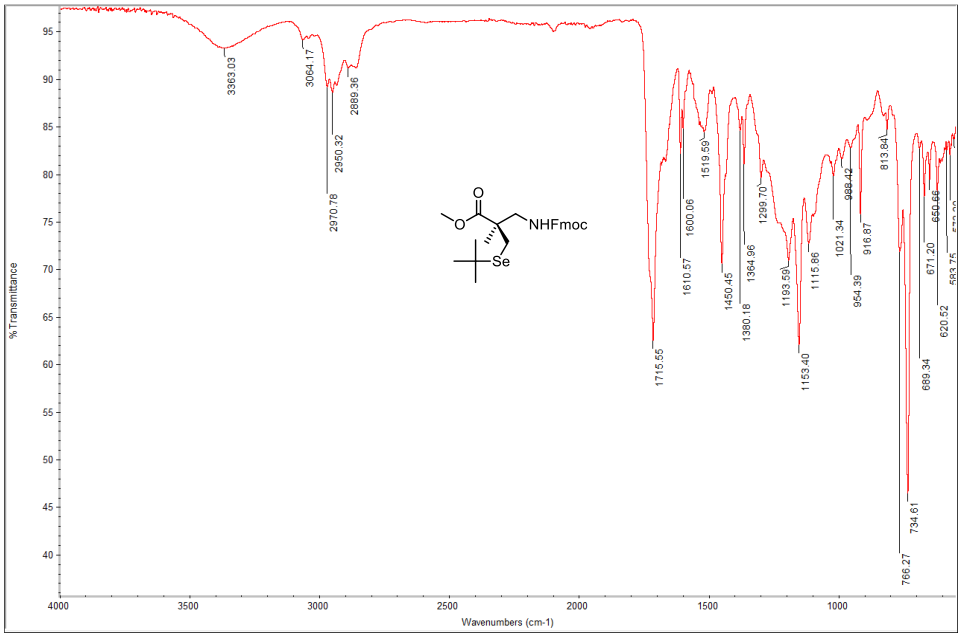
% Transmittance
95
90
85
80
75
70
65
60
55
50
45
40
4000
3500
3000
2500
2000
1500
1000
Wavenumbers (cm-1)
3363.03
3064.17
2970.78
2950.32
2889.36
1715.55
1610.57
1600.06
1519.59
1450.45
1380.18
1364.96
1299.70
1193.59
1153.40
1115.86
1021.34
988.42
954.39
916.87
813.84
766.27
734.61
689.34
671.20
650.66
620.52
583.75
NHFmoc
O
O
Se

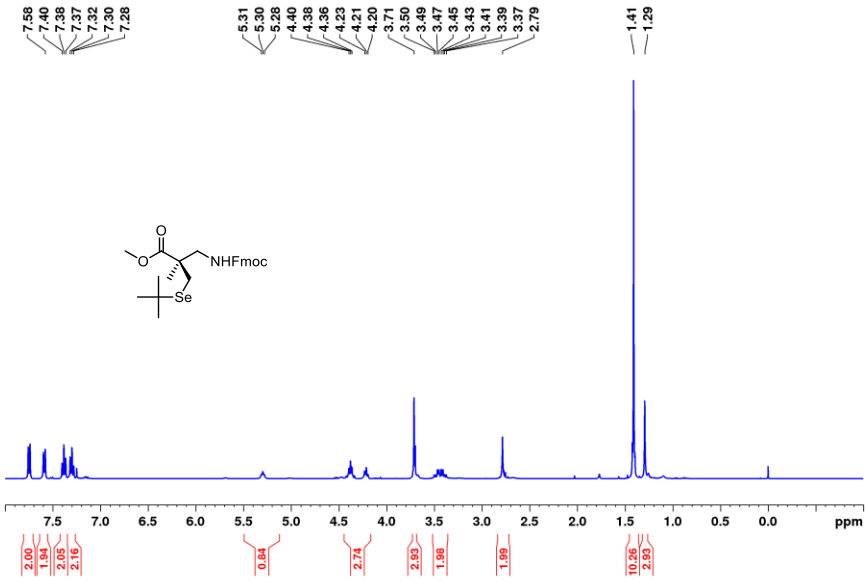
7.58
7.40
7.38
7.37
7.32
7.30
7.28
5.31
5.30
5.28
4.40
4.38
4.36
4.23
4.21
4.20
3.71
3.50
3.49
3.47
3.45
3.43
3.41
3.39
3.37
2.79
1.41
1.29
O
O
NHFmoc
Se
7.5
7.0
6.5
6.0
5.5
5.0
4.5
4.0
3.5
3.0
2.5
2.0
1.5
1.0
0.5
0.0
ppm
2.00
1.94
2.05
2.16
0.84
2.74
2.93
1.98
1.99
10.26
2.93

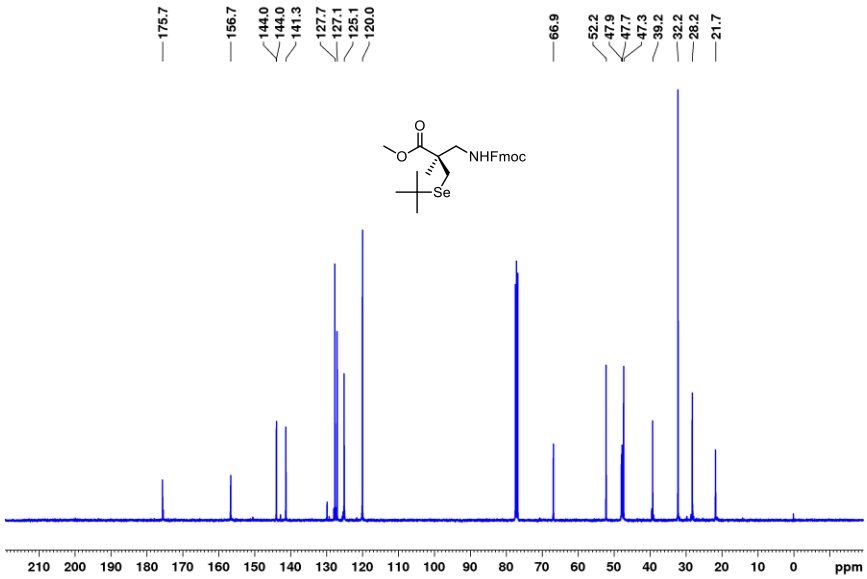
175.7
156.7
144.0
144.0
141.3
127.7
127.1
125.1
120.0
66.9
52.2
47.9
47.7
47.3
39.2
32.2
28.2
21.7
O
O
NHFmoc
Se
210
200
190
180
170
160
150
140
130
120
110
100
90
80
70
60
50
40
30
20
10
0
ppm

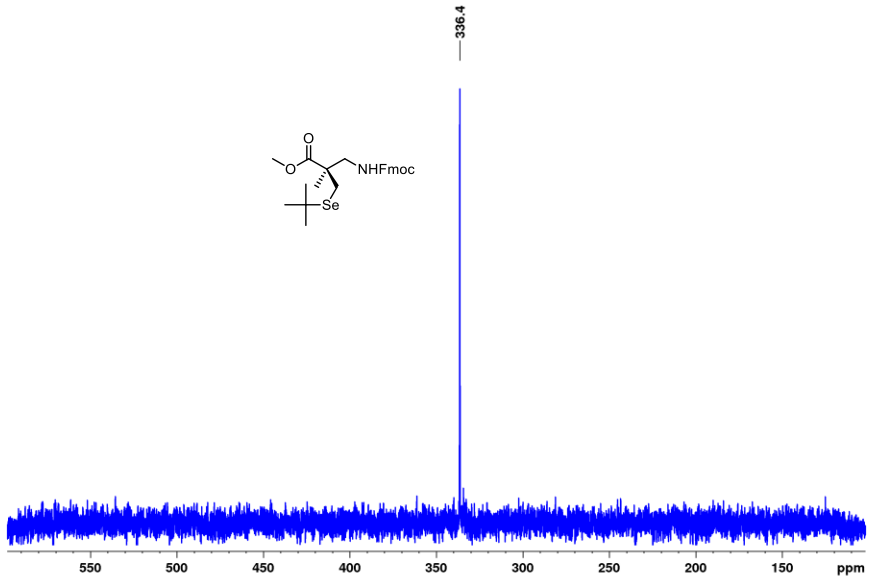
336.4
NHFmoc
Se
550
500
450
400
350
300
250
200
150
ppm

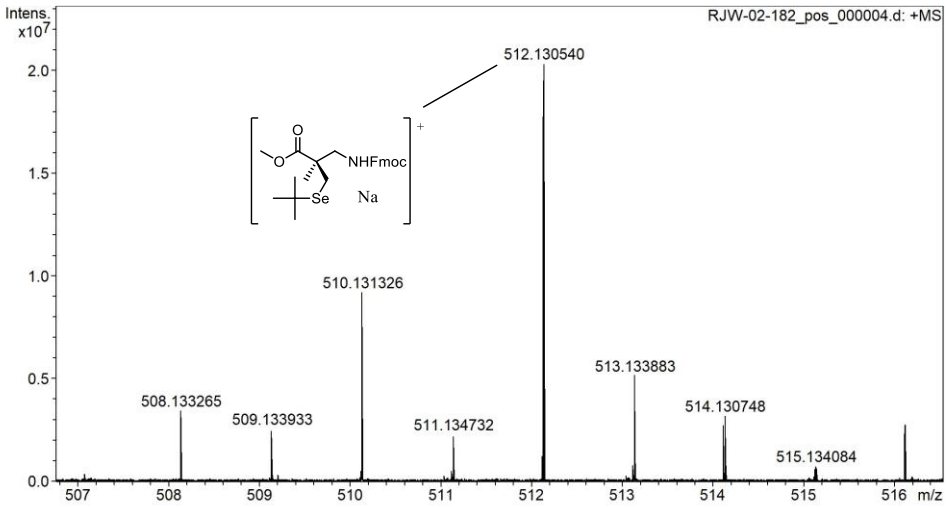
Intens.
x10^7
RJW-02-182_pos_000004.d: +MS
512.130540
NHFmoc
Se
Na
510.131326
513.133883
508.133265
509.133933
514.130748
511.134732
515.134084
2.0
1.5
1.0
0.5
0.0
507
508
509
510
511
512
513
514
515
516
m/z

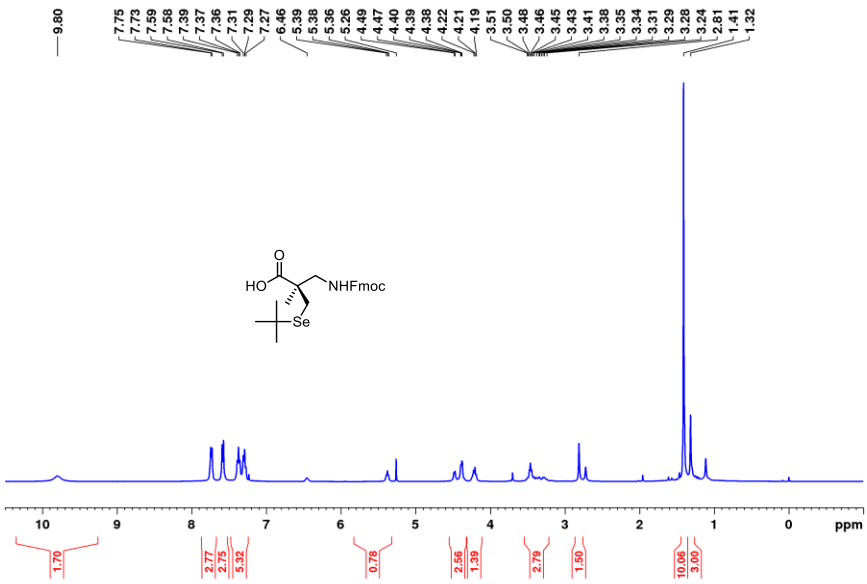
9.80
7.75
7.73
7.59
7.58
7.39
7.37
7.36
7.31
7.29
7.27
6.46
5.39
5.38
5.36
5.26
4.49
4.47
4.40
4.39
4.38
4.22
4.21
4.19
3.51
3.50
3.48
3.46
3.45
3.43
3.41
3.38
3.35
3.34
3.31
3.29
3.28
3.24
2.81
1.41
1.32
HO
O
NHFmoc
Se
10
9
8
7
6
5
4
3
2
1
0
ppm
1.70
2.77
2.75
5.32
0.78
2.56
1.39
2.79
1.50
10.06
3.00

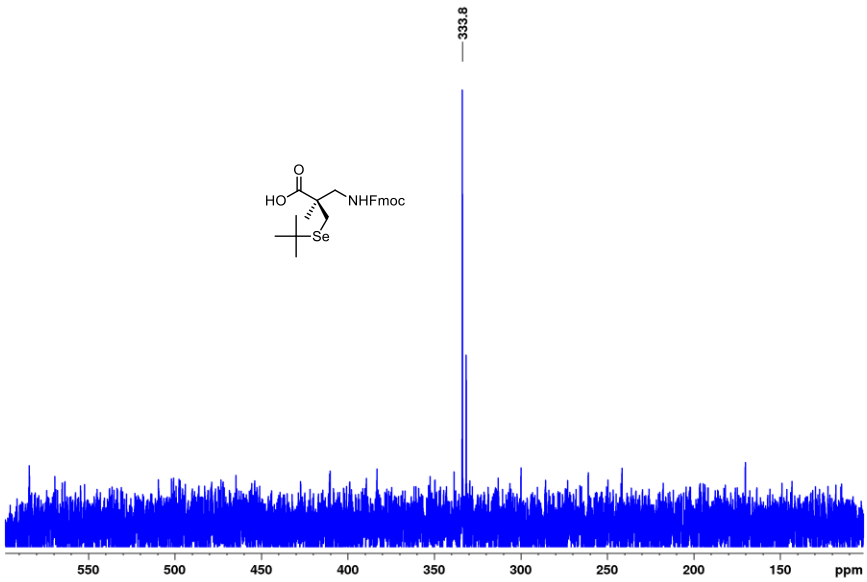
333.8
HO
O
NHFmoc
Se
550
500
450
400
350
300
250
200
150
ppm

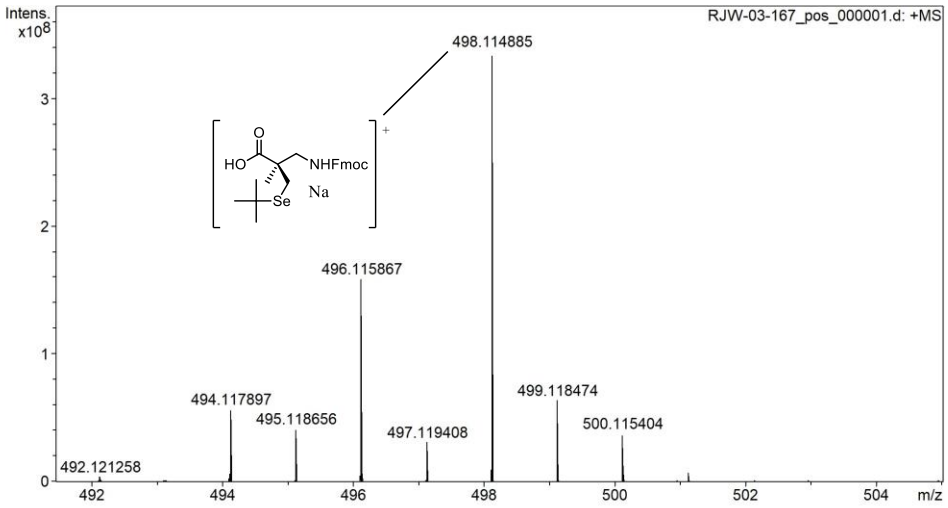
Intens.
x10^8
RJW-03-167_pos_000001.d: +MS
498.114885
496.115867
494.117897
495.118656
497.119408
499.118474
500.115404
492.121258
HO
NHFmoc
Na
Se
m/z

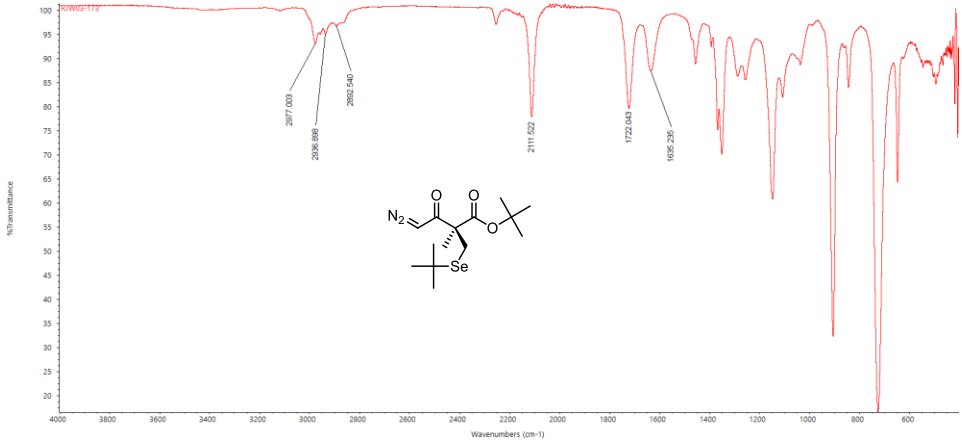
2977.003
2936.898
2892.540
2111.522
1722.043
1635.235
N2
Se
Wavenumbers (cm-1)

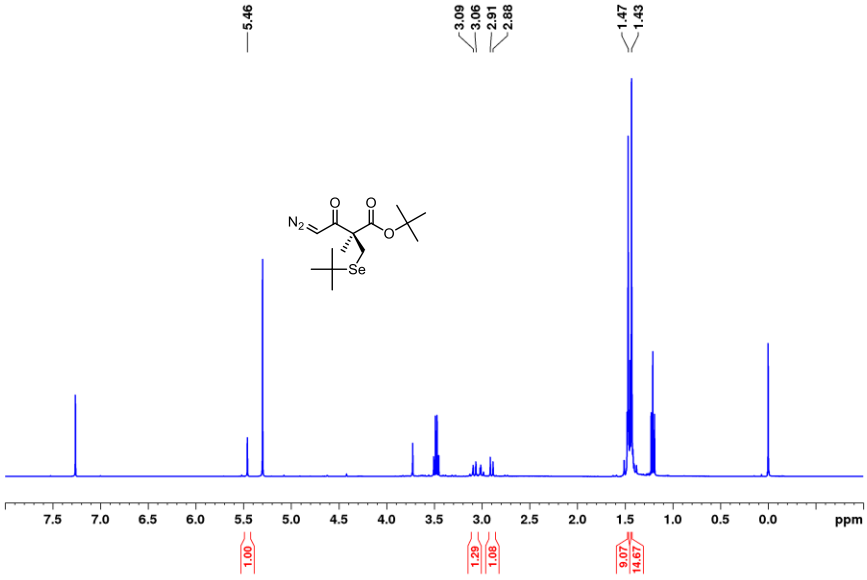
5.46
3.09
3.06
2.91
2.88
1.47
1.43
N2
O
O
O
Se
7.5 7.0 6.5 6.0 5.5 5.0 4.5 4.0 3.5 3.0 2.5 2.0 1.5 1.0 0.5 0.0 ppm
1.00
1.29
1.06
9.07
14.67

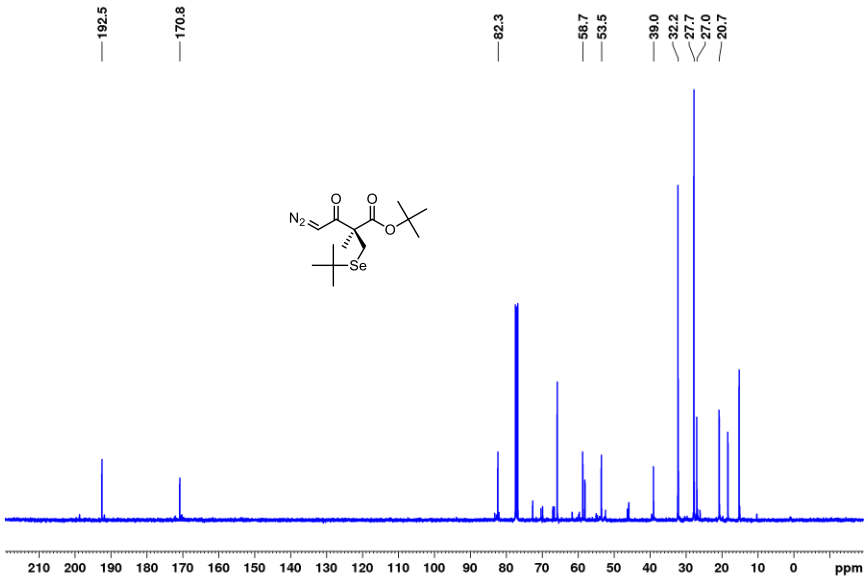
192.5
170.8
82.3
58.7
53.5
39.0
32.2
27.7
27.0
20.7
N2
O
O
O
Se
210 200 190 180 170 160 150 140 130 120 110 100 90 80 70 60 50 40 30 20 10 0 ppm

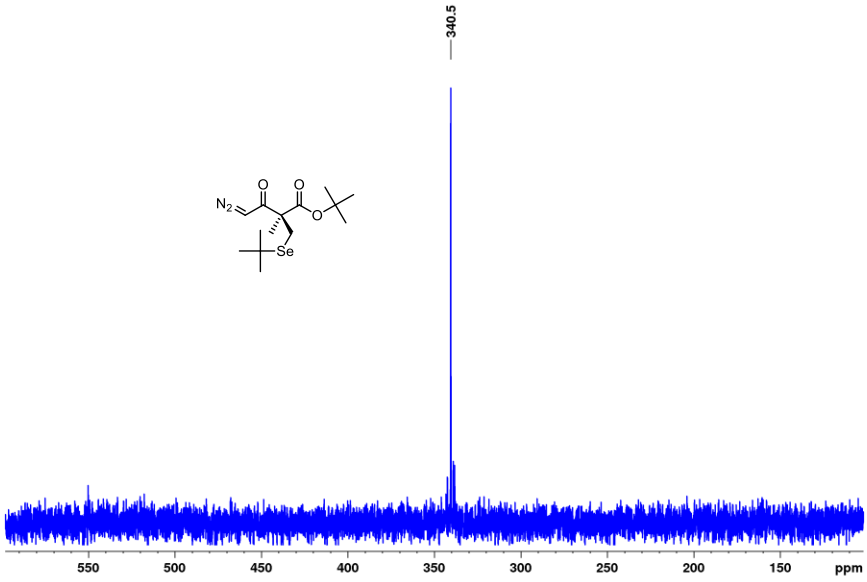

A.2 Chapter 3 Spectra

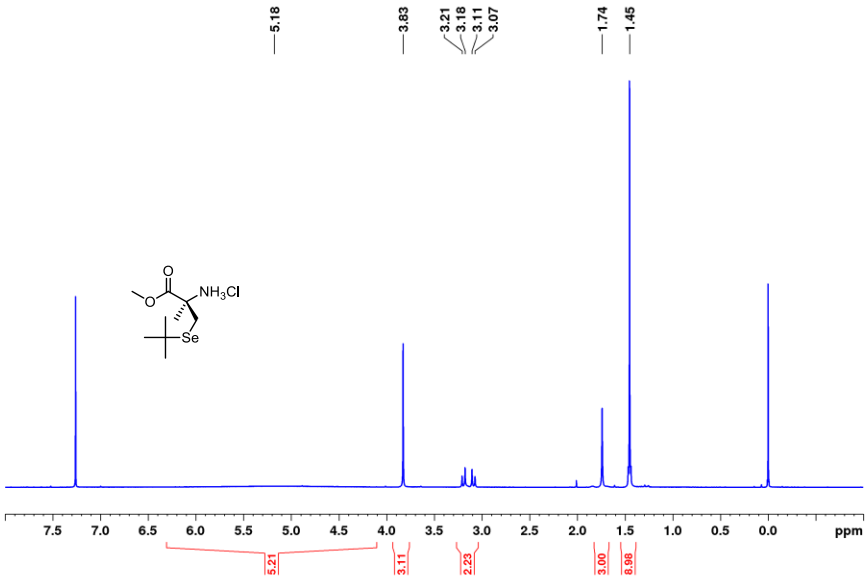

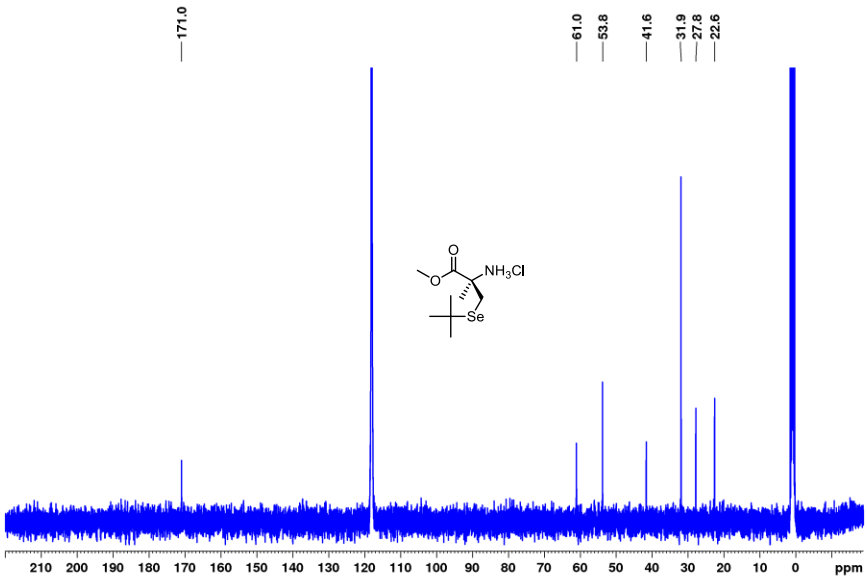
171.0
61.0
53.8
41.6
31.9
27.8
22.6
O
O
NH3Cl
Se
210 200 190 180 170 160 150 140 130 120 110 100 90 80 70 60 50 40 30 20 10 0 ppm

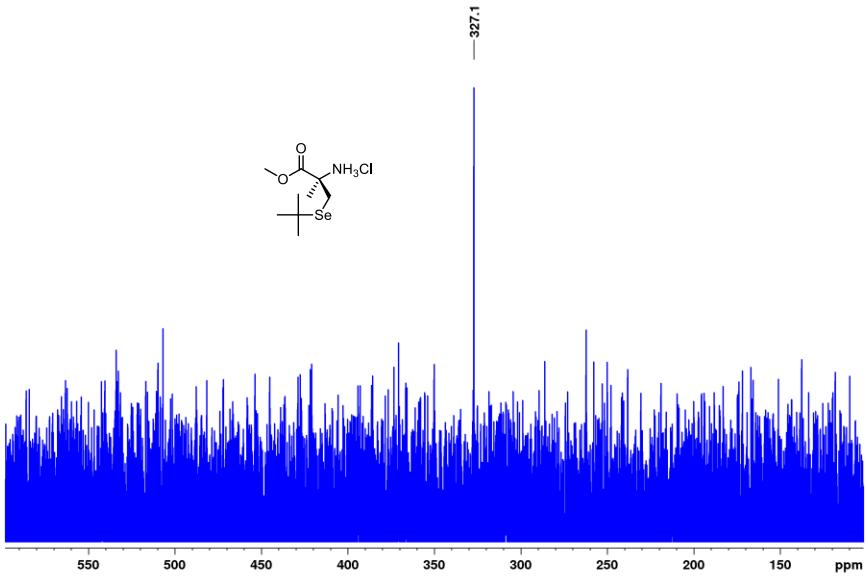
327.1
O
O
NH3Cl
Se
550 500 450 400 350 300 250 200 150 ppm

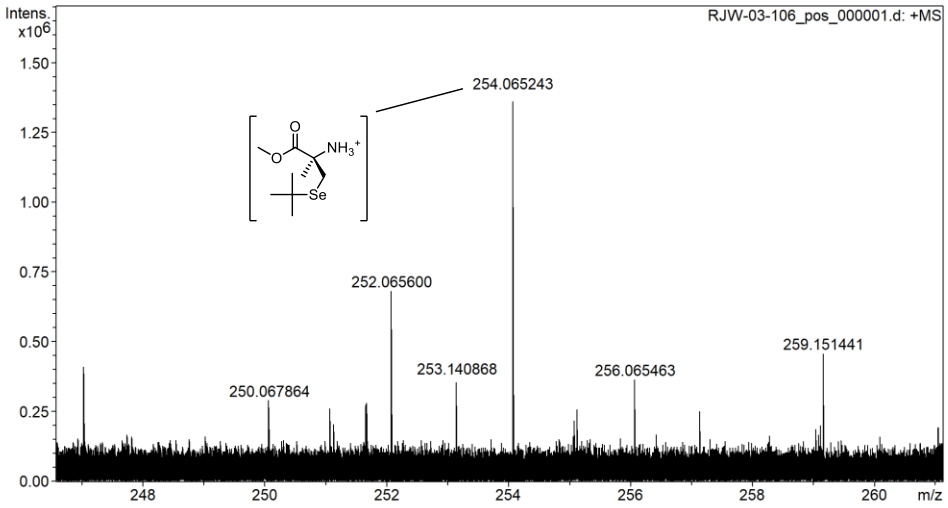
Intens.
x10^6
RJW-03-106_pos_000001.d: +MS
254.065243
252.065600
253.140868
250.067864
256.065463
259.151441
m/z

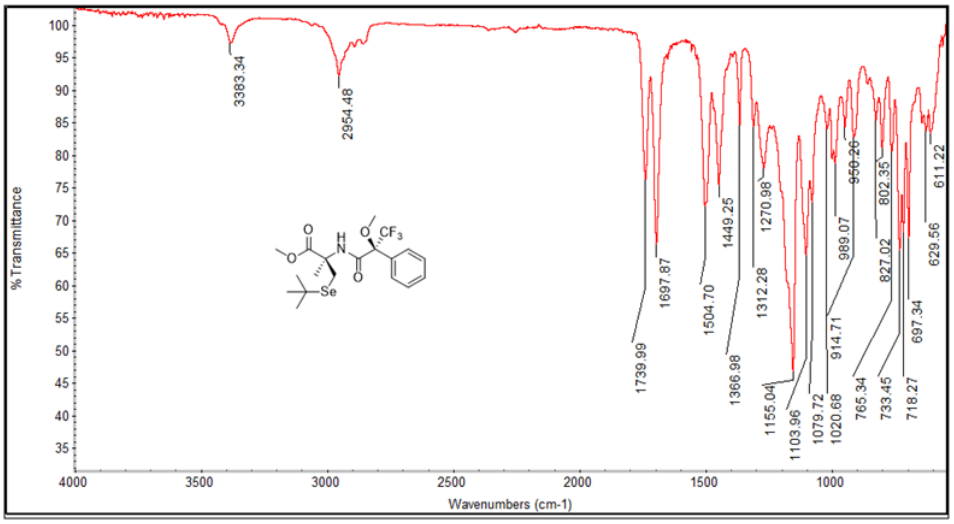
%Transmittance
Wavenumbers (cm-1)
3383.34
2954.48
1739.99
1697.87
1504.70
1449.25
1366.98
1312.28
1270.98
1155.04
1103.96
1079.72
1020.68
989.07
950.26
914.71
827.02
802.35
765.34
733.45
718.27
697.34
629.56
611.22

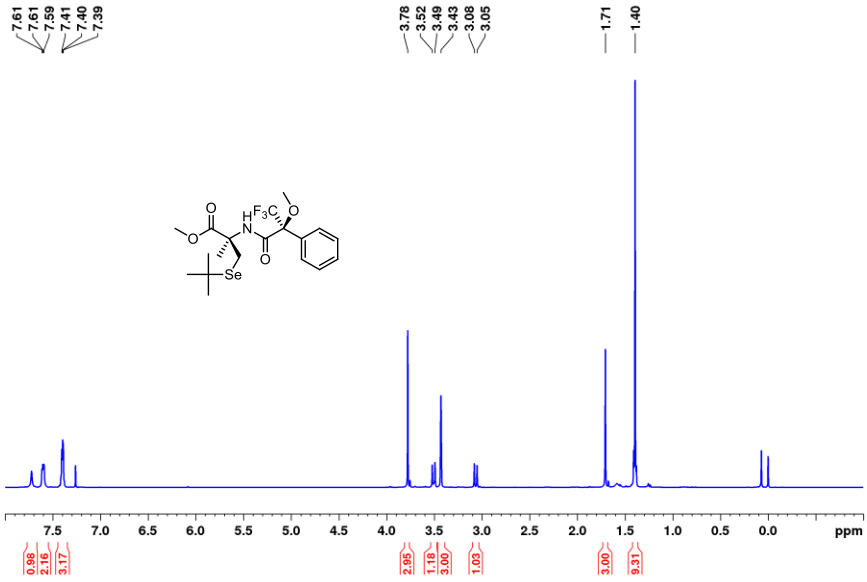
7.61
7.61
7.59
7.41
7.40
7.39
3.78
3.52
3.49
3.43
3.08
3.05
1.71
1.40
F3C
O
N
H
O
O
O
Se
7.5
7.0
6.5
6.0
5.5
5.0
4.5
4.0
3.5
3.0
2.5
2.0
1.5
1.0
0.5
0.0
ppm
0.98
2.16
3.17
2.95
1.18
3.00
1.03
3.00
9.31

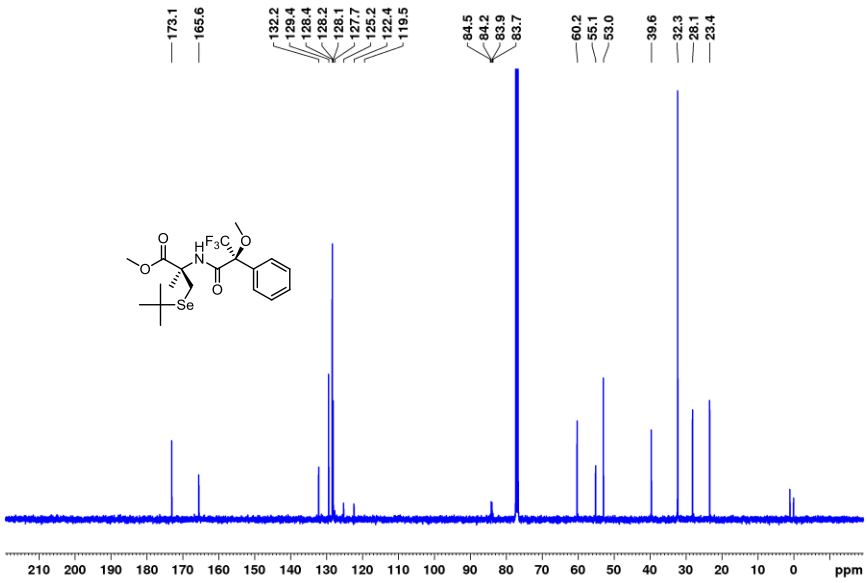
173.1
165.6
132.2
129.4
128.4
128.2
128.1
127.7
125.2
122.4
119.5
84.5
84.2
83.9
83.7
60.2
55.1
53.0
39.6
32.3
28.1
23.4
F3C
O
N
H
O
O
O
Se
210
200
190
180
170
160
150
140
130
120
110
100
90
80
70
60
50
40
30
20
10
0
ppm

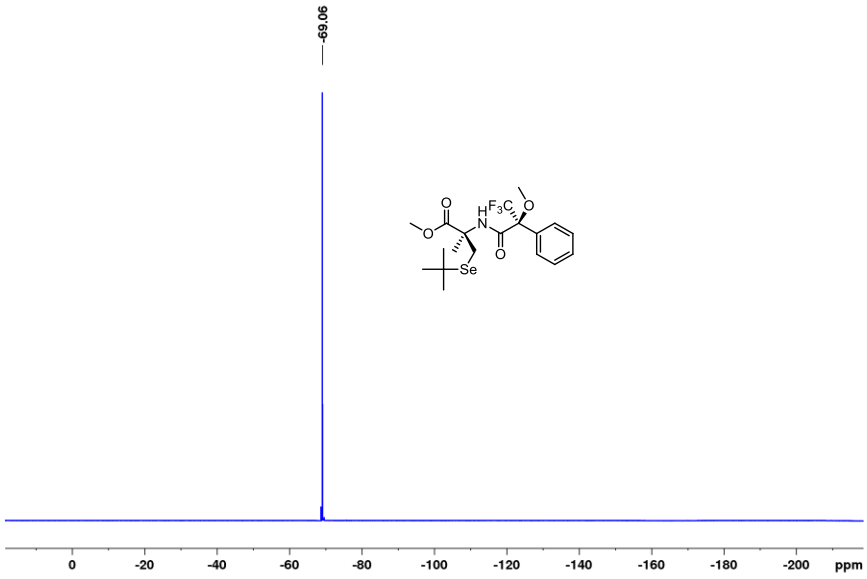
-69.06
0
-20
-40
-60
-80
-100
-120
-140
-160
-180
-200
ppm

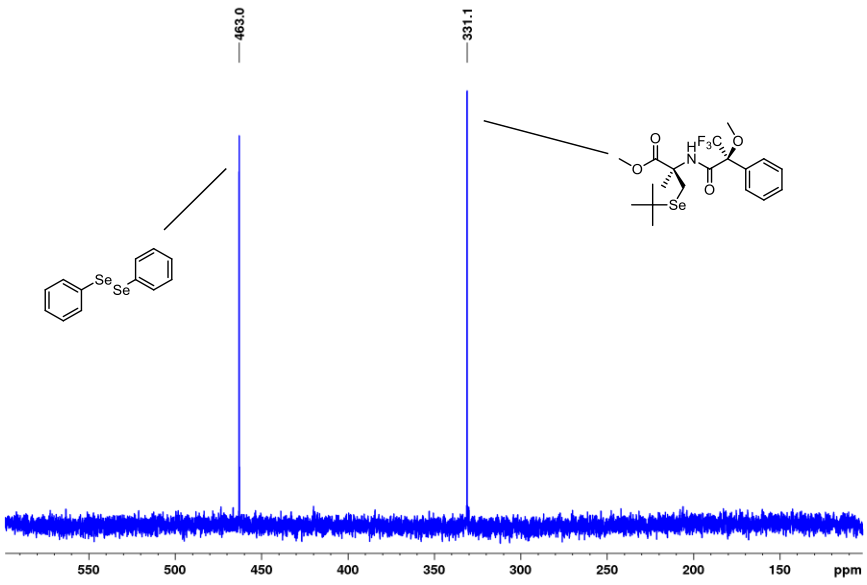
463.0
331.1
550
500
450
400
350
300
250
200
150
ppm

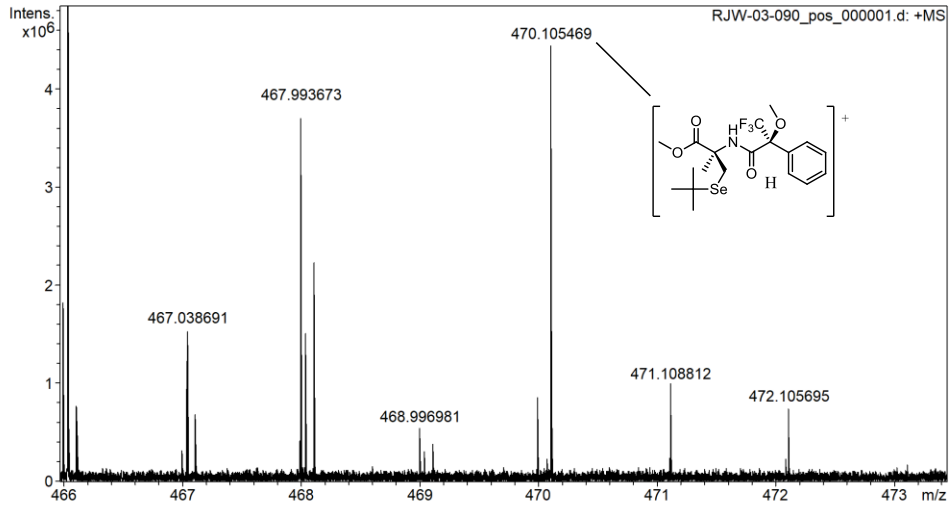
RJW-03-090_pos_000001.d: +MS
Intens.
x10^6
470.105469
467.993673
467.038691
471.108812
472.105695
468.996981
m/z

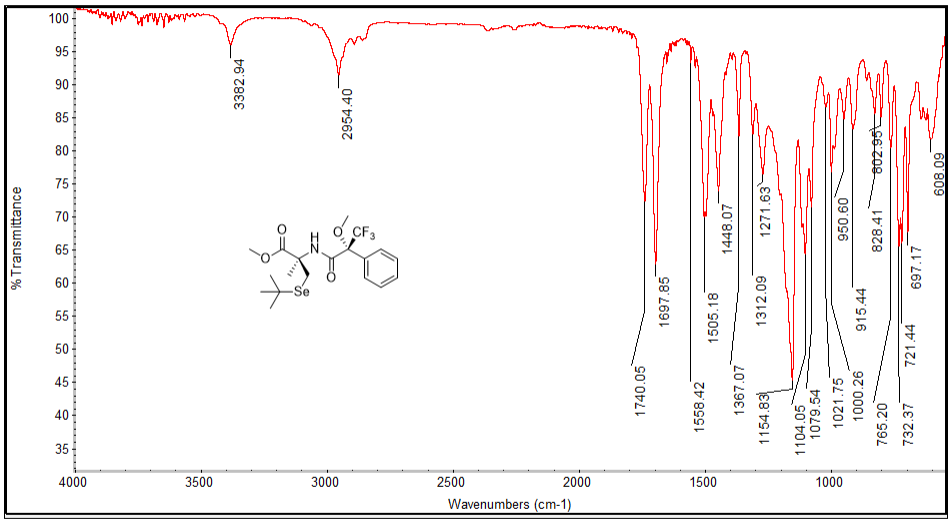
%Transmittance
Wavenumbers (cm-1)
3382.94
2954.40
1740.05
1697.85
1558.42
1505.18
1448.07
1367.07
1312.09
1271.63
1154.83
1104.05
1079.54
1021.75
1000.26
950.60
915.44
828.41
802.95
765.20
732.37
721.44
697.17
608.09

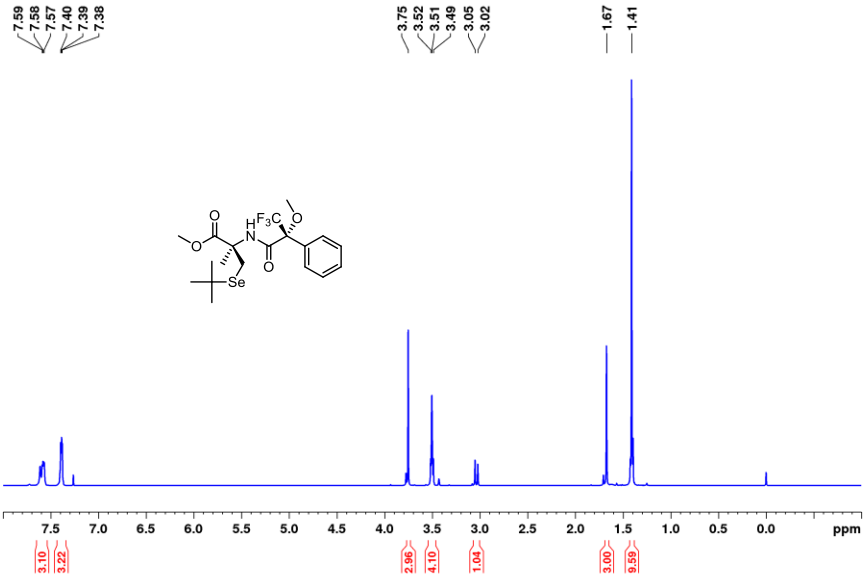
7.59
7.58
7.57
7.40
7.39
7.38
3.75
3.52
3.51
3.49
3.05
3.02
1.67
1.41
7.5
7.0
6.5
6.0
5.5
5.0
4.5
4.0
3.5
3.0
2.5
2.0
1.5
1.0
0.5
0.0
ppm
3.10
3.22
2.96
4.10
1.04
3.00
9.59

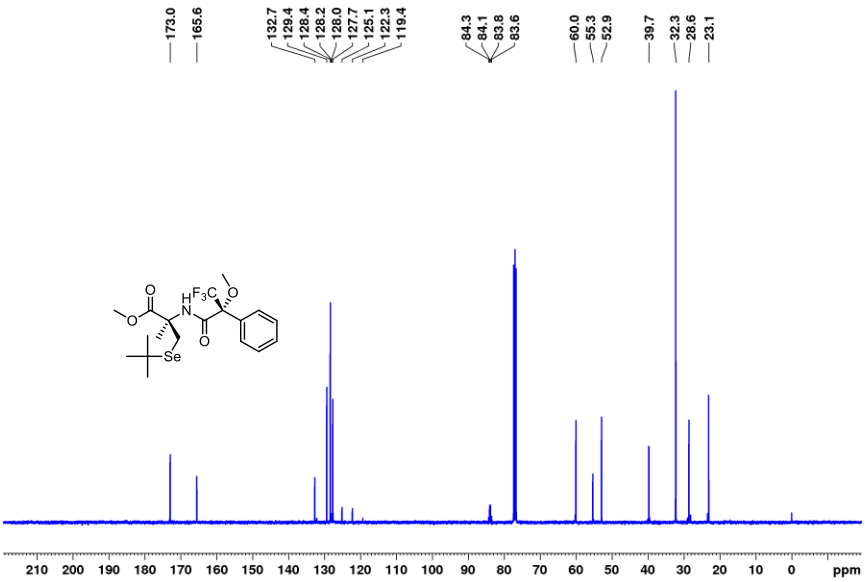
173.0
165.6
132.7
129.4
128.4
128.2
128.0
127.7
125.1
122.3
119.4
84.3
84.1
83.8
83.6
60.0
55.3
52.9
39.7
32.3
28.6
23.1
210
200
190
180
170
160
150
140
130
120
110
100
90
80
70
60
50
40
30
20
10
0
ppm

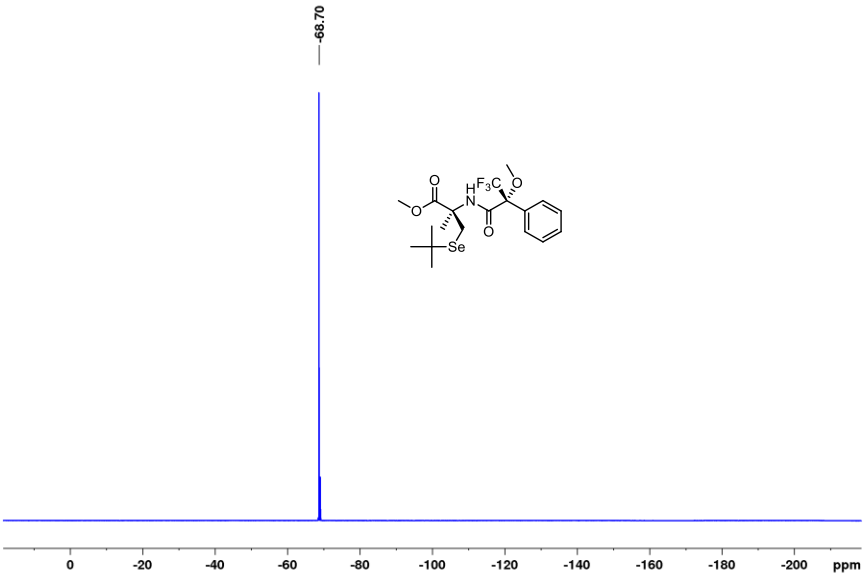
-68.70
0
-20
-40
-60
-80
-100
-120
-140
-160
-180
-200
ppm

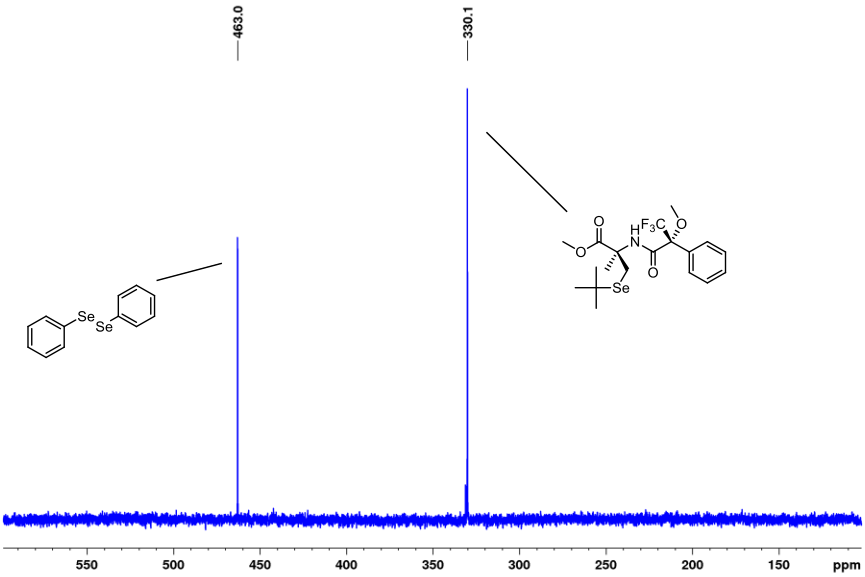
463.0
330.1
550
500
450
400
350
300
250
200
150
ppm

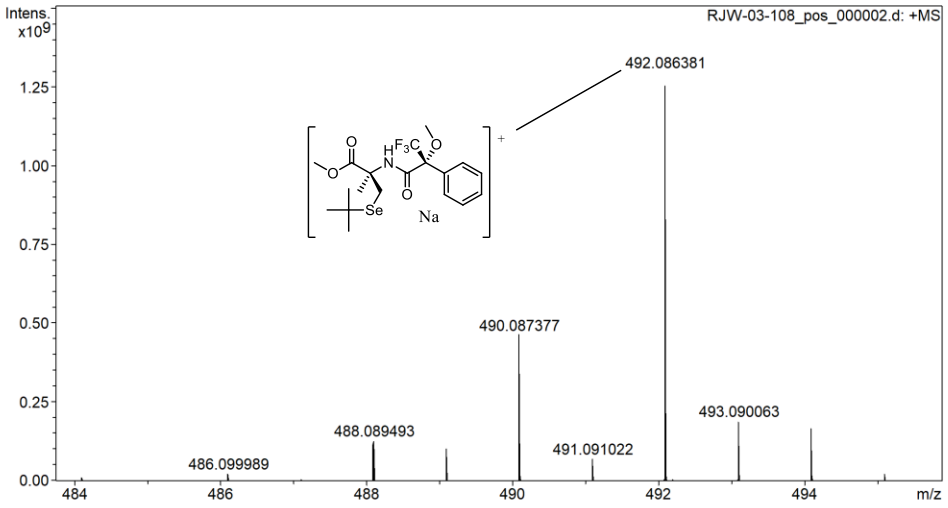

A.3 Chapter 4 Spectra

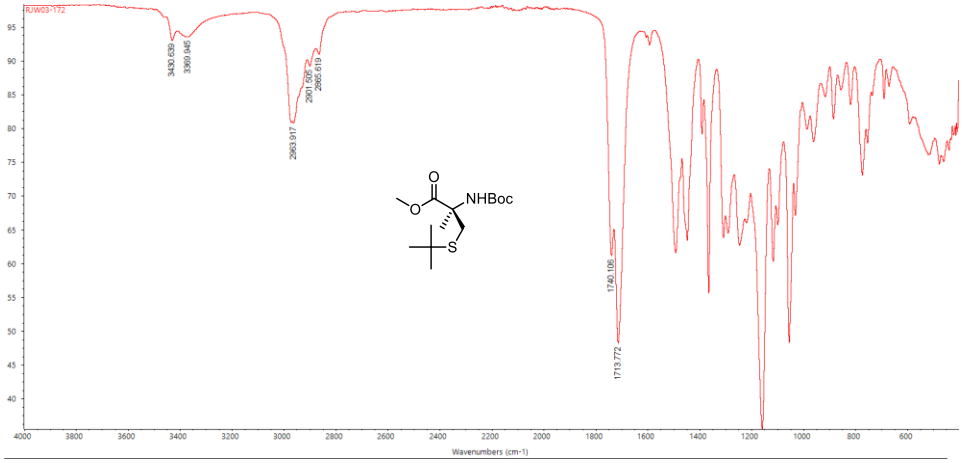

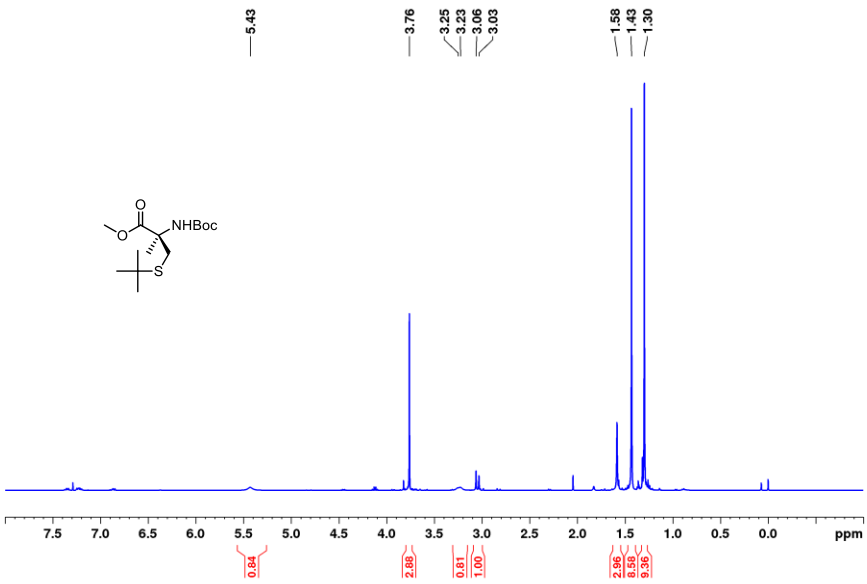
5.43
3.76
3.25
3.23
3.06
3.03
1.58
1.43
1.30
NHBoc
O
O
S
7.5 7.0 6.5 6.0 5.5 5.0 4.5 4.0 3.5 3.0 2.5 2.0 1.5 1.0 0.5 0.0 ppm
0.84
2.68
0.81
1.00
2.96
8.58
9.36

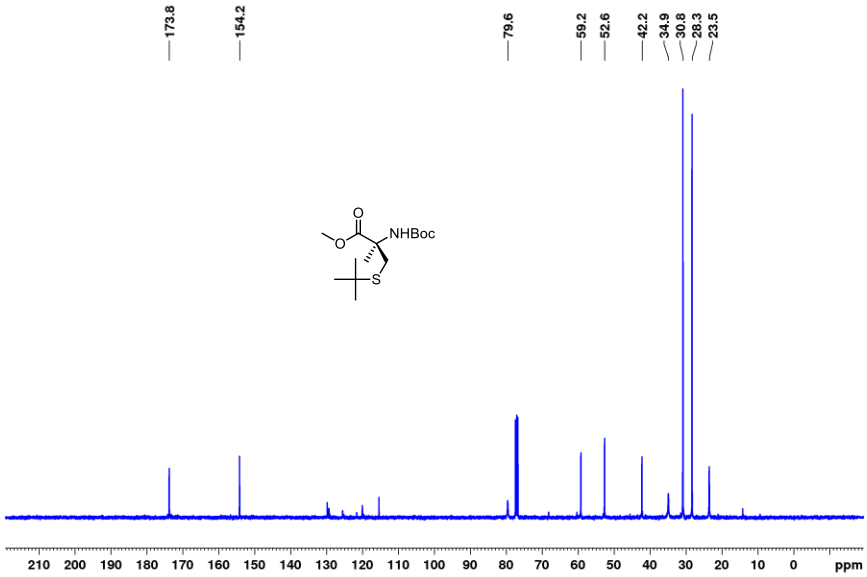
173.8
154.2
79.6
59.2
52.6
42.2
34.9
30.8
28.3
23.5
NHBoc
O
O
S
210 200 190 180 170 160 150 140 130 120 110 100 90 80 70 60 50 40 30 20 10 0 ppm

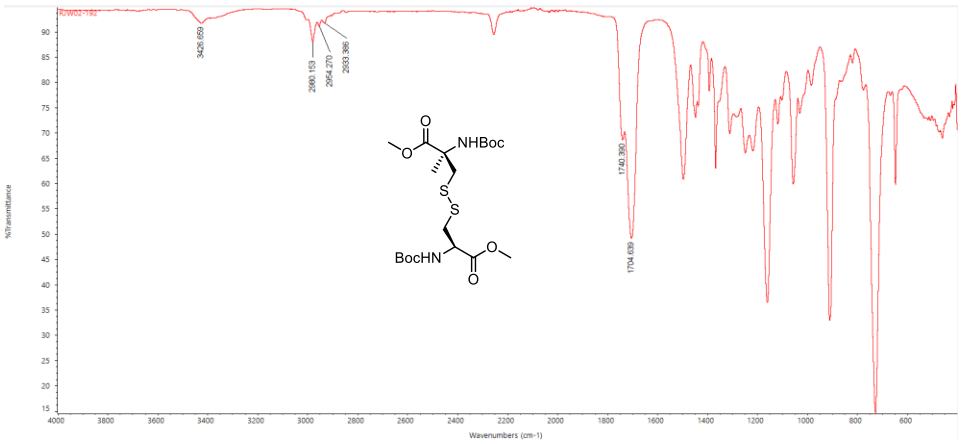
3426.659
2960.153
2954.270
2933.386
1740.390
1704.639
%Transmittance
Wavenumbers (cm-1)
NHBoc
BocHN

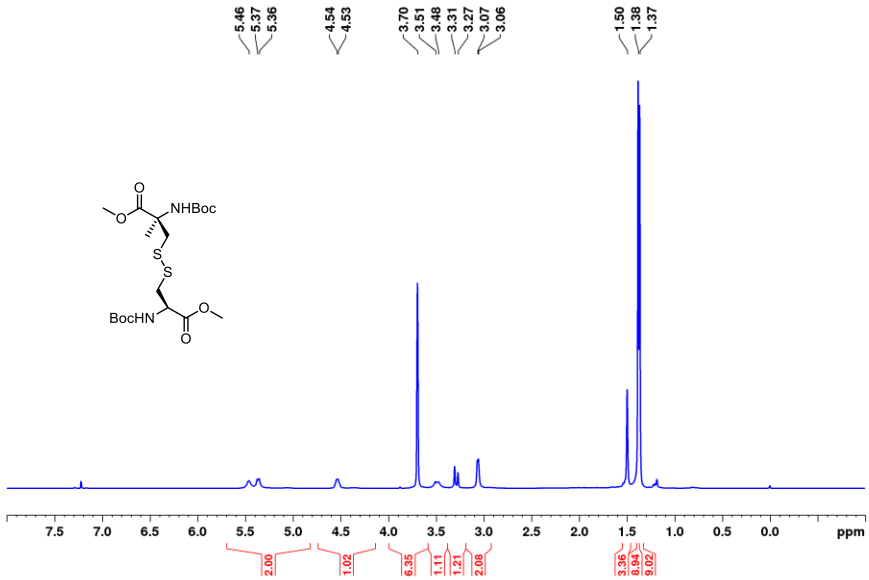
5.46
5.37
5.36
4.54
4.53
3.70
3.51
3.48
3.31
3.27
3.07
3.06
1.50
1.38
1.37
NHBoc
BocHN
ppm
2.00
1.02
6.35
1.11
1.21
2.08
3.36
8.94
9.02

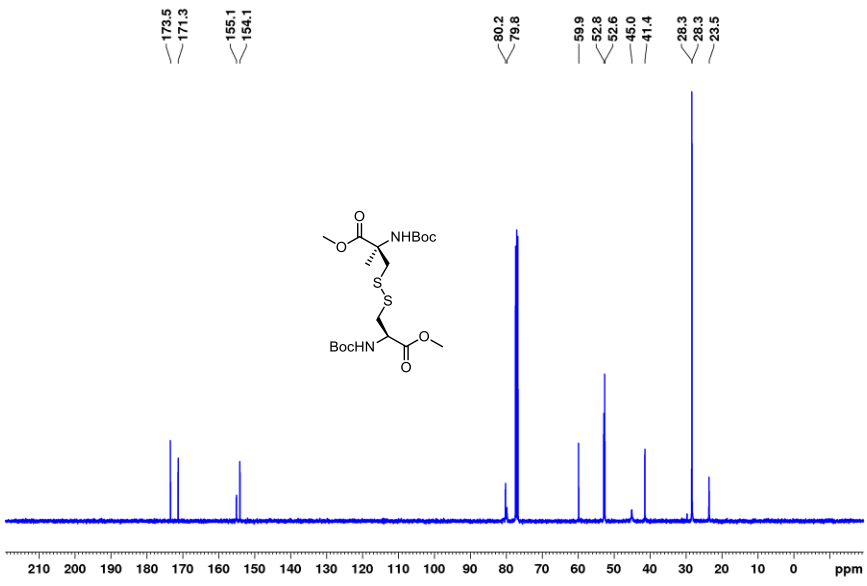
173.5
171.3
155.1
154.1
80.2
79.8
59.9
52.8
52.6
45.0
41.4
28.3
28.3
23.5
NHBoc
BocHN
210 200 190 180 170 160 150 140 130 120 110 100 90 80 70 60 50 40 30 20 10 0 ppm

REFERENCES

1. Li, F.; Lutz, P. B.; Pepelyayeva, Y.; Arner, E. S.; Bayse, C. A.; Rozovsky, S., Redox active motifs in selenoproteins. *Proc. Natl. Acad. Sci. U. S. A.* **2014,** *111* (19), 6976-81.
2. Hekimi, S.; Lapointe, J.; Wen, Y., Taking a "good" look at free radicals in the aging process. *Trends Cell Biol.* **2011,** *21* (10), 569-76.
3. Wrobel, J. K.; Power, R.; Toborek, M., Biological activity of selenium: Revisited. *IUBMB Life* **2016,** *68* (2), 97-105.
4. Pizzino, G.; Irrera, N.; Cucinotta, M.; Pallio, G.; Mannino, F.; Arcoraci, V.; Squadrito, F.; Altavilla, D.; Bitto, A., Oxidative Stress: Harms and Benefits for Human Health. *Oxid. Med. Cell. Longev.* **2017,** *2017*, 8416763.
5. Bartolini, D.; Sancineto, L.; Fabro de Bem, A.; Tew, K. D.; Santi, C.; Radi, R.; Toquato, P.; Galli, F., Selenocompounds in Cancer Therapy: An Overview. *Adv. Cancer Res.* **2017,** *136*, 259-302.
6. Krol, A., Evolutionarily different RNA motifs and RNA–protein complexes to achieve selenoprotein synthesis. *Biochimie* **2002,** *84* (8), 765-774.
7. Oliveira, A. R. M. d.; Piovan, L.; Simonelli, F.; Barison, A.; Santos, M. d. F. C.; de Mello, M. B. M., A ^{77}Se NMR study of elemental selenium reduction using $NaBH_4$. *J. Organomet. Chem.* **2016,** *806*, 54-59.
8. Spallholz, J. E., On the nature of selenium toxicity and carcinostatic activity. *Free Radical Biol. Med.* **1994,** *17* (1), 45-64.
9. Böck, A.; Forchhammer, K.; Heider, J.; Leinfelder, W.; Sawers, G.; Veprek, B.; Zinoni, F., Selenocysteine: the 21st amino acid. *Mol. Microbiol.* **1991,** *5* (3), 515-520.
10. Atkins, J. F.; Gesteland, R. F., The twenty-first amino acid. *Nature* **2000,** *407* (6803), 463, 465.
11. Kryukov, G. V.; Castellano, S.; Novoselov, S. V.; Lobanov, A. V.; Zehtab, O.; Guigo, R.; Gladyshev, V. N., Characterization of mammalian selenoproteomes. *Science* **2003,** *300* (5624), 1439-43.
12. Hondal, R. J.; Raines, R. T., Semisynthesis of proteins containing selenocysteine. *Methods Enzymol.* **2002,** *347*, 70-83.
13. Besse, D.; Siedler, F.; Diercks, T.; Kessler, H.; Moroder, L., The Redox Potential of Selenocystine in Unconstrained Cyclic Peptides. *Angew. Chem. Int. Ed.* **1997,** *36* (8), 883-885.
14. Press, D. J.; McNeil, N. M.; Hambrook, M.; Back, T. G., Effects of methoxy substituents on the glutathione peroxidase-like activity of cyclic seleninate esters. *J. Org. Chem.* **2014,** *79* (19), 9394-401.
15. Wilson, S. R.; Zucker, P. A.; Huang, R. R. C.; Spector, A., Development of synthetic compounds with glutathione peroxidase activity. *J. Am. Chem. Soc.* **1989,** *111* (15), 5936-5939.
16. Prabhu, P.; Singh, B. G.; Noguchi, M.; Phadnis, P. P.; Jain, V. K.; Iwaoka, M.; Priyadarsini, K. I., Stable selones in glutathione-peroxidase-like catalytic cycle of selenonicotinamide derivative. *Org. Biomol. Chem.* **2014,** *12* (15), 2404-12.

17. Steinbrenner, H.; Speckmann, B.; Klotz, L. O., Selenoproteins: Antioxidant selenoenzymes and beyond. *Arch. Biochem. Biophys.* **2016,** *595*, 113-9.
18. Lesser, R.; Weiss, R., Aromatic compounds containing selenium. VI. *Ber. Dtsch. Chem. Ges. B* **1924,** *57B*, 1077-82.
19. Müller, A.; Cadenas, E.; Graf, P.; Sies, H., A novel biologically active seleno-organic compound—1. *Biochem. Pharmacol.* **1984,** *33* (20), 3235-3239.
20. Ogawa, A.; Yoshimoto, T.; Kikuchi, H.; Sano, K.; Saito, I.; Yamaguchi, T.; Yasuhara, H., Ebselen in acute middle cerebral artery occlusion: a placebo-controlled, double-blind clinical trial. *Cerebrovasc. Dis.* **1999,** *9* (2), 112-8.
21. Yang, C. F.; Shen, H. M.; Ong, C. N., Intracellular thiol depletion causes mitochondrial permeability transition in ebselen-induced apoptosis. *Arch. Biochem. Biophys.* **2000,** *380* (2), 319-30.
22. Yang, C. F.; Shen, H. M.; Ong, C. N., Ebselen induces apoptosis in HepG(2) cells through rapid depletion of intracellular thiols. *Arch. Biochem. Biophys.* **2000,** *374* (2), 142-52.
23. Ma, S.; Caprioli, R. M.; Hill, K. E.; Burk, R. F., Loss of selenium from selenoproteins: Conversion of selenocysteine to dehydroalanine in vitro. *J. Am. Soc. Mass. Spectrom.* **2003,** *14* (6), 593-600.
24. Brigelius-Flohe, R.; Maiorino, M., Glutathione peroxidases. *Biochim. Biophys. Acta* **2013,** *1830* (5), 3289-303.
25. Wessjohann, L. A.; Schneider, A.; Abbas, M.; Brandt, W., Selenium in chemistry and biochemistry in comparison to sulfur. *Biol. Chem.* **2007,** *388* (10), 997-1006.
26. Shen, Q. C., Fong Fong; Newburger, Peter E., Sequences in the 3'-untranslated region of the human cellular glutathione peroxidase gene are necessary and sufficient for selenocysteine incorporation at the UGA codon. *J. Biol. Chem.* **1993,** *268* (15), 11463-9.
27. Osawa, S.; Jukes, T. H.; Watanabe, K.; Muto, A., Recent evidence for evolution of the genetic code. *Microbiol. Rev.* **1992,** *56* (1), 229-64.
28. Berry, M. J.; Banu, L.; Chen, Y. Y.; Mandel, S. J.; Kieffer, J. D.; Harney, J. W.; Larsen, P. R., Recognition of UGA as a selenocysteine codon in type I deiodinase requires sequences in the 3' untranslated region. *Nature* **1991,** *353* (6341), 273-6.
29. Turanov, A. A.; Xu, X. M.; Carlson, B. A.; Yoo, M. H.; Gladyshev, V. N.; Hatfield, D. L., Biosynthesis of selenocysteine, the 21st amino acid in the genetic code, and a novel pathway for cysteine biosynthesis. *Adv. Nutr.* **2011,** *2* (2), 122-8.
30. Wang, C.; Guo, Y.; Tian, Q.; Jia, Q.; Gao, Y.; Zhang, Q.; Zhou, C.; Xie, W., SerRS-tRNASec complex structures reveal mechanism of the first step in selenocysteine biosynthesis. *Nucleic Acids Res.* **2015,** *43* (21), 10534-45.
31. Hondal, R. J.; Ruggles, E. L., Differing views of the role of selenium in thioredoxin reductase. *Amino Acids* **2011,** *41* (1), 73-89.
32. Patora-Komisarska, K.; Jadwiga Podwysocka, D.; Seebach, D., Preparation of the β^2-Homoselenocysteine Derivatives Fmoc-(*S*)-β^2hSec(PMB)-OH and Boc-(*S*)-β^2hSec(PMB)-OH for Solution and Solid-Phase Peptide Synthesis. *Helv. Chim. Acta* **2011,** *94* (1), 1-17.
33. Gieselman, M. D.; Xie, L.; van der Donk, W. A., Synthesis of a Selenocysteine-Containing Peptide by Native Chemical Ligation. *Org. Lett.* **2001,** *3* (9), 1331-1334.
34. Stryer, L., *Biochemistry*. 3rd ed.; W. H. Freeman: New York, 1988; p 1136.

35. Eckenroth, B. E.; Rould, M. A.; Hondal, R. J.; Everse, S. J., Structural and biochemical studies reveal differences in the catalytic mechanisms of mammalian and Drosophila melanogaster thioredoxin reductases. *Biochemistry* **2007,** *46* (16), 4694-705.
36. Reich, H. J., Organoselenium chemistry. Benzeneselenenyl trifluoroacetate additions to olefins and acetylenes. *J. Org. Chem.* **1974,** *39* (3), 428-429.
37. Reich, H. J.; Renga, J. M.; Reich, I. L., Organoselenium chemistry. Conversion of cyclic ketones and β-dicarbonyl compounds to enones. *J. Org. Chem.* **1974,** *39* (14), 2133-2135.
38. Reich, H. J.; Reich, I. L.; Renga, J. M., Organoselenium chemistry. α-Phenylseleno carbonyl compounds as precursors for α,β-unsaturated ketones and esters. *J. Am. Chem. Soc.* **1973,** *95* (17), 5813-5815.
39. Levengood, M. R.; van der Donk, W. A., Dehydroalanine-containing peptides: preparation from phenylselenocysteine and utility in convergent ligation strategies. *Nat. Protoc.* **2006,** *1* (6), 3001-10.
40. Zhu, Y.; van der Donk, W. A., Convergent Synthesis of Peptide Conjugates Using Dehydroalanines for Chemoselective Ligations. *Org. Lett.* **2001,** *3* (8), 1189-1192.
41. Cho, C. S.; Lee, S.; Lee, G. T.; Woo, H. A.; Choi, E. J.; Rhee, S. G., Irreversible inactivation of glutathione peroxidase 1 and reversible inactivation of peroxiredoxin II by H_2O_2 in red blood cells. *Antioxid. Redox Signal* **2010,** *12* (11), 1235-46.
42. Wehrle, R. J.; Ste Marie, E. J.; Hondal, R. J.; Masterson, D. S., Synthesis of alpha-methyl selenocysteine and its utilization as a glutathione peroxidase mimic. *J. Pept. Sci.* **2019**, e3173.
43. Khoury, G. A.; Baliban, R. C.; Floudas, C. A., Proteome-wide post-translational modification statistics: frequency analysis and curation of the swiss-prot database. *Sci. Rep.* **2011,** *1*.
44. Altmann, K.-H.; Altmann, E.; Mutter, M., Confromational Studies on Peptides Containing Enantiometric α-Methyl α-Amino Acids. Part I. Differential conformational properties of (*R*)- and (*S*)-2-methylaspartic acid. *Helv. Chim. Acta* **1992,** *75* (4), 1198-1210.
45. Sagan, S.; Karoyan, P.; Lequin, O.; Chassaing, G.; Lavielle, S., N- and Cα-methylation in biologically active peptides: synthesis, structural and functional aspects. *Curr. Med. Chem.* **2004,** *11* (21), 2799-822.
46. Stroud, E. D.; Fife, D. J.; Smith, G. G., A method for the determination of the pKa of the α-hydrogen in amino acids using racemization and exchange studies. *J. Org. Chem.* **1983,** *48* (26), 5368-5369.
47. Bada, J. L., Kinetics of racemization of amino acids as a function of pH. *J. Am. Chem. Soc.* **1972,** *94* (4), 1371-1373.
48. Khosla, M. C.; Stachowiak, K.; Smeby, R. R.; Bumpus, F. M.; Piriou, F.; Lintner, K.; Fermandjian, S., Synthesis of [α-methyltyrosine-4]angiotensin II: studies of its conformation, pressor activity, and mode of enzymatic degradation. *Proc. Natl. Acad. Sci. U. S. A.* **1981,** *78* (2), 757-60.
49. Shapiro, R.; Vallee, B. L., Interaction of human placental ribonuclease with placental ribonuclease inhibitor. *Biochemistry* **1991,** *30* (8), 2246-55.

50. Kedrowski, B. L.; Gutow, J. H.; Stock, G.; Smith, M.; Jordan, C.; Masterson, D. S., Glutathione reductase activity with an oxidized methylated glutathione analog. *J. Enzyme Inhib. Med. Chem.* **2014,** *29* (4), 491-4.
51. Nakazawa, H.; Kumagai, H.; Yamada, H., Decarboxylation Reaction of α-Methyl Amino Acid Catalyzed by Aromaticl-Amino Acid Decarboxylase fromMicrococcus percitreus. *Agr. Biol. Chem. Tokyo* **2014,** *49* (1), 159-165.
52. Heitbaum, M.; Glorius, F.; Escher, I., Asymmetric heterogeneous catalysis. *Angew. Chem. Int. Ed.* **2006,** *45* (29), 4732-62.
53. Grubbs, R. H.; Trnka, T. M., Ruthenium-Catalyzed Olefin Metathesis. **2005**, 153-177.
54. Kolb, H. C.; VanNieuwenhze, M. S.; Sharpless, K. B., Catalytic Asymmetric Dihydroxylation. *Chem. Rev.* **1994,** *94* (8), 2483-2547.
55. Koshland, D. E., The Key–Lock Theory and the Induced Fit Theory. *Angew. Chem. Int. Ed.* **1995,** *33* (2324), 2375-2378.
56. Fischer, E., Einfluss der Configuration auf die Wirkung der Enzyme. *Ber. Dtsch. Chem. Ges.* **1894,** *27* (3), 2985-2993.
57. Smith, M. E.; Banerjee, S.; Shi, Y.; Schmidt, M.; Bornscheuer, U. T.; Masterson, D. S., Investigation of the Cosolvent Effect on Six Isoenzymes of PLE in the Enantioselective Hydrolysis of Selected α,α-Disubstituted Malonate Esters. *ChemCatChem* **2012,** *4* (4), 472-475.
58. Smith, M. E.; Fibinger, M. P. C.; Bornscheuer, U. T.; Masterson, D. S., An Investigation of the Interaction of Co-Solvent with Substrates in the Pig Liver Esterase-Catalyzed Hydrolysis of Malonate Esters. *ChemCatChem* **2015,** *7* (19), 3179-3185.
59. Schmid, R. D.; Verger, R., Lipases: Interfacial Enzymes with Attractive Applications. *Angew. Chem. Int. Ed.* **1998,** *37* (12), 1608-1633.
60. Luyten, M.; Müller, S.; Herzog, B.; Keese, R., Enzyme-Catalyzed Hydrolysis of Some Functionalized Dimethyl Malonates. *Helv. Chim. Acta* **1987,** *70* (5), 1250-1254.
61. Zhu, L.-M.; Catriona Tedford, M., Application of Pig Liver Esterases (PLE) in Asymetric Synthesis. *Tetrahedron* **1990,** *46* (19), 6587-6611.
62. Toone, E. J.; Werth, M. J.; Jones, J. B., Enzymes in organic synthesis. 47. Active-site model for interpreting and predicting the specificity of pig liver esterase. *J. Am. Chem. Soc.* **1990,** *112* (12), 4946-4952.
63. Fredga, A., Synthesis of α,α'-diaminodiseleniumdihydroacrylic acid. *Sven. Kem. Tidskr.* **1936,** *48*, 160-5.
64. Metanis, N.; Keinan, E.; Dawson, P. E., Synthetic seleno-glutaredoxin 3 analogues are highly reducing oxidoreductases with enhanced catalytic efficiency. *J. Am. Chem. Soc.* **2006,** *128* (51), 16684-91.
65. Stocking, E. M.; Schwarz, J. N.; Senn, H.; Salzmann, M.; Silks, L. A., Synthesis of L-selenocystine, L-[^{77}Se]selenocystine and L-tellurocystine. *J. Chem. Soc., Perkin Trans. 1* **1997,** (16), 2443-2448.
66. Shirahama, H.; Sakai, M.; Hashimoto, K., Synthesis of Optically Pure β-Phenylselenoalanine Through Serine-β-lactone: A Useful Precursor of Dehydroalanine. *Heterocycles* **1997,** *44* (1), 319.

67. Reich, H. J.; Jasperse, C. P.; Renga, J. M., Organoselenium chemistry. Alkylation of acid, ester, amide, and ketone enolates with bromomethyl benzyl selenide and sulfide. Preparation of selenocysteine derivatives. *J. Org. Chem.* **1986,** *51* (15), 2981-2988.
68. Sharpless, K. B.; Young, M. W.; Lauer, R. F., Reactions of selenoxides: Thermal -elimination and $H_2{}^{18}O$ exchange. *Tetrahedron Lett.* **1973,** *14* (22), 1979-1982.
69. Jones, D. N.; Mundy, D.; Whitehouse, R. D., Steroidal selenoxides diastereoisomeric at selenium; *syn*-elimination, absolute configuration, and optical rotatory dispersion characteristics. *J. Chem. Soc. D* **1970,** (2), 86.
70. Sharpless, K. B.; Lauer, R. F., Selenium dioxide oxidation of olefins. Evidence for the intermediacy of allylseleninic acids. *J. Am. Chem. Soc.* **1972,** *94* (20), 7154-7155.
71. Arigoni, D.; Vasella, A.; Sharpless, K. B.; Jensen, H. P., Selenium dioxide oxidations of olefins. Trapping of the allylic seleninic acid intermediate as a seleninolactone. *J. Am. Chem. Soc.* **1973,** *95* (23), 7917-7919.
72. Jensen, H. P.; Sharpless, K. B., Selenium dioxide oxidation of *d*-limonene. Reinvestigation. *J. Org. Chem.* **1975,** *40* (2), 264-265.
73. Potapov, V. A., Organic Diselenides, Ditellurides, Polyselenides and Polytellurides. Synthesis and Reactions. In *The Chemistry of Organic Selenium and Tellurium Compounds*, Rappoport, Z., Ed. 2013; Vol. 4, pp 765-843.
74. Klayman, D. L.; Griffin, T. S., Reaction of selenium with sodium borohydride in protic solvents. A Facile Method for the introduction of selenium into organic molecules. *J. Am. Chem. Soc.* **1973,** *95* (1), 197-199.
75. Panguluri, N. R.; Panduranga, V.; Prabhu, G.; Vishwanatha, T. M.; Sureshbabu, V. V., Synthesis of chiral N^{β}-protected amino diselenides from the corresponding amino alkyl iodides using $NaBH_2Se_3$as a selenating reagent and their conversion to seleninic acids. *RSC Adv.* **2015,** *5* (64), 51807-51811.
76. Krief, A.; Derock, M., Synthesis of diselenides and selenides from elemental selenium. *Tetrahedron Lett.* **2002,** *43* (16), 3083-3086.
77. Gray, I. P.; Bhattacharyya, P.; Slawin, A. M.; Woollins, J. D., A new synthesis of $(PhPSe_2)_2$ (Woollins reagent) and its use in the synthesis of novel P-Se heterocycles. *Chem. Eur. J.* **2005,** *11* (21), 6221-7.
78. Makiyama, A.; Komatsu, I.; Iwaoka, M.; Yatagai, M., One-Pot Conversion of Serine and α-Methylserine Derivatives to the Corresponding Cysteines and Selenocystines by Using Chalcogenophosphate Reagents. *Phosphorus Sulfur Relat. Elem.* **2010,** *186* (1), 125-133.
79. Iwaoka, M.; Ito, S.; Miyazaki, I.; Michibata, M., Synthesis of L-Selenocysteine and α-Methyl-L-Selenocysteine Derivatives Using Woollins' Reagent and Their Application as Chiral Selenium Catalysts. *Proc. Natl. Acad. Sci., India, Sect. A Phys. Sci.* **2016,** *86* (4), 499-509.
80. Charton, M., Steric effects. III. Bimolecular nucleophilic substitution. *J. Am. Chem. Soc.* **1975,** *97* (13), 3694-3697.
81. Koh, H. J.; Lee, H. W.; Lee, I., Bimolecular nucleophilic substitution (S_N2) reactions of neopentyl arenesulfonates with anilines and benzylamines in methanol. *J. Chem. Soc., Perkin Trans. 2* **1994,** (2), 253.
82. Rozovsky, S., *^{77}Se NMR Spectroscopy of Selenoproteins*. American Chemical Society: 2013; Vol. 1152, p 127-142.

83. McKillop, A.; Koyunçu, D.; Krief, A.; Dumont, W.; Renier, P.; Trabelsi, M., Efficicient, high yield, oxidation of thiols and selenols to disulphides and diselenides. *Tetrahedron Lett.* **1990,** *31* (35), 5007-5010.
84. Kedrowski, B. L., Synthesis of orthogonally protected (*R*)- and (*S*)-2-methylcysteine via an enzymatic desymmeterization and Curtius rearrangement. *J. Org. Chem.* **2003,** *68* (13), 5403-6.
85. Spino, C.; Joly, M. A.; Godbout, C.; Arbour, M., Ti-catalyzed reactions of hindered isocyanates with alcohols. *J. Org. Chem.* **2005,** *70* (15), 6118-21.
86. Sutton, C. C. R.; Lim, C. Y.; Silva, G., Self-catalyzed keto-enol tautomerization of malonic acid. *Int. J. Quantum Chem.* **2019,** *120* (5).
87. Petersen, K. S., Chiral Bronsted Acid Catalyzed Kinetic Resolutions. *Asian J Org Chem* **2016,** *5* (3), 308-320.
88. King, R. P.; Wagner, A. J.; Burtea, A.; King, S. M., Asymmetric Synthesis and Absolute Configuration Determination of an Enantioenriched Alcohol: A Discovery-Based Undergraduate Laboratory Experiment. *J. Chem. Educ.* **2020,** *97* (3), 793-800.
89. Kelley, A. M.; Minerali, E.; Wilent, J. E.; Chambers, N. J.; Stingley, K. J.; Wilson, G. T.; Petersen, K. S., Asymmetric synthesis of novel spirocycles via a chiral phosphoric acid catalyzed desymmetrization. *Tetrahedron Lett.* **2019,** *60* (18), 1262-1264.
90. Zimmerman, H. E.; Traxler, M. D., The Stereochemistry of the Ivanov and Reformatsky Reactions. I. *J. Am. Chem. Soc.* **1957,** *79* (8), 1920-1923.
91. Dale, J. A.; Mosher, H. S., Nuclear magnetic resonance enantiomer regents. Configurational correlations via nuclear magnetic resonance chemical shifts of diastereomeric mandelate, *O*-methylmandelate, and α-methoxy-α-trifluoromethylphenylacetate (MTPA) esters. *J. Am. Chem. Soc.* **1973,** *95* (2), 512-519.
92. Allen, D. A.; Tomaso, A. E.; Priest, O. P.; Hindson, D. F.; Hurlburt, J. L., Mosher Amides: Determining the Absolute Stereochemistry of Optically-Active Amines. *J. Chem. Educ.* **2008,** *85* (5), 698.
93. Hoye, T. R.; Jeffrey, C. S.; Shao, F., Mosher ester analysis for the determination of absolute configuration of stereogenic (chiral) carbinol carbons. *Nat. Protoc.* **2007,** *2* (10), 2451-8.
94. Karunakaran, C.; Santharaman, P.; Balamurugan, M., ^{1}H and ^{13}C Nuclear Magnetic Resonance Spectroscopy. **2018**, 49-110.
95. Raban, M.; Mislow, K., The determination of optical purity by nuclear magnetic resonance spectroscopy. II. Compounds which owe their dissymmetry to deuterium substitution. *Tetrahedron Lett.* **1966,** *7* (33), 3961-3966.
96. Dale, J. A.; Dull, D. L.; Mosher, H. S., α-Methoxy-α-trifluoromethylphenylacetic acid, a versatile reagent for the determination of enantiomeric composition of alcohols and amines. *J. Org. Chem.* **1969,** *34* (9), 2543-2549.
97. Dale, J. A.; Mosher, H. S., Nuclear magnetic resonance nonequivalence of diastereomeric esters of α-substituted phenylacetic acids for the determination of stereochemical purity. *J. Am. Chem. Soc.* **1968,** *90* (14), 3732-3738.
98. Dörrich, S.; Falgner, S.; Schweeberg, S.; Burschka, C.; Brodin, P.; Wissing, B. M.; Basta, B.; Schell, P.; Bauer, U.; Tacke, R., Silicon-Containing Dipeptidic Aspartame and Neotame Analogues. *Organometallics* **2012,** *31* (16), 5903-5917.

99. Cogan, D. A.; Ellman, J. A., Asymmetric Synthesis of α,α-Dibranched Amines by the Trimethylaluminum-Mediated 1,2-Addition of Organolithiums to *tert*-Butanesulfinyl Ketimines. *J. Am. Chem. Soc.* **1999,** *121* (1), 268-269.
100. Sullivan, G. R.; Dale, J. A.; Mosher, H. S., Correlation of configuration and ^{19}F chemical shifts of α-methoxy-α-trifluoromethylphenyl acetate derivatives. *J. Org. Chem.* **1973,** *38* (12), 2143-2147.
101. Rieser, M. J.; Hui, Y. H.; Rupprecht, J. K.; Kozlowski, J. F.; Wood, K. V.; McLaughlin, J. L.; Hanson, P. R.; Zhuang, Z.; Hoye, T. R., Determination of absolute configuration of stereogenic carbinol centers in annonaceous acetogenins by ^{1}H- and ^{19}F-NMR analysis of Mosher ester derivatives. *J. Am. Chem. Soc.* **1992,** *114* (26), 10203-10213.
102. Ohtani, I.; Kusumi, T.; Kashman, Y.; Kakisawa, H., High-field FT NMR application of Mosher's method. The absolute configurations of marine terpenoids. *J. Am. Chem. Soc.* **1991,** *113* (11), 4092-4096.
103. Izumi, S.; Moriyoshi, H.; Hirata, T., Identification of Absolute Configuration of Tertiary Alcohols by Combination of Mosher's Method and Conformational Analysis. *B. Chem. Soc. Jpn.* **1994,** *67* (9), 2600-2602.
104. Kotapati, H. K.; Lawrence, D. R.; Thames, S. O.; Masterson, D. S., Enzyme mediated concise synthesis of NH-Fmoc-*S*-Trityl-Cα-Methyl Cysteine. *Tetrahedron Lett.* **2016,** *57* (39), 4389-4391.
105. Lardon, M., Selenium and proton nuclear magnetic resonance measurements on organic selenium compounds. *J. Am. Chem. Soc.* **1970,** *92* (17), 5063-5066.
106. Krause, L.; Herbst-Irmer, R.; Sheldrick, G. M.; Stalke, D., Comparison of silver and molybdenum microfocus X-ray sources for single-crystal structure determination. *J. Appl. Crystallogr.* **2015,** *48* (Pt 1), 3-10.
107. Sheldrick, G. M., SHELXT - integrated space-group and crystal-structure determination. *Acta Crystallogr., Sect. A: Found. Crystallogr.* **2015,** *71* (Pt 1), 3-8.
108. Sheldrick, G. M., Crystal structure refinement with SHELXL. *Acta Crystallogr., Sect. C: Cryst. Struct. Commun.* **2015,** *71* (Pt 1), 3-8.
109. Parsons, S.; Flack, H. D.; Wagner, T., Use of intensity quotients and differences in absolute structure refinement. *Acta Crystallogr., Sect. B: Struct. Sci.* **2013,** *69* (Pt 3), 249-59.
110. Bergman, J.; Brynolf, A., Synthesis of Chrysogine, a Metabolite of Penicillium chrysogenum and some related 2-substituted 4-(*3H*)-Quinazolinones. *Tetrahedron* **1990,** *46* (4), 1295-1310.
111. Goto, K.; Nagahama, M.; Mizushima, T.; Shimada, K.; Kawashima, T.; Okazaki, R., The First Direct Oxidative Conversion of a Selenol to a Stable Selenenic Acid: Experimental Demonstration of Three Processes Included in the Catalytic Cycle of Glutathione Peroxidase. *Org. Lett.* **2001,** *3* (22), 3569-3572.
112. Mapson, L. W.; Goddard, D. R., Reduction of glutathione by co-enzyme II. *Nature* **1951,** *167* (4259), 975-6.
113. Rall, T. W.; Lehninger, A. L., Glutathione reductase of animal tissues. *J. Biol. Chem.* **1952,** *194* (1), 119-130.
114. Racker, E., Glutathion reductase from Bakers' yeast and beef liver. *J. Biol. Chem.* **1955,** *217* (2), 855-866.

115. Masterson, D.; Kedrowski, B.; Blair, A., An Improved Method for the Preparation of Protected (*R*)-2-Methylcysteine: Solution-Phase Synthesis of a Glutathione Analogue. *Synlett* **2010,** *2010* (19), 2941-2943.
116. Smithies, O., Disulfide-Bond Cleavage and Formation in Proteins. *Science* **1965,** *150* (3703), 1595-1598.
117. Nagy, P., Kinetics and mechanisms of thiol-disulfide exchange covering direct substitution and thiol oxidation-mediated pathways. *Antioxid. Redox Signal* **2013,** *18* (13), 1623-41.
118. Fava, A.; Iliceto, A.; Camera, E., Kinetics of the Thiol-Disulfide Exchange. *J. Am. Chem. Soc.* **1957,** *79* (4), 833-838.
119. (Phenylthio)Nitromethane. *Organic Syntheses* **1990,** *68*, 8.
120. Wardell, J. L.; Clarke, P. L., Reactions of organotin sulphides II. Cleavage of organotin sulphides by aromatic sulphenyl compounds and divalent sulphur chlorides. *J. Organomet. Chem.* **1971,** *26* (3), 345-352.
121. Bunte, H., Zur Constitution der unterschwefligen Säure. *Ber. Dtsch. Chem. Ges.* **1874,** *7* (1), 646-648.
122. Hiver, P.; Dicko, A.; Paquer, D., Medium effects in unsymmetrical disulfides compounds synthesis from bunte salts. *Tetrahedron Lett.* **1994,** *35* (51), 9569-9572.
123. Okuma, K.; Koike, T.; Yamamoto, S.-i.; Takeuchi, H.; Yonekura, K.; Ono, M.; Ohta, H., Reaction of Olefins with Dimethyl(methylthio)sulfonium Salts in the Presence of Triphenylphosphine. Preparation of Vinylphosphonium Salts. *B. Chem. Soc. Jpn.* **1992,** *65* (9), 2375-2380.
124. Poulsen, L. T.; Heuckendorff, M.; Jensen, H. H., On the generality of the superarmament of glycosyl donors. *Org. Biomol. Chem.* **2018,** *16* (13), 2269-2276.
125. Hiskey, R. G.; Carroll, F. I.; Babb, R. M.; Bledsoe, J. O.; Puckett, R. T.; Roberts, B. W., A Synthesis of Unsymmetrical Aliphatic Disulfides. *J. Org. Chem.* **1961,** *26* (4), 1152-1155.
126. Harpp, D. N.; Ash, D. K.; Back, T. G.; Gleason, J. G.; Orwig, B. A.; VanHorn, W. F.; Snyder, J. P., A new synthesis of unsymmetrical disulfides. *Tetrahedron Lett.* **1970,** *11* (41), 3551-3554.
127. Mukaiyama, T.; Takahashi, K., A convenient method for the preparation of unsymmetrical disulfides by the use of diethyl azodicarboxylate. *Tetrahedron Lett.* **1968,** *9* (56), 5907-5908.
128. Hunter, R.; Caira, M.; Stellenboom, N., Inexpensive, one-pot synthesis of unsymmetrical disulfides using 1-chlorobenzotriazole. *J. Org. Chem.* **2006,** *71* (21), 8268-71.
129. Nishimura, O.; Kitada, C.; Fujino, M., New method for removing the S-*p*-methoxybenzyl and S-*t*-butyl groups of cysteine residues with mercuric trifluoroacetate. *Chem. Pharm. Bull.* **1978,** *26* (5), 1576-1585.
130. Muraki, M.; Mizoguchi, T., Use of N,S-Bis-*tert*-butoxycarbonyl-L-cysteine for Synthesis of Glutathione. *Chem. Pharm. Bull.* **1971,** *19* (8), 1708-1713.
131. Grotjahn, D.; Kragulj, E.; Gustafson, J., A Convenient Method for Regeneration of Free Thiol from a *tert*-Butyl Thioether. *Synlett* **2007,** *2007* (18), 2851-2854.
132. Masterson, D. S.; Roy, K.; Rosado, D. A.; Fouche, M., A divergent approach to the preparation of cysteine and serine analogs. *J. Pept. Sci.* **2008,** *14* (11), 1151-62.